Behavioral and synaptic consequences following removal of the Il1rapl1 gene in mice, a model of intellectual disability

Xander Houbaert

université de BORDEAUX

THESE

Pour le

DOCTORAT De L'UNIVERSITE DE BORDEAUX

Ecole Doctorale des Sciences de la Vie et de la Santé

Présentée et soutenue publiquement

Le 28 novembre 2014

Par Xander Houbaert

Behavioral and synaptic consequences following removal of the *Il1rapl1* gene in mice, a model of intellectual disability

Membres du Jury

M. le Dr. Bertrand Lambolez (DR CNRS)…… (rapporteur externe)
M. le Dr Nael Nadif Kasri (Assistant Professor)…… (rapporteur externe)
M. le Dr. Carlo Sala (Senior Researcher)…… (examinateur)
M. le Dr. Cyril Herry (CR Inserm)…… (examinateur)
M. le Dr. Yann Humeau (CR CNRS)…… (directeur de thèse)

Table of contents

I) Remerciements

Je remercie sincèrement mon directeur de thèse, le Dr. Yann Humeau, de m'avoir offert la chance de rejoindre son équipe il y a de ça déjà presque quatre ans. Depuis, l'équipe et les projets scientifiques continuent de se diversifier et le fait d'assister et de participer à cette évolution fut très enrichissant. Je tiens à le remercier pour sa disponibilité et pour les nombreuses discussions que nous avons pu avoir au cours de ma thèse. Il a su m'initier au monde de l'électrophysiologie et me transmettre sa passion pour ce domaine. Un grand merci également pour la liberté qu'il m'a laissée afin de développer mes propres idées et expériences. Travailler avec lui fut un plaisir et j'espère que nos chemins se recroiseront dans l'avenir. J'oubliais presque, merci de m'avoir offert la possibilité de participer à de grands congrès scientifiques dont celui à Copenhague qui me tenait vraiment à cœur pour la recherche de mon futur post-doc.

Je remercie également le directeur de l'Institut Interdisciplinaire des Neurosciences (IINS), le Dr. Daniel Choquet, de m'avoir accueilli au sein de son institut, qui fut pour moi un lieu propice à de nombreuses rencontres et qui reste aujourd'hui un pôle d'excellence pour l'étude des neurosciences en France.

Je souhaiterais également exprimer ma reconnaissance à toutes les personnes qui ont pris le temps d'étudier ce manuscrit. En particulier, le Dr. Bertrand Lambolez et le Dr. Nael Nadif Kasri d'avoir accepté d'évaluer mon travail en tant que rapporteur. Je remercie le Dr. Bertrand Lambolez de présider le jury de cette thèse ainsi que les Dr. Cyril Herry et Carlo Sala d'avoir bien voulu examiner ce travail.

Je remercie également tous mes collègues de travail sans qui la publication de mes résultats n'aurait pas été possible. Travailler avec eux pendant ces trois ans fut un vrai bonheur. Je pense notamment à toutes les blagues très fines ou répliques cultes qui mériteraient à elles-seules un livre entier. Il me faut commencer par remercier Chun-Lei qui a grandement contribué à la publication de mes résultats et m'a fait découvrir plusieurs spécialités culinaires de son pays. Je n'oublie pas non plus Elisabeth de m'avoir formé à la chirurgie et à la bonne pratique

expérimentale des animaux. Encore pardon pour le « coup de boule » accidentel lors de notre tentative de danse sur le dancefloor à Chypre. Une pensée bien sûr pour Marilyn et son aide précieuse dans l'analyse des images et pour ses conseils lors d'achats vestimentaires à Barcelone. Je tiens à lui souhaiter le meilleur pour la future naissance de son bébé. Je remercie aussi Etienne qui fut toujours de bon conseil et dont la bonne humeur est fatalement contagieuse. Personnellement, je garderai en mémoire la soirée où il nous a fait découvrir les « chupitos » dans les rues endiablées de Barcelone. Merci à Elisa d'avoir supporté mes blagues concernant sa tragique chute en vélo à Bordeaux, cela ne reflétait que mon amitié pour elle. Je pense aussi à Mélissa, Audrey et Florien qui se sont occupés de mes précieux animaux tout au long de ma thèse. Pour finir, j'aimerais remercier particulièrement Frédéric de m'avoir formé à la pose de « fenêtres crâniennes » sur la souris. Merci aussi à Mattia et Fréderic d'avoir suscité en moi l'envie de faire la fête en boîte de nuit à Bordeaux, chose qui n'est pas dans mes habitudes.

Pour conclure, je tiens à remercier de tout mon cœur mes parents d'avoir cru en moi et de m'avoir fait confiance depuis le début. Votre soutien et les nombreux repas gastronomiques passés ensemble dans les quatre-coins de la France sont toujours des moments agréables. Je pense aussi tout particulièrement à mes deux frères Anaxi et Khéphren. A Anaxi à qui je souhaite le meilleur pour sa thèse, c'est une expérience inoubliable. Je n'oublierai jamais que nous avons survécu ensemble aux crêtes du Néouvielle dans les Pyrénées. A Khéphren pour sa réussite dans son nouveau travail, je suis sûr qu'il s'y plaira. J'attends avec impatience le jour où il pourra me fabriquer une planche de surf personnalisée. Je ne pourrais conclure sans remercier ma compagne Véronique. Faire sa connaissance est la meilleure chose qui me soit arrivée et vivre avec elle est un bonheur de tous les instants. Elle a su m'apporter du soutien pendant les moments difficiles et je tiens à lui dire que je serai toujours là pour soutenir ses rêves et ses ambitions.

II) Résumé en français

Les désordres intellectuels (DI) représentent une collection très hétérogène de maladies neuro-développementales qui trouvent leur origine pendant l'enfance. Ils ont une incidence variant entre 1 et 3% dans la population générale et les origines sont multiples, combinant des facteurs environnementaux et génétiques. Pendant ma thèse, je me suis particulièrement intéressé aux DI qui résultent de mutations qui affectent la fonction d'un seul gène. Les produits protéiques de ces gènes remplissent des fonctions très différentes dans le fonctionnement du cerveau. De plus, ces protéines sont souvent exprimées à la synapse, suggérant que leur absence pourrait altérer le fonctionnement synaptique et entraîner ainsi des désordres cognitifs. Mon travail a consisté à utiliser un modèle animal de souris génétiquement modifiée mutée pour le gène *Il1rapl1* ou Interleukin-1 receptor accessory protein-like 1 (souris KO *Il1rapl1*). En effet, des micro-délétions ou mutations dans la séquence d'*Il1rapl1* sont directement impliquées dans le développement de DI et de certaines formes d'autisme chez l'homme. IL1RAPL1 est une protéine transmembranaire qui de par ses interactions avec plusieurs partenaires pré, post et trans-synaptiques serait impliquée dans la formation et la stabilisation de synapses excitatrices dans le cerveau. Néanmoins, la fonction précise d'IL1RAPL1 à des niveaux intégrés reste peu étudiée. Notre stratégie expérimentale visait à trouver des liens forts entre la fonction synaptique et déficits comportementaux. Afin de déceler des déficits cognitifs chez la souris KO *Il1rapl1*, j'ai réalisé des expériences comportementales de peur conditionnée. Cette tâche consiste à associer la présentation d'un stimulus (son, contexte…) à un événement aversif (choc électrique) créant ainsi une forte mémoire. Mes résultats montrent un déficit dans la capacité des animaux *Il1rapl1* KO à former une mémoire associative au son ainsi qu'une forte baisse de l'expression de la peur contextuelle. L'aptitude à former une mémoire de peur à un son ou d'exprimer de la peur contextuelle est soutenue par deux noyaux distincts de l'amygdale : le noyau latéral de l'amygdale (LA) et le noyau basolatéral de l'amygdale (BLA) respectivement.

Des enregistrements électrophysiologiques réalisés dans le LA et le BLA ont prouvé l'existence d'une dérégulation de la balance entre la transmission inhibitrice et excitatrice (balance I/E) suite à l'absence d'IL1RAPL. En effet, l'excitation reçue suite à la stimulation de projections

excitatrices contactant les neurones pyramidaux du LA ou du BLA était amoindrie chez les animaux *Il1rapl1* KO tandis que l'inhibition reçue par les neurones pyramidaux était préservée. Dans le LA et le BLA les neurones pyramidaux sont régulés par l'activation d'interneurones locaux. L'inhibition des neurones pyramidaux étant préservée, nous avons voulu tester l'excitation des interneurones suite à la stimulation des mêmes afférences. En réalisant des expériences électrophysiologiques ciblées sur les interneurones du LA, j'ai ainsi pu démontrer que l'absence d'IL1RAPL1 n'affectait pas les synapses excitatrices des interneurones et en conclure que l'identité de la cellule postsynaptique (excitatrice ou inhibitrice) définit la vulnérabilité des synapses suite à l'absence d'IL1RAPL1.

Nous avons alors fait l'hypothèse que l'altération de la balance I/E était à l'origine des déficits comportementaux observés. J'ai ainsi découvert que le déficit des animaux *Il1rapl1* KO dans la formation de la mémoire de peur au son résultait d'une perte des processus de plasticité synaptique qui sous-tendent la formation de la mémoire. En effet, j'ai pu montrer que la dérégulation de la balance I/E empêchait l'induction de la potentiation à long terme dans le LA expliquant le déficit comportemental. Ensuite, nous avons voulu restaurer le comportement des animaux *Il1rapl1* KO en utilisant des approches pharmacologiques et optogénétiques censées corriger la balance I/E dans l'animal *in vivo* juste avant la phase de formation de la mémoire. De façon surprenante, les deux traitements étaient capables de normaliser la formation de peur conditionnée au son chez les animaux *Il1rapl1* KO, ceci prouvant des liens étroits entre la balance I/E et le déficit comportemental.

Afin de mieux caractériser le déficit d'expression de peur contextuelle, nous avons analysé l'activation du BLA et de l'hippocampe suite à la réexposition d'animaux *Il1rapl1* KO à un contexte aversif, laquelle entraîne l'expression d'une peur contextuelle. Cette expérience révèle une forte diminution de l'activité du BLA et de la zone ventrale de l'hippocampe (vHPC). Le vHPC envoie des afférences sur le BLA, or, le rôle de ces projections dans la régulation de l'expression de la peur contextuelle restait peu étudié avant nos recherches. Nous avons alors fait l'hypothèse que le dysfonctionnement des projections de l'hippocampe ventral sur le BLA pourrait être à l'origine du déficit d'expression de la peur contextuelle chez les animaux *Il1rapl1* KO. Pour tester notre hypothèse nous avons appliqué un protocole de potentiation des

projections du vHPC sur le BLA par optogénétique, et ce avant la réexposition de l'animal au contexte aversif. Cette intervention a permis de restaurer l'expression de la peur contextuelle sur les souris mutées, montrant l'importance de cette projection dans la régulation de la peur contextuelle. La question se pose : quel rapport y-a-t-il avec la dérégulation de la balance I/E dans le BLA ? Nous pensons que la faible activation des cellules pyramidales du BLA lors de la réexposition au contexte aversif est une conséquence directe de la modification de la balance I/E dans le BLA. La potentiation des projections du vHPC sur le BLA permettrait de contourner cette balance I/E ce qui permet l'activation des cellules pyramidales du BLA lors de l'expression de la peur contextuelle.

En conclusion, le disfonctionnement synaptique lié à la modification de la balance I/E peut entraîner des déficits cognitifs à plusieurs niveaux. Ainsi, dans le LA cela a pour conséquence d'empêcher la formation d'une mémoire de peur en empêchant l'induction de mécanismes de plasticité synaptique. Dans le BLA, la balance I/E empêche une population neuronale de s'activer bloquant ainsi l'expression de mémoires précédemment formées. Ceci ouvre la perspective intéressante que les déficits d'apprentissage et de mémoire pourraient être corrigés à plusieurs niveaux. Pour finir, mes travaux montrent l'importance de l'hétérogénéité synaptique dans certains aspects pathologiques des désordres intellectuels. En effet, seules les synapses excitatrices des neurones pyramidaux excitateurs étaient concernées par l'absence d'IL1RAPL1, ce qui suggère un rôle différentiel de la protéine en fonction du type de synapse étudiée. De nombreux déficits cognitifs pourraient ainsi être causés par la perte de la fonction d'une protéine à divers types synaptiques. Ainsi, la compréhension des désordres intellectuels nécessite une stratégie nous permettant d'aborder la question de l'hétérogénéité synaptique en utilisant des approches expérimentales *in vitro* et plus encore *in vivo*.

III) Abstract en français

Les désordres intellectuels (DI) comprennent une collection hétérogène de désordres neurodéveloppementaux qui émergent pendant l'enfance. Ils ont une incidence de 1 à 3% dans la population et sont associés avec des déficits dans les fonctions mentales et adaptives. De nombreuses mutations ont été identifiées dans des gènes codant pour des protéines qui remplissent des fonctions biologiques très diverses dans le cerveau. Parmi ces protéines, certaines sont enrichies à la synapse, supposant que les déficits cognitifs associés aux DI pourraient être reliés à des déficits synaptiques. L'objectif scientifique de notre équipe et de comprendre le rôle de certaines protéines dans la fonction synaptique et la cognition en utilisant des souris génétiquement modifiées portant des mutations dans le gène correspondant. Je me suis concentré sur *Il1rapl1*, un gène codant pour la protéine Interleukin-receptor-accessory-protein-like-1. Des mutations ou micro-délétions dans ce gène sont liés au développement de DI chez l'homme. Dans les neurones, *Il1rapl1* code pour une protéine transmembranaire qui serait impliquée dans la formation et/ou la stabilisation de synapses excitatrices. Les conséquences de l'absence d'IL1RAPL1 à des niveaux plus intégrés restaient peu étudiées lors du début de ma thèse. J'ai utilisé une souris déficiente pour IL1RAPL1 (KO) afin de comprendre le lien entre les déficits comportementaux et la fonction synaptique. Pour cela, j'ai soumis des souris KO à des taches comportementales de peur conditionnée. J'ai ensuite utilisé une combinaison d'approches *in vitro, ex vivo* et *in vivo* afin de caractériser la fonction synaptique dans les circuits neuronaux dédiés : l'amygdale latérale et basolatérale. Des enregistrements electrophysiologiques ont montré une dérégulation de la balance entre la transmission inhibitrice et excitatrice (I/E) dans l'amygdale de souris *Il1rapl1* KO, causant ainsi des déficits dans la capacité d'acquérir et d'exprimer la mémoire de peur conditionnée. La correction de ce déficit synaptique *in vivo* par pharmacologie ou par optogénétique a permis de restaurer le comportement chez les souris KO.

Mots clés : IL1RAPL1, désordre intellectuel, balance inhibition/excitation, peur conditionnée, amygdale, optogénétique

IV) Abstract

Intellectual disability (ID) comprises a highly heterogeneous collection of neurodevelopmental disorders that arise during childhood. They have an incidence of 1-3% in the population with impairments in mental and adaptive functions. While the etiologies of IDs are thought to be very heterogeneous, a significant proportion of ID has genetic origins. Mutations in single ID genes lead to dysfunctions in proteins that fulfill highly different biological functions in the brain. Interestingly, ID-related proteins are often found enriched at synapses, suggesting that cognitive impairments defining ID could be related to alterations of synaptic function. The main goal of our research team is to understand the role of ID-related proteins in synaptic function and cognition using mouse models bearing gene mutations associated to ID in humans. My research focused on the study of *Il1rapl1, a* gene coding for the Interleukin-receptor-accessory-protein-like-1 protein. Micro-deletions or point mutations in this gene are directly linked to the development of ID and autism spectrum disorder in humans. In neurons, *Il1rapl1* encodes a trans-membrane protein and several *in vitro* experiments point to its important role in the differentiation and formation/stabilization of excitatory synapses trough interactions with presynaptic, trans-synaptic or postsynaptic partners. However, the consequences of *Il1rapl1* deficiency at more integrated levels remains poorly understood. The principal objective of my thesis is to explore the link between synaptic deficits and behavioral impairments in *Il1rapl1*-deficient mice. To achieve that, wild-type and mutant animals were first submitted to fear learning tasks. I then used a combination of *in vivo*, *ex vivo* and *in vitro* functional essays to characterize synaptic functions in behaviorally relevant neuronal circuits. Ultimately, our working hypothesis were challenged *in vivo* by pharmacological and optogenetic approaches to normalize behavioral deficits in *Il1rapl1* KO mice. Altogether my work demonstrates that Inhibitory/Excitatory imbalances associated with the absence of *Il1rapl1* impaired both the capacity to form new memories as well as the expression of previously formed memories.

Key words: IL1RAPL1, intellectual disability inhibitory/excitatory balance, fear conditioning, amygdala, optogenetics

V) Abbreviations

AC: Adenylate Cyclase

AMPA: α-Amino-3-hydroxy-5-methyl-4-isoxazolepropionic acid

ASD: Autism Spectrum Disorder

BLA: Basolateral amygdala

CA: Cornu Ammonis

CAM: Cell Adhesion Molecules

CAMKII: $Ca^{2+/}$calmodulin-dependent protein kinase II

cAMP: Cyclic Adenosine Monophosphate

CD: Cognitive disorder

CE: Central amygdala

CS: Conditioned stimulus

CT: Carboxyl terminal

DG: Dentate Gyrus

DIC: Differential Interference Contrast

E/I: Excitatory/inhibitory

EM: Electron microscopy

EPSC: Excitatory postsynaptic current

EPSP: Excitatory postsynaptic potential

FACS: Fluorescence Activated Cell Sorting

FASS: Fluorescence Activated Synaptosome Sorting

FFI: Feed-forward inhibition

FMR2: Fragile mental retardation 2

FRAP: Fluorescence Recovery After Photobleaching

GABA: γ-Aminobutyric acid

GAD67: Glutamate decarboxylase 67

GAP: GTP-ase activating protein

GDI: Guanine dissociation inhibitor

GDP: Guanosine Di-Phosphate

GEF: Guanine nucleotide exchange factors

GFP: Green Fluorescent Protein

GluN: Glutamate NMDA Receptor subunit

GluR: Glutamate AMPA Receptor subunit

GTP: Guanosine Tri-Phosphate

Homer: Homer protein homolog 1

ID: Intellectual Disability

IL: Infralimbic

IL1RAPL1: Interleukin 1 Receptor Accessory Protein-Like 1

ISI: Interstimulus Interval

ITC: Intercalated cell cluster

LA: Lateral amygdala

LTP: Long term potentiation

MAGUK: Membrane-associated guanylate kinases

mEPSC: Miniature excitatory postsynaptic current

mPFC: Medial prefrontal cortex

NLG: Neuroligin

NMDA: N-Methyl-D-aspartate

NRX: Neurexin

OPHN1: Oligophrenin 1

PKA: Protein Kinase A

PKC: Protein Kinase C

PL: Prelimbic

PPF: Paired Pulse Facilitation

PPR: Paired Pulse Ratio

PSD: Postsynaptic Density

PTX: Picrotoxin

PV: Parvalbumin

RIM: Rab-interacting molecule

ROCK: Rho-associated protein kinase

RRP: Ready releasable pool

SHANK: SH3 and multiple ankyrin repeat domains

SM: Sec1/Munc18like proteins

SNAP-25: Synaptosomal-associated protein 25

SNARE: Soluble N-éthylmaleimide-sensitive-factor Attachment protein Receptor

STDP: Spike Timing Dependent Plasticity

TETO: Tetracycline response element

TIR: Toll/interleukin-1 receptor

tTa: Tetracycline transactivator

US: Unconditioned stimulus

VGCC: Voltage-gated calcium channel

VGLUT: Vesicular Glutamate Transporter

vHPC: Ventral hippocampus

VI) Introduction

Although the causes of intellectual disabilities (ID) are highly heterogeneous, an increasing number of genetic factors have been discovered that contribute to the development of ID in humans. Amongst them, single gene mutations lead to the absence or the partial loss of discrete proteins that fulfill highly different biological functions in the brain. However, whether and how the loss of function of those proteins relates to cognitive impairment remains unclear. The main goal of our team is to understand ID pathophysiology at synaptic, neuronal, network and behavioral levels by using genetically engineered mice mimicking single gene mutations found in human patients. This optimizes the well-established strategy that consists of deciphering normal brain function by studying the physiological consequences of perturbing mutations.

Single gene mutations in ID-related genes impact several biological functions including brain development or general brain function. Severity of ID pathology depends on the nature of the disrupted biological processes. For example, mutations in genes underlying the initial stages of brain development often lead to irreversible changes in brain circuitry and severe deficits in cognitive functions. My interest being more to look at the role of synapses in adult circuitry, I decided to focus on a mild form of ID caused by the mutation of the *Il1rapl1* gene. Indeed, *Il1rapl1*-deficiency is thought to preserve brain development in humans and rodents (at least the initial stages), allowing studying the consequences of the mutation in a correctly established mature brain. In contrast, *Il1rapl1,* as many other ID-related genes, is enriched in both pre- and postsynaptic compartments, a crucial place for information transfer and processing in neurons. This has led to the idea that the specific absence of IL1RAPL1 at synapses may be responsible of the reported cognitive impairments. Furthermore, it is well established now that the absence of proteins essential for synaptic function leads to lethality. As a consequence, we hypothesize that because *Il1rapl1* deficiency only leads to mild behavioral changes, IL1RAPL1 may regulate more subtle aspects of synaptic physiology and understanding their function is of crucial importance.

The consequences of ID-related mutations at more integrated levels such as neuronal coding of behaviors are far less described. The originality of my contribution was to use *Il1rapl1*-deficient mice to understand how synaptic deficits associated to the absence of IL1RAPL1 affect mice behaviors. To achieve that, I used an associative learning task, the pavlovian fear conditioning, as it is well understood at neuronal and synaptic levels, and perturbed in *Il1rapl1* KO mice. Moreover, regulation of fear behavior involves projections between different brain areas and interactions between both excitatory and inhibitory cells. This makes associative fear an ideal model to look at the consequences of *Il1rapl1* mutation at the circuit, cellular, synaptic and behavioral levels.

The following introductory paragraphs are organized according to my experimental strategy. The first part covers intellectual disabilities by providing some general definitions and their etiologies. In order to understand ID pathology, one has to understand how the normal brain operates. Thus, I'll describe how brain processes information, as well as the underlying cellular and synaptic mechanisms. For the sake of clarity synaptic function has been separated in pre- and postsynaptic function and a few examples of ID-related mutations illustrate how their absence may lead to disruptions in synaptic function. Brain is also subject to morphological changes throughout life and depends on the local action of different ID-related proteins. Thus, I added a chapter on brain development and how mutations in ID-related genes can interfere with this essential biological process. Finally, after discussing briefly how ID is currently studied in humans, I'll show the importance of animal models in the study of the pathology of intellectual disabilities and shed some light on current therapeutic perspectives that could improve some core symptoms of the disease.

The second part aims at reviewing the current knowledge on the gene I have studied during my PhD: the *Il1rapl1* gene. First, I provide some evidence that, in humans, genetic abnormalities in *Il1rapl1* gene are directly linked with the development of ID and other cognitive disorders like autism. I present all current experimental data reporting a role of IL1RAPL1 protein in the mammalian brain both *in vitro* and *in vivo*. Finally, the last part of the introduction further explains my choice in using associative fear learning tasks on *Il1rapl1* KO mice. I focus

specifically on the neural circuits and the cellular/synaptic mechanisms leading to the formation and expression of fear memories.

1 Intellectual disabilities

1.1 General definitions

Intellectual disability (ID) defines a large and heterogeneous collection of neurodevelopmental disorders that arise during early childhood. Until recently called mental retardation, these disorders are now referred to as intellectual disabilities as the old designation was considered outdated by American health services. ID and related cognitive disorders (CD) have a high incidence in our modern societies, affecting approximately 1-3% of the population. Patients show impairments of general mental abilities that impact adaptive functioning in three areas: conceptual (language, reading, writing, reasoning, knowledge and memory), social (empathy, social judgment, communication skills…) and practical (self-management, job responsibilities, organization…). IDs are chronic and often co-occur with other mental conditions like depression, attention-deficit/hyperactivity disorder, and autism spectrum disorder (ASD) (Won et al., 2013). ASD is a group of developmental disabilities characterized by abnormal social interaction and communication and stereotyped/repeated behaviors with restricted interests. ID and ASD have strongly overlapping symptoms, but stereotyped/repeated behaviors with restricted interests are specific to ASD.

Intellectual disabilities are classified in different categories depending on intellectual quotient (IQ) levels of the patients. Persons suffering from ID have an IQ lower than 70 (Figure 1) and the severity of ID can be divided into mild (IQ between 50 and 69), moderate (IQ between 35 and 49), severe (IQ between 20 and 34) and profound (IQ lower than 20). Genetic forms of ID are often distinguished in two categories: non-syndromic and syndromic ID. Non-syndromic ID patients suffer from cognitive impairments solely, whereas syndromic ID patients often show other radiological, biological or metabolic defects (van Bokhoven, 2011). However, the classification between syndromic and non-syndromic forms of ID is not always easy to establish as different individuals can show heterogeneity in symptoms following a mutation in the same

genetic locus (Frints et al., 2002). Patients that present syndromic forms of ID often also present strong morphological brain abnormalities like micro-and macrocephaly or deficits in neuronal migration. These abnormalities are likely to contribute to cognitive deficits, thus preventing from understanding the precise role of the gene product in brain cognitive functions.

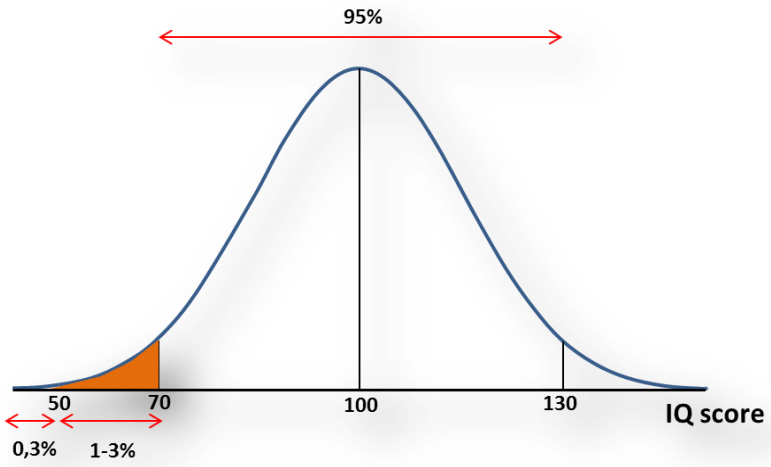

Figure 1: Gaussian representing IQ scores in the general population. The vast majority of human IQ profiles vary between 70 and 130. Intellectual disabilities are represented by IQ levels under 70. Most ID patients (1-3%) have IQ levels between 50 and 70 and 0,3% of them present more severe forms of ID.

The causes of ID and ASD are highly heterogeneous, including environmental factors (pesticides, prenatal alcohol exposure…) that influence the development of the nervous system, and genetic causes including single gene mutations, copy number variants or chromosomal abnormalities (Chelly et al., 2006). Characterization of the genetic factors that determine ID started in the 90's with the discovery of *Fmr2* gene, an X-linked gene which's mutation causes fragile X syndrome (Gecz et al., 1996). Initially, the identification of ID-related genes focused mostly on the X chromosome, most likely because their recessive nature and the presence of a single copy in male patients facilitates the relation between genetic abnormalities and behaviors (Figure 2). An increasing number of ID-related genes were then identified with more than several hundred genes discovered to date. However, the number of identified ID genes is expected to increase dramatically (several thousand) with the development of next-generation sequencing

technologies (Gilissen et al., 2014) (Figure 2). Interestingly, these technologies may also for the first time give access to a large number of autosomal genes.

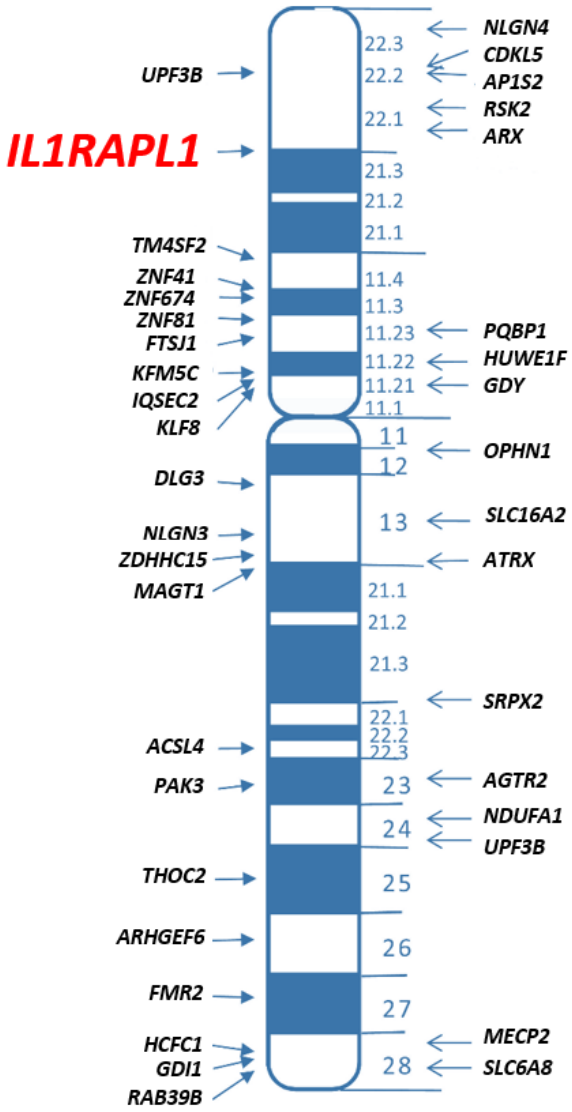

Figure 2: Scheme representing some identified X-linked genes causing ID in humans. On the left are presented genes which's mutation causes non syndromic ID, while the genes on the right cause both syndromic and non syndromic ID. The *Il1rapl1* gene is depicted in big on the left because it causes a non syndromic form of ID. Adapted from Lubs et al. 2012

In our team, we take advantage of the monogenic aspects that determine development of ID mainly because it facilitates the generation of animal models mimicking mutations found in human patients. Within that framework, my PhD was dedicated to the study of a non-syndromic monogenetic ID model, in order to unravel the link between brain dysfunction and cognitive

features in ID. Indeed, both non-syndromic human patients and rodent models show no gross morphological alterations, which favor the study of functional consequences of mutations on roughly normally developed brains. We decided to focus our attention on the X-related *Il1rapl1* gene that encodes Interleukin 1 Receptor Accessory Protein-like 1 (Figure 2).

Mutations in the *Il1rapl1* gene are associated with both ASD and ID in humans. (Carrié et al., 1999; Piton et al., 2008). The reasons behind genetic heterogeneity in the development of ID and ASD remain largely unknown. One possibility could rely in the exact position of the mutation within the gene that would lead either to subtle or profound (including the complete absence) changes in the protein. In this line, some biological functions/interactions of the protein could be preserved, leading to differences in phenotype expression. Alternatively, environmental factors may emphasize differences in epigenetic regulation of genes, resulting in different phenotypic expression patterns in individuals (Rzhetsky et al., 2014).

1.2 Function of ID-related genes

In humans, knowledge about the pathological consequences of ID- and ASD related genes at cellular and subcellular levels is limited by ethical issues. Most data available originate from post-mortem tissue of ID and ASD patients. They often reveal deficits in the wiring of the brain or in the number/morphology of dendritic spines (Kaufmann, 2000; Purpura, 1974).

ID-related genes code for proteins that can be divided in distinct functional categories including enzymes, mediators of signal transduction, transcriptional regulators, transporters, cell adhesion and structural molecules, motor proteins… (Vaillend et al., 2008). Proteins belonging to these categories fulfill a wide array of cellular functions to regulate neuronal function (van Bokhoven, 2011). Interestingly, a lot of ID and ASD-related proteins are often found localized and expressed at the synaptic level, thereby emphasizing their biological function at the synapse. This has led to the emergence of the term “synaptopathy”, a term implying that global function and/or structure of the synaptic compartment is disrupted, at least partly, in ID pathology.

1.3 Physiology of the brain in health and disease

Dissecting the neural and cellular mechanisms involved in high cognitive functions is a key yet unresolved question in neuroscience. Classically, this has been addressed by identifying and dissecting how high cognitive functions are perturbed in ID model. ID patients show strong sensory, motor and general cognitive abnormalities, suggesting that the cellular and molecular mechanisms underlying information transfer and processing in the brain could be disrupted. Because of the high enrichment of ID-related proteins at synapses, this chapter aims at reviewing some basic principles of how the brain integrates and treats information by emphasizing the role that synapses play in this essential biological process. For the sake of clarity, synaptic function has been separated in two parts according to the anatomical organization of the synapse, being pre-and postsynaptic compartments. Of course, ID-related proteins not only impact mature brain function. A high proportion of ID's are indeed thought to result from deficits in brain development and reorganization of existing connections throughout life. Thus, I also added a paragraph on brain development which focuses mainly on the mechanisms regulating synaptic formation.

1.3.1 Synaptic integration

Probably one of the most exciting yet very complex matter in neuroscience is the understanding of how neurons process and integrate information and how this underlies high cognitive functions (Spruston, 2008). Synapses are specialized anatomical entities that mediate information transfer between neurons. Typically a synapse is composed of tightly apposed pre- and postsynaptic sites separated by the synaptic cleft (Figure 3), a very thin zone where presynaptic neurotransmitter-filled vesicles are released. Synapses can be distinguished by their location on the neuron and the identity of the pre-and postsynaptic element. The vast majority of synapses in the brain are axo-dendritic synapses: the axon travels through a defined region and makes "en passant" boutons that contact the dendrites of postsynaptic neurons. However, synapses may also be axo-somatic, axo-axonal, dendro-dendritic, somato-somatic or somato-dendritic. Interestingly, these different types of synapses fulfill highly different functions in the

regulation of neuronal responsiveness and integration and aren't mediated by the same cellular types in the brain.

The brain is composed of many different neuronal cell types. However, two types largely underlie the vast majority of information processing in the brain: excitatory (principal) neurons use glutamate as neurotransmitter and interneurons which mostly exert an inhibitory role by releasing GABA. Principal cells developed specialized structures on their dendrites called dendritic spines that are supposed to increase the number of possible contacts between neurons. In contrast, Inhibitory neurons are usually described as "low spiny" neurons. Nonetheless, it has to be noted that some brain structures do possess spiny interneurons, a feature not shared by the majority of interneurons in the brain. Excitatory and inhibitory neurons not only differ in the way they are contacted, but also in the way they contact other cells. For example, the axons of interneurons preferentially make axo-axonic or axo-somatic on pyramidal cells to regulate their activity (see below) while principal cells mostly contact other cells (pyramidal or interneurons) through axo-dendritic synapses (Tritsch et al., 1998).

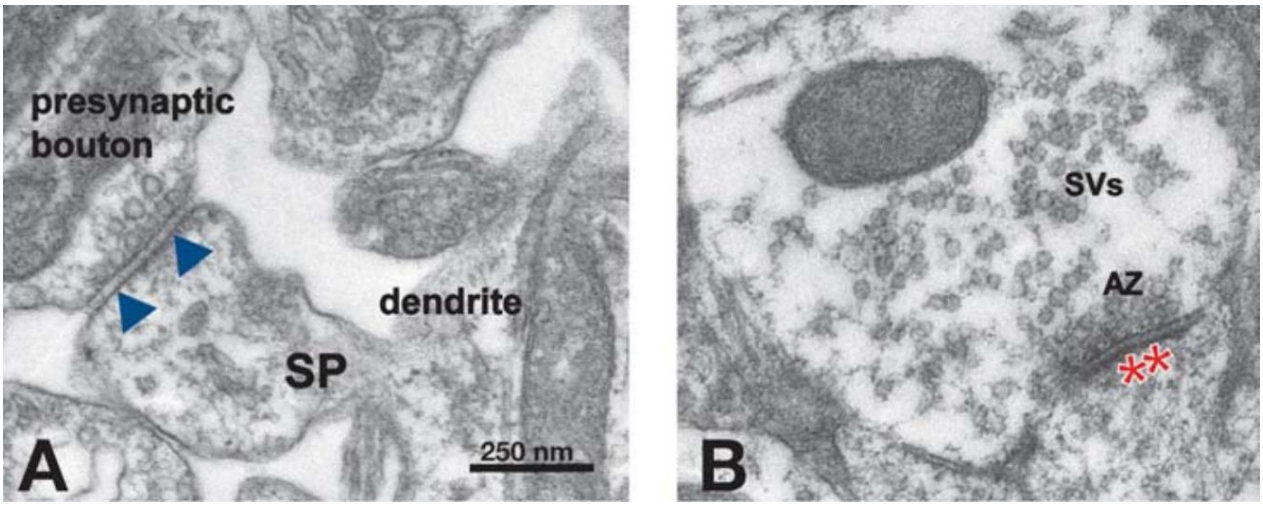

Figure 3: Electron microscopy pictures of two typical excitatory glutamatergic synapses of hippocampal cells in culture. A: Typical excitatory synapse between a presynaptic bouton and a postsynaptic dendritic spine (SP). Docked synaptic vesicles can be seen and the synaptic cleft is indicated by arrowheads. B: Synapse with many of the classical features of chemical synapses: a presynaptic bouton containing synaptic vesicles (SVs), an electron dense active zone (AZ) and an apposed postsynaptic density (PSD) indicated by asterisks. From Waites et al. 2005

Excitatory principal cells compose the large majority of neurons in the brain, underlie local information processing/storage, and represent the major sources of output to distinct brain regions. In addition of these long range projections, principal cells also mutually connect to each other, thereby generating excitatory transmission to neighboring neurons through local circuits. Interneuron's axons, however, are often limited to single brain regions, regulating the activity of local circuits (Markram et al., 2004).

A crucial question is to understand how principal cells transform incoming information into specific pattern of action potential output. Axon potential initiation occurs in anatomically defined zone called the axonal initiation segment which is located close to the soma. Principal cell receive a large amount of excitatory and inhibitory synaptic inputs that are spread across their dendritic arbor, but also at their soma or axon. Most of the excitatory drive arrives through the dendrites. Interestingly, integration of excitatory inputs is greatly influenced by their location on the dendrite. Synapses on dendrites that are located far from the soma are thought to amplify signals with high gain and over broader time windows to compensate for their electrotonic disadvantage, thus having stronger influence over action potential initiation (Branco and Häusser, 2010; Williams and Atkinson, 2008). In contrast, the soma and the axon of principal cells receive mainly inhibitory GABA-ergic inputs originating from local interneurons, regulating output of principal cells.

Interestingly, distinct populations of interneurons target specific cellular domains on pyramidal neurons (Markram et al., 2004). These interneurons not only differ in their morphological aspect and their electrophysiological properties (DeFelipe et al., 2013), but especially in the way they contact pyramidal cells. For example, while some interneurons clearly target the soma or the axon to regulate AP initiation, others exert their effect through inhibition of the dendritic arbor of principal cells, regulating the activation of distal synapses (Pouille and Scanziani, 2004). Two functional microcircuits involving interneurons and controlling principal cells integration have been described: feed-forward or feed-back inhibitory circuits (Figure 4). During feed-forward inhibition, interneurons are activated by the same projections that activate principal cells, regulating principal cell excitation and output. In contrast, feed-back inhibition is only activated when principal cells fire an AP, thus limiting sustained pyramidal-neuron firing. Feed-forward

and feed-back inhibition have been shown to be important physiologically to reduce the number of simultaneously active principal cells, working towards the creation of sparse representations, but also in the regulation of synaptic plasticity mechanisms. In addition, interneurons have been shown to coordinate network oscillations within/between brain areas (Isaacson and Scanziani, 2011), a process that has been shown to generate certain behaviors (Courtin et al., 2014). The balance between excitatory and inhibitory (E/I balance) transmission in the brain is crucial for information processing and output responsiveness (Yizhar et al., 2011). Moreover, a growing body of evidence suggests that disrupted E/I balance in the CNS may be implicated in the pathology of neurodevelopment disorders including autism and IDs (Baroncelli et al., 2011; Gatto and Broadie, 2010).

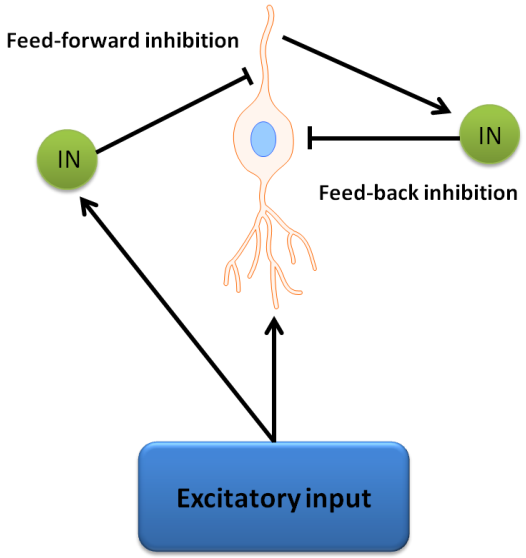

Figure 4: Scheme representing feed-forward (FFI) and feed-back (FBI) inhibition of a principal neuron. During FFI, the same axons contact principal cell and interneuron. In contrast, FBI is only elicited when the principal cell fire an AP.

In conclusion, neuronal integration in a particular network depends on a strong interaction between excitatory principal cells and inhibitory interneurons. The relative strength of excitation and inhibition and their temporal relationship orchestrates brain function. The large diversity of cellular types in the brain and the way they connect to each other allows the brain

to elaborate a wealth of different cognitive features. This diversity also suggests that multiple actors regulating neuronal integration could be differentially impacted following ID gene mutations. For example, the disruption of E/I balance in ID could result from differential effects of ID-gene mutations on excitatory vs. inhibitory cells; to my knowledge, only a few studies have addressed the consequences of ID-related gene mutations on both excitatory and inhibitory cells. In my opinion, to understand how ID genes impact neuronal integration and cognition, one has to consider all elements of a neuronal circuit to get a clear picture on how synaptic proteins may contribute to brain function.

1.3.2 Synaptic function

In neuronal cell cultures, ID-related proteins are often found enriched at pre- and/or postsynaptic compartments, leading to the hypothesis that cognitive impairments associated with ID could be related to local alterations at the synaptic level (Humeau et al., 2009). While in some cases, some clear pre-or postsynaptic functions have been attributed to ID proteins, some are present in both compartments. Thus, the next chapters focus on pre- and postsynaptic function and provide some examples of ID gene mutations that impact these crucial biological processes.

1.3.2.1 Presynaptic function

Classically, the presynaptic site is composed of the active zone, an electron-dense, protein rich zone where vesicles fuse with plasma membrane and release their content in neurotransmitters. This tightly regulated ultra-fast mechanism achieves the release of chemical compound at high rate and in a very precise manner through the interaction of a large number of proteins over several steps (Sudhof, 2004). Moreover, neurotransmitter release can be modified by neuronal activity, a phenomenon called synaptic plasticity (see synaptic plasticity paragraph below). Neurotransmitter secretion follows a well characterized sequence of events including: 1) the filling of vesicles with neurotransmitters, 2) the docking and priming of vesicles into the active zone, 3) the calcium-mediated fusion of the vesicle, 4) the release of its content, and 5) its recycling (Figure 5). Neurotransmitters first need to be loaded into vesicles by a regulated transport. Each vesicle is endowed with specialized transporters that allow charging

the vesicle with specific neurotransmitters. For example, VGLUT transporters specifically handle the loading of the excitatory neurotransmitter glutamate into the synaptic vesicle (Fremeau et al., 2004). Interestingly, three transporters for glutamate have been identified and show different expression patterns throughout the brain, which endows certain heterogeneity in the identity of presynaptic compartments (Herzog, 2004).

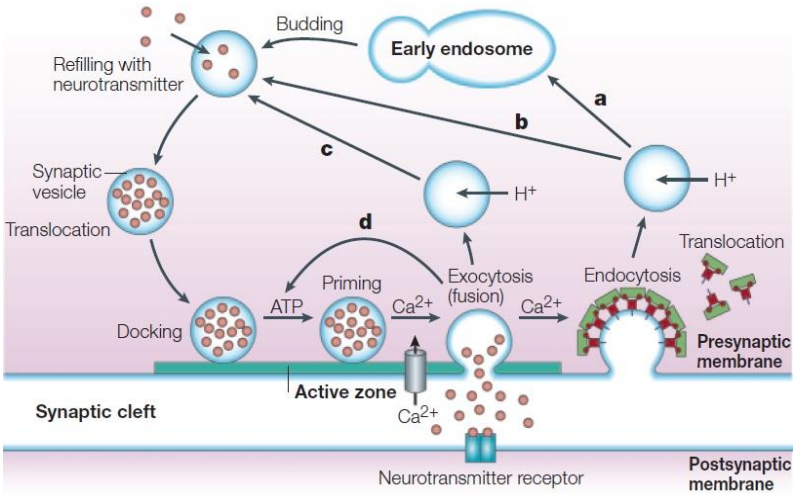

Figure 5: Scheme representing the key steps in vesicle-mediated neurotransmission. Initially, vesicles are filled with neurotransmitters. Then, they are translocated to the active zone, tethered (docking) and primed for release. In response to a Ca^{2+} influx, they undergo exocytosis and release neurotransmitters in the synaptic cleft. Finally, vesicles are retrieved by various ways, but the most described one is clathrin-mediated endocytosis with (or without) a recycling through the endosome. From Gundelfinger et al. 2003

Once filled, vesicles are translocated to the presynaptic active zone where they are docked and get primed for release. Docking of vesicles to the plasma membrane involves the formation of a protein complex composed of SNARE (Soluble N-éthylmaleimide-sensitive-factor Attachment protein Receptor) and SM (Sec1/Munc18like proteins) proteins that undergo a cycle of association/dissociation during the fusion reaction of the vesicle membrane with the plasma membrane (Sudhof, 2013) (Figure 6B). First, the vesicular SNARE (v-SNARE) protein synaptobrevin (or VAMP) assembles with syntaxin-1 and SNAP-25 (also called t-SNAREs). This binding is tightly regulated by the so called SM proteins Munc18-1 and complexin (Shen et al.,

2007; Wragg et al., 2013) (Figure 6B). During membrane fusion, the assembly (before transmitter release) and disassembly (after transmitter release) of the SNARE/SM complex is regulated by chaperone proteins (Acuna et al., 2014). Once primed to the plasma membrane at the level of the active zone, vesicles are ready for pore opening and neurotransmitter release.

Upon arrival of an action potential in the presynaptic compartment, there is activation of voltage-dependent calcium channels (VGCCs) that are located at the active zone. Voltage-gated calcium channels are a large family of proteins with multiple members but synchronous release is believed to depend mainly on N and P/Q calcium channels (Kamp et al., 2012). Their activation leads to a spatially restricted increase in calcium concentration within the active zone next to primed vesicles. This leads to binding of Ca^{2+} ions to the synaptotagmin protein, which binds at his turn to the SNARE/SM complex and phospholipids, allowing pore opening and release of neurotransmitters in the synaptic cleft (Südhof, 2013). Finally, the families of RIM and RIM-binding proteins collaborate to recruit calcium channels to the release sites, allowing the fine spatial localization of Ca2+ influx to couple action potential to neurotransmitter release (Han et al., 2011; Kaeser et al., 2011).

RIM proteins bind to vesicular Rab proteins, involved in the trafficking of vesicles to the presynaptic terminal. Rab proteins are part of the Ras family of small GTPases, which are typically active in their GTP-bound state and inactive in their GDP-bound state (D'Adamo et al., 2014). The GDP-GTP-bound state is controlled by GTPase-activating proteins (GAPs) and guanine-nucleotide-dissociation inhibitors (GDIs), which promote the inactive state and guanine-nucleotide-exchange factors (GEFs) that stimulate Rab activity. The interaction of RIM with Rab3 (Figure 6B) has an important regulatory role in calcium mediated vesicular fusion with the active zone (Han et al., 2011).

A last crucial step involves the recycling of emptied vesicles. This step is mandatory to maintain the pool of available vesicles in order to further allow continuous neurotransmission (Rizzoli, 2014). This mainly occurs through clathrin-mediated endocytosis, a conserved mechanism that involves the coating of vesicles with clathrin through the coordinated assembly of a large number of proteins (Godlee and Kaksonen, 2013). Once endocytosis occurred, vesicles may

either transit through the endosomes or bypass this route (Figure 5). Alternatively, some vesicles are supposed to be recycled just after the release of their neurotransmitters without leaving the active zone, a process called kiss and run. However, the existence of this process remains unclear (Alabi and Tsien, 2013).

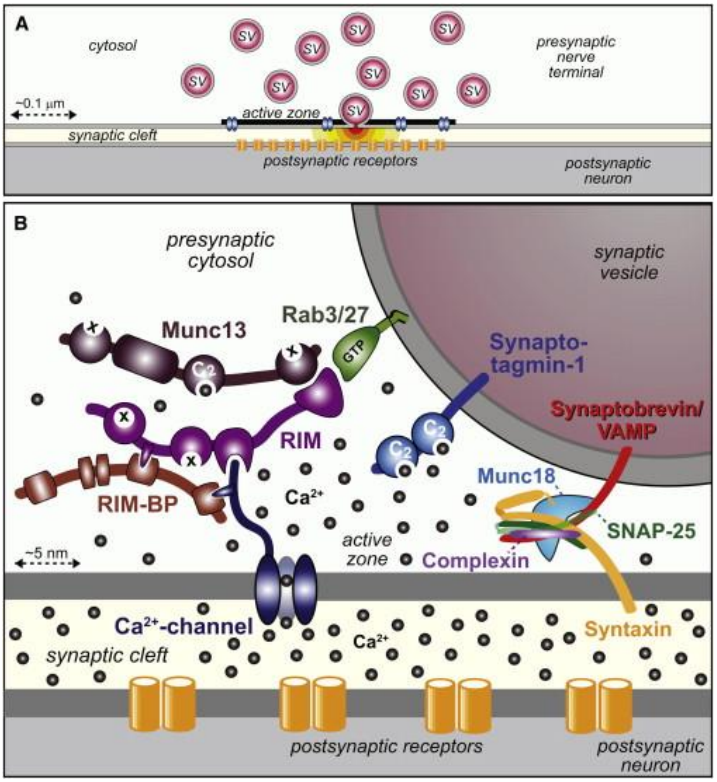

Figure 6: (A) Drawing of a synapse with synaptic vesicles (SV, red), an active zone containing Ca2+ channels (blue), and a postsynaptic cluster of receptors (orange). (B) Schematic of the molecular machinery mediating Ca2+-triggered vesicle fusion. On the right is depicted the SNARE/SM complex composed of vesicular protein synaptobrevin (VAMP) interacting with Syntaxin and SNAP-25, a recognition itself regulated by Munc18 and Complexin. The Ca2+ sensor synaptotagmin-1 is depicted in the middle. On the left are RIM and RIM-BP proteins recruit Ca2+ channels close to release sites by binding with vesicular Rab proteins. From Sudhöf 2013

Not surprisingly, genetic abnormalities of proteins involved in all steps leading to neurotransmission have severe consequences in humans. For example, mutations in the *Stxbp1* gene, which codes for Munc18-1, are the cause of Ohtahara syndrome, encompassing infantile epileptic encephalopathy and severe ID (Hamdan et al., 2011). Interestingly, two proteins involved in the regulation of Rab protein activity have been associated with ID: GDIα and

Rab3GAP. GDIα is located on the X chromosome and maintains Rab proteins in the inactive state by binding Rab-GDP. GDI1 KO mice have deficits in the synaptic vesicle pools and short term-synaptic plasticity defects (Bianchi et al., 2009). However, mutations seem to have little effect on Rab3a, and the cognitive defects might be exerted through other neuronal Rab proteins. For example, mutations in Rab39B lead to a form of non syndromic ID with deficits in the number of neurite growth cones and presynaptic boutons, suggesting that Rab39B could be involved in synaptic formation and maintenance (Giannandrea et al., 2010). Rab3GAP, another direct regulator of presynaptic Rab proteins, specifically limits the amount of GTP bound to Rab3A. Mutations in Rab3GAP are found in Warburg-Micro syndrome, a recessive ID syndrome comprising microcephaly, eye anomalies, and hypogenitalism (Aligianis et al., 2005).

Recently, re-sequencing of a large number of X-linked ID patients has identified (Tarpey et al., 2009) new mutations in the gene coding for the synaptophysin protein. The replication of these mutations in cultured cells revealed that synaptophysin may control the retrieval of synaptobrevin during endocytosis of vesicles, suggesting that the recycling of vesicles could be perturbed in certain forms of ID (Gordon and Cousin, 2013). Mutations in OPHN1 protein are directly linked to the development of ID in humans. OPHN1 encodes a synaptic Rho-GAP protein that is expressed throughout the brain and the protein product is present in axons, dendrites and spines, pointing to a role of the protein at both the presynaptic and postsynaptic site. At the presynaptic site, OPHN1 was shown to interact with endophilin A1, a protein involved in recruiting other protein to mediate membrane curvature during endocytosis. Following shRNA-mediated knockdown of OPHN1, there was a reduction in the endocytosis of presynaptic synaptic vesicles in cortical neurons (Nakano-Kobayashi et al., 2009). This suggests that presynaptic recycling of vesicles might contribute to the pathogenesis of ID. Recently, absence of *Rsk*2 (*Rsk2* encodes a serine/threonine kinase called ribosomal S6 serine/threonine kinase) was shown to impair neurite outgrowth in cultured cortical cells, possibly through the activation of PLD1. PLD1 is a phospholipase protein involved in the hydrolysis of membrane lipids and its activation by RSK2 is thought to have a regulatory role in vesicular fusion at the active zone (Ammar et al., 2013).

In conclusion, several mechanisms can be disrupted following mutations in presynaptic proteins: docking and fusion of the vesicle with presynaptic plasma membrane, calcium-mediated release, recycling of vesicles after release of their neurotransmitter content... In line with this, some mouse models of ID present some electrophysiological properties that can be explained by alteration in presynaptic function. For example, *Ophn1* KO mice have a reduction in paired pulse facilitation in CA1 region of hippocampus (Khelfaoui et al., 2007). However, the pathophysiological consequences of ID pathophysiology at the presynaptic site remain largely unexplored. This can probably be explained by the fact that a lot of mutations of presynaptic proteins are lethal in mice (Atasoy et al., 2007) limiting the study of ID-related genes to proteins that are not absolutely essential for synaptic function but that would be regulating this essential process in more subtle ways.

1.3.2.2 Postsynaptic function

As stated earlier, the postsynaptic compartment can be distinguished either by the anatomical location of the contact (dendrite, soma, and axon) or the identity of the postsynaptic cell (excitatory or inhibitory). This potentially leads to an array of synaptic subtypes in the brain which could be differentially impacted by ID gene mutations. Indeed, most attention regarding the synaptic role of ID-related proteins has been on the study of excitatory transmission, although deficits in inhibitory GABA transmission have also been implicated in ID and ASD (Deidda et al., 2014). However, at excitatory and inhibitory synapses, the identity of the postsynaptic cell has been neglected in most physiological studies. Thus, increasing our knowledge of ID pathology would probably profit from an approach were the study of pathological consequences wouldn't be limited to excitatory transmission as this likely doesn't reflect the complexity of mechanisms leading to disease. Instead, the consequences of protein absence should be studied at all postsynaptic compartments and on the different cellular types that compose a circuit. Nonetheless, as a large majority of postsynaptic sites contacted by glutamatergic synapses are dendritic spines and the next paragraph will use this synapse as an example to explain the functioning and the elements that compose the postsynaptic site.

Dendritic spines are tiny protrusions composed of a spine head that is anchored to the dendritic shaft through a thin neck. Most importantly, they are supposed to be the anatomical proxies for synaptic plasticity mechanisms and memory storage. Indeed, dendritic spines may experience structural changes in response to synaptic plasticity protocols, with stimuli that induce long-term potentiation (LTP) causing spine growth (Matsuzaki et al., 2004; De Roo et al., 2008) and stimuli that induce long-term depression (LTD) causing spine shrinkage (Zhou et al., 2004). Both spine head enlargement and shrinkage are mediated by NMDA receptors. Interestingly, spines are continuously generated and eliminated in the naïve adult cortex. This phenomenon may be enhanced by learning or sensory experience, indicating that morphological changes of spines are activity-dependent and highly dynamic (Holtmaat and Svoboda, 2009). Dendritic spines are therefore thought to be central to the brain's capacity to change its connectivity, increasing the dendrites ability to connect with axons that are not in direct contact with the dendritic shaft. Thus, connections are continuously remodeled in the adult brain and this underlies cognitive fitness.

The head of the dendritic spine contains an electron-dense zone called the postsynaptic density (PSD) containing the postsynaptic receptors that bind released neurotransmitters, but also a large amount of proteins regulating dendritic spine morphology and function (Nair et al., 2013). The two main types of ionotropic glutamate receptors are AMPA and NMDA receptors. AMPARs are heterotetramers that are usually formed of two different subunits. The different subunits are GluR1, GLuR2, GluR3 and GluR4. Most receptors in the CNS are GluR1/R2 or GluR2/R3 receptors. The glutamate-mediated transmission of AMPA receptors is influenced by their subunit composition, post-transcriptional and post-traductional mechanisms, the number of AMPA receptors at the membrane and their interactions with auxiliary proteins. NMDA receptors are heterotetramer combinations of GluN1, GLuN2 (GluN2A, B, C and D) and GluN3 subunits. Functional receptors are composed of two GluN1 subunits and a combination of GluN2 and/or GluN3 subunits. AMPA receptors mediate fast excitatory neurotransmission (they are permeable to Na^+ and K^+ ions) in the brain and their number on the surface of the dendritic spine determines synaptic strength. They also play a key role in synaptic plasticity, as this mechanism often involves the trafficking and insertion of new receptors in the postsynaptic

membrane (Fanselow and Poulos, 2005). NMDA receptors also play a key role in synaptic plasticity by mediating calcium entry in the postsynaptic compartment, but only after the relief of the Mg^{2+}-block following initial depolarization of the membrane by AMPA receptors (see synaptic plasticity paragraph). Interestingly, principal cells and interneurons have differences in the subunit composition of AMPA and NMDA receptors at their glutamatergic synapses, leading to differences in synaptic function and plasticity mechanisms in these two cell populations (Spampanato et al., 2011).

AMPA and NMDA receptors are anchored to the underlying PSD by a variety of interactions with scaffolding proteins allowing them to be positioned directly above their signaling machinery and the actin cytoskeleton (Figure 7). The actin cytoskeleton is a key player in the general morphology of dendritic spines (Bosch and Hayashi, 2012; Sala and Segal, 2014). MAGUK (membrane-associated guanylate kinases) and other PDZ-containing domain proteins have a major role in scaffolding the PSD and in the trafficking of ion channels and postsynaptic receptors. Indeed, AMPA and NMDA receptors are continuously travelling in and out of the membrane by exo-and endocytosis events that occur at extrasynaptic sites but also by lateral diffusion in the plasma membrane (Choquet and Triller, 2013). Among the large family of scaffold proteins, PSD-95 and SAP-102 associate to NMDA receptors and other major PSD proteins, such as HOMER, calmodulin-dependent protein kinase II (CAMKII), guanylate kinase-associated protein (GKAP) and several SH3 and multiple ankyrin repeat domain proteins (SHANKs) (Figure 7). HOMER and SHANK are very abundant in the PSD and form a polymeric network structure serving as an assembly platform for other PSD proteins (Sheng and Kim, 2011). GKAP is involved in linking PSD-95 and NMDA receptors to underlying HOMER and SHANK complexes (Shin et al., 2012). Dynamics of AMPA receptors also dependent on several interactions with scaffold proteins (Anggono and Huganir, 2012). For example, interaction of GluR1 subunit with SAP-97 underlies dynamics of AMPA receptors (Waites et al., 2009). GRIP (AMPA binding proteins) proteins are involved in the dynamics of GluR2/R3 AMPA receptors at the synapse (Dong et al., 1997). In addition, several post traductional modifications are involved in the regulation of AMPARs dynamics. Phosphorylation of GluR1 subunit by PKA leads to an increase of the delivery of AMPARs to the plasma membrane (Esteban et al., 2003).

Interestingly, NMDA receptors are also the target of post traductional modifications like phosphorylation (Murphy et al., 2014). Thus, the dynamics of AMPA and NMDA receptors involve a large wealth of interactions with scaffold proteins but also post-traductional modifications that are under dependence of neuronal activity.

Unlike excitatory synapses, inhibitory synapses are characterized by the presence of postsynaptic $GABA_A$, $GABA_B$ receptors and glycine receptors and are formed on dendritic shafts or near the cell body. Interestingly, recent evidence suggests that GABARs could also be present on some dendritic spines (Gambino and Holtmaat, 2012). $GABA_A$ receptors are ionotropic and hyperpolarize the postsynaptic site by entry of Cl^- ions while $GABA_B$ receptors are metabotropic and exert their effects at both the pre-and postsynaptic site (Pinard et al., 2010). Presynaptically, activation of $GABA_B$ receptors regulates calcium channels and neurotransmission while postsynaptically they regulate mainly the activity of inwardly-rectifying K^+-channels leading to hyperpolarization. The PSD of inhibitory synapses appears fainter on electron microscopy, suggesting that the postsynaptic specialization is less elaborate than for excitatory synapses. $GABA_A$ and glycine receptors interact with gephyrin, a well-known postsynaptic scaffold of inhibitory synapses (Tyagarajan and Fritschy, 2014). A lot of binding partners of gephyrin have been identified, allowing close apposition with the actin cytoskeleton and thus regulation of the morphology of the postsynaptic site. For example, gephyrin has been shown to interact with proteins such as profilin and Mena/VASP, linking postsynaptic GABARs with the actin cytoskeleton (Tyagarajan and Fritschy, 2014). Thus, various scaffold proteins in the PSD of inhibitory and excitatory synapses underlie the close apposition of postsynaptic receptors with the actin cytoskeleton.

Remarkably, a high number of genetic abnormalities associated with cognitive disorders have been identified in proteins regulating the organization of the PSD. Mutations in AMPA subunit GluR3 and in NMDA subunits NR2A and NR2B are associated with ID and epilepsy (Endele et al., 2010; Wu et al., 2007). SHANK2 and SHANK3 mutations cause ID and autism in humans (Berkel et al., 2012; Durand et al., 2012). In addition, mutations in SAP-102 have been found in ID patients (Tarpey et al., 2004). At the postsynaptic site, OPHN1 has been shown to control synapse maturation and plasticity by stabilizing AMPA receptors (Nadif Kasri et al., 2009). This

effect is activity dependent and thought to be mediated by local changes in RhoA signaling, a major downstream target of OPHN1 implicated in the dynamics of the actin cytoskeleton (Khelfaoui et al., 2007). In addition, OPHN1 has been shown to be important for the endocytosis of AMPA receptors by interacting with endophilin A2/3 and reducing internalized AMPA receptors (Nadif Kasri et al., 2011). Recently, L Van Aelst group has reported a role of the interaction of OPHN1 with homer 1b/c in the positioning of the endocytic zone and the regulation of internalization of AMPA receptors (Nakano-Kobayashi et al., 2014). Disruption of this pathway leads to deficits in synaptic maturation and plasticity.

In conclusion, mutations in several proteins regulating the stability and organization of the PSD are found to cause ID and/or ASD, suggesting that some changes in the morphology of dendritic spines in ID patient's brains could be linked to a disruption of the mechanisms regulating the organization of the postsynaptic site. Noteworthy, morphological remodeling of the dendritic spines is not only limited to the initial formation of synapses. Instead, spines are believed to be highly dynamic throughout life, a process which has been shown to depend on activity and/or experience (Holtmaat and Svoboda, 2009). This suggests that mutations in ID-related genes could also potentially disrupt activity-dependent remodeling and dendritic spine turnover throughout life.

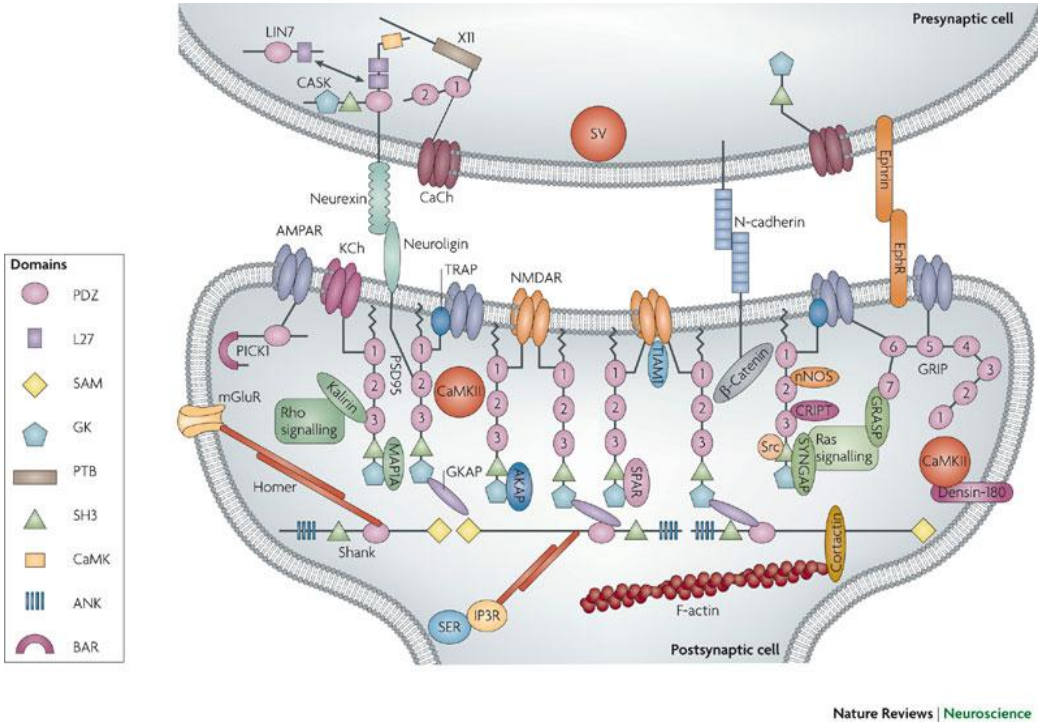

Figure 7: Scheme representing major partners in the organization of the post synaptic density (PSD) of an excitatory synapse. Some proteins are depicted with their functional domains, other by simple shapes. The PSD is composed of postsynaptic receptors (AMPA and NMDA mainly), but also ion channels. The scaffold proteins PSD-95, Shank family and Homer family are very abundant in the PSD. Shank and PSD-95 are bridged by the GKAP protein. Shank-family scaffolds are linked to the actin cytoskeleton by adaptor proteins. The presynaptic and postsynaptic membranes are connected by cell-adhesion molecules (neurexin/neuroligin; N-caherins; Ephrin and EphR…). Are also represented some cell signaling proteins that interact with PSD proteins. From Feng and Zhang 2009

1.3.3 Brain development and ID

The human brain is an amazingly complex organ composed of trillions of neurons. During development, connections are made creating highly complex neuronal networks that will underlie future cognitive and learning abilities. The biological mechanisms leading to the development and formation of brain circuitry are highly regulated. Development of the brain starts during embryogenesis and continues throughout early life with the formation of synaptic contacts. Indeed, embryogenesis is characterized by the production of new neurons (neurogenesis) and their migration to their final location while the formation of new synapses is specific to post-natal stages. Obviously mutations in genes that regulate neurogenesis and the

migration of neurons have profound consequences on normal brain anatomy and patients usually exhibit severe forms of ID with strong morphological abnormalities (Chelly et al., 2006; Vaillend et al., 2008).

Neurogenesis is achieved by the cooperative action of several gene products that encode mitotic proteins mediating neuronal proliferation but also transcriptional regulators controlling cell cycle division. For example, microcephaly involves at least four genes: microcephalin (MCPH1), Abnormal spindle-like microcephaly-associated protein (ASPM), cyclin-dependent kinase 5 regulatory associated protein 2 (CDK5RAP2) and centromere-associated protein J (CENPJ) (Vaillend et al., 2008). All of them contribute to neuron generation by controlling cell cycle and thus ultimately brain size. Another important function that can be affected in ID is neuronal migration, a process where newly produced neurons migrate to their final location. Abnormalities in neuronal migration often arise from mutations in microtubule-associated proteins or in proteins mediating interactions between the cytoskeleton, membrane and extracellular matrix (Vaillend et al., 2008).

As we decided to focus on a non-syndromic form of ID, I will not further discuss these early phases of brain development which are thought to be unaltered in *Il1rapl1* patients (see below). While production and migration of neurons is mostly prenatal, postnatal development is characterized by the formation of new synapses. This is a particularly important phase in brain development, especially when one keeps in mind the large heterogeneity of synapses underlying integration of neuronal information (see synaptic integration). Thus, during postnatal development, the brain could be particularly sensitive ("critical period") to mutations in genes mediating synaptogenesis, leading to irreversible deficits in normal brain wiring (Kroon et al., 2013). This suggests that a lot of cognitive dysfunctions associated with ID could originate in deficits that occur during synaptogenesis.

1.3.3.1 Synaptogenesis

The formation of synapses in vertebrates spans from embryogenesis to early postnatal life. However, recent reports show that synapses can also appear (or disappear) during adult life and some reports suggested that ID-related genes could perturb the formation of synapses at

different phases in life including adulthood (Isshiki et al., 2014). Synaptogenesis refers to all processes involved in the formation of synapses. This includes cell-cell contact, differentiation of nascent pre- and postsynaptic terminals, development of morphological specializations and ultimately the organization of mature synaptic inputs (Figure 8).

Initially, when neurons differentiate, they extend axonal and dendritic processes and expression of synaptic proteins is turned on. This results in the formation, accumulation and directional trafficking of vesicles carrying pre-and postsynaptic protein complexes (Waites et al., 2005). During this time, axons and dendrites make transient contacts, a mechanism involving a large diversity of secreted factors, receptors and signaling molecules that make neurons receptive to form synapses. This is also facilitated by sets of cell surface adhesion molecules (CAMs), a large family of transmembrane proteins expressed at both the pre-and postsynaptic site that interact in a pair wise fashion across the synaptic cleft (Dalva et al., 2007) (Figure 8). Several sub groups of CAMs have been discovered: N-cadherins, neurexin/neuroligin, Ephrin receptors and their ligands, IgCAMs (immunoglobulin cell adhesion molecules)… CAMs are involved in cell-cell recognition and induce signals that trigger the initial stages of synapse formation, leading to the formation of pre-and postsynaptic specializations. Indeed, during this phase, there is an accumulation/delivery of both pre-and postsynaptic components at the synapse. At the pre-synapse this is characterized by accumulation of presynaptic scaffold proteins like Piccolo, Bassoon or Rab3. At the post-synapse, there is a gradual increase of PSD-95 levels and other scaffold proteins like Shank or Homer family of proteins. In addition to the clear role of CAMs in synaptogenesis, it has also been shown that CAMs are important in mature synapses (Thalhammer and Cingolani, 2014), regulating synaptic function and/or modulating synaptic plasticity (Figure 8).

Genetic abnormalities or mutations in proteins that regulate synaptogenesis can have profound effects on mental health. This is well illustrated by the neurexin/neuroligin adhesion couple proteins, as mutations in both neuroligin3 and neuroligin4 have been associated with ID and ASD (Jamain et al., 2003). Neurexins are specific to the presynaptic site and recognize postsynaptic neuroligins (Sudhof, 2008). They have been shown to be important in synaptic differentiation and specifically in the specification of excitatory versus inhibitory synapses (Craig

and Kang, 2007). Indeed, synaptic specificity seems to result from the action of specific splice variants of neurexin and neuroligin that are specifically involved in the formation of excitatory and inhibitory synapses (Graf et al., 2004). Interestingly, other CAM proteins are specific to excitatory or inhibitory synapses, showing the strong heterogeneity in mechanisms mediating synapse specification. The specification of excitatory vs. inhibitory synapses is particularly important because proper brain function requires the integration of excitatory and inhibitory inputs at the level of individual neurons but also at the level of neural circuits (Xue et al., 2014). Thus, it has been proposed that diseases like ID and autism could be considered as "critical period diseases", the mutations in several genes associated with ID/ASD (for example neuroligins/neurexins) possibly affecting the early inhibition-excitation balance necessary for development of brain areas related to sensory coding, motor learning or cognition (Fernandez and Garner, 2007).

Several animal models of ID have been shown to have I/E imbalances in the brain. For example, in Mecp2 mutant mice there is a shift of the balance towards inhibition due to a specific impact of the mutation on miniature excitatory currents (mEPSCs), leaving miniature inhibitory currents intact (Dani et al., 2005). Interestingly, Shank3 mutant mice also show a reduction of excitation at cortico-striatal synapses (Peca et al., 2011), although inhibition wasn't specifically addressed. In a mouse model of Down Syndrome, the Ts65Dn mouse, there is an increased inhibition due to a specific decrease of excitatory synapses. Interestingly, lowering inhibitory load with an $GABA_A$ antagonist was able to restore cognitive function and LTP in hippocampus (Fernandez et al., 2007). In contrary, inhibition/excitation balance can also be shifted to higher excitation, which also affects information processing in the brain (Yizhar et al., 2011).

In conclusion, ID pathophysiological studies demonstrated that mutations in genes that mediate or regulate synaptogenesis have deleterious consequences in adult brain function. Furthermore, the impact of the mutations at adult synapses may depend on the anatomical location and intrinsic nature of the neurons. In this line, the consequences of mutations in ID-related genes in synaptogenesis could be limited to certain synaptic types, cells or even particular periods throughout life were synapses appear and/or disappear. For example, the initial formation in

early life could be disrupted while the activity-dependent remodeling and formation of synapses might be preserved.

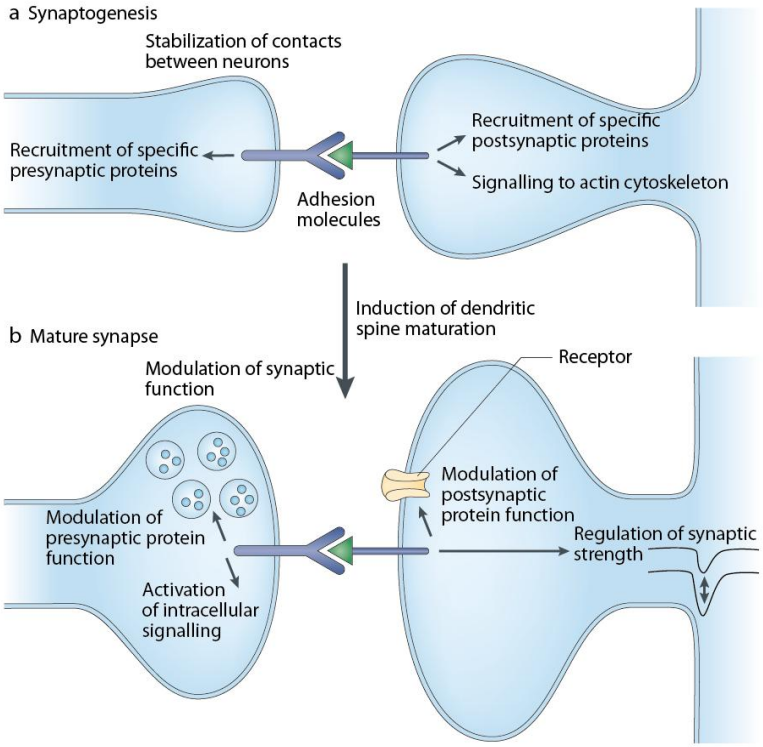

Figure 8: Scheme representing the importance of cell adhesion molecules at the synapse. a: During synaptogenesis, synaptic adhesion molecules stabilize the initial contact between axons and dendrites by transsynaptic interactions. Their binding leads to clustering and recruitment of specific pre-and postsynaptic proteins via specific binding domains. Interactions between adhesion molecules can also lead to the activation of signaling pathways involved in dendritic spine maturation and morphology (e.g. actin cytoskeleton). b: In the mature synapse, synaptic adhesion molecules can modulate synaptic function, either by interacting with synaptic proteins or by the activation of signaling pathways. From Dalva et al. 2007

1.4 Animal models of ID

The technological advances in genetics and molecular biology have allowed creating animal models of IDs, reproducing the genetic mutations observed in human patients. The most widely used laboratory species are undoubtedly rodents. Due to the relative phylogenetic proximity with other mammals, they provide insights linking specific genes to high cognitive functions and are the most amenable to genetic manipulations. However, to consider a genetically manipulated mouse as being a valid model for human disease, three criteria have to be met (Banerjee et al., 2014). First, the etiology of the disorder has to be similar between the animal

model and the disorder in humans (same genetic mutation…). Second, the symptoms in the animal model have to share similar behavioral and physical outputs to the human disorder. It becomes clear that appropriate phenotyping, including behavioral characterization is critical. Ideally, the testing of a genetically modified mouse is realized by subjecting them to a battery of behavioral tests that assess motor and sensory, as well as cognitive functions. Finally, the predictive validity indicates a similar response in the mouse model to an intervention that is known to be effective in human patients with the disorder. This last criterion is very difficult to achieve as there are currently very few treatments available in humans to treat these disorders (Delorme et al., 2013). Thus, the best animal model would be one where the etiology and the symptoms share common features with the human disease. Eventually, this would allow unveiling the pathophysiological mechanisms of the disease and opening the possibility to develop therapeutic interventions that could eventually be used in human patients.

Several mouse models of ID and ASD have already been created and replicate some of the symptoms observed in humans with syndromic ID. For example, knockout mice for *Mecp2* reproduce the motor and social interaction deficits observed in humans affected by Rett syndrome (Moretti et al., 2006) as well as social and feeding behavior (Fyffe et al., 2008). Knockout mice for SHANK3 exhibit deficits in social interaction, a recurrent trait of ID (Peca et al., 2011). *Fmr1* mutant mice also display deficits in social behavior, as well as motor deficits and synaptic dysfunctions (Ronesi et al., 2012). Moreover, these mice also replicate some morphological deficits like macro-orchidy.

1.5 Towards ID therapeutics?

IDs and ASD are highly heterogeneous diseases with different etiologies, phenotypic outcomes and ages of onset. The first cognitive disabilities associated with ID are often detected after the critical time periods where the brain is subject to plasticity and is particularly sensitive to mutations of specific genes. Thus, for a long time, ID and ASD have been considered as neurodevelopmental disorders with irreversible cognitive deficits. However, an increasing number of studies in mouse models of ASD have shown that certain neuronal defects can be reversed in the mature mouse brain (Delorme et al., 2013), and that certain phenotypical

characteristics can be improved. Moreover, many ID-related proteins converge on similar molecular and signaling pathways, suggesting that some treatments could alleviate symptoms associated with different genetic causes (Pavlowsky et al., 2012).

Different "correcting" strategies have been undertaken, ranging from genetic manipulation and cellular therapeutics, to pharmacological treatments or environmental stimulation. Most studies investigating the possibility of treating mouse models of ASD or ID have been performed on two most highly occurring monogenic syndromes: fragile X syndrome and Rett syndrome. Patients suffering from Fragile X present genetic abnormalities in the *FMR1* gene coding for the FMRP protein, which acts as a RNA-binding protein allowing local regulation of translation (Darnell and Klann, 2013). Thus, when translational control is lost illegitimate translation occurs in the absence of stimuli (Maurin et al., 2014). Expression of a human form of *FMR1* gene in *Fmr1* KO mice restored social behavior and sensory gating (Paylor et al., 2008; Spencer et al., 2008). Pharmacological treatments aiming at counteracting the excessive mGluR5 signaling following FMR1 removal were also ameliorating certain cognitive features in FMR1 KO mice (Michalon et al., 2012; Yan et al., 2005).

Rett syndrome is caused by a de novo mutation in the *MECP2* gene coding for the methyl-CpG-binding protein which acts as a transcriptional modulator. In *Mecp2* mutated mice, reactivation of the gene by Cre-lox technology allowed improving morphological defects in the motor cortex and led to a marked improvement in respiratory and sensorimotor functions (Guy et al., 2007). Moreover, a pharmacological treatment aiming at restoring functional plasticity during development in *Mecp2* mutant mice was able to alleviate certain symptoms and synaptic functioning (Tropea et al., 2009). Mice that are mutated for *Shank2* present NMDA receptor hypofunction and pharmacological treatments aiming at correcting this deficit was able to restore social interactions and AMPA/NMDA ratio, but had globally no effect on social recognition (Won et al., 2012).

In conclusion, correcting or curing ID requires a fine understanding of the cellular and synaptic dysfunctions caused by the absence of a certain protein, including the compensatory mechanisms that have been activated by the loss of function of the gene product. Given the

high heterogeneity in phenotypic outcomes in ID it is probably optimistic to think that therapeutic strategies in adults would have some effects on all aspects of the disease. However, improving some core symptoms of the disease like sensory and motor deficits would definitely improve the life quality of patients.

2 A model of intellectual disability: mutations in the *Il1rapl1* gene

As stated above, animal models are crucial to improve our understanding of the pathophysiology of ID as they allow us to use "invasive" methods that can't be applied on human patients, but which are mandatory to study the link between synaptic function and cognition. During my PhD thesis, I focused on a knock out mouse for the IL1RAPL1 protein (see material and methods). In humans, a similar loss of function has been recurrently associated with ID or ASD (Carrié et al., 1999; Piton et al., 2008). Although previous findings of our team and others suggested a role of IL1RAPL1 in synaptic function, its precise integrated function remained largely unexplored when I started my project. Next paragraphs will review the current knowledge on IL1RAPL1 in brain function and disease.

2.1 Structure of IL1RAPL1

In humans, the *IL1RAPL1* gene is composed by 11 exons and is located on the p arm of X chromosome. It encodes a transmembrane protein of 696 amino acids called Interleukin-1 Receptor Accessory Protein Like-1 (IL1RAPL1). IL1RAPL1 shows strong homology with interleukin-1 receptor accessory protein (IL1RaP) family, except for the C-terminal 150 amino acid domain, which is present only in IL1RAPL1. This led to the idea that IL1RAPL1 could have a role in the mediation of the immune response (Carrié et al., 1999). However, IL1RAPL1 does not seem to be involved in interleukin-1 (IL-1) pathway (Bahi, 2003; Born et al., 2000), although the activation of a IL-1-mediated signaling cascade through IL1RAPL1 has been reported previously (Pavlowsky et al., 2010a). Altogether, this suggests that IL1RAPL1 could function as a new class of receptors within this family.

Structurally, IL1RAPL1 protein contains an extracellular domain with three extracellular immunoglobulin-like (Ig) motifs, an intracellular Toll/Il-1 Receptor (TIR) domain and a specific 150 amino acids extension at C-terminal (CT domain) (Figure 9 and 10). In situ hybridization revealed a ubiquitous low level expression in the fetal and adult brain (Carrié et al., 1999). Overall, the highest expression of *Il1rapl1* transcripts was observed in brain structures that correspond to the primary olfactory cortex, entorhinal cortex, hippocampus including the

dentate gyrus, perirhinal and occipito-parietal cortices. These brain areas are known to be involved in learning and memory processes, suggesting a role of IL1RAPL1 in cognitive features. In cultured cells, IL1RAPL1 protein can localize to both pre-and postsynaptic compartments (Pavlowsky et al., 2010b; Valnegri et al., 2011; Yoshida et al., 2011) suggesting that IL1RAPL1 could exert its role at both sites. However, the exact localization of IL1RAPL1 *in vivo* remains controversial and the lack of specific antibodies haven't helped in this matter.

2.2 *IL1RAPL1* and ID in humans

The first report of the involvement of *IL1RAPL1* in the pathology of ID dates back to 1999, when microdeletions were discovered in the coding region of *IL1RAPL1* in multiple patients (Carrié et al., 1999). For most patients, these microdeletions span exons 3-7, leading to the absence of the protein and the development of ID (Figure 9). In the same report, another patient was shown to have a nonsense mutation in exon 11 leading to a premature STOP codon and a protein lacking half of the TIR domain and the entire C-terminal domain. Similarly, the fine analysis of a family with ID revealed the presence of a point mutation leading to a truncated IL1RAPL1 protein lacking half of the TIR domain and the entire CT domain (Tabolacci et al., 2006). Interestingly, it was shown that point mutations and intragenic deletions of *Il1rapl1* are associated with the development of autism spectrum disorder (ASD) (Piton et al., 2008). Globally, however, most of *IL1RAPL1*-deficient patients are only diagnosed with ID and it remains difficult to link the loss of particular IL1RAPL1 domains with disease severity.

Several other reports have shown intragenic deletions in the parts coding for the extracellular Ig-like domains (Behnecke et al., 2011; Whibley et al., 2010) or spanning the Ig-like domains until the CT domain (Youngs et al., 2012). All these deletions lead to ID in concerned patients. Interestingly, most affected patients are males, as the gene is located on the X chromosome. Originally, patients with genetic abnormalities in the *IL1RAPL1* gene were considered as non-syndromic. However, several patients also present some morphological deficits (facial abnormalities, body size…), but show global normal brain morphology. How mutations in *Il1rapl1* lead to inter-individual variability remains unknown. One possibility is the influence of environmental factors; another is the location where the mutation occurred, disrupting certain

interactions of IL1RAPL1 with other partners and leaving others unaltered. Surely, research would benefit from studies that would link the presence of a particular mutation with the disruption of specific signaling pathways that underlie synaptic function. Eventually this could allow developing personalized treatments to improve life quality or at least some core symptoms of the disease in ID patients.

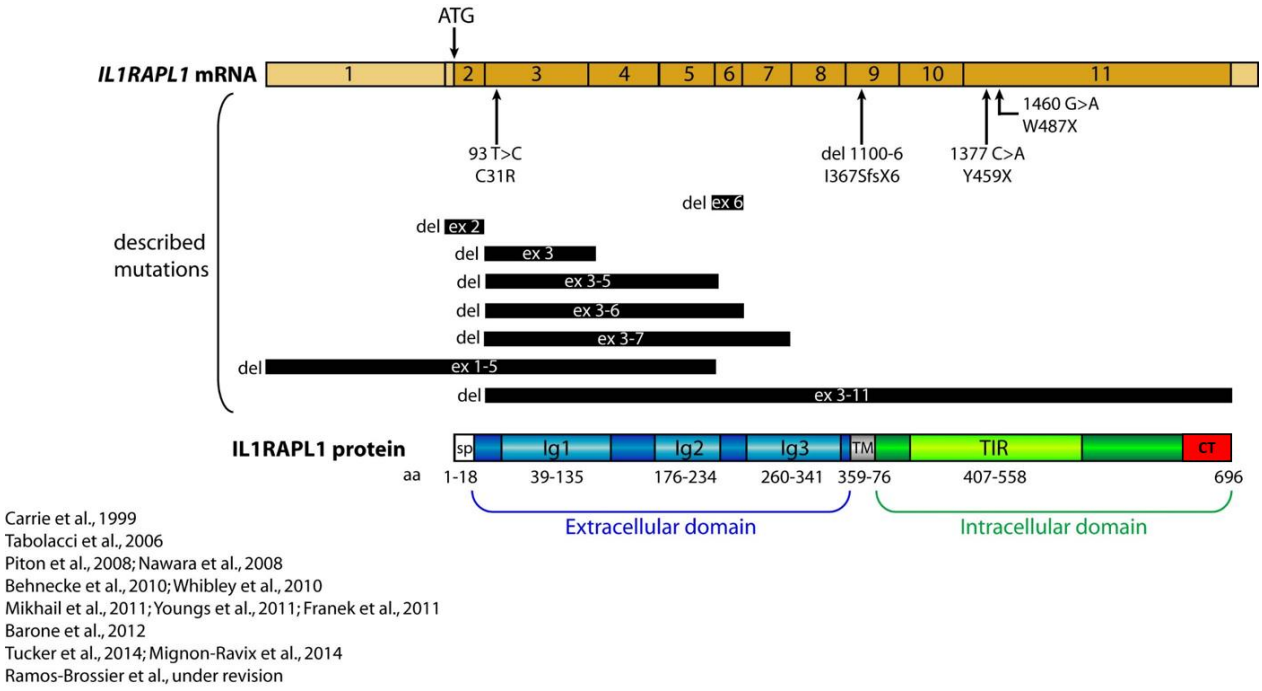

Figure 9: Scheme representing *Il1rapl1* mRNA (11 exons) and the associated protein sequence with the main functional domains. Some mutations are point mutations, leading to the substitution of a single base and the traduction of incomplete proteins. Others lead to deletions of larger fragments that can encompass one or several exons and lead to the complete absence of the protein. Most mutations are located within the first exons that code for the extracellular Ig-like domains. Adapted from M. Ramos

2.3 Biological role of IL1RAPL1

Most experimental data on IL1RAPL1 function has been obtained from cultured cell models and suggest that IL1RAPL1 is enriched at the synapse. Its synaptic functions have been shown to depend on several protein/protein interactions between specific domains of IL1RAPL1 and its binding partners leading to the activation of distinct signaling. The next paragraphs review all

current knowledge about the possible role of IL1RAPL1 at the synapse and, for the sake of clarity, have been separated according to the anatomical organization of the synapse.

2.3.1 Presynaptic

Using a yeast two-hybrid screening it was shown that IL1RAPL1 interacts with the neuronal calcium sensor-1 (NCS-1) protein trough the CT domain (Bahi, 2003) (Figure 10). This interaction was also confirmed in non-neuronal mammalian cells. NCS-1 belongs to a large Ca^{2+}-binding protein family implicated in the regulation of Ca2+-dependent exocytosis and in the modulation of Ca2+ channels trafficking and activity (Burgoyne, 2007). An overexpression experiment of IL1RAPL1 in PC-12 cells revealed a negative effect on an exocytosis assay. Using PC-12 cells again, it was shown that NCS-1/IL1RAPL1 interaction is important for the regulation of N-type voltage-gated calcium channel activity (Gambino et al., 2007). These channels are important for regulation of neurotransmitter release at the presynaptic terminal, proving that IL1RAPL1-NCS-1 interaction could be important to regulate this process. On top of this, IL1RAPL1 lowered Nerve Growth factor (NGF)-mediated neurite elongation in PC-12 cells, an effect that depended on functional NCS-1/IL1RAPL1 interaction.

Using an olfactory sensory neuron-specific gene manipulation system in combination with *in vivo* imaging of transparent zebrafish embryos, the group of Mishina has shown the role of the zebrafish orthologue of human IL1RAPL1, IL1RAPL1b, in presynaptic differentiation of olfactory sensory neurons looking at both synaptic vesicle accumulation and subsequent morphological remodeling (Yoshida and Mishina, 2008). Interestingly, these two processes appeared to be mediated by distinct domains, namely the CT and TIR domain respectively.

Taken together, these papers suggest that, presynaptically, IL1RAPL1 could be involved in both synaptic activity and/or building-up in the nervous system. Noteworthy, these effects were mediated by the CT and/or the TIR domain of IL1RAPL1, pointing their crucial role in these biological processes. Nonetheless, caution should be taken in the interpretation of these results as the precise localization of endogenous IL1RAPL1 at the presynaptic site is still not clear and presynaptic effects could merely be the result of post- and/or transsynaptic consequences of IL1RAPL1 absence.

2.3.2 Postsynaptic

Most of the work aiming at understanding IL1RAPL1 function has been realized at the postsynaptic site, because of its high enrichment at the PSD (Pavlowsky et al., 2010b). A yeast two-hybrid experiment conducted on human fetal c-DNA library revealed a specific interaction of IL1RAPL1 with PSD-95 through a noncanonical PDZ-binding motif (Pavlowsky et al., 2010b) (Figure 10). PSD-95 is a major component of excitatory postsynaptic compartment and serves as an anchoring protein for synaptic proteins. IL1RAPL1/PSD-95 interaction was confirmed using transfection in cultured cells and with co-immunoprecipitation experiments. As said above, in cultured hippocampal neurons, IL1RAPL1 colocalized with PSD-95 at postsynaptic excitatory dendritic spines. In addition, overexpression of IL1RAPL1 led to an increase of excitatory synapse number (seen by PSD-95 clusters) both *in vitro* and *in vivo*. Moreover, this was accompanied by an increase in the frequency of miniature EPSCs (mEPSCs), indicating that these synapses are functional. The increase in spine number was shown to be mediated by the CT domain of IL1RAPL1 which positively regulates c-Jun N-terminal kinase (JNK) signaling activity in neurons. JNK has been shown to phosphorylate PSD-95 in neurons, regulating its synaptic localization (Pavlowsky et al., 2010b). Loss of IL1RAPL1 led to a constitutive decrease of JNK activity, ultimately leading to lower phosphorylation of PSD-95 and its recruitment to the postsynaptic density. Finally, a lack of maintenance of theta-burst induced synaptic plasticity at SC-CA1 synapses was observed in *Il1rapl1* KO mice (Pavlowsky et al., 2010b). Together, these results suggest an involvement of IL1RAPL1 in promoting the formation or in the stabilization of excitatory synapses and in the correct function of these contacts. It remains to be studied how IL1RAPL1 can activate JNK, as no ligand has been characterized until now.

Recently, with the aim of further characterizing the partners of IL1RAPL1 important for the formation and maintenance of spines, a team has used affinity chromatography on mouse forebrain and could identify several new proteins (Hayashi et al., 2013). Amongst them, they identified MCF2L, which binds to IL1RAPL1 through the TIR domain (Figure 10). MCF2L is a Rho guanine nucleotide exchange factor (RhoGEF) that activates Rho-A and CDC42. Rho-A has been previously shown to control the cytoskeletal dynamics that induce structural change of excitatory spines and actin cytoskeletal dynamics are regulated by Rho-A dependent activation

of ROCK (Govek et al., 2005). This suggests that IL1RAPL1 could control dendritic spine formation though MCF2L/RhoA/ROCK pathway. Indeed, treatment with a shRNA against *Mcf2l* or treatment with a ROCK inhibitor was able to reduce IL1RAPL1-induced increase of dendritic protrusions (Hayashi et al., 2013). In addition they showed that overexpression of IL1RAPL1 increased the replacement of GluA1-containing AMPA receptors with GluA2/A3-containing ones at newly formed spines. This effect was shown to be dependent on MCF2L/RhoA/ROCK signaling pathway, providing the first evidence that IL1RAPL1 could control glutamate receptor dynamics. Other proteins were also shown to interact with the intracellular domain of IL1RAPL1: PKCε with the TIR domain and PLCβ1, SNIP, RASAL1 with the CT domain. However, this paper didn't focus on the role of these protein/protein interactions, suggesting that additional signaling pathways besides MCF2L/RhoA/ROCK could coexist. Noteworthy, PSD-95 and RhoGAP2 were not identified with their affinity chromatography, probably because of different experimental conditions.

2.3.3 Transsynaptic

Recently, two studies aimed at understanding how IL1RAPL1 regulates the formation of synaptic contacts and trough which domains of the protein (Valnegri et al., 2011; Yoshida et al., 2011). Valnegri et al. expressed two constructs in hippocampal neurons that mimic some mutations found in human patients. One construct lacked a part of the TIR domain and the full CT domain while the other one was missing a part of the extracellular Ig-like domains. Transfection experiments revealed that the extracellular domain is required to induce presynaptic formation although both the extracellular and intracellular domains are required for inducing dendritic spine formation. Yoshida et al. found similar results when expressing different IL1RAPL1 constructs in cortical neurons and were also able to show a reduction in this effect when expression of *Il1rapl1* was abolished by cellular expression of a specific shRNA. These results suggested the existence of a presynaptic partner through which postsynaptic IL1RAPL1 could induce presynaptic differentiation and that the intracellular domains act in concert to control the formation of the postsynaptic spines. Affinity chromatography between a tagged IL1RAPL1 protein and synaptosomal fraction of rat brains (Valnegri et al., 2011) or total mouse brain proteins (Yoshida et al., 2011) revealed an interaction between the extracellular domain of

IL1RAPL1 and a new unidentified partner: the protein tyrosine phosphatase delta (PTPδ) which is located at the presynaptic site and widely expressed in the mouse brain (Kwon et al., 2010). PTPδ is part of the LAR family of proteins which bind to netrin-G ligand-3 (NGL-3) (Woo et al., 2009) and induce pre- and postsynaptic differentiation in neurons. The interaction between IL1RAPL1 and PTPδ is very strong and is determined through their respective extracellular Ig-like domains, making this a transsynaptic interaction. Moreover, co-culture of transfected IL1RAPL1 cells with cortical neurons from PTPδ KO mice was unable to induce presynaptic differentiation, unambiguously showing the role of IL1RAPL1/PTPδ in this process (Yoshida et al., 2011). The role of this interaction was also proved *in vivo*, as infection of layer 2/3 cortical neurons with IL1RAPL1 protein lacking the Ig-like domains reduced spine density. Nonetheless, these results don't tell us what postsynaptic proteins and/or signaling cascades could be activated to mediate dendritic spine formation.

In order to identify which partners could interact with the intracellular domains of IL1RAPL1 and that might be required for dendritic spine formation, Valnegri and colleagues used a yeast two-hybrid system that could show that the C-terminal domain of IL1RAPL1 interacted with RhoGAP2, a novel RhoGTPase-activating protein II (Valnegri et al., 2011). Pull-down and co-immunoprecipitation experiments revealed that this interaction also depends on the TIR domain of IL1RAPL1, showing that the interaction between both proteins involves different parts of the C-terminal domain of IL1RAPL1. RhoGAP2 is expressed in cortex, hippocampus and cerebellum and its overexpression in neurons leads to the accumulation of different postsynaptic markers through Rho signaling pathway (Govek et al., 2005). Other overexpression experiments revealed that the interaction between IL1RAPL1 and PTPδ is necessary for recruitment of RhoGap2 to the synapse (Valnegri et al., 2011). In conclusion, IL1RAPL1 can be considered as a synaptogenic protein that promotes presynaptic differentiation and formation of excitatory spines through transsynaptic interactions, a mechanism that closely resembles the role of adhesion molecules (Sakisaka and Takai, 2005), some of them being closely related to ID and/or ASD (Sudhof, 2008).

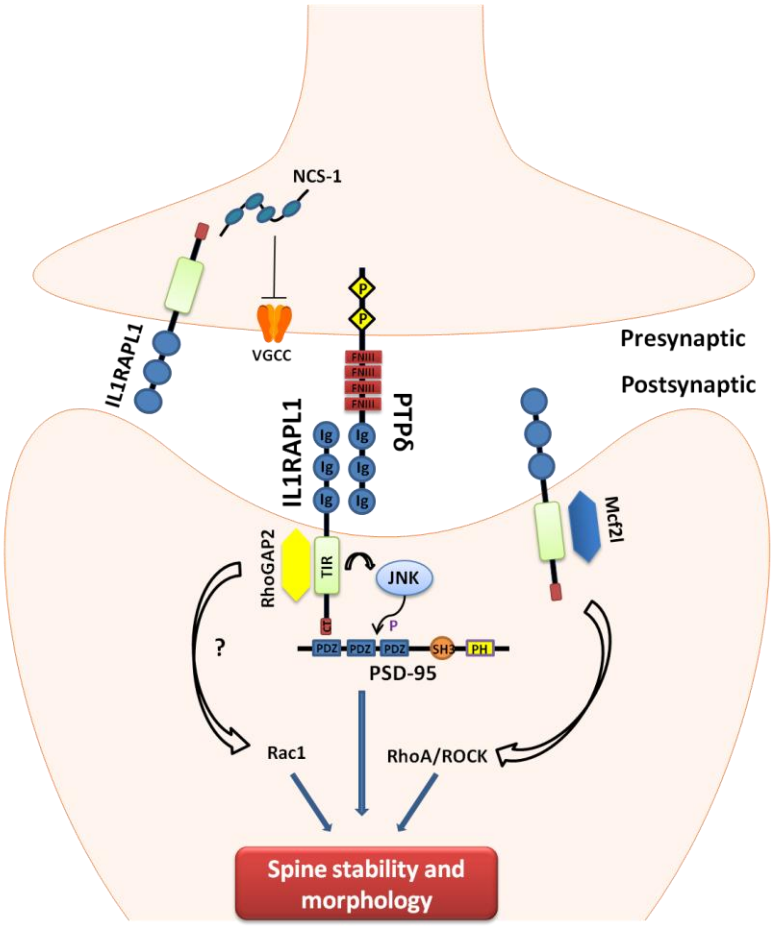

Figure 10: Scheme representing the proposed role of IL1RAPL1 at the synapse. Presynaptically, IL1RAPL1 interacts with the calcium sensor NCS-1, regulating the activity of N-type VGCCs. Postsynaptically, IL1RAPL1 interacts with RhoGAP2, possibly regulating Rac1 activity, a protein involved in cytoskeletal organization. RhoGAP2's interaction with IL1RAPL1 depends on the transsynaptic interaction between presynaptic PTPδ and postsynaptic IL1RAPL1. This interaction involves the Ig-like domains of both partners. At the postsynaptic level, IL1RAPL1 also interacts with PSD-95 and this interaction is possibly regulated through the regulation of JNK activity. Finally, postsynaptic IL1RAPL1 also interacts with MCF2L, leading to the regulation of RhoA/ROCK pathway, a signaling pathway regulating cytoskeletal organization.

2.3.4 *In vivo* role of IL1RAPL1

Neuronal cultures have unveiled a large amount of information on the role of IL1RAPL1 at the synapse and have allowed identifying several possible binding partners through which IL1RAPL1 could exert its function. However, studies on the *in vivo* consequences of IL1RAPL1 deficiency were still lacking when I started my PhD. Thus, there was an urge to understand what could be the precise function of IL1RAPL1 in the brain, and how its absence could lead to cognitive

deficits in ID patients. Although some small effects on spine density were noticed *in vivo*, the pathophysiological mechanisms underlying functional and behavioral impairments following *Il1rapl1* deletion remain poorly studied, especially in intact organisms.

Previous work from our lab has started addressing the role of IL1RAPL1 *ex vivo* by looking at the consequences of *Il1rapl1* deletion in cerebellum-containing brain slices of *Il1rapl1* KO mice (Gambino et al., 2009). Indeed, cerebellar abnormalities are often found in autistic patients (Carper, 2002). Following IL1RAPL1 removal there was a higher excitability of molecular layer interneurons (MLI) that control the activity of Purkinje cells in early development (P10-P12). The latter cells are large GABA-ergic cells that control the activity of deep cerebellar neurons (DCNs), the main output cells of the cerebellum. The higher inhibition received by Purkinje cells resulted in a disinhibition of DCN neurons. How exactly MLI neurons became more excitable is still unclear but doesn't seem to result from higher excitatory drive on MLIs.

Interestingly, this was the first paper to show a deregulation of I/E balance following IL1RAPL1 removal, an effect that was consecutive to the specific effect of the mutation on a particular cell type within a circuit. In line with this paper, I decided to further characterize *Il1rapl1* KO mice in order to make causal links between synaptic function and behavior by using the neural circuits of associative fear conditioning as a model.

3 Associative learning as a tool to measure cognition on an ID model

Cognition refers to all higher order mental processes like reasoning, memory, decision making and executive functions, but also more general processes like perception, motricity and emotions. Cognitive aspects are often disrupted in ID patients but the underlying pathophysiological mechanisms are not well understood. For obvious reasons, cognition is a quite difficult phenomenon to study in animals, as none of them show high order mental processes as they exist in humans. Nonetheless, simple behavioral paradigms have been developed that allow assessment of learning and memory processes in animals. A classical and robust form of learning that is often used in animal models is associative learning where animals memorize the co-occurrence of two events and was first developed by the researcher Pavlov.

Associative fear learning has been particularly useful in the last decades to unveil learning and memory mechanisms in rodents. Most importantly, the neural circuits as well as the cellular and synaptic mechanisms underlying associative fear are well characterized, making this an ideal model to link behavior with synaptic function. The previous expertise of our team in fear conditioning and associated synaptic mechanisms accelerated our choice to use this behavioral paradigm to characterize learning and memory in *Il1rapl1* KO mice.

3.1 Fear conditioning

Fear is a basic emotion present in all mammals and has a protective role, thus providing an evolutionary advantage. A lot of psychiatric illnesses are associated with dysregulations of the mechanisms regulating fear behavior, leading to anxiety disorders. The neuronal substrates of fear behavior and the cellular and molecular mechanisms governing them are starting to be well documented (Pape and Pare, 2010). During associative fear conditioning, animals learn to associate the presentation of a neutral sensory stimulus (conditioned stimulus or CS) with a coinciding aversive stimulus (unconditioned stimulus or US). Subsequent exposure to the CS alone after conditioning elicits a conditioned fear response (CR) with associated physiological autonomic components: increased heart rate and blood pressure, release of stress hormones, analgesia… During the conditioned fear response rodents adopt an immobile posture called

freezing. Freezing is easy to quantify with adapted devices and its duration reflects the strength of fear memory.

Cued fear conditioning is a behavioral protocol where the CS is a cue, typically a sound, which is associated with a mild foot shock, the US, to the paw of the animal. This type of learning is rapidly acquired, needs few associations and is long lasting. However, the US is also typically associated with the context in which it has been applied creating a contextual fear memory. A context is broadly defined as the set of circumstances around an event (Maren et al., 2013). This context is often composed of different sensory modalities and is continuously present during an experiment. Conditioned fear can also be decreased by a process called extinction (Herry et al., 2010). During extinction procedures, the subject is submitted multiple times with the previously conditioned CS alone, which typically leads to a progressive decline of the conditioned response. Importantly, extinction is believed to generate a new associative learning ("CS/safety") that doesn't completely erase the previous associative fear memory. Thus, fear and extinction co-exist and interact to regulate fear behavior.

3.2 Neuronal substrates

A tremendous amount of studies have attempted to define the neuronal substrates of fear and the mechanisms involved in the regulation of fear behavior. Those studies all point to the crucial role of the amygdala, a component of the limbic system and the main structure involved in emotional learning (McGaugh, 2004)(Berlau and McGaugh, 2006). Multiple reports indicate that the amygdala is involved in the formation, extinction and expression of associative fear memories (Herry et al., 2010; Pape and Pare, 2010). The amygdala has extensive connections with other brain structures allowing fine regulation of fear behavior. Among them, two actors emerge: the hippocampus and the medial prefrontal cortex (mPFC). The mPFC is known for its role in fear extinction and fear expression (Courtin et al., 2013) while the hippocampus regulates contextual aspects of fear memory (Maren et al., 2013). In the next chapters I decided to focus mainly on the amygdala and the hippocampus because of their involvement in cued fear conditioning and contextual fear conditioning, two learning tasks that I characterized in *Il1rapl1* KO mice.

3.2.1 The amygdala

3.2.1.1 General anatomy and connectivity

The amygdala is located in the anterior portion of the temporal lobe and is comprised of different nuclei that can be separated upon their cellular composition or connectivity (Pape and Pare, 2010) (Figure 11). These nuclei mainly include the lateral amygdala (LA; can be divided in a dorsal and ventral part), the basolateral amygdala (BA; also called BLA), the central amygdala (CE; can be further subdivided in CeL and CeM) and the intercalated cell masses (ITC). Amygdala has strong intra-nuclear connections and extensive inter-nuclear connections that follow a dorsal to ventral direction. Indeed, LA sends projections to the BA which in turn sends projections to the CE (Figure 11). The CE is the main the output station of the amygdala and sends projections to the hypothalamus and different structures in the brainstem to orchestrate conditioned autonomic and motor responses.

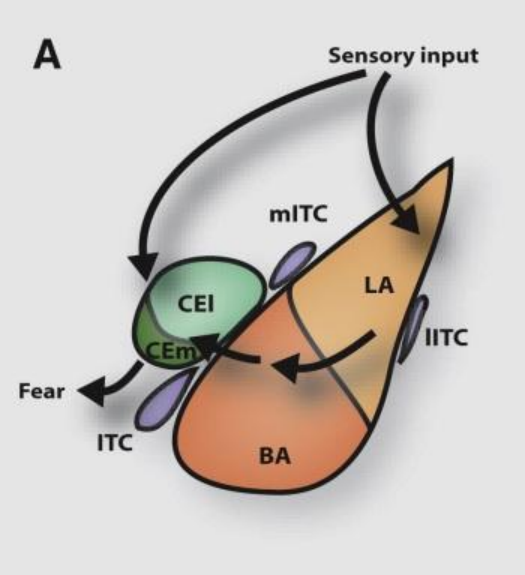

Figure 11: A: Scheme representing the main nuclei composing the amygdala. The three main nuclei are depicted: the LA (light orange), the BA (dark orange) and the central amygdala (green). Are also depicted the ITC cell clusters that border the LA and BA. The CE can be further divided in CEl and CEm. The LA receives sensory input from the thalamus and the cortex. From Ehrlich et al. 2009

The amygdala is also strongly innervated by cortical and sub-cortical structures. The LA serves as the primary sensory interface as it receives inputs carrying information about the CS and the US

originating from thalamus and cortex. Thalamic projections originate from the posterior intralaminar nucleus (PIN) and the medial geniculate nucleus (MGm) while cortical projections mainly originate from temporal auditory cortical fields (Pape and Pare, 2010) (that is for auditory cues). Axonal projections from cortical fields are located in a dense fiber bundle called the external capsule that borders the LA laterally. Thalamic projections are more diffuse and reach the amygdala through the internal capsule which is positioned medially to the LA and dorsally to the CE. It is now widely accepted that the association/storage of CS and US takes place in LA and that this process involves synaptic plasticity mechanisms (Pape and Pare, 2010). Moreover, pharmacological inactivation of LA is sufficient to impair cued fear acquisition in rodents (Maren and Quirk, 2004). In addition, electrophysiological recordings have shown an increase in auditory evoked firing of LA principal cells after fear conditioning (Quirk et al., 1997). More recently, an elegant study using a cellular imaging technique with immediate early genes (catFISH) suggested that CS and US information converge on the same populations of neurons in LA (Barot et al., 2009).

The BA not only receives information from the LA but is also strongly interconnected with other brain regions like hippocampus and mPFC. Axonal projections from the hippocampus to the BA all originate from the ventral hippocampus while BA sends projections to all different parts of hippocampus (PITKÄNEN et al., 2006). An important anatomical distinction exists in the mPFC which is subdivided in two parts: prelimbic cortex (PL) and infralimbic cortex (IL). Importantly, both divisions have strong reciprocal, but different connections with BA. This suggests that BA could function as a hub orchestrating fear behavior and extinction (Herry et al., 2008).

3.2.1.2 Cellular composition

The different nuclei of amygdala are highly differing in their cell type compositions: while the LA and the BA are mostly composed of excitatory cells (about 80%, the remaining 20% being inhibitory), CE and ITCs are composed only of inhibitory cells (Figure 11 and 12). Excitatory principal cells of amygdala have large somata and are densely covered with spines while inhibitory interneurons have smaller somata and have spine-sparse dendrites.

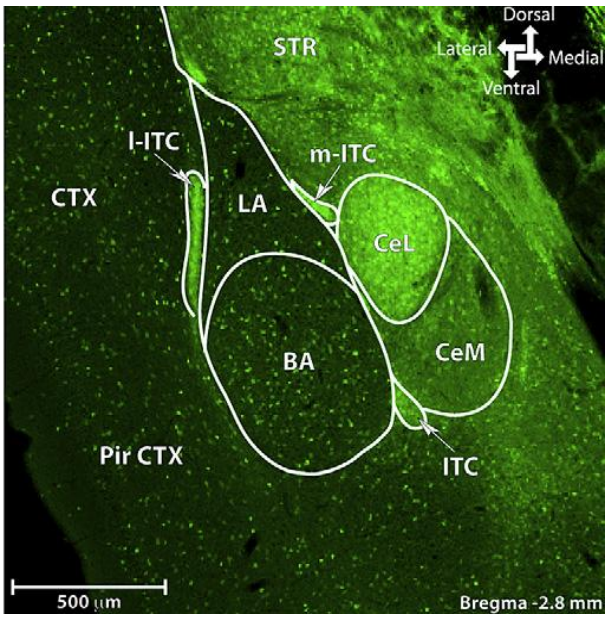

Figure 12: Brain slice representing interneurons in the amygdala. The slice was taken from a GAD67-eGFP mouse, where all interneurons are green. LA and BA are mostly composed of excitatory cells, with a smaller proportion of inhibitory cells. CE is composed solely of interneurons, as are the ITC clusters. From Spampanato et al. 2011

Interneurons are composed of multiple subtypes and up to date very little knowledge exist on their specific contributions to the different aspects of fear conditioning and extinction (Ehrlich et al., 2009). Recently a paper has attempted to classify LA interneurons based upon their molecular and electrophysiological properties (Sosulina et al., 2010). Although this led to the classification of interneurons in 5 subtypes, no evidence clearly shows their involvement in fear conditioning. Recently, however, a study from the Lüthi group has shown the role of a disinhibitory circuit of amygdala interneurons regulating fear conditioning (Wolff et al., 2014).

It has to be noted that the different interneuron subtypes make contacts on different areas of principal neurons, thus regulating excitability and plasticity at different levels (Muller et al., 2007; Woodruff and Sah, 2007). In addition, interneurons are under strong neuromodulatory control (Pinard et al., 2008; Zhang et al., 2013) which may allow to adapt inhibition depending on the emotional/behavioral state of the animal. Interneurons can be further subdivided based on the expression of specific markers, different electrophysiological parameters or on projection properties (Sosulina et al., 2010). In recent years considerable progress has been made in the

development of genetically modified animals allowing the visualization and manipulation of specific interneuron subtypes (Taniguchi, 2014). With no doubt the use of these animal models will allow unraveling the complexity and diversity of interneuron function in learning and memory processes.

3.2.2 Hippocampus

3.2.2.1 General anatomy

The hippocampus is a brain structure located in the medial temporal lobe. Briefly, the hippocampus can be subdivided in four main fields: the dentate gyrus (DG), the CA3 (Cornu Ammonis 3), the CA2 and the CA1 (Figure 13). DG and CA1-3 areas are filled with granule and pyramidal cells respectively and communicate in a unidirectional way. That is, granule cells of the DG send their axons (mossy fibers) to CA3, and pyramidal cells of CA3 send their axons (Schaffer collaterals) to CA2 and CA1. Sensory information reaches the hippocampus through projections originating from the entorhinal cortex (perforant path), specifically the medial and lateral layers II and III (Figure 13). CA1 then sends projections back to layer V of entorhinal cortex. The hippocampus has a strong caudal extension and can be further divided in dorsal (DH) and ventral hippocampus (VH). Thus, the different fields of hippocampus all have dorsal and ventral extensions. Interestingly, dorsal and ventral hippocampus are thought to underlie different aspects of cognition (Fanselow and Dong, 2010). Interestingly, the dorsal and ventral hippocampus show distinct extrinsic connectivity and projections to the amygdala all originate from the ventral hippocampus. The ventral CA1 sends axons to a structure called the subiculum which is the main output region of the hippocampus and sends strong projections to the BLA (see material and methods).

The hippocampus is known for its role in declarative memory as pharmacological lesions interfere with previously formed memories (Sanders et al., 2003). Moreover, decades of experimental evidence have shown a role of hippocampus in spatial representation and navigation (Smith and Bulkin, 2014). Hippocampus sends and receives projections from both amygdala and mPFC suggesting that it could also be involved in the regulation of fear behavior.

Here I focus mainly on the role of hippocampus in the representation of contextual information and how this information can be used to regulate fear behavior.

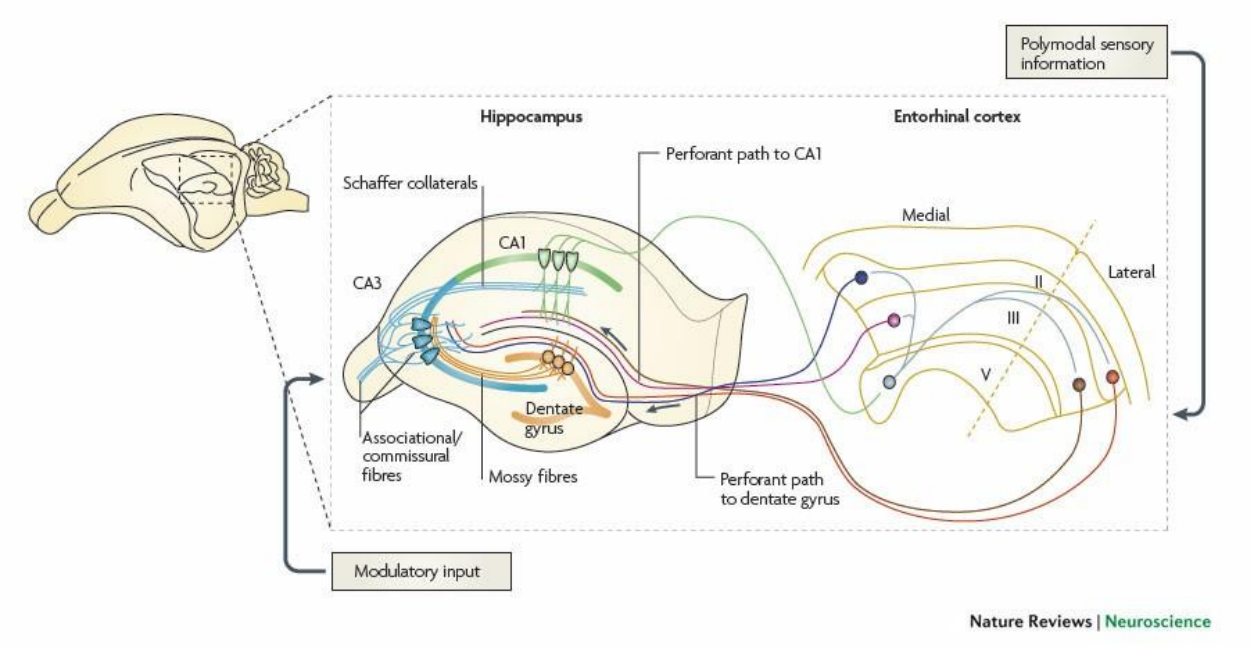

Figure 13: General anatomy of the hippocampus in rodents. The wiring diagram of the hippocampus is traditionally presented as a tri-synaptic loop. The major input originates from entorhinal cortex sending axons through the perforant path to DG granule cells (in orange). Granule cells of DG contact CA3 (in blue) pyramidal cells by projections called mossy fibers. Finally CA3 pyramidal cells, contact CA1 (in green) pyramidal cells through projections called Schaffer collaterals. Note that CA1 cells also receive projections from the entorhinal cortex. Finally, CA1 sends afferents back to entorhinal cortex in layer V. From Neves et al. 2008

3.2.2.2 Hippocampus in contextual coding

Unlike discrete cues (e.g. sound), contexts are multisensory, diffuse and continuously present. When performing a fear conditioning task on an animal, the initial step for the association to occur is the encoding/representation of the context in the animal's brain. Indeed, if the animal is shocked before it had time to explore the context, no association occurs with the context. Several pharmacological studies have pointed to the role of hippocampus in contextual encoding, consistent with the large amount of literature showing its role in spatial representation and navigation (Smith and Bulkin, 2014). Interestingly, each context is encoded by distinct neural ensembles within the hippocampus, as was shown elegantly using *in vivo* recordings in rats (Kelemen and Fenton, 2010).

While dorsal hippocampus is mainly responsible for contextual encoding, ventral hippocampus is important for anxiety and expression of previously formed fear, pointing a strong dichotomy between dorsal and ventral hippocampus function {Fanselow:2010dk}. It has to be noted that the neocortex is also involved in the storage of the contextual memory as it is believed there is a gradual transfer of information from hippocampus to cortical regions with time {Goshen:2011gh}{Frankland:2005kf}. During contextual fear conditioning, the encoded context is associated with the aversive foot shock. The main question that one could ask is where this association takes place. One candidate for the storage of the context/shock association is the amygdala as it has been shown that BLA is essential for contextual fear learning and expression (Fanselow and Poulos, 2005) Interestingly, BLA and hippocampus show strong reciprocal connections (PITKÄNEN et al., 2006) and synaptic plasticity between hippocampus and BLA can be induced *in vivo* (Maren et al., 1995).

More recent work has shown that the regulation in the expression of contextual fear depends on strong interactions between the PL, the BLA and the ventral hippocampus (Orsini et al., 2011; Sotres-Bayon et al., 2012) (Figure 14). This is especially true for contextual renewal of fear after extinction. Indeed, after an initial cued fear conditioning task the fear disappears in animals that were extinguished in the fearful context but renews as soon as the tone is presented in a non-extinguished context (Herry et al., 2010). BLA receives long range projections from both PL and VH and it is believed that, during contextual fear renewal, contextual representations are integrated in BLA trough both projections (Orsini et al., 2013). Recently two cell populations that correlate with high or low levels of fear have been discovered in BLA (Herry et al., 2008). Those two distinct cell populations are differentially connected with the prefrontal cortex and the hippocampus and were respectively called “fear” or “extinction” neurons. BLA fear neurons were indeed connected preferentially with ventral hippocampus and extinction neurons with IL. This key paper puts BLA as a central hub that can orchestrate behavior by allowing switching between states of high or low fear. Recently, using *in vivo* electrophysiological recordings, a report has shown that a subtype of BLA interneurons is recruited by hippocampal theta rhythm to promote hippocampo-BLA synchrony during emotional memory formation and presentation of noxious stimuli (Bienvenu et al., 2012).

However, hippocampal projections onto BLA are poorly characterized and their physiological role was still unexplored when I started my PhD. These projections have been difficult to study because of the difficulty in separating axonal projections of other brain structures with classical recordings (see material and methods). Using optogenetic approaches, however, I was able to shed some light on the importance of these projections *in vivo* (see results, paper 2).

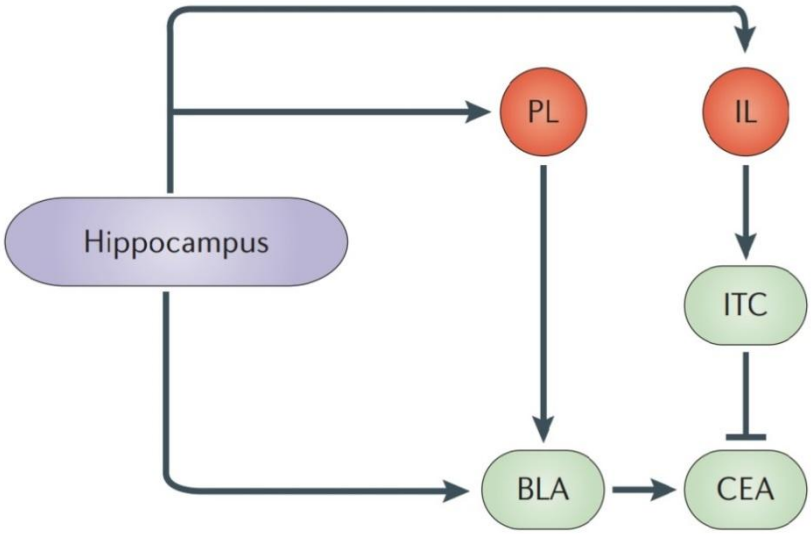

Figure 14: Neural circuit underlying context-dependent regulation of fear memory. Hippocampus sends projections to both mPFC (PL and IL) and BLA. Direct projections from hippocampus to BLA or indirect projections through PL might be crucial for the renewal of fear after extinction. Projections from hippocampus to IL might be important for the suppression of fear expression by a disinhibitory circuit passing through ITC cells. From Maren 2013

3.3 Synaptic plasticity in associative learning

One of the most important properties of the brain is its plasticity, which is the capacity of neuronal activity generated by an experience to modify neuronal circuit function. Synaptic plasticity refers to the activity-dependent modification of the synaptic strength and goes hand in hand with morphological remodeling of pre-and postsynaptic compartments (Bosch and Hayashi, 2012). Interestingly, a lot of ID mouse models present some – although divergent - deficits in synaptic plasticity, possibly explaining some cognitive abnormalities (Humeau et al., 2009). Fear conditioning is an ideal model because the synaptic plasticity mechanisms

associated with it have been well characterized. In the next paragraphs I introduce some general features of synaptic plasticity and provide some experimental evidence linking synaptic plasticity at particular synapses to fear conditioning behavior.

3.3.1 Synaptic plasticity, general principles

Learning and memory result from changes in activity-dependent changes in synaptic strength. This view, originally postulated by Hebb (1949) says that a synaptic input can be strengthened when activity in the presynaptic neuron co-occurs with activity (depolarization) in the postsynaptic neuron, pointing to the associative nature of the phenomenon. This postulate was first demonstrated in the rabbit hippocampus, more precisely in the dentate gyrus (Bliss and Lomo 1973) and was called long term potentiation (LTP). From now we know that LTP is mediated by various mechanisms depending on the brain structure, the experimental protocol or the considered cellular or synaptic types (Citri and Malenka, 2008). Originally, LTP between Schaffer collaterals (CA3 projections) and the CA1 region of the hippocampus is considered as the "canonical" LTP, as being the most studied form of synaptic plasticity in the brain. Thus, most studies have focused on synaptic plasticity on excitatory synapses of principal cells (see below). Noteworthy, synaptic plasticity of glutamatergic synapses onto interneurons has also been reported (Bauer and LeDoux, 2004), and may exhibit some distinctions with those of principal cells (Spampanato et al., 2011).

A temporal distinction can be made between the induction and the expression of LTP. Induction refers to the synaptic mechanisms initiating plasticity while expression designates the processes leading to stabilization of plasticity and often involves the traduction of new proteins (maintenance phase). Induction of LTP on excitatory cells involves the two main types of glutamatergic receptors: AMPA and NMDA. AMPA receptors have fast kinetics and open at resting membrane potential, leading to depolarization of the postsynaptic membrane by influx of cations. NMDA receptors, closed at resting membrane potential by a Mg^{2+}-mediated block, open when the postsynaptic membrane depolarizes, allowing the relieve of the Mg^{2+} ion and the Ca^{2+} entry within the cell (Citri and Malenka, 2008). The increase in calcium concentration then activates a large number of signaling pathways that ultimately lead to the strengthening of

the synapse. The role of CaMKII in this process has been clearly established (Opazo et al., 2010) but also of other proteins like PKA or PKC (Maren and Quirk, 2004). Interestingly, during fear conditioning, amygdalar cells that express higher levels of CREB are preferentially recruited into a memory trace (Han et al., 2007) and the reactivation of these cells is necessary for the expression of the fear memory (Kim et al., 2014). Also, *ex vivo* experiments showed that cells with higher CREB levels were more excitable than CREB-negative cells, possibly favoring their recruitment in a memory trace (Han et al., 2007). Thus, these results suggest that a specific subpopulation of cells become tagged during learning and are re-activated upon retrieval of memories.

Experimentally, induction of LTP can be achieved by applying high-frequency tetanic stimulation to presynaptic projections. Alternatively, pairing protocols consist of depolarization of the postsynaptic neuron with a sustained low-frequency presynaptic stimulation. Other protocols that are often used are called “spike-time dependent plasticity” (STDP) protocols, consisting of stimulating the presynaptic projection in a narrow time-window before firing of the postsynaptic cell (Caporale and Dan, 2008). Expression of LTP depends on the modification of existing proteins or production of new proteins that will contribute to the strengthening of the synapse. The major mechanism of expression of LTP involves an increase in the incorporation of AMPARs within the postsynaptic density. This is achieved by activity-dependent changes in AMPARs trafficking within the plasma membrane (Rumpel et al., 2005) and is tightly regulated (Opazo and Choquet, 2011). Alternatively, the electrophysiological properties of AMPARs can be modified to increase permeability.

Dendritic spines undergo strong morphological changes during synaptic plasticity. A recent study has shown that LTP induction is characterized by a strong reorganization and stabilization of the actin cytoskeleton (Bosch et al., 2014). The protein synthesis-dependent PSD enlargement was seen only 60min after LTP induction, as suggested by the increase of HOMER1B and SHANK1B proteins.

In CA1 LTP, both induction and expression are mediated by postsynaptic mechanisms. However, this is not necessarily the case at all synapses and some types of LTP are generated by

presynaptic mechanisms. In contrast to NMDAR-dependent LTP, the induction and expression of presynaptic LTP are characterized by an increase of neurotransmitter release leading to an increase of the postsynaptic response. Following high frequency tetanic stimulation, VGCCs mediate the increase of presynaptic calcium levels leading to the activation of a calcium/calmodulin-dependent adenylyl cyclase (AC). This in turn increases presynaptic cAMP levels and activates PKA, which phosphorylates critical presynaptic substrates, such as RIM1α, to cause a long-lasting enhancement in transmitter release (Fourcaudot et al., 2008).

3.3.2 Synaptic plasticity related to fear conditioning

One question that has been difficult to resolve is which forms of LTP can be directly linked/causing the newly acquired behavior. Indeed, it is not easy to characterize the physiological conditions under which LTP is initiated in the behaving animal. The synaptic mechanisms leading to the formation of fear memory have been extensively studied in the past years, especially in the amygdala. Indeed, both *in vitro* and *in vivo* studies have revealed the existence of LTP-like mechanisms in the lateral amygdala (Sah et al., 2008). In lateral amygdala, two forms of LTP have been shown to coexist (Shin et al., 2010). Indeed, projections from cortex to lateral amygdala (cortico-LA) underlie a form of LTP that is expressed presynaptically with an increase in the probability in neurotransmitter release (Humeau et al., 2003). Alternatively, LTP induced by stimulation of thalamic projections impinging on lateral amygdala (thalamo-LA) is expressed postsynaptically with incorporation of new AMPA receptors at the postsynaptic site (Rumpel et al., 2005).

An interesting approach to answer this is *ex vivo* electrophysiology where recordings are realized on brain slices of previously conditioned animals. When occlusion of LTP occurs in brain slices, one can assume that similar LTP-like mechanisms occur *in vivo* during learning. Projections from auditory cortex to lateral amygdala are modified during acquisition of fear conditioning and LTP couldn't be induced in previously conditioned animals (Tsvetkov et al., 2002). This suggested that presynaptic cortico-LA LTP underlies, at least partly, the acquisition of cued fear conditioning. Similarly, projections from the thalamus to the lateral amygdala show postsynaptic plasticity mechanisms that are occluded in previously conditioned animals (Hong

et al., 2012; Rumpel et al., 2005). Taken together, those two studies show that different forms of LTP are directly implicated in fear acquisition although their specific relevance is still a matter of debate. Interestingly, research from our lab has shown, using KO mouse models for GluR1 and GLuR3 subunits, that thalamo-LA LTP relies on GluR1-dependent synaptic plasticity mechanisms while cortico-LA LTP depended on both GluR1 and GLuR3 subunits (Humeau et al., 2007). Recently, an optogenetic study has shown that fear memory could be activated or inactivated by potentiation (LTP) or depressing (LTD) projections from thalamus and cortex (Nabavi et al., 2014).

3.3.3 Modulation of synaptic plasticity by inhibitory cells

To understand the mechanisms governing memory formation and expression the main focus has been on excitatory cells in the brain. However, interneurons are critical components in brain function as they regulate overall balance of network excitability but also synaptic integration, spike timing, and synchrony of a neuronal ensemble (Isaacson and Scanziani, 2011). Pyramidal cells of lateral amygdala are under strong inhibitory control and have very low spontaneous activity. Cortical and thalamic projections that reach LA also contact local interneurons that provide feed-forward inhibition to pyramidal cells (Szinyei et al., 2007) thereby tightly controlling their activity and thus the induction of synaptic plasticity (Figure 15). Interestingly, although synaptic plasticity at those two afferents differs in their induction and expression mechanisms, LTP gating is largely dependent on the activation of inhibitory cells in lateral amygdala (Ehrlich et al., 2009).

Thalamic LTP is induced postsynaptically through NMDA-receptor activation and is particularly sensitive to feed-forward inhibition. Indeed, induction of LTP at this pathway needs the relieve of $GABA_A$-mediated inhibition, for example following dopaminergic modulation of interneuronal subtypes (Bissière et al., 2003). At the cortical pathway, homosynaptic induction of presynaptic LTP is prevented by the GABA released from local feed-forward interneurons that activates presynaptic $GABA_B$ receptors negatively regulating glutamate release (Szinyei et al., 2007). Relieving $GABA_B$ mediated presynaptic inhibition at cortico-LA afferents unmasks a NMDA-receptor-independent presynaptic LTP at this afferent (Shaban et al., 2006). Thus, the level of

feed-forward inhibition in LA sets the balance between two types of LTP induction mechanisms at cortico-LA afferents. Taken together these results unambiguously show a role of inhibition in shaping activity and plasticity of thalamic and cortical afferents reaching pyramidal neurons in LA (Figure 15).

However, it is still a matter of debate which interneurons provide the feed-forward inhibition, but regular, high spiking, parvalbumin (PV)-expressing interneurons appear as good candidates as they are contacted by both thalamic and cortical afferents in LA (Szinyei et al., 2007).

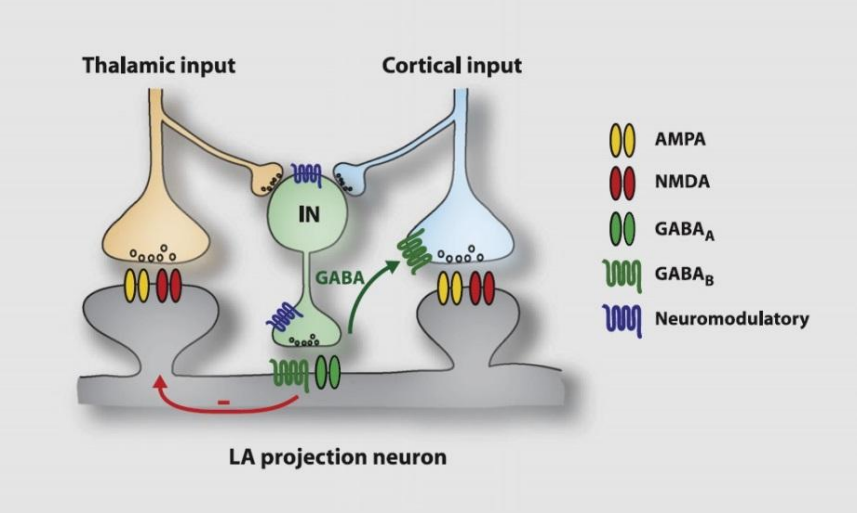

Figure 15: Cortical and thalamic inputs converge on LA projection (principal/pyramidal) neurons. The same afferents also contact local interneurons which provide feed-forward inhibition on projection neurons. LTP is tightly regulated by GABA released from feed-forward local interneurons. At thalamic afferents this control is mainly postsynaptic via $GABA_A$ receptors. At cortical afferents this control is presynaptic via $GABA_B$ receptors. Moreover, interneurons are under neuromodulatory control, providing an additional level of regulation. From Ehrlich et al. 2009

VII) Materials and methods

Cognitive disabilities in ID are thought to result from the functional absence of proteins that fulfill various functions in the brain. Therefore, understanding of ID pathology requires a combination of experimental techniques that allow studying the functional consequences of the absence of the protein at different analytical levels (behavior, cellular and synaptic). My main scientific goal was to link behavior with synaptic function using KO *Il1rapl1* mice. To achieve this, I have submitted *Il1rapl1* KO mice to associative fear learning tasks and performed *in vitro* electrophysiological recordings in physiologically relevant brain structures. *In vivo* pharmacological and optogenetic approaches were used to specifically act on synaptic function while the animals were performing behavioral tasks, allowing us to make causal links between possible behavioral and synaptic deficits in *Il1rapl1*-deficient mice. In this section I focus mostly on the experimental techniques that I have personally used and developed during my PhD. These include behavioral learning (fear conditioning), *in vitro* electrophysiology on acute brain slices and *in vivo* and *in vitro* optogenetic approaches. Several other experimental techniques were used to further dissect pathology of ID in *Ilrapl1*-deficient mice like immunohistology and imaging, but they appear me quite secondary. However, the reader can access further information in the material and methods section of the published papers present in the manuscript.

1 Animals

Il1rapl1 KO mice were generated by Pierre Billuart, in the group of Jamel Chelly (Cochin Institute, Paris) using a Cre/Lox technology and leading to the insertion of a stop codon within the 6th exon of the *Il1rapl1* gene (Figure 16). The first description and use was done in 2009, in a previous publication from the lab (Gambino et al., 2009). Briefly, an 18-kb BamHI DNA fragment containing exons 4–5 from the mouse *Il1rapl1* gene was isolated from an SV129 genomic library (RPCI21483014, RZPD, Berlin, Germany) and sub-cloned to construct a targeting vector. A pgk-hygromycin resistant gene cassette flanked with LoxP sites was inserted into in the intron 5 at

the KpnI position to allow positive selection of the homologous recombination event. Another LoxP site was inserted into the intron 4 at the PstI position. The genomic region surrounding exon 5 was targeted by homologous recombination in embryonic stem cells leading to the insertion of a tri-loxed sequence containing the exon 5 and a phosphoglycerolkinase-hygromycin-resistant gene cassette. A first transgenic line containing this allele was established and crossed with a transgenic line expressing the Cre recombinase in the germline cells. The Cre recombinase catalysed the deletion of sequences between LoxP sites and a secondary line was selected in the F1 generation with a complete deletion of both exon 5 and the selective cassette. The final *Il1rapl1*-mutated allele used in this study has exon 5 deleted and the spliced resulting mRNA contains a STOP codon in exon 6.

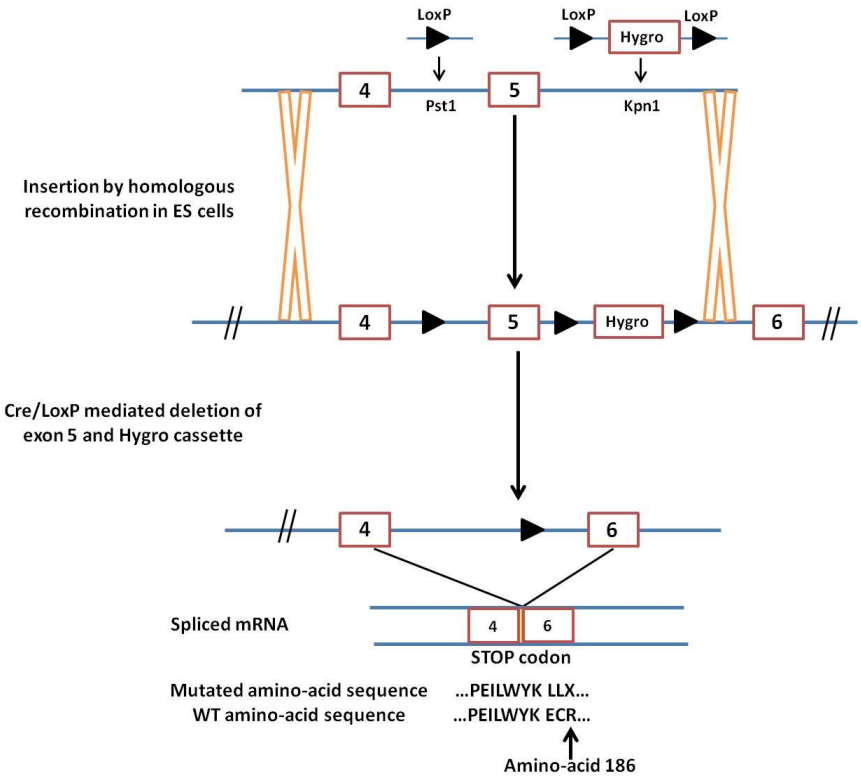

Figure 16: Strategy used to create the KO *Il1rapl1* mouse model. The strategy is based on the genomic deletion of the fifth exon, leading to the disruption of the open reading frame after transcription and splicing of exon 4–6 in the *Il1rapl1* mRNA. This frame shift mutation leads to a premature STOP codon in the beginning of the second Ig-like loop of the extracellular domain. Adapted from Gambino et al. 2007

We maintained an *Il1rapl1* colony in Bordeaux animal facility by crossing female KO *Il1rapl1* mice with heterozygous males. In dedicated experiments aiming at recording GABA-ergic interneurons, we crossed *Il1rapl1* mice with GAD67-eGFP mice (Tamamaki et al., 2003) (kindly provided by A. Lüthi's lab, FMI, Basel). The breeding scheme consisted of crossing a heterozygous female *Il1rapl1 +/-* mouse with a GAD67eGFP KI male. Animals expressing eGFP were then selected for electrophysiological recordings.

Animals were housed under a 12h light/dark cycle and provided with food and water ad libitum. All procedures were performed in accordance with the European guide for the care and use of laboratory animals and the animal care guidelines issued by the animal experimental committee of Bordeaux Universities (CE50) (A5012009). All behavioral experiments were realized on adult animals (2-6 months age). Electrophysiological recordings on LA principal cells were realized on young adult mice (3 weeks old) or on older animals (~ 2 months old) when performing BLA recordings.

2 Fear conditioning

2.1 Cued fear conditioning

Mice were housed individually in a ventilation area before the start of behavioral training. Animals were handled every day before the start of the experiment during a week. On training day 1, animals were transferred to the conditioning context (context A, Figure 17) for habituation. During this phase I presented two different sounds to the animals: the CS+ which will be later on coupled with the foot shock and the CS- which serves as a control. Both CS+ (total CS duration of 30s, consisting of 50-ms pips repeated at 0.9 Hz, pip frequency 7.5 kHz, 80 dB sound level) and CS- (30s, consisting of white noise pips repeated at 0.9Hz, 80dB sound level) were presented 4 times at variable inter stimulus intervals (ISI). On day 2, I proceeded with the conditioning phase. The protocol consisted of 5 pairings of CS+ with the US onset coinciding with the CS+ offset (1s foot shock, 0.6mA, ISI 10-60s). In all cases, CS- presentations were intermingled with CS+ presentations and ISI was variable over the whole training course. Cued memory was tested (recall) 24 hours after conditioning by analyzing the freezing levels at the

first CS+ presentations in context B (Figure 17). Freezing behavior was quantified automatically in each behavioral session using a fire-wire CCD-camera (Ugo Basile, Italy, Figure 17) connected to an automated freezing detection software (ANY-maze, Stoelting Co, US). To test for animal exploration and activity, the animal displacement in the context was traced and analyzed with software programmed and provided by Dr. Jiyun Peng (Fudan, Shanghai, China).

2.2 Contextual fear conditioning

Mice were housed individually in a ventilation area before the start of behavioral training. Animals were handled every day before the start of the experiment during a week. On day 1, animals were transferred to the conditioning context (context A, Figure 17) for habituation, which consisted of a 2min exploration period. On day 2, I proceeded with the conditioning phase. The protocol typically consisted of three 2s foot shock presentations of 0.6mA separated by a 60 sec time interval between shocks. Discriminative contextual fear memory was tested 24 hours after conditioning by analyzing the freezing levels in context B VS context A (Tests B/A, Figure 16). Freezing behavior was quantified as above.

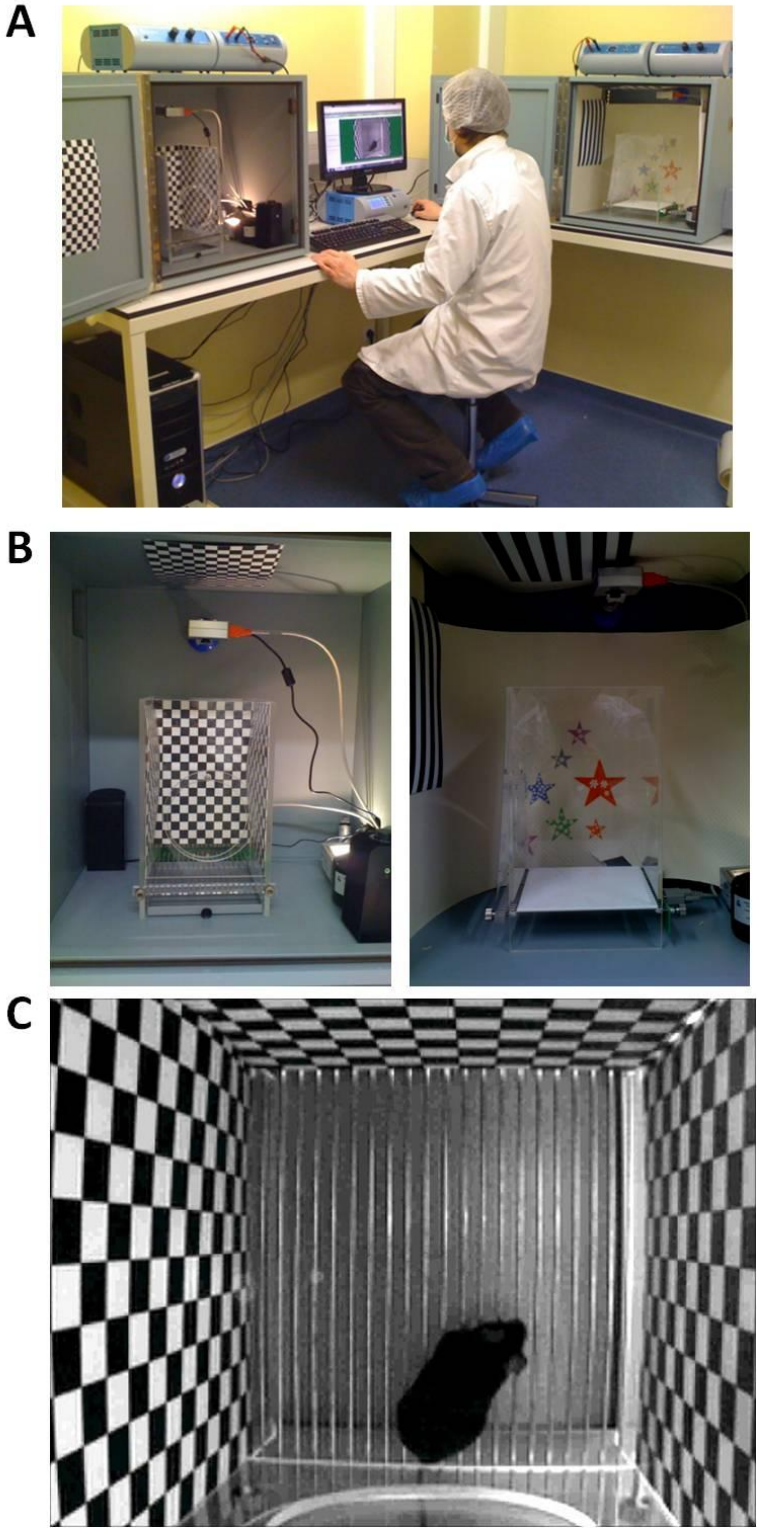

Figure 17: Fear conditioning apparatus. A: Picture showing the arrangement of our fear conditioning behavior device. Each context is placed in an isolated box to reduce background noise that could interfere with behavior. Sound and shock generators are connected and controlled by a computer interface. B: Picture of context A (left) and context B (right). The contexts differed in olfactory, visual, and sensory modalities in order to be very different from one another. C: Mouse freezing episodes were automatically detected by a camera placed above the conditioning cage.

3 Optogenetics

Previously, the role of certain brain areas in memory processes was based on a combination of physical, pharmacological and genetic lesions together with electrical or pharmacological stimulation of these same areas. Nevertheless, those techniques lack temporal and spatial specificity and didn't allow assessing the role of certain neuronal populations in real-time when the animal is performing a behavioral task. Probably one of the major breakthroughs in modern neuroscience is the implementation of optogenetic, a recently developed technique that combines optical stimulations and genetically driven cellular expression of light-sensitive proteins to control well-defined events within neural circuits with fine temporal and spatial specificity.

Opsins are bacterial channels that respond to illumination by certain wavelengths of light with depolarizing currents, hyperpolarizing currents or specified signal-transduction event (Papagiakoumou, 2013), allowing neuronal activation or silencing depending on experimental demands. Channelrhodopsin-2 (Chr2) is an opsin that depolarizes membranes (by cation influx) following stimulation with blue light and that can be used to trigger spikes in neurons (Boyden et al., 2005) (Figure 18). Undoubtedly, this is the most used tool to activate neurons *in vitro* or *in vivo* and multiple genetic variants have been engineered to modify current amplitude, time of desensitization… (Lin, 2011). On the other side, neuronal silencing has been achieved mainly by two types of opsins: halorhodopsin (NpHR; chloride influx) and archaerhodospin (Arch; proton outflow), which are both sensitive to yellow light (Chow et al., 2010; Gradinaru et al., 2010) (Figure 18). When expressed in neurons, opsins locate to the soma but also to axonal projections. This allows one to study firing properties of neurons while stimulating the soma or to limit the light stimulation to presynaptic projections (Tye and Deisseroth, 2012).

I used optogenetics both for *in vivo* and *in vitro* purposes. Most my experiments were realized by using the original Chr2 construct. To achieve Chr2 expression in the brain I used stereotaxic injections of AAV viruses containing Chr2 (see surgeries). A few experiments were realized using the Arch construct.

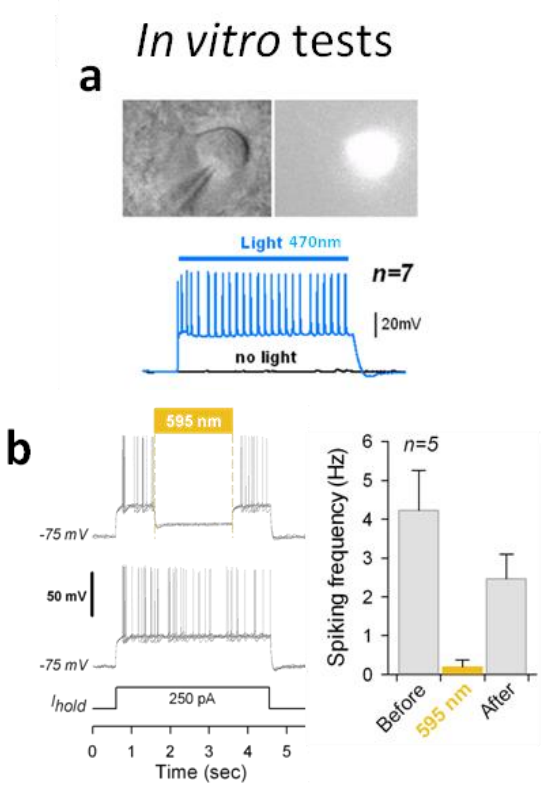

Figure 18: Effect of Chr2 and Arch on spiking activity of principal cells on acute brain slices. a: Expression of the opsin (Chr2 or Arch) was visualized by fluorescence. 470nm blue light excitation of Chr2 elicited strong spiking activity. b: depolarizing current injections led to spiking of the cell and this spiking could be repressed by 595nm yellow light excitation of Arch. Spiking frequency was completely abolished by yellow light illumination.

For *in vitro* experiments, light was delivered through a 500µm fiber which was placed just on top of the brain slice with a micromanipulator, allowing a large field of illumination. To record for hippocampo-BLA light-evoked currents on principal cells, 5ms flashes were elicited, delivered by an ultra-high power 460nm LED (Prizmatix Ltd, Israel) at maximal intensity.

For *in vivo* experiments, light was delivered through implanted guide cannulas (Plastics One, US) positioned above the brain area of interest. To achieve this, an optical polymer fiber (Prizmatix Ltd, Israel) was placed in the guide cannula and light was produced by a 460nm ultra high power LED device (UHP-460, Prizmatix Ltd., Israel). The fiber was allowed to project out of the guide cannula tip, thus placing the fiber just above the structure of interest. Two main *in vivo*

experiments were realized using this strategy, although the stimulation locus differed (LA or BLA):

- Rescue of cued fear conditioning in *Il1rapl1* mice (publication 1, figure 8)
- Rescue of contextual fear conditioning in *Il1rapl1* mice (publication 2, figure 4)

For the behavioural rescue of cued fear conditioning, we applied a protocol based on previous results showing that an artificial fear memory can be created in LA by using optogenetic-helped amygdala stimulation (Johansen et al., 2010). This protocol consists of pairing the presentation of the CS together with light-mediated depolarization of LA principal cells, replacing or reinforcing US-induced depolarization. In our hands, CS were delivered together with trains of blue light pulses (20 Hz, 30 sec, 2msec light pulses) and terminated with US application. Thus, we boosted LA principal cell depolarization during CS/US pairing. 24 hours later, the mice were presented with CS+ in another context B (Recall) and the freezing response was analysed.

For the behavioral rescue of contextual fear conditioning, we restricted the light stimulation to the ventral hippocampus projections to the BLA. First, mice were submitted to a classical habituation/conditioning/test sequence (see above). One hour before being re-exposed to the fearful context they received bursting light stimulation above the BLA. This illumination was performed in their homecage. The bursting protocol was composed of 5 burst episodes separated by 30 sec. Each burst is composed of 20 trains (applied at 5Hz) of 4 light flashes (intra-train frequency: 100Hz) (Figure 19).

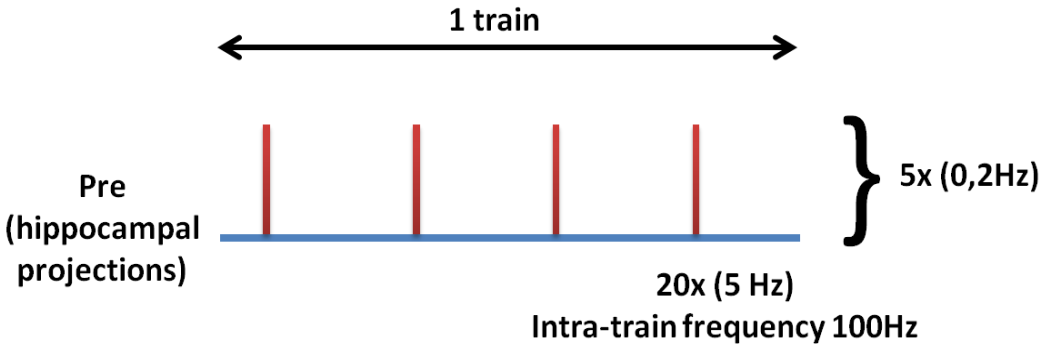

Figure 19: Scheme representing the bursting protocol we have used for stimulation and/or priming of hippocampal projections in BLA in acute slices and *in vivo* respectively

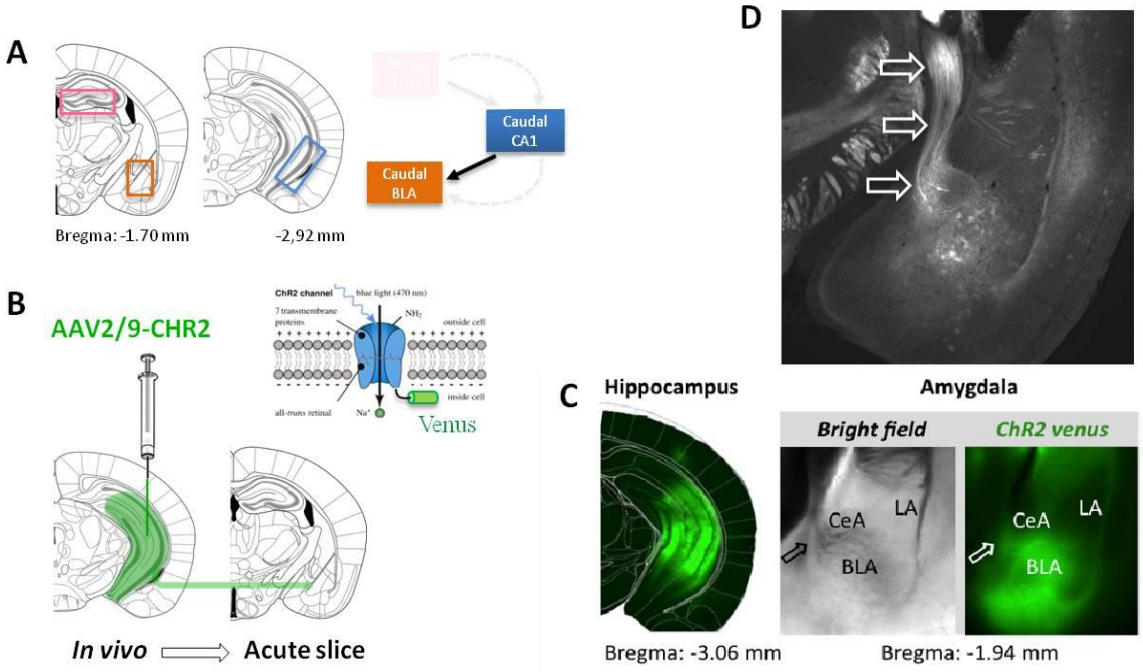

Figure 20: Scheme showing the strategy to infect hippocampus with Chr2. A: Left: Brain slices depicting amygdala (left, bregma -1,70) or caudal hippocampus (right, bregma -2,92). Caudal hippocampus (CA1, subiculum) sends projections to BLA. B: An AAV virus coding for Chr2-Venus (GFP) was injected in caudal hippocampus *in vivo*. Few weeks after infections, brains were dissected and acute brain slices containing BLA were prepared. C: Infection site in ventral hippocampus. D: Top: Picture of an amygdala-containing coronal slice allowing visualizing hippocampal fibers reaching the BLA (arrows). Bottom: Bright field picture of BLA-containing slice (left) and fluorescent picture of the same coronal slice showing Chr2-GFP expression in hippocampal projections.

4 Surgeries

- AAV injections. Adeno-associated viruses (AAV2/9.CAG.ChR2-Venus.W.SV40-p1468, ref Addgene-20071, $5.82E^{12}$ vector genomes (vg)/ml)) were packaged at the University of Pennsylvania Vector Core. The AAV Arch-GFP was kindly provided by Cyril Herry. Around 2 months old mice (over 20g) were prepared for the stereotaxic injection. Beforehand, mice were treated with buprenorphine (0.1 mg/kg, i.p), and positioned in a stereotaxic apparatus (David Kopf Instruments, Tujunga, CA) under continuous anaesthesia with isoflurane. During the surgery, the mice were warmed on a 33-35°C heating pad. The virus was bilaterally pressure-injected through glass pipettes (Hirschmann Laborgerate, ringcaps, tips pulled O.D 30-50 µm) using a Picosprizer (Parker Co). The positions of Bregma and Lambda points were defined and adjusted to the same horizontal level. Coordinates for the LA [AP] -

1.7 mm, [ML] ± 3.1 mm, [DV] -3.2 mm BLA: [AP] -1.5-1.7 mm, [ML] ±3.2-3.4 mm, [DV] -4.8 mm, or caudal HPC: [AP] -3.1-3.3 mm, [ML] ±3.2-3.4 mm, [DV] -4.0 mm.

- Cannula implantation. Stainless steel guide cannula (26 or 24 gauge; Plastics-One, Roanoke, VA, USA) were bilaterally implanted above the LA [AP] -1.7 mm, [ML] ± 3.1 mm, [DV] -2.8~3 mm, BLA: [AP] -1.5-1.7 mm, [ML] ±3.2-3.4 mm, [DV] -3.4-3.5 mm, or caudal HPC: [AP] -3.1-3.3 mm, [ML] ±3.2-3.4 mm, [DV] -3.0-3.1 mm. Cannula was secured to the skull using dental cement (Super-Bond, Sun Medical Co. Ltd, Moriyama, Shiga, Japan). In the end, dummy cannula was inserted into the guide cannula to reduce the risk of infection. In the next 2 weeks of cannula surgery recovery, or 4-6 weeks of virus transfection, body weight and symptoms of sickness were monitored carefully.

5 *In vitro* electrophysiology on acute brain slices

5.1 Slice preparation

Protocols to prepare acute brain slices were adapted depending on the brain structure studied and the age of the animal. Indeed, the quality of acute brain slices heavily depend on animal age, and special dissecting procedures have to be applied to record for adult neurons in these preparations (Figure 21). All recordings of LA neurons (publication 1) were performed on slices from 3-4 weeks old animals while recordings of BLA neurons were performed on slices of older mice (~1,5 month). For lateral amygdala (LA) recordings, I used a standard procedure as previously described {Humeau:2005kz}. Briefly, mice were anesthetized under isoflurane and the brain rapidly removed. Then, the brain was dissected in ice-cold artificial cerebrospinal fluid (ACSF) containing (in mM): 124 NaCl, 2.7 KCl, 2 $CaCl_2$, 10 $MgSO_4.7H_2O$, 26 $NaHCO_3$, 1.25 NaH_2PO_4, 18.6 glucose and 2.25 ascorbic acid; the brain was mounted against an agar block and sliced (300µm thick) with a vibratome (Leica VT1200s; Germany) at 4°C. Slices were maintained for 45 min at 37°C in an interface chamber containing ACSF equilibrated with 95% O_2/5% CO_2 and then for at least 45 min at room temperature before being transferred to a perfused recording chamber. In the perfused ACSF the $MgSO_4$ was decreased to 1.3mM.

For the preparation of 1,5 to 3 months old BLA-containing acute slices, a different protocol was used to improve slice preservation (Peca et al., 2011)(Figure 21). Briefly, mice were anesthetized with a mixture of ketamine/xylazine (100mg/kg and 10mg/kg respectively) and cardiac-perfused with ice-cold, oxygenated (95% O2, 5% CO2) cutting solution (NMDG) containing (in mM): 93 NMDG, 93 HCl, 2.5 KCl, 1.2 NaH_2PO_4, 30 $NaHCO_3$, 25 Glucose, 10 $MgSO_4$, 0.5 $CaCl_2$, 5 Sodium Ascorbate, 3 Sodium Pyruvate, 2 Thiourea and 12mM N-Acetyl-L-cystéïne (pH 7.3-7.4, with osmolarity of 300-310 mOsm). The brains were rapidly removed and placed in the ice-cold and oxygenated NMDG cutting solution described above.

Coronal slices (300 µm) were prepared using a Vibratome (VT1200S, Leica Microsystems, USA) and transferred to an incubation chamber held at 32°C and containing the same NMDG cutting solution. After this incubation the slices were maintained at room temperature in oxygenated modified ACSF containing (mM): 92 NaCl, 2.5 KCl, 1.2 NaH_2PO_4, 30 $NaHCO_3$, 20 HEPES, 25 Glucose, 2 $MgSO_4$, 2 $CaCl_2$, 5 Sodium Ascorbate, 3 Sodium Pyruvate, 2 Thiourea and 12mM N-Acetyl-L-cystéïne (pH 7.3-7.4, with osmolarity of 300-310 mOsm) until recording.

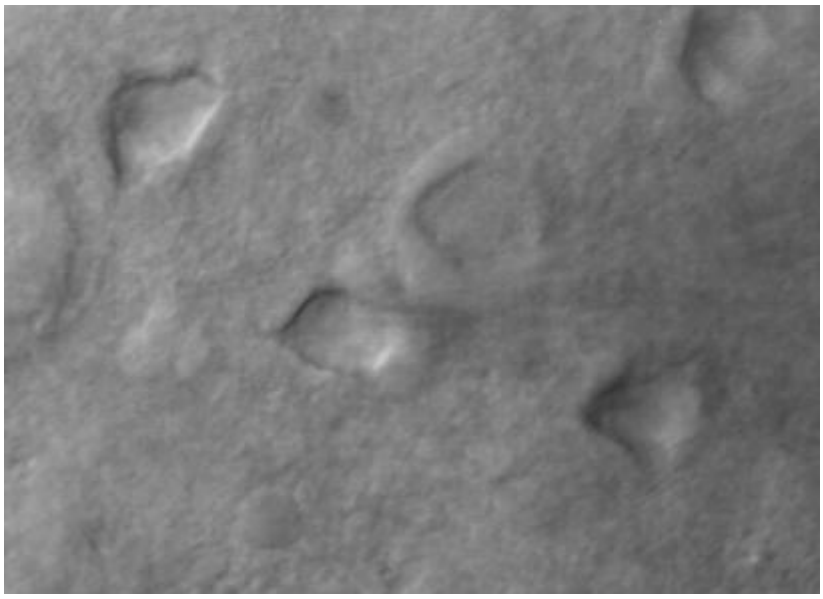

Figure 21: Differential interference contrast (DIC) picture of a BLA-containing acute slice showing some principal cells in BLA. NMDG-based cutting solution drastically improved slice quality in BLA.

5.2 Electrophysiological recordings

Whole-cell recordings of LA or BLA principal cells were performed at 30-32°C in a perfused chamber. Neurons were visually identified with infrared videomicroscopy using an upright microscope equipped with a 60x objective. Patch electrodes (3-5 MΩ) were pulled from borosilicate glass tubing. For voltage clamp recordings pipettes were filled with a low-chloride solution containing (in mM): 140 Cs-methylsulfonate, 5 QX314-Cl, 10 HEPES, 10 phosphocreatine, 4 Mg-ATP, and 0.3 Na-GTP (pH adjusted to 7.25 with CsOH, 300 mOsm). For dedicated current-clamp experiments, Cs-methylsulfonate was replaced with equimolar K-gluconate to allow spike discharge. In case of interneuron recordings, GFP labeled cells were targeted in acute slices by fluorescence imaging.

Long range cortical and thalamic projections towards LA principal neurons were performed following electrical stimulation of thalamic or cortical fibers with a bipolar twisted platinum/10% iridium wire (Figure 22). Stimulation intensity was adjusted to obtain baseline EPSC amplitudes between 100 to 200pA (voltage clamp experiments) or EPSP amplitudes of 4 to 6mV (current clamp experiments). In the voltage clamp mode, recordings of synaptic current at both -70 mV and 0mV allowed me to separate excitatory and inhibitory conductances.

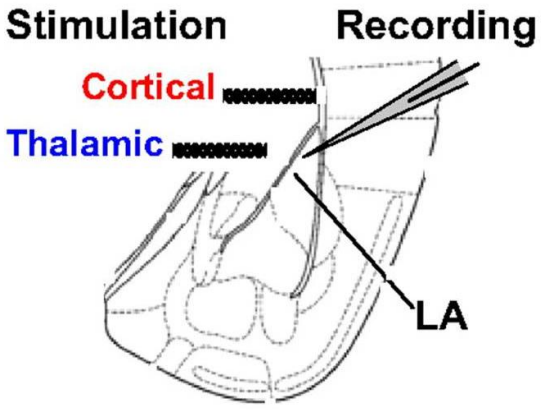

Figure 22: Scheme depicting an acute slice containing LA. Stimulation electrodes were placed in external capsule (cortical afferents) or internal capsule (thalamic afferents) and evoked responses were recorded on LA principal cells or LA interneurons

- Input/output curves were obtained by plotting the recorded amplitude of the evoked currents according to the stimulation intensity.

- Inhibition/excitation ratio was calculated by dividing the evoked amplitude of inhibition by the evoked amplitude of excitation for the strongest stimulation intensity.

- Thalamic LTP experiments on LA principal cells. All LTP experiments were performed in the presence of picrotoxin (PTX, 100 µM), except when stated otherwise. LTP was induced using a spike-timing dependent plasticity protocol (STDP), consisting of pairing three presynaptic stimulation followed by three postsynaptic spike discharges (10ms delay). This induction protocol was repeated 15 times at a rate of 0,2Hz (Figure 23).

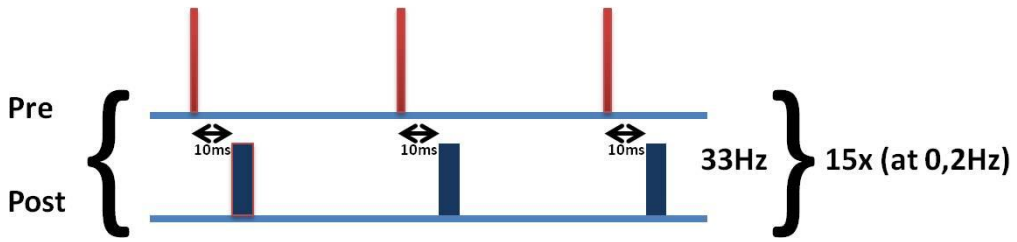

Figure 23: STDP plasticity protocol. Three monosynaptic EPSPs were paired with postsynaptic current injections leading to spike discharge. This was repeated 15 times at a frequency of 0,2 Hz

- Spiking activities. LA interneurons recordings were performed on *Il1rapl1*/GAD67-eGFP mice, which allowed me to visualize cells by fluorescence. Interneuronal populations were further separated based on the spiking patterns of the recorded cells. To elicit spikes, cells were maintained at -70 mV in current clamp mode and submitted to repeated, 400 msec long, current steps of increasing intensity: -50, 50, 150, 250 and 350 pA. IN classification was essentially based on the number of observed spikes and the degree of spike adaptation. Occasionally, I also used spike half-width and the initial spike frequency to allow classifying some borderline cases.

- Light-evoked synaptic currents. All *in vitro* BLA recordings were performed following light-induced stimulation of hippocampo-BLA projections (see optogenetics section).

Similarly as for LA recordings (see above), voltage clamp mode was used to estimate excitatory and inhibitory conductances and to calculate I/E ratio. For LTP experiments, cells were clamped in current clamp, allowing cells to depolarize.

5.3 Data acquisition and analysis

Data were recorded with a Multiclamp700B (Molecular Devices, USA), filtered at 2 kHz and digitized at 10 kHz. Data were acquired and analysed with pClamp10.2 (Molecular Devices). In all experiments, series resistance was monitored throughout the experiment, and if it changed by more than 15%, the data were not included in the analysis. Changes were quantified by normalizing and averaging EPSP slope during the last 5 min. of the experiments relative to the 5 min. of baseline prior to LTP induction or drug application.

VIII) Results

The main aim of my thesis was to use a KO mouse model of *Il1rapl1* and find links between cognitive features and synaptic function. The starting point of my experimental strategy was to characterize behavioral deficits in *Il1rapl1* KO mice. Once I had defined the behavioral deficit, I would use an array of experimental techniques (see material and methods) to understand how IL1RAPL1 absence led to the observed deficit at the synaptic level. Initially, my objective was to submit a first cohort of *Il1rapl1*-deficient animals to a full fear conditioning/extinction protocol. Indeed, fear conditioning and extinction depend on different neural circuits (see introduction) thus increasing the possibility of finding behavioral deficits at multiple steps of the fear learning procedure. In practice, animals were first submitted to cued fear conditioning which was followed by an extinction phase and the subsequent testing of extinction memory (retrieval) and contextual aspects of fear memory (renewal) (Figure 24). During retrieval animals are resubmitted to the extinction context to test for extinction memory. Renewal consists of re-exposing animals to the cued conditioning context and is often used to test for contextual aspects of fear memory after extinction learning. Thus, this protocol would allow me to test both the capacity of animals to form and retrieve cued-and extinction fear memories but at the same time give me some information on the contextual aspects of the fear memory.

This pioneer experiment revealed a delay in the capacity of animals to acquire cued fear memory but also some deficits during renewal, suggesting that acquisition of cued fear and some contextual aspects of fear were impaired following absence of IL1RAPL1 (Figure 24). Interestingly, extinction was preserved in *Il1rapl1*-deficient animals proposing that the neural circuits underlying extinction were preserved. Thus, these findings suggested that neural circuits of fear conditioning and extinction could be differentially vulnerable to *Il1rapl1* mutation (Figure 24). In order to further characterize cued and contextual fear deficits in KO animals, I submitted two other cohorts of animals to a cued fear conditioning (see material and methods) and a pure contextual fear learning task (see material and methods) respectively. Indeed, during contextual fear only the context becomes associated with the shock, contrasting with renewal where contextual and cued aspects of fear are intermingled.

In accordance with my previous results, I found that *Il1rapl1*-deficient mice were strongly impaired in both cued fear conditioning and in contextual fear conditioning. Because the two deficits appear to be of different nature, the dataset was finally published in two parts that are presented sequentially. For each study, I will provide a summary of the main outcomes with a small discussion of some methodological aspects. A more complete overview of the findings and perspectives are discussed in the general discussion section.

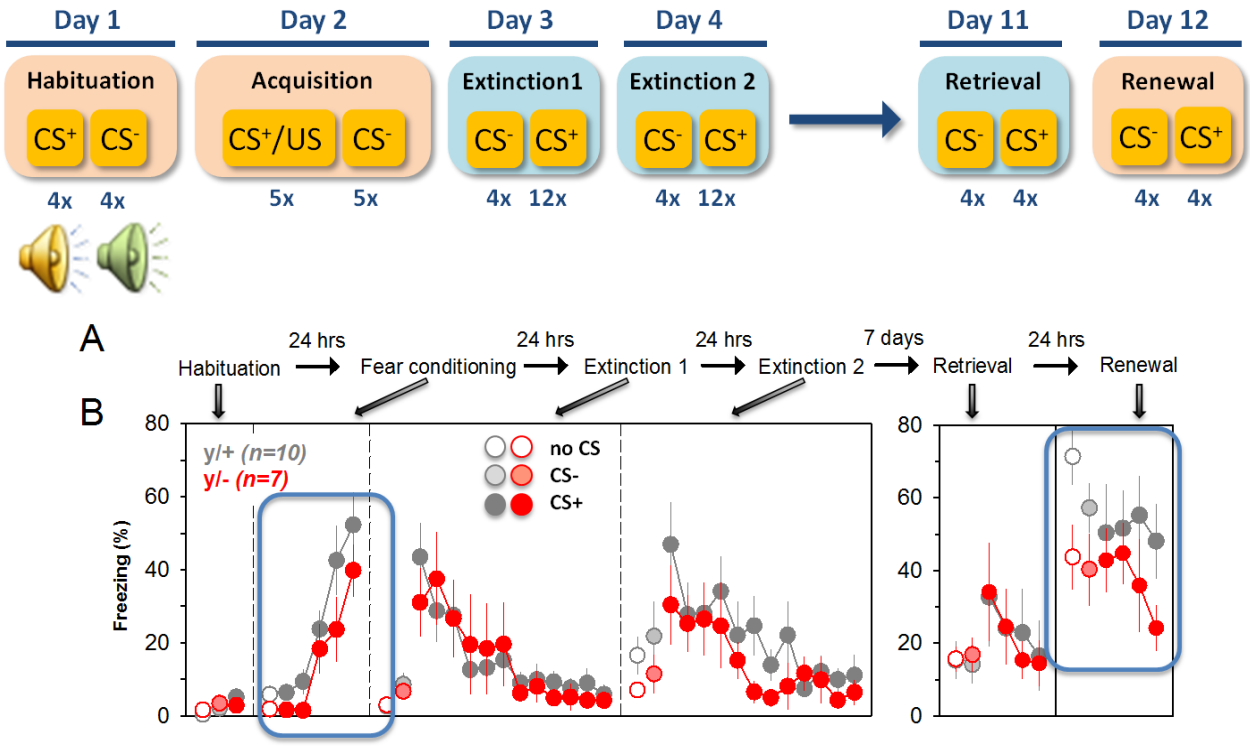

Figure 24: Scheme representing the initial full behavioral screening of fear behavior in a cohort of *Il1rapl1*-deficient animals (in red) and their WT littermates (in grey). First animals were habituated to the presentation of the CS+ (sound that will be coupled to the shock) and the CS- (control sound, not coupled to the shock) without presentation of foot shocks. Freezing levels were very low during this initial phase. The next day, animals were submitted to acquisition, which is the conditioning itself. During acquisition animals learn to associate the CS+ to the shock and freezing levels gradually increase. *Il1rapl1* KO animals presented a delay in the initiation of the fear response. The next two days animals were submitted to an extinction procedure consisting of presenting several times the CS+ without shock resulting in a gradual decrease of the fear response. Note that extinction is performed in another context to specifically look at the cued aspects of the fear memory. Retrieval is performed a week later and allows measuring the strength of the extinction memory. Both extinction and retrieval were similar between genotypes. Renewal consists of re-exposing animals to the conditioning context to measure contextual aspects of fear memory. I observed a strong deficit in *Il1rapl1* KO animals compared to their WT littermates.

1 Publication 1: "Target-specific vulnerability of excitatory synapses leads to deficits in associative memory in a model of intellectual disorder"

1.1 Results summary

Learning and memory capacity of *Il1rapl1* KO mice were determined by submitting animals to an associative cued fear learning paradigm. This behavioral task consists of pairing a neutral sound (conditioned stimulus, CS) with a noxious foot shock (unconditioned stimulus, US). The process during which animals learn to associate CS with US is called acquisition, resulting in a gradual increase of the fear reaction together with the number of CS/US pairings. During acquisition, an unspecific stress is also generated by the US repetition. Thus, sound-specific associative learning has to be measured by comparing freezing levels observed between CS- vs. Cs+ presentations. In contrast, 24 hours later, CS+/CS- presentations led to very different behavioral responses: only the CS+ led to freezing behavior whose strength is typically related to the intensity of the associative fear memory. *Il1rapl1*-deficient mice presented a slower acquisition of the task compared to their WT littermates, as reflected by lower freezing levels during CS/US pairings (publ. Figure 1). Recall of the fear memory was also lower in *Il1rapl1* KO animals, possibly reflecting lower fear acquisition in those animals (publ. Figure 1).

Because of the strong deficit in fear response exhibited by in *Il1rapl1*-deficient mice within the acquisition session, I decided to record for synaptic features in the main brain area responsible for acquisition of associative fear learning: the lateral amygdala (LA). I performed whole cell recordings of LA principal cells and tested synaptic properties and plasticity at major afferents carrying sensory information about CS and US, namely thalamic projections to the LA. Thalamo-LA synapses are thought to be the locus of associative plasticity mechanisms that mediate CS/US association, a lack of which would explain the lack of memory imprinting in *Il1rapl1* KO mice. As said above, the induction of this postsynaptic plasticity is strongly regulated by local inhibition, mainly originating through feed-forward inhibition carried by local interneurons in the LA. To determine whether absence of IL1RAPL1 affected information processing in the LA, I recorded both excitatory responses and feed-forward inhibitory transmission occurring on LA

principal cells following stimulation of thalamic projections in acute brain slices. Strikingly, following stimulation of thalamic projections, *Il1rapl1*-deficient mice presented lower evoked excitatory transmission onto LA principal cells (publ. Figure 3). However, a surprising accompanying result was that feed-forward inhibitory transmission reaching LA principal cells and evoked under the very same conditions remained unaffected, leading to an increase of the inhibitory/excitatory (I/E) balance in *Il1rapl1*-deficient mice (publ. Figure 3). In other words, the specific decrease of excitation leads to higher inhibitory drive in the LA of *Il1rapl1* mutant mice. Keeping in mind that feed-forward inhibition tightly controls plasticity on LA principal cells, I hypothesized that the shift in I/E balance following *Il1rapl1* removal could interfere with plasticity mechanisms essential for fear acquisition.

To test this, I performed *ex vivo* LTP experiments on brain slices of previously conditioned animals and compared them to non-conditioned animals (publ. Figure 2). *Ex vivo* electrophysiological studies principle is based on the fact that learning-induced and electrically-induced LTP elicited in slices share common mechanisms and may not occur twice at the same synapse. Then, if LTP already occurred *in vivo*, it will not be possible to induce it on slices of previously conditioned animals: a phenomenon called occlusion (Hong et al., 2012). Interestingly, unlike WT animals, conditioned *Il1rapl1*-deficient animals didn't show total occlusion of LTP, suggesting some deficits in learning-induced LTP during fear acquisition (publ. Figure 2). In naïve (non-conditioned) animals the amount of LTP that could be generated in absence of inhibition was similar between genotypes. Thus, this occlusion experiment strongly suggested that local I/E imbalance could perturb LTP induction during CS/US associations. Most importantly, this working model could be challenged *in vivo* using pharmacological and optogenetic approaches aiming at correcting or by-passing the inhibitory gate at the time of acquisition (publ. Figures 7 and 8).

The fact that the inhibitory component of LA principal cells carried by local feed-forward circuits was unaltered suggested us that the excitatory synapses onto the local LA interneurons must remain unaffected by IL1RAPL1 deficiency (publ. Figure 3). Thus to study excitatory synapses onto LA interneurons, we crossed the *Il1rapl1* KO mice with GAD-67-eGFP reporter line, thereby allowing to target GABA-ergic interneurons. Because highly heterogeneous in their intrinsic

properties, LA interneurons were classified based on several electrophysiological parameters to test for a possible effect of the mutation on a subclass of interneurons. No effect on excitatory transmission from long-range cortical and thalamic projections was observed for any of the subclasses of interneurons following *Il1rapl1* removal (publ. Figure 4). This led us to conclude that *Il1rapl1* removal had a differential impact on excitatory synapses, depending on the postsynaptic target (principal cell or inhibitory neuron). This could ultimately generate a local I/E imbalance impacting the capacity of the LA principal neurons to depolarize upon presynaptic discharge and thus to induce LTP induction at active synapses, leading to learning impairments in *Il1rapl1* KO mice.

With this working model in hands, we wanted to test if any functional I/E correction could be effective in restoring learning ability in *Il1rapl1*-deficient mice by acting on I/E imbalance just before fear acquisition (publ. Figure 7 and 8). The pharmacological strategy aimed at correcting I/E imbalance in LA by lowering inhibition with a $GABA_A$ blocker (bicuculline) just before the acquisition of the learning task. This treatment was able to restore normal learning in *Il1rapl1*-deficient mice, bringing their freezing to similar levels as their WT littermates (publ. Figure 7).

In addition to local intra amygdala bicuculline treatments, we used a less invasive method to test for the impact of I/E imbalance on fear acquisition. $GABA_A$ α5 subunit-containing receptors are expressed in LA and an inverse agonist has been used to lower $GABA_A$ α5 inhibition *in vivo*. Such strategy was shown to be effective in correcting spatial learning deficits in a mouse model of Down syndrome (Braudeau et al., 2011). Crucially, this drug is able to cross the blood brain barrier, opening the possibility to inject it intraperitoneally (IP). *In vitro* experiments on acute slices confirmed the reduction of IPSC amplitude following α5IA injection (Figure 25). Injecting the drug just before the acquisition of cued fear conditioning was also effective in restoring some aspects of fear learning. Indeed, we observed a normalization of freezing levels during recall in *Il1rapl1* KO animals (Figure 25), but not during acquisition (data not shown). Taken together, these pharmacological experiments strengthen a causal link between I/E imbalance and the learning deficit.

The optogenetic approach aimed at bypassing I/E imbalance in LA by directly depolarizing LA principal cells *in vivo* when the animal was submitted to the CS/US pairs (publ. Figure 8). Indeed, *in vitro* experiments suggested that LA principal neurons were hardly stimulated by incoming thalamic input and that could possibly be restored by Chr2 expression. Upon optogenetic "help" as well as during pure light/CS association, the amount of conditioned response was undistinguishable between genotypes, providing strong evidence that correcting I/E imbalance during the formation of new memories (CS/US association) is able to rescue behavioral deficits in *Il1rapl1* KO mice (publ. Figure 8).

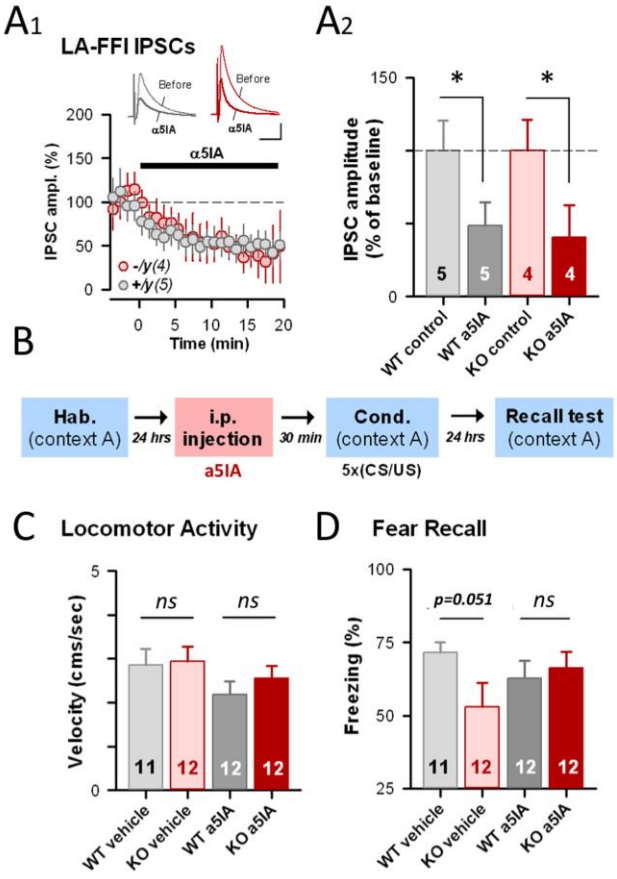

Figure 25: Blocking of GABA α5-containing receptors with an inverse agonist before cued fear acquisition. A: Application of the inverse agonist on acute brain slices lowered IPSC amplitude in both genotypes. B: Fear protocol and application of the inverse agonist just before conditioning. C: Locomotor activity was preserved between genotypes after drug application. D: Fear recall was normalized between genotypes after application of the drug.

1.2 Discussion

Using a combined approach at behavioral, cellular and synaptic levels I characterized the consequences of *Il1rapl1* deletion on cued fear related amygdala neuronal networks and could propose a scenario explaining the learning deficit in these mice: *Il1rapl1* mutation specifically impacted excitatory synapses onto principal cells, leaving connections to inhibitory cells intact. This led to a local I/E imbalance in LA by affecting associative LTP induction necessary for CS/US association. Importantly, behavioral deficits could be rescued by correcting I/E imbalance, suggesting that some cognitive features defining intellectual disabilities could be restored in the mature brain.

ID is often characterized by deficits in sensorimotor processing. To eliminate any possible confusion in my behavioral results due to possible consequences of *Il1rapl1* removal on sensorimotor function, I checked motor activity and general reaction to the shock (vocalization and jumping responses). These experiments revealed no differences in sensorimotor function between WT and KO animals (Figure 1 in paper). However, I cannot exclude that other components of sensorimotor function are impacted in *Il1rapl1* mutated mice. A more extensive behavioral screening of *Il1rapl1* KO mice would have been benefic to definitely eliminate any sensory (e.g. hearing) or motor deficits that could explain delay in the acquisition of fear memory. However, taken together, my experiments suggest that sensorimotor function is globally normal in *Il1rapl1 KO* mice and that the behavioral deficit could be directly linked to a local synaptic dysfunction. Furthermore, the pharmacological and optogenetic procedures are likely to act downstream of sensory processing and normalized fear acquisition in *Il1rapl1* KO animals. Indeed, optogenetic pairing of CS+ with light stimulation was able to induce artificial learning in both WT and KO animals, a protocol which is independent of US presentation and thus circumvents possible problems in sensory integration of the US.

The lower evoked excitation received by thalamic projections could indicate a lower number of functional synapses in LA. Interestingly, a study reported a decrease – even if really mild - in dendritic spine density in the hippocampus of *Il1rapl1* KO mice (Pavlowsky et al., 2010b). Using loading of LA principal cells in both genotypes, I quantified the morphology and density of

dendritic spines, but did not observe any evidence for such a defect in amygdala neurons. This was further corroborated by some electrophysiological measures where I recorded for miniature excitatory postsynaptic currents (mEPSC) in LA principal cells in both genotypes. Changes in frequency of miniature events inform about the number of functional synapses while amplitude informs about the number of postsynaptic receptors. I observed no differences for both amplitude and frequency between WT and KO animals (publ. Figure 5). Moreover, I didn't see any differences in AMPA/NMDA ratio. In contrast with my findings, over expression and knockdown of IL1RAPL1 in cultured hippocampal neurons led to an increase or decrease in frequency of miniature events respectively (Pavlowsky et al., 2010b). However, the same report didn't observe an effect on basal synaptic transmission parameters when recording from hippocampal brain slices. Given the space clamp limitations in LA principal cells and the mild effect seen on dendritic spine density in the hippocampus, I cannot exclude that some mild defect in dendritic spines may exist in the amygdala of *Il1rapl1*-deficient mice.

This is somehow paradoxical with the strong deficit in evoked excitatory transmission I have observed on LA principal cells (publ. Figure 3). This discrepancy may find its explanation at the molecular level. First, morphologically, the synaptogenic effect of IL1RAPL1 may be compensated by multiple redundancies supporting the formation of dendritic spines in the KO mice. Second, if still present, the synapses may not be fully functional and as robust as in normal mice. Indeed, by refining our observation to thalamic afferents contacting LA principal cells (which express VGLUT2 at the presynaptic level) we could show that VGLUT2 clusters opposed to PSD-95 puncta were of lower intensity in *Il1rapl1*-deficient mice, suggesting that those synapses may be particularly impacted by *Il1rapl1* mutation (publ. Figure 5).

Another possibility would reside in the replacement of synapses from long range projections by local synaptic contacts. Indeed, a theory was recently developed in order to explain functional deficits observed in adults suffering from neurodevelopmental disorders (NDDs): it states that long range connections are impaired in ID and/or ASD and that this is accompanied by local hyper-connectivity in other brain areas (Kroon et al., 2013). Thus, intra LA connectivity might be overdeveloped to compensate for dysfunctional long-range projections. Yet, I have no evidence that intra-LA connectivity is boosted in *Il1rapl1* KO mice. To demonstrate that, one would need

to record for pairs of principal neurons and compare connectivity parameters between genotypes.

Concerning the link between I/E imbalance and learning-induced LTP in LA, I could show that *Il1rapl1*-deficient mice have a deficit in LTP induction during fear acquisition. Indeed, brain slices of previously conditioned animals revealed a deficit in LTP occlusion in *Il1rapl1* KO animals. However, partial occlusion occurs in KOs, as LTP levels of conditioned animals didn't return to levels of naïve levels. This suggests that LTP was not completely induced *in vivo* in KO animals and that some LTP induction remains despite I/E imbalance in LA. In other words, I/E imbalance probably isn't severe enough to completely prevent LTP induction. The impairment of LTP induction in *Il1rapl1* KO mice is in line with previous observations in a Down syndrome mouse model presenting deficits in the induction of hippocampal LTP following increased inhibition in dentate gyrus (Kleschevnikov et al., 2004). Formation of associative memory might be impaired in other brain regions following absence of *Il1rapl1*, particularly when induction of LTP depends on feed-forward inhibition and more globally on local I/E balance.

However, with this *ex vivo* approach we couldn't differentiate cells that had been previously activated to create the memory trace with cells that didn't. Indeed, only a subpopulation of cells is believed to be recruited in a memory trace (see introduction) and *ex vivo* electrophysiology experiments don't allow discriminating between cells that were activated during fear acquisition or not. One way to circumvent this would be to use a model that allows the labeling of activated cells during learning, in order to patch recruited and non-recruited cells and possibly refine my results (but see general discussion). Nonetheless, it remains very surprising that occlusion of LTP in slices of previously conditioned WT animals is complete. Indeed, this means that all recorded cells show this occlusion contrasting with the theory that states that only a subpopulation of cells are recruited in a memory trace, and that a subset of synapses undergo plasticity. The mechanisms mediating this are still unknown but one can imagine that because of the strength of the US and the relative poverty of sensory experiences of laboratory animals, some neural circuits might become saturated, limiting any further plasticity mechanisms. Alternatively, neuromodulatory systems activated by fear learning could interfere with some plasticity mechanisms by currently unknown mechanisms.

Recordings of LA interneurons didn't reveal an effect of the mutation on excitatory synapses of interneurons although I did observe a tendency for lower excitation on regular spiking interneurons. In this regard, it would be particularly interesting to know which interneuronal populations provide feed-forward inhibition on LA principal cells. Knowing the importance of inhibitory neurons in the regulation of fear behavior and associated plasticity, disruption of a particular subtype of interneuron could have profound consequences on behavior. This was recently demonstrated in the LA by an elegant study showing the existence of disinhibitory circuits between parvalbumin and somatostatin interneurons in the control of cued fear learning (Wolff et al., 2014). To record for specific interneurons on brain slices, one can imagine crossing *Il1rapl1* KO mice with transgenic mouse lines in which specific subtypes of interneurons are labeled. This would allow studying the consequences of IL1RAPL1 absence on different categories of interneurons. Another possibility is to record for interneurons and realize post hoc labeling with specific antibodies directed against molecular markers of interneurons.

Pharmacological and optogenetic experiments aiming at correcting I/E imbalance were effective in restoring fear acquisition in *Il1rapl1* KO mice. Interestingly, the normalization of freezing behavior during the acquisition was only present at the end of CS/US pairings (publ. Figure 8). This could be explained by an incomplete blockade of inhibitory system that remains too efficient or a lack of excitation by incoming inputs at the first CS/US associations. Also, I cannot exclude that bicuculline spilled over, albeit slightly, in other amygdala nuclei and impacted fear learning in some way. Similarly, optogenetic approaches also led to unwanted effects: although freezing levels were normalized for CS+ presentations across genotypes (publ. Figure 8), we observed some fear generalization to the CS-. Thus, artificially boosting LA principal neuron activity probably interfered with CS+/CS- specificity. However, together, pharmacological and optogenetic experiments convincingly show a normalization of cued fear acquisition and recall after *in vivo* pharmacological manipulations of the LA ionotropic GABA-ergic system at the time of CS/US association.

1.3 Conclusion

This paper highlights the consequences of IL1RAPL1 absence in the capacity to acquire cued fear memory and how this relates to synaptic function (Figure 26). Acquisition of fear conditioning depends on synaptic integration on LA excitatory principal cells which is tightly regulated by local feed-forward inhibitory circuits. Here, I could built a working model after being in position to record for three different synaptic populations in the same circuit: excitatory thalamo-LA synapses on principal cells, feed-forward inhibition on LA principal cells and excitatory thalamo-LA synapses on interneurons. Interestingly, *Il1rapl1* mutation didn't impact all synaptic types. Indeed, evoked excitation was only lowered on LA principal cells and not on LA interneurons.

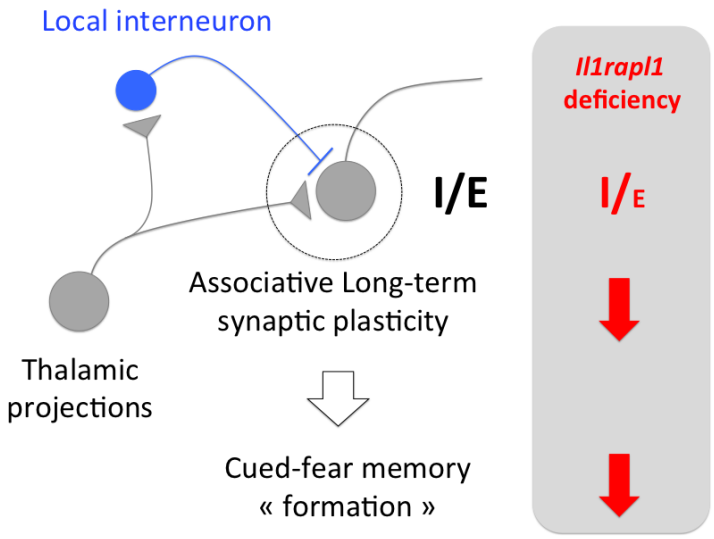

Figure 26: Scheme representing the consequences of *Il1rapl1* deficiency on behavior and synaptic function. Thalamic projections contact LA principal cells (in circle) and interneurons that provide FFI on principal cells. Excitatory synapses of LA principal cells were specifically affected, leading to a local I/E imbalance in LA. This I/E imbalance impacted associative long-term synaptic plasticity mechanisms necessary for the formation of the cued fear memory.

Thus, the identity of the postsynaptic cell defines the functional impact of *Il1rapl1* mutation, suggesting that excitatory synapses on principal cells and interneurons don't show the same vulnerability to IL1RAPL1 absence. In conclusion, the target-specific effect of IL1RAPL1 led to an imbalance between excitatory and inhibitory transmission in a crucial brain structure mediating

formation of associative fear memories. Most importantly, my paper suggests that learning and memory impairments in ID pathophysiology are more likely to be understood only if one can have access to multiple cellular and synaptic types in an isolated neuronal circuit.

Systems/Circuits

Target-Specific Vulnerability of Excitatory Synapses Leads to Deficits in Associative Memory in a Model of Intellectual Disorder

Xander Houbaert,[1]* Chun-Lei Zhang,[1]* Frédéric Gambino,[2] Marilyn Lepleux,[1] Melissa Deshors,[1,3] Elisabeth Normand,[3] Florian Levet,[4] Mariana Ramos,[5] Pierre Billuart,[5] Jamel Chelly,[5] Etienne Herzog,[1] and Yann Humeau[1]

[1]Team synapse in cognition, Institut Interdisciplinaire de Neuroscience, Centre National de la Recherche Scientifique CNRS UMR5297, Université de Bordeaux, 33077 Bordeaux, France, [2]Institut des neurosciences cellulaires et intégratives, Centre National de la Recherche Scientifique CNRS UPR3212, Université de Strasbourg, 67000 France, [3]Pole in vivo, Institut Interdisciplinaire de Neuroscience, Centre National de la Recherche Scientifique CNRS UMR5297, Université de Bordeaux, 33077 Bordeaux, France, [4]Team imaging the cell, Institut Interdisciplinaire de Neuroscience, Centre National de la Recherche Scientifique CNRS UMR5297, Université de Bordeaux, 33077 Bordeaux, France, and [5]Centre National de la Recherche Scientifique, Université Paris Descartes, Institut National de la Santé et de la Recherche Médicale, UMR8104, Institut Cochin, 75014 Paris, France

Intellectual disorders (IDs) have been regularly associated with morphological and functional deficits at glutamatergic synapses in both humans and rodents. How these synaptic deficits may lead to the variety of learning and memory deficits defining ID is still unknown. Here we studied the functional and behavioral consequences of the ID gene *il1rapl1* deficiency in mice and reported that *il1rapl1* constitutive deletion alters cued fear memory formation. Combined *in vivo* and *in vitro* approaches allowed us to unveil a causal relationship between a marked inhibitory/excitatory (I/E) imbalance in dedicated amygdala neuronal subcircuits and behavioral deficits. Cell-targeted recordings further demonstrated a morpho-functional impact of the mutation at thalamic projections contacting principal cells, whereas the same afferents on interneurons are unaffected by the lack of Il1rapl1. We thus propose that excitatory synapses have a heterogeneous vulnerability to *il1rapl1* gene constitutive mutation and that alteration of a subset of excitatory synapses in neuronal circuits is sufficient to generate permanent cognitive deficits.

Introduction

Learning-related forms of persisting synaptic plasticity (LTP) at excitatory synapses were initially discovered in the hippocampus (Bliss and Lomo, 1973). Although diverse in their molecular and cellular mechanisms, LTP has now been found in most brain areas, including amygdala (Rumpel et al., 2005). Meanwhile, >450 gene mutations have been identified as causing intellectual disorders (IDs) (van Bokhoven, 2011). Studies on human and animal models consistently reported that ID gene mutations primarily impact the morphology and/or function of excitatory synapses (Purpura, 1974). Remarkably, deficits in LTP in ID models remain poorly documented (Vaillend et al., 2008; Humeau et al., 2009), although an increasing number of ID gene products are involved in LTP-relevant signaling pathways (Pavlowsky et al., 2011).

In mammals, pairing an initially neutral stimulus (conditioned stimulus [CS]) with an aversive stimulus (unconditioned stimulus [US]) leads to the formation of a robust and long-lasting associative fear memory (Ledoux, 2000). During CS/US associations, long-lasting synaptic potentiation is induced at excitatory synapses impinging onto principal cells of the lateral nucleus of the amygdaloid complex (LA) (Rumpel et al., 2005; Humeau et al., 2007). Interestingly, the gating of this form of LTP is only possible in conditions lowering the influence of feedforward GABAergic inhibition (Bissière et al., 2003; Ehrlich et al., 2009), implying that a functional adaptation of the inhibition/excitation (I/E) balance is required to allow suprathreshold, postsynaptic depolarization during fear conditioning. Moreover, I/E balance alterations have been recurrently associated with neurological and ID animal models (Kleschevnikov et al., 2004; Dani et al., 2005; Baroncelli et al., 2011; Pizzarelli and Cherubini, 2011; Yizhar et al., 2011), including *il1rapl1* mutant mice (Gambino et al., 2009).

In humans, *il1rapl1* mutation leads to a spectrum of cognitive defects, ranging from nonsyndromic intellectual disorders to au-

Received April 3, 2013; revised July 20, 2013; accepted July 23, 2013.

Author contributions: J.C. and Y.H. designed research; X.H., C.-L.Z., F.G., M.L., M.D., E.N., P.B., and Y.H. performed research; F.L., M.R., and P.B. contributed unpublished reagents/analytic tools; X.H., C.-L.Z., F.G., M.L., and Y.H. analyzed data; E.H. and Y.H. wrote the paper.

This work was supported by Agence Nationale pour la Recherche (J.C., E.H., and Y.H.), the European Neuroscience Institutes Network (Y.H.), and the Gencodys FP7 program (Y.H. and J.C.). We thank Drs Shona Osborne, Cyril Herry, Andréas Lüthi, Julien Dupuis, and François Georges for their critical reading of the manuscript; Dr. Jiyun Peng for helping in the tracking of mouse activities; and the Pole In Vivo and animal facilities of the Bordeaux University for the animal care. The microscopy was done at the Bordeaux Imaging Center of the University of Bordeaux Segalen, with the help of Sébastien Marais and Magali Mondin.

The authors declare no competing financial interests.

*X.H. and C.-L.Z. contributed equally to this work.

Correspondence should be addressed to Dr. Yann Humeau, UMR5297 Institut Interdisciplinaire de Neuroscience, Centre de génomique fonctionnelle, 146 rue Léo Saignat, 33077, Bordeaux cedex, France. E-mail: yann.humeau@u-bordeaux2.fr.

F. Gambino's present address: Département des neurosciences fondamentales, CMU, Genève, Suisse.

DOI:10.1523/JNEUROSCI.1457-13.2013

 0270-6474/13/3313805-15$15.00/0

tistic spectrum disorders (ASDs) (Piton et al., 2008). Il1rapl1 is a member of a novel family of IL1/Toll receptors enriched at excitatory synapses (Pavlowsky et al., 2010). Il1rapl1 induces excitatory presynapse formation by interacting trans-synaptically with the protein tyrosine phosphatase δ (PTPδ) (Valnegri et al., 2011; Yoshida et al., 2011) but also interacts with some components of the postsynaptic density, such as PSD95, RhoGAP2, and Mcf2l (Pavlowsky et al., 2010; Valnegri et al., 2011; Hayashi et al., 2013), enabling morphological and functional maintenance of excitatory dendritic spines and glutamate receptor insertion (Hayashi et al., 2013). Il1rapl1 also regulates N-type voltage-gated calcium channel and neurite elongation in neuroendocrine cells through its interaction with the neuronal calcium sensor-1 (Gambino et al., 2007). Thus, current data support the notion that Il1rapl1 is important for the formation, maintenance, and function of excitatory synapses by converging presynaptic, postsynaptic, and trans-synaptic effects.

Yet, the consequences of *il1rapl1* deletion onto physiological properties of mature neuronal networks and related behavioral paradigms remain unexplored. Here we identified an I/E imbalance in the amygdala circuits of adult *il1rapl1* constitutive mutant mice, resulting from a heterogeneous vulnerability of excitatory synapses to Il1rapl1 removal. We then determined how these functional perturbations of amygdala circuit impact fear memory formation.

Materials and Methods

Animals

Most experiments were performed using male *il1rapl1−/y* and their control *+/y* littermates (2–3 months old, C57BL/6 background), housed in 12/12 LD with *ad libitum* feeding. Some crossings with GAD67-eGFP mice (Tamamaki et al., 2003) (kindly provided by A. Lüthi's laboratory, FMI, Basel, Switzerland) were made in house to allow visualizing amygdala interneurons. Every effort was made to minimize the number of animals used and their suffering. The experimental design and all procedures were in accordance with the European guide for the care and use of laboratory animals and the animal care guidelines issued by the animal experimental committee of Bordeaux Universities (CE50; A5012009).

Fear conditioning

Mice were housed individually in a ventilation area before the start of behavioral training. Animals were handled every day before the start of the experiment during a week. On day 1, animals were transferred to the conditioning context (Context A) for habituation. Both CS^+ (total CS duration of 30 s, consisting of 50 ms pips repeated at 0.9 Hz, pip frequency 7.5 kHz, 80 dB sound pressure level) and CS^- (30 s, consisting of white noise pips repeated at 0.9 Hz, 80 dB sound pressure level) were presented 4 times with a variable interstimulus interval (ISI). On day 2, we proceeded with the conditioning phase. The protocol consisted of 5 pairings of CS^+ with the US onset coinciding with the CS^+ offset (1 s foot shock, 0.6 mA, ISI 10–60 s). In all cases, CS^- presentations were intermingled with CS^+ presentations and ISI was variable over the whole training course. Cued memory was tested 24 h after conditioning by analyzing the freezing levels at the first CS^+ presentations in Context B (recall). Freezing behavior was quantified automatically in each behavioral session using a fire-wire CCD camera (Ugo Basile) connected to automated freezing detection software (ANY-maze, Stoelting). To test for animal exploration and activity, the animal displacement in the context was traced and analyzed with software programmed and provided by Dr. Jiyun Peng (Fudan, Shanghai, China).

Electrophysiology

Slice preparation. Standard procedures were used to prepare 300- to 330-μm-thick coronal slices from 4-week-old up to 2.5-month-old male wild-type or mutant mice following a protocol approved by the European and French guidelines on animal experimentation. Briefly, the brain was dissected in ice-cold artificial CSF (ACSF) containing the following (in mM): 124 NaCl, 2.7 KCl, 2 $CaCl_2$, 10 $MgSO_4$, 7 H_2O, 26 $NaHCO_3$, 1.25 NaH_2PO_4, 18.6 glucose, and 2.25 ascorbic acid; the brain was mounted against an agar block and sliced with a vibratome (Leica VT1200 s) at 4°C. Slices were maintained for 45 min at 37°C in an interface chamber containing ACSF equilibrated with 95% O_2/5% CO_2 and then for at least 45 min at room temperature before being transferred to a superfusing recording chamber. In the perfused ACSF, the $MgSO_4$ was decreased to 1.3 mM.

Recordings. Whole-cell recordings from LA principal neurons were performed at 30–32°C in a superfusing chamber as previously described (Humeau et al., 2005). Neurons were visually identified with infrared videomicroscopy using an upright microscope equipped with a 60× objective. Patch electrodes (3–5 MΩ) were pulled from borosilicate glass tubing and filled with a low-chloride solution containing the following (in mM): 140 Cs-methylsulfonate, 5 QX314 Cl, 10 HEPES, 10 phosphocreatine, 4 Mg-ATP, and 0.3 Na-GTP (pH adjusted to 7.25 with CsOH, 300 mOsm). For dedicated current-clamp experiments, Cs-methylsulfonate was replaced with equimolar K-gluconate. All LTP experiments were performed in the presence of picrotoxin (100 μM), except the no-PTX experiments shown in Figure 2. Monosynaptic EPSCs or EPSPs exhibiting constant 10–90% rise times and latencies were elicited by stimulation of afferent fibers with a bipolar twisted platinum/10% iridium wire (25 μm diameter). In all experiments, stimulation intensity was adjusted to obtain baseline EPSC amplitudes between 100 and 200 pA (CC mode) or 4–6 mV (IC mode). In some experiments, the capacitance of recorded cells was measured to evaluate the cell size. We used an exponential fit adjusted to the capacitive current generated by 100 ms/10 mV hyperpolarizing steps under the voltage-clampmode (see Fig. 4, seal tests).

LA interneuron classification. GAD-67-eGFP-expressing interneuron separation was based on the spiking patterns of recorded cells. To elicit spikes, cells were maintained at −70 mV in current-clamp mode and submitted to repeated, 400-ms-long, current steps of increasing intensity: −50, 50, 150, 250, and 350 pA, to explore a variety of potential response. In most cases, spiking inactivation was seen at the end of high intensity trains, indicating that the cell has reached its maximal spiking capacity. Otherwise, additional current injections of greater intensities were applied to reach spike inactivation. The last current step not inducing spike inactivation was retained for analysis. We analyzed neuronal discharge by measuring each spike amplitude and interspike intervals (ISI) observed during the train. IN classification was essentially based on the number of observed spikes (REG > BIM > ADA > SADA) and the degree of spike adaptation (last ISI/first ISI: BIM > ADA, SADA > REG). Occasionally, we also used spike half-width (REG < BIM < ADA, SADA) and the initial spike frequency (BIM > SADA, ADA, REG) to allow classifying some borderline cases.

Data acquisition and analysis. Data were recorded with a Multiclamp700B (Molecular Devices), filtered at 2 kHz and digitized at 10 kHz. Data were acquired and analyzed with pClamp10.2 (Molecular Devices). In all experiments, series resistance was monitored throughout the experiment; and if it changed by >15%, the data were not included in the analysis. Changes were quantified by normalizing and averaging EPSP slope during the last 5 min of the experiments relative to the 5 min of baseline before LTP induction or drug application.

Morphological analysis

In situ hybridization of il1rapl1 mRNA. This protocol was performed by a service company (Oramacell). Detection of each mRNA (VGLUT1, solute carrier family 17, member 7, slc17a7; NM_182993), glutamate decarboxylase 1 (gad1; NM_008077), and interleukin 1 receptor accessory protein-like 1 (il1rapl1; NM_001160403.1) was achieved by design of antisense oligonucleotides using Helios ETC oligo design software (Oramacell). For *il1rapl1* mRNA detection, two sets of oligonucleotides were designed: one specific for exon 5 (2 oligonucleotides) and one nonspecific of exon 5 (5 oligonucleotides). For slc17a7 and gad1 mRNA detection, a set of 3 oligonucleotides was designed for mRNA. Each oligonucleotide and a mix of two or three labeled oligonucleotides were tested for the hybridization step. Same results were obtained for each

mRNA for the four probes. *In situ* hybridization was performed as described previously (Moutsimilli et al., 2005). Briefly, oligonucleotides were labeled with [^{35}S]-dATP using terminal transferase to a specific activity of 5×10^8 dpm/μg. Experimental slides were fixed in 4% formaldehyde in PBS, washed with PBS, rinsed with water, dehydrated in 70% ethanol, and air-dried. Sections were then covered with 140 μl of a hybridization medium (Oramacell) containing 3–5 $\times 10^5$ dpm of the labeled oligonucleotide mix. Slides were incubated overnight at 42°C, washed, and exposed to a BAS-SR Fujifilm Imaging Plate for 15 d. The plates were scanned with a Fujifilm BioImaging Analyzer BAS-5000 and analyzed with MultiGauge software. Slides were then dipped in Kodak NTB emulsion, exposed for 6 weeks, developed and counterstained with toluidine blue.

Neurobiotin-based dendritic spine analysis. Amygdala-containing coronal sections (300 μm thick) in which LA principal cells were loaded with neurobiotin (0.02% in intracellular medium) for at least 20 min in open whole-cell configuration were first fixed in PFA 10% and then treated with PBS solution containing Triton 0.4% and 33 mM NaH_4Cl to block PFA aldehydic functions. Neurobiotin was then revealed using streptavidin-conjugated with AlexaFluor-568. Sections were then coverslipped with Vectashield, and *z*-stack images performed using confocal microscopy (Leica SP2, 63× oil-immersion objective) with a lateral resolution of ~200 nm. Spine number, spine length, spine head diameter, and spine type (mushroom, thin, stubby) were analyzed using Neuron Studio software (Rodriguez et al., 2008) (http://research.mssm.edu/cnic/tools.html). The first step consists of adjusting settings and software calibration to automatically detect dendritic spines. In all cases, automatic results were manually checked on the 3D reconstruction to delete false-positive and add nondetected spines. Values for each branch segment were expressed as spine number/μm.

Presynaptic and postsynaptic apposed clusters analysis. To prepare amygdala coronal sections, 3 and 3 *Il1rapl1* +/*y* and −/*y* mice were anesthetized with pentobarbital and fixed by intracardiac perfusion with 4% paraformaldehyde in PBS. The brains were dissected, postfixed during 24 h, and coronal, 50-μm-thick sections were obtained using a vibratome (Leica 1200 s). The brain sections were maintained in a blocking buffer (PBS solution containing 0.3% Triton X-100 and 2% gelatin) for 1 h at room temperature. Thereafter, sections were incubated at 4°C overnight with monoclonal antibody against PSD95 (1:600; Abcam, ab2723) and polyclonal antibodies against VGlut2 (1:10,000) from Millipore (AB2251) diluted in the blocking buffer. Slices were rinsed three times in PBS and incubated for 2 h at room temperature with Alexa488- and Alexa647-labeled goat anti-mouse or anti-guinea pig Ig G secondary antibodies (1:1000, Invitrogen), rinsed in PBS before being mounted with Vectashield.

Amygdala *z*-stacks were captured with confocal microscope (Leica SPE, 63× oil-immersion objective), at a constant depth from the surface. To compute apposition between the presynaptic and the postsynaptic staining, a plugin developed within ImageJ and based on wavelets transform was used to perform image processing and analysis. At first, each staining is segmented (by the use of "à trous" wavelets, see below) in a set of objects. Afterward, these two segmentations were used in a pixel-based technique to determine their appositions.

Segmentation. The input signal (i.e., the image) is analyzed by using the coefficients of a low-pass filter. Because wavelets are a multiresolution representation, the low-pass filter was stretched depending on the resolution level. As a result, each resolution level generated a different set of coefficients. To filter unwanted background noise while keeping details of interest, it was sufficient to directly set the threshold for the wavelet coefficient sub-bands in which the size of the filter is close to the size of the desired objects (in our case, there were the two first ones). Results of this filtering were two binary images (one for each staining) with clusters being identified as individual objects.

Apposition. To determine whether the presynaptic staining was apposed to the postsynaptic one at a given location, each cluster was tagged with a value: 0 for background, 1 for presynaptic, and 2 for postsynaptic clusters. A new image was created, which is the result of the addition of all the presynaptic and postsynaptic clusters. Once all the objects of this image were identified, we could easily determine whether there were apposed clusters. If an object was not composed of a single value (either 1 or 2), then it was an apposed cluster. Two cases were possible: if the two objects were touching themselves with no overlapping pixels, they were perfectly apposed. On the contrary, if some overlapping pixels were present, the objects were just apposed. In this study, all apposed events were counted. Because the technique is pixel-based, apposition was determined at the resolution level of the images.

Cannula implantation and drug administration

Cannula implantation. Stainless steel guide cannula (26 gauge; Plastics-One) were bilaterally implanted above amygdala under continuous anesthesia with isoflurane. Beforehand, mice were treated with buprenorphine (0.1 mg/kg, i.p) and positioned in a stereotaxic apparatus (David Kopf Instruments). The positions of bregma and λ points were defined and adjusted to the same horizontal level. Coordinates were as follows: LA, anteroposterior, −1.7 mm, mediolateral, ±3.1 mm, and dorsoventral, −2.8–3 mm. Cannula was secured to the skull using dental cement (Super-Bond, Sun Medical). In the end, the mice woke up on a 35°C heating pad, and a dummy cannula was inserted into the guide cannula to reduce the risk of infection.

Drug administration. To reduce stress during drug injection, the mice were trained with dummy cannula removal and insertion 1 week before use. To perform freely moving drug injection, the dummy cannula was replaced by an infusion cannula (33 gauge; connected to a 1 μl Hamilton syringe via polyethylene tubing) projecting out of the guide cannula with 1 mm to target LA. As previously described (Herry et al., 2008), the GABA-A receptor antagonist bicuculline (20 ng/200 nl in saline) was infused bilaterally at a rate of 0.1 μl/min in a volume of 200–250 nl per side by an automatic pump (Legato 100, Kd Scientific) 30–60 min before learning. To allow penetration of drug, the injector was maintained for an additional 3 min. After injection, mice were put back in the cages before behavioral testing. Importantly, no seizures were observed upon bicuculline treatment in all cohorts analyzed and presented here.

Controls. To analyze the location and extent of the injections, brains were injected with a fluorophore BODIPY TMR-X (Invitrogen; 5 mM in PBS 0.1 M, DMSO 40%). Then slices (60 μm) were imaged using a 5× epifluorescence microscope (Leica DM5000). The mice we considered for further analysis had at least one side precisely targeted above the LA and where each side was covered by >25% bodipy fluorescence.

Freely moving optical stimulation

AAV injections: adeno-associated viruses. AAV constructs and viruses were obtained from the U-penn Vector Core. We used AAV2/9 vectorsencodingforChR2-Venusexpression(AAV2/9.CAG.ChR2-Venus.W.SV40) (Addgene ref. 20071; $5.82E^{12}$ vector genomes, vg/ml). The injection of AAV-ChR2-virus was made through a guide cannula targeting the LA at least 2 weeks before behavioral testing (see above). Body weight and symptoms of sickness were monitored. One week before use, the mice were trained with dummy cannula removal and fiber insertion.

Optical stimulation and behavioral testing. To be tightly fixed to the guide cannula pedestal, an optical polymer fiber (200 μm of diameter, Prizmatix) was glued through an infusion cannula holder and assembled with a locking cap collar (Plastics One). The projection distance out of the guide cannula tip (1–1.5 mm) was set to allow positioning the fiber above the LA. One day before acquiring the associative fear, all the mice explored freely the Context A for 3 min and then habituated to tones. The following day, CS were delivered together with trains of blue light pulses (20 Hz, 30 s, 2 ms light pulses generated by pClamp10 software) produced by a 460 nm ultra high-power LED (UHP-460, Prizmatix) and terminated or not with US application (see Fig. 8). Then, mice were presented with CS^+ in another Context B (Recall), and the freezing response was analyzed.

Statistical analysis

Most data were analyzed using Student's *t* tests. However, when data were not following a normal distribution, we applied the Mann–Whitney rank-based statistical test. When studying the impact of two factors (genotype and treatment) in pharmacological rescue experiments (bicuculline), we used two-way ANOVA Student-Newman-Keuls *post hoc*

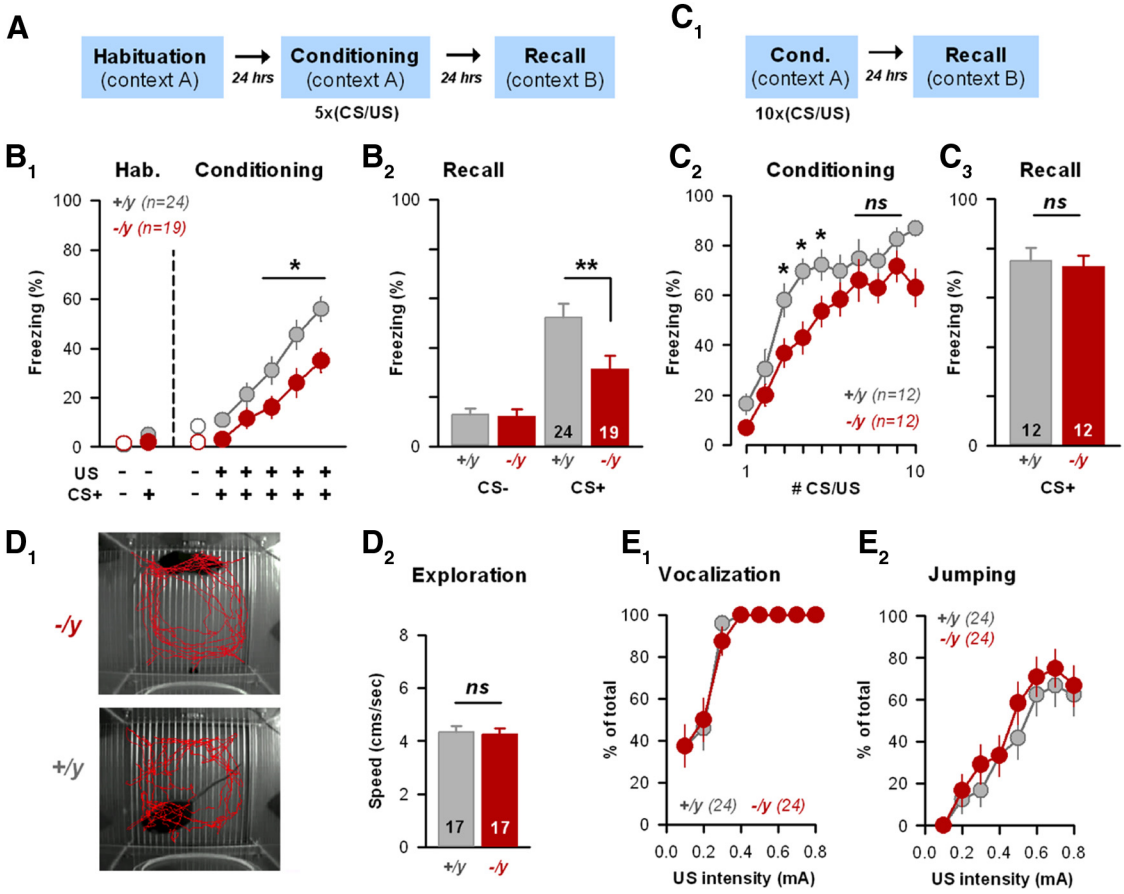

Figure 1. Deficits in cued fear learning in the absence of the ID-gene *il1rapl1*. ***A***, ***C*$_1$**, Behavioral paradigms. ***B***, ***C***, Freezing levels observed before and during CS/US pairings (***B*$_1$**,***C*$_2$**) or during the recall test (***B*$_2$**,***C*$_3$**) in *il1rapl1* WT (+/y, gray circles/bars) or KO (−/y, red circles/bars) mice submitted to normal (5 × CS/US) or reinforced (10 × CS/US) cued fear conditioning, respectively. The number of animals in each genotype is indicated. *$p < 0.05$. **$p < 0.01$. ns, Not significant. ***D***, Locomotor activity was tested in *il1rapl1* WT and KO mice during the exploration phase (first 2 min in the Context A) before CS presentations. No difference was detected between genotypes (***D*$_2$**). ***E***, Pain sensitivity was tested in WT and KO animals by scoring the vocalization (***E*$_1$**) and escaping responses (***E*$_2$**) for shocks of increasing intensities. WT and KO animals exhibited similar behavioral responses.

analysis to test for differences between groups of interest. Amplitude and frequency of spontaneous or miniature events were analyzed, and medians were directly compared as described above. Occasionally, cumulative distributions were compared using the nonparametric Kolgomorov–Smirnov test. Box plots in Figure 5 were done using SigmaPlot software (Systat Software).

Reagents

Picrotoxin was from Sigma-Aldrich, and QX-314 was from Alomone Labs. TTX was purchased from Latoxan and stock solution prepared in acetate buffer at pH 4.5. Bicuculline was purchased from Ascent Scientific.

Results

Deficits in cued fear learning in the absence of the ID-gene *il1rapl1*

Associative fear learning can easily be induced in rodents (Ledoux, 2000) and is classically monitored by measuring the degree of freezing reaction elicited upon subsequent presentations of the sole conditioning stimulus. We thus tested *il1rapl1*−/y and +/y littermates using a discriminative, associative fear learning/recall test paradigm (Fig. 1). After habituation in Context A, animals were submitted 5 times to 2 distinct tones: the CS$^+$ tone coupled to a foot shock (US) and an uncoupled CS$^-$ tone (see Materials and Methods). The following day, in another context (Context B), animals were submitted to a single CS$^+$ presentation (Recall, Fig. 1*A*,*B*$_2$). We first noticed that *il1rapl1*−/y animals exhibited a significant delay in expressing the conditioned fear response to the last three CS presentations (Fig. 1*B*$_1$; $p < 0.05$). Accordingly, when tested, the recall of cued associative memory was also altered in KO mice: *il1rapl1*−/y mice exhibited a lower fear response than their WT littermates while hearing the first CS (*il1rapl1*+/y, 47 ± 5%; *Il1rapl1*−/y, 29 ± 5%, $p < 0.01$; Fig. 1*B*$_2$). To test for an eventual deficit in memory retention, animals were submitted to a reinforced conditioning session (10 CS/US pairings, Fig. 1*C*). Interestingly, under these strong learning conditions, *il1rapl1* KO mice did not exhibit any deficit in both the level of freezing at the last CS/US presentations (CS/US$_{7–9}$, $p > 0.05$) (Fig. 1*C*$_2$) and during the recall test (*il1rapl1*+/y, 75 ± 5%; *il1rapl1*−/y, 73 ± 5%, $p > 0.05$, Fig. 1*C*$_3$). This indicates that, once formed, cued fear memory is well retained, and also that the potency of learning is preserved in the absence of *Il1rapl1*.

To avoid confusion from potential locomotor hyperactivity, we analyzed the mean distance run by the mice during the habituation/exploration period, which did not differ between KO mice and their WT littermates (Fig. 1*D*). In addition, we challenged the mice for pain thresholds: *il1rapl1*−/y and +/y animals started vocalization (Fig. 1*E*$_1$) and escaping–jumping responses (Fig. 1*E*$_2$) for the same shock intensity, indicating that pain sensitivity was not altered in *il1rapl1* mutant animals. Together, these results suggest that information processing within the amygdala may be impacted by *il1rapl1* mutation.

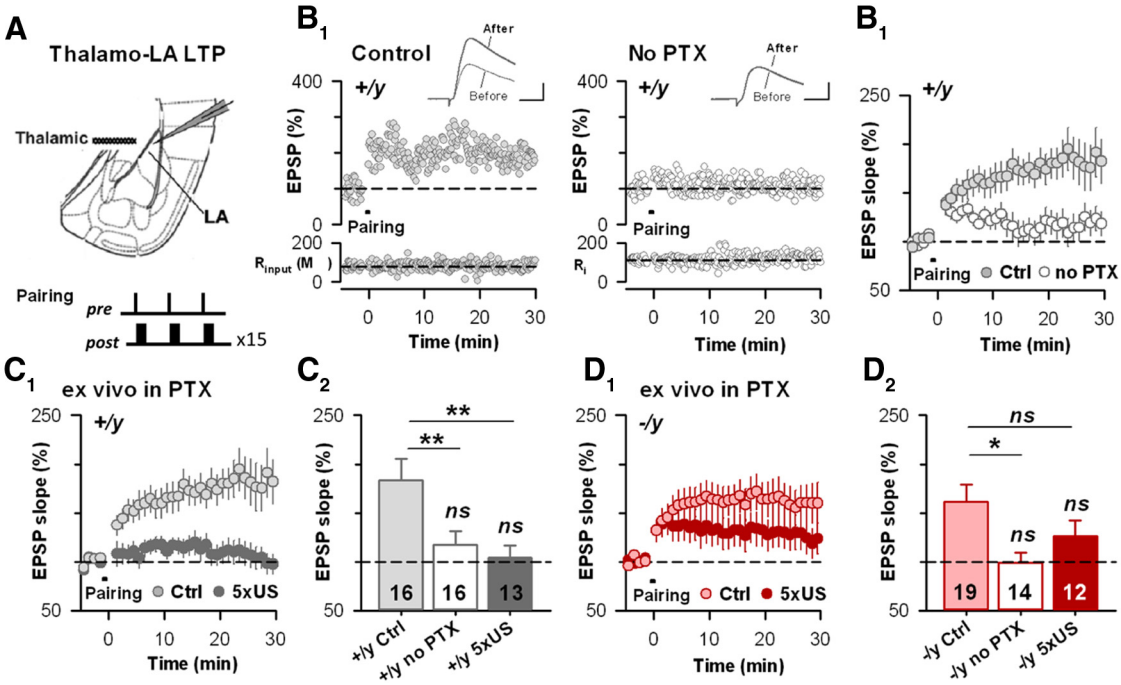

Figure 2. Constitutive *il1apl1* deletion impairs fear-learning associated LTP induction *in vivo*. ***A***, Scheme of the acute slice preparation with the positioning of recording and stimulating electrodes. The pairing protocol used to induce LTP is indicated. ***B*$_1$**, Typical time course of EPSP slope in WT animals after associative STDP-pairing application in control and no PTX conditions. Insets, Typical EPSPs. Calibration: 4 mV, 5 ms. ***B*$_2$**, Average time courses in both conditions in WT mice. ***C***, Fear learning mediates thalamo–LA LTP occlusion in *il1rapl1+/y* mice. ***C*$_1$**, Time course of thalamo–LA EPSP slope before and after pairing in *il1rapl1+/y* naive (Ctrl) and conditioned (5 × US) adult mice. ***C*$_2$**, Mean LTP in naive *il1rapl1+/y* in both control and no PTX conditions, and fear-conditioned *il1rapl1+/y* adult mice. $^{**}p < 0.01$. ***D***, Fear learning did not induce complete thalamo–LA LTP occlusion in *il1rapl1−/y* mice. ***D*$_1$**, Time course of thalamo–LA EPSP slope before and after pairing in *il1rapl1−/y* naive (Ctrl) and conditioned (5 × US) adult mice. ***D*$_2$**, Mean LTP in naive *il1rapl1−/y* in both control and no PTX conditions, and fear-conditioned *ll1rapl1−/y* adult mice. $^{*}p < 0.05$.

Constitutive *il1rapl1* deletion impairs fear associated LTP induction *in vivo*

Associative long-term synaptic plasticity at thalamo–LA synapses underlies the acquisition of fear conditioning (Rumpel et al., 2005; Humeau et al., 2007). Thus, the behavioral deficits observed in *il1rapl1*-deficient mice within the acquisition session must be linked to a decrease in the gating of amygdala associative synaptic plasticity. We therefore examined the induction of associative, postsynaptic LTP at thalamo–LA synapses *il1rapl1* KO and WT in acute brain slices (Fig. 2). At adult synapses, as in juveniles (Bissière et al., 2003), a robust LTP can be triggered by coincident bursts of preactivites and postactivities, but only in the presence of the GABAA-R antagonist PTX (100 μM) (Fig. 2*B*). Interestingly, when tested in these standard conditions, both *il1rapl1* WT and KO animals exhibited similar levels of LTP (*il1rapl1+/y*, 183 ± 23%; *il1rapl1−/y*, 161 ± 18%, $p > 0.05$; Fig. 2*C*,*D*), indicating that *il1rapl1* deletion did not alter the capability of thalamo–LA synapses to produce postsynaptic LTP.

Noteworthy, these experiments were conducted in the absence of ionotropic GABAergic transmission, therefore bypassing an eventual GABAergic modulation. Thus, to examine the occurrence of genuine thalamo–LA LTP *in vivo* during associative fear learning, we tested LTP levels in slices from fear-conditioned KO and WT animals. Indeed, it was previously reported that fear conditioning led to occlusion of thalamo–LA LTP in brain slices (Hong et al., 2011). *il1rapl1−/y* and *+/y* animals were first submitted to the associative fear conditioning described above (5 CS/US), and brain slices were prepared 24 h after the last CS/US presentation. Compatible with an effect of fear conditioning in both genotypes, LTP levels in conditioned animals were nonsignificant ($p > 0.05$ compared with baseline; Fig. 2*C*,*D*). However, while in conditioned WT mice, a pronounced occlusion of LTP was observed (*il1rapl1+/y* LTP_{naive}, 183 ± 23%; $LTP_{5CS/US}$, 104 ± 12%, $p < 0.01$) (Fig. 2*C*), LTPs obtained in naive and conditioned *il1rapl1* KO slices were not significantly different (*il1rapl1−/y* LTP_{naive}, 161 ± 18%; $LTP_{5CS/US}$, 126 ± 16%, $p > 0.05$). This indicates that fear-induced LTP occlusion is only partial in *il1rapl1* KO mice, probably because of a lower LTP induction *in vivo* during fear acquisition. We propose that this impairment of LTP induction could, at least partially, contribute for both the delay in fear acquisition and the deficit in the recall of cued fear memory observed in *il1rapl1*-deficient animals.

Increased I/E balance in LA principal cells is associated with *il1rapl1* mutation

Gating of AMPAR-mediated, NMDAR-dependent postsynaptic LTP requires the relief of the magnesium block of NMDA receptors through the firing of postsynaptic cells. Previous studies demonstrated the crucial role of local GABAergic interneurons in controlling the postsynaptic discharge (Pouille and Scanziani, 2001; Gabernet et al., 2005), thereby limiting the gating of synaptic plasticity through postsynaptic hyperpolarization (Bissière et al., 2003). Thus, we examined feedforward inhibition (FFI) in the LA of *il1rapl1* KO and WT mice after activation of major excitatory inputs (Fig. 3). To achieve that, LA principal cells were recorded at two different membrane potentials, −70 and 0 mV in physiological chloride, while stimulating thalamic excitatory fibers (Humeau et al., 2005; Gambino et al., 2010) (Fig. 3*A*). Through this electrophysiological manipulation of the membrane potential, we could isolate AMPAR-mediated excitation (EPSCs, at −70 mV) and GABAA-R-mediated inhibition (IPSCs, at 0 mV) based on their different reversal potential (Fig. 3*A*$_2$).

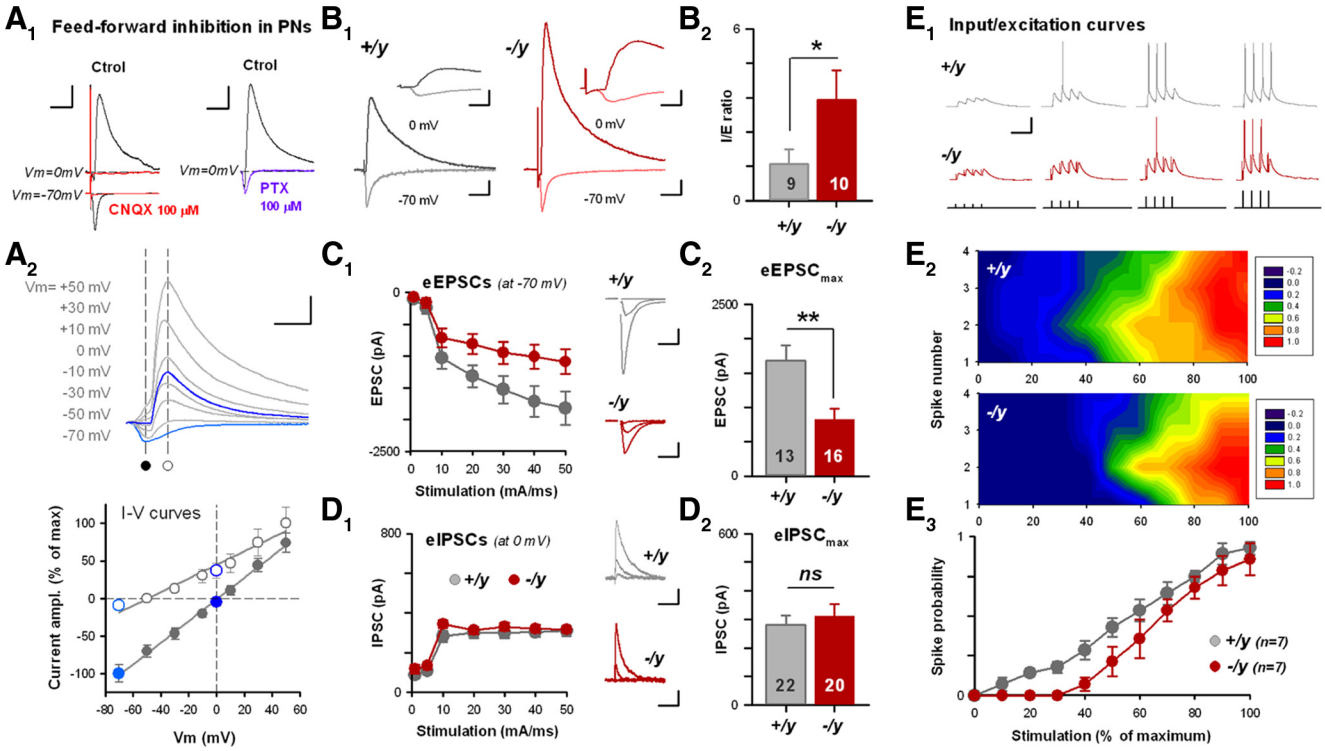

Figure 3. Increased I/E balance and lack of activation in LA principal cells are associated with *il1rapl1* mutation. ***A***, FFI measurements in LA principal cells. ***A*$_1$**, Pharmacological controls demonstrating that FFI is induced after thalamic fiber stimulations. ***A*$_2$**, AMPAR and GABAA-R-mediated PSCs can be isolated by their differential reversal potential. ***B***, FFI is increased in il1rapl1 KO mice (red traces). ***B*$_1$**, Typical FFI recordings using similar EPSC values. Calibration: top, 150 pA, 5 ms; bottom, 50 pA, 20 ms. ***B*$_2$**, Mean I/E ratio obtained at thalamo–LA synapses in +/*y* and −/*y* preparations. *$p < 0.05$. The number of recorded cells is indicated. ***C***, Evoked excitatory transmission at thalamo–LA synapses is affected by *il1rapl1* mutation. ***C*$_1$**, Left, average I/O curves. Right, Typical EPSCs recorded for 0.1, 1, and 10 mA stimulations in +/*y* and −/*y* preparations. Number of recorded cells is indicated. Calibration: 200 pA, 30 ms. ***C*$_2$**, Mean EPSC amplitude for 10 mA stimulations. **$p < 0.01$. ***D***, Same presentation as in ***C*** but describing thalamic-evoked IPSCs. Calibration: 100 pA, 60 ms. *ns*, Not significant. ***E***, Activation of LA principal cells by incoming thalamic excitation is decreased in *il1rapl1*-deficient mice. ***E*$_1$**, Typical recordings of LA-PNs V_m upon thalamic fiber stimulations of increasing intensity in +/y and −/y preparations. Calibration: 20 mV, 40 ms. ***E*$_2$**, Probability map of spike occurrence at each stimulation time point (1, 2, 3, or 4) and for each stimulation intensity (0–100%). Seven and seven cells were recorded in each genotype. ***E*$_3$**, Spike probability curve showing that LA cells are less efficiently activated by thalamic input in *il1rapl1*-deficient mice.

Accordingly, inward currents recorded at −70 mV were completely blocked by the AMPAR antagonist CNQX (100 μM; Fig. 3*A*$_1$, left), whereas the outward current recorded at 0 mV was sensitive to the GABAA-R antagonist picrotoxin (100 μM; Fig. 3*A*$_1$, right). Moreover, this last component was also sensitive to AMPAR blockade (Fig. 3*A*$_1$, left, at 0 mV), indicating the recruitment of local interneurons as a feedforward circuit (FFI). Importantly, I/V curves recorded in WT and KO preparations were similar and could be greatly approximated by a linear fit, indicating their correct measurements (data not shown).

To directly compare FFI in WT and KO preparations, we first elicited thalamo–LA EPSCs of comparable size in LA principal cells (at −70 mV, 130–60 pA, $p > 0.05$ between both groups) and compared the amplitude of the outward inhibitory current recorded at 0 mV (Fig. 3*B*). Strikingly, IPSCs were found to be significantly higher in KO preparations (Fig. 3*B*$_1$), and the I/E ratio was exacerbated in *il1rapl1* mutant mice (Fig. 3*B*$_2$). Theoretically, the increase of I/E balance (calculated here as a ratio) in *il1rapl1* KOs could result from an increase in inhibitory, or a decrease in the excitatory, transmission onto LA principal cells. To refine our observation, we compared eEPSC and eIPSC amplitudes for increasing stimulation intensities (Fig. 3*C*,*D*). As shown in Figure 3*C*, input/output (I/O) relationships of thalamo–LA eEPSCs were clearly impacted by *il1rapl1* mutation ($eEPSC_{max}$, $p < 0.01$). Thus, recurrent to some observations in pyramidal cells in hippocampus (Pavlowsky et al., 2010), the absence of Il1rapl1 led to a reduction of glutamatergic transmission in pyramidal cells. In stark contrast, inhibitory I/O curve was not modified by the mutation (Fig. 3*D*), indicating that the observed change in the I/E ratios (Fig. 3*B*) can be mostly attributed to a decrease in the excitatory component.

To assess for the functional consequences of these synaptic defects on amygdala output, we tested the ability of thalamic inputs to elicit spike discharges in LA principal neurons (Fig. 3*E*). Bursts of 4 presynaptic stimulations (at 20 Hz) were applied at various intensities and eventual postsynaptic spikes counted. Noteworthy, in KO preparations, the first generated spikes occur for greater stimulation intensities than in WT preparations (Fig. 3*E*), suggesting that *il1rapl1* mutation lowers LA-PN activation by incoming thalamic synaptic inputs.

Impact of *il1rapl1* deletion onto excitatory synaptic inputs to LA interneurons

Local interneurons of the LA account for ~20% of cell bodies (McDonald, 1982), tightly regulating principal cell excitability by providing strong feedforward inhibition (Szinyei et al., 2000; Chu et al., 2012). Moreover, accumulating evidence points for a role of GABAergic transmission in regulating fear conditioning (Ehrlich et al., 2009). To answer whether *il1rapl1* mutation had a specific impact on excitatory level reaching interneurons, we crossed *il1rapl1* mutant mice with GAD67-eGFP transgenic mice (Tamamaki et al., 2003), making it easy to visualize interneurons with fluorescence (Fig. 4*A*$_1$). Interneurons, although highly variable in their electrophysiological parameters and expression of specific

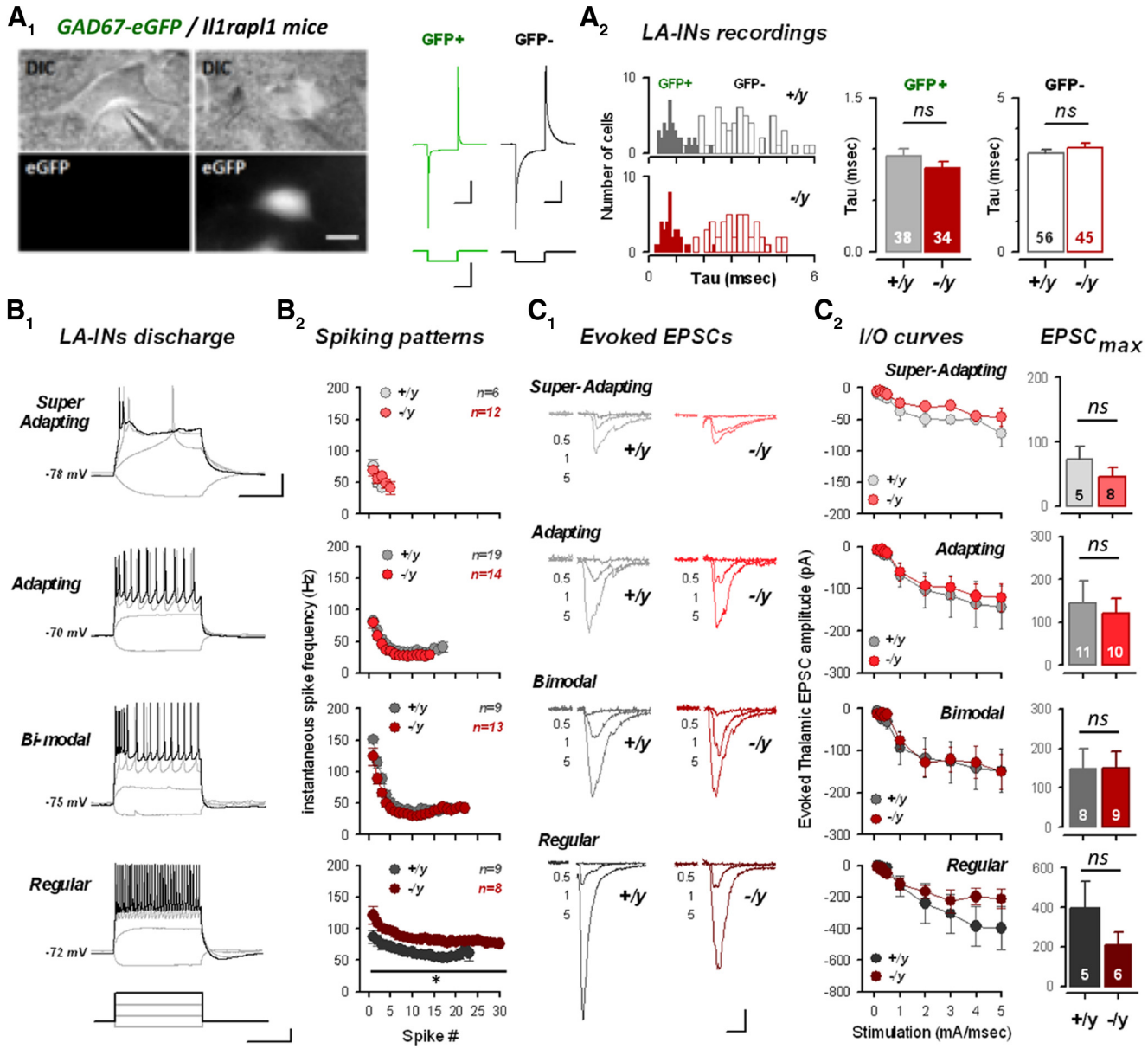

Figure 4. Excitatory transmission onto amygdala interneurons is preserved in *il1rapl1*-deficient mice. ***A***, Amygdalar GABAergic neurons were directly visualized and recorded by GFP fluorescence after crossing *il1rapl1* mutant mice with GAD67-eGFP mice (see Materials and Methods). ***A*$_1$**, Principal cells can be separated from interneurons by looking at cellular capacitance during the seal test. ***A*$_2$**, Density and capacitance of GABA-ergic (GFP$^+$) and principal (GFP$^-$) cells in Il1rapl1 WT and KO preparations. Number of recorded cells is indicated. ***B***, Spiking patterns of LA interneurons. ***B*$_1$**, LA interneurons were classified in four subclasses based on spiking behavior (for a detailed description of interneuron classification, see Materials and Methods). ***B*$_2$**, Mean spiking frequency against spike number for each subclass of interneuron. ***C***, Excitatory evoked transmission of LA interneurons after thalamic stimulation. ***C*$_1$**, Mean EPSC amplitude for 0.5, 1, and 5 mA stimulations in WT and KO interneurons. Calibration: 100 pA, 20 ms. ***C*$_2$**, Left, I/O curves of LA interneurons for a 5 mA stimulation in WT and KO interneurons. Right, Mean EPSC amplitude at 5 mA stimulation intensity for all LA interneurons. Number of recorded cells is indicated.

biological markers (Spampanato et al., 2011), could be distinguished from principal cells by cellular capacitance. Indeed, measurement of the exponential τ of the cellular response to a −10 mV voltage jump revealed a clear segregation with principal cells, a parameter that was not itself modified by *Il1rapl1* mutation for both cell populations (Fig. 4*A*$_2$). Interneurons were classified in different subclasses based on a previous study looking at diverse electrophysiological parameters of LA interneurons (Sosulina et al., 2010). Indeed, mRNA expression of different calcium binding proteins and neuropeptides was not very conclusive to further classify these populations (Sosulina et al., 2006). Thus, interneurons were assigned to a specific population looking solely at electrophysiological parameters (see Materials and Methods). To that end, we performed whole-cell patch-clamp recordings in current-clamp mode from GFP-expressing LA cells in *il1rapl1* KO and WT mice (Fig. 4*B*,*C*). Combined analysis of spiking pattern and other electrophysiological parameters allowed us to separate interneurons into four classes (Fig. 4*B*$_1$). Superadapting neurons showed a few spikes in the beginning of the depolarizing pulse before exhibiting spike failure/adaptation. Adapting neurons were characterized by a strong adaptation of spiking pattern during the depolarizing current step. Bimodal neurons, on the other hand, started spiking in a burst-fashion manner before adapting their firing pattern. Finally, regular spiking neurons were characterized by very low spike adaptation (Fig. 4*B*$_1$). Apart from superadapting neurons, all our subclasses share common

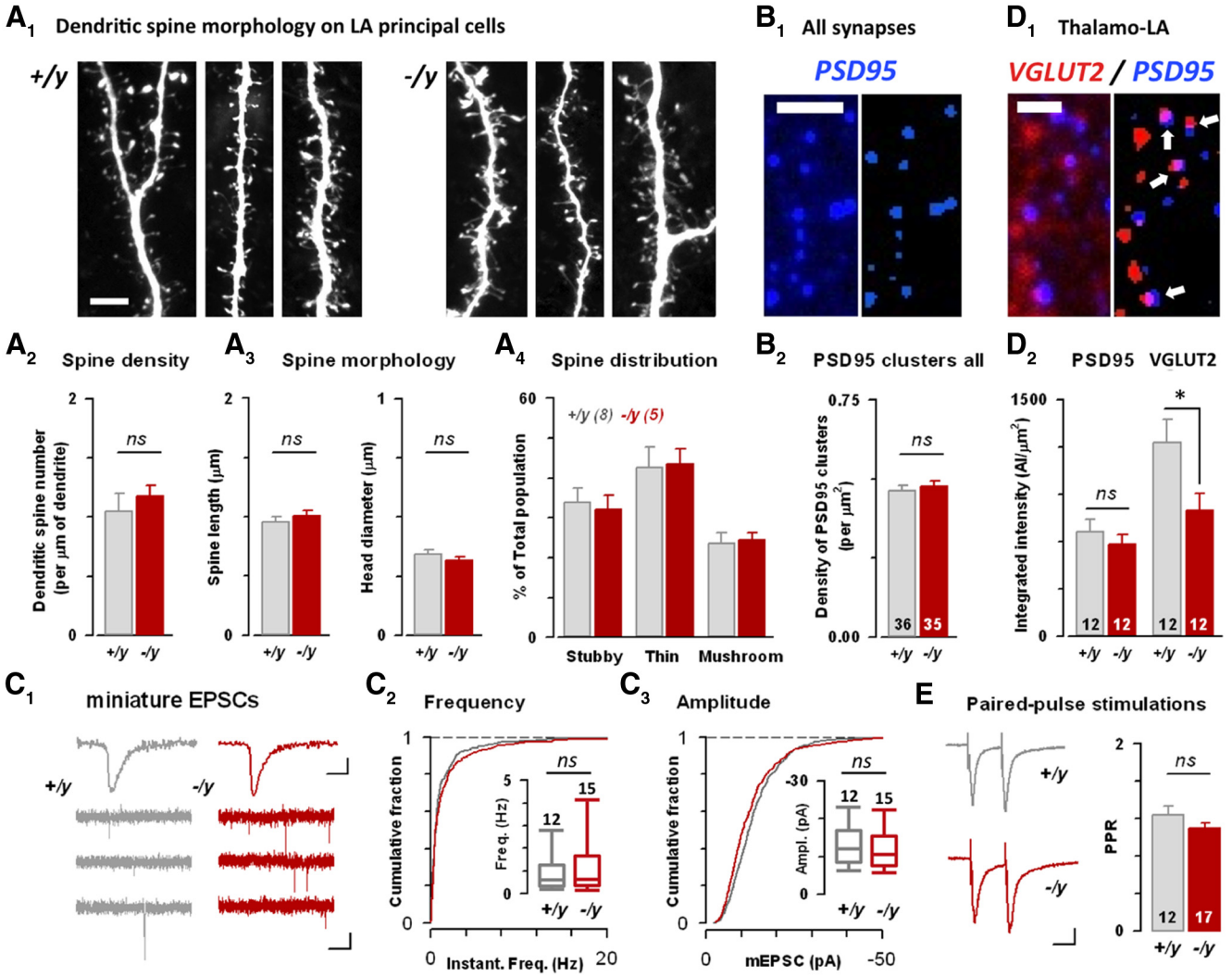

Figure 5. Morphology of LA excitatory synapses in constitutive *il1rapl1* mutant mice. ***A***, Morphology of LA principal cell dendrites is preserved in *il1rapl1*-deficient mice. ***A*$_1$**, Portions of neurobiotin-filled LA principal cell dendrites were analyzed and compared between genotypes. ***A*$_{2-4}$**, Analysis of spine density, morphology, and distribution of different spine types. ***B***, Morphological examination of LA synaptic contacts. ***B*$_1$**, Typical immunolabeling against PSD95. ***B*$_2$**, Density of PSD95 clusters for both genotypes. ***C***, Miniature EPSC recordings on LA principal cells for both genotypes. ***C*$_1$**, Representative trace of mEPSC recordings in both genotypes. ***C*$_{2-3}$**, Cumulative distribution of mEPSC frequency and amplitude for both genotypes. Insets, Medians of frequency and amplitude, respectively. ***D***, Putative synapses were identified as closely apposed VGLUT2/PSD95 clusters (see Materials and Methods). Scale bars, 2 μm. ***D*$_1$**, Typical immunolabeling showing apposed PSD95/VGLUT2 clusters. ***D*$_2$**, Integrated intensity of PSD95 and VGLUT2 in apposed clusters for both genotypes. $^*p < 0.05$. ***E***, Paired pulse recordings for both genotypes. PPR was calculated as the ratio of the second response to the first one.

electrophysiological parameters with previously defined subtypes of LA interneurons (Sosulina et al., 2010). In both genotypes, plotting spiking frequency against spike number showed clear differences in the spiking behavior of these different populations (Fig. 4*B*$_2$); no differences were observed between genotypes, except for regular spiking neurons, which display a higher frequency in KO animals ($p < 0.05$). Next, we assessed excitatory signals reaching those categories by constructing I/O curves after thalamic stimulation (Fig. 4*C*). In stark contrast with the situation found in LA principal cells, none of the interneuron groups displayed significantly different I/O curves between WT and KO preparations (Fig. 4*C*). Noteworthy, superadapting and regular-spiking neurons exhibited a tendency to a decrease of thalamic EPSCs, which remained nonsignificant ($p = 0.093$ and $p = 0.217$, respectively). We raise two major conclusions from these genetically driven recordings: (1) the lack of impact of *il1rapl1* mutation onto excitatory transmission in LA interneurons may largely contribute to the increase of FFI described above (Fig. 3); and (2) Il1rapl1 may play a functional role in the postsynaptic compartment, as LA recordings involving the same presynaptic but different postsynaptic compartments exhibited or not a functional impact of the mutation (see also Discussion).

Morphological and functional characterization of excitatory synaptic inputs to LA principal neurons in *il1rapl1* WT and KO mice

We next performed morphological analysis of dendritic spines from LA principal cells to determine whether Il1rapl1 plays a role in synapse formation and/or maturation in the amygdala (Fig. 5). We filled LA principal cells with neurobiotin during whole-cell patch-clamp recordings and thoroughly analyzed dendritic spine density and morphology after fixation (see Materials and Methods) (Fig. 5*A*). Using this method, we could not find any differences between genotypes (Fig. 5*A*), which was in good line with two other observations. First, global analysis of PSD95 cluster density using immunocytochemistry did not allow separating

WT and KO preparations (Fig. 5*B*). Furthermore, no impact of the mutation on mEPSC frequency or amplitude recorded in LA principal cells could be detected (Fig. 5*C*), thus suggesting that the amygdala neuropile was not strongly affected by the removal of Il1rapl1.

Then, taking benefit of differential VGLUT1/VGLUT2 expression in amygdala-projecting brain structures (Fremeau et al., 2001), we specifically examined the morphology of thalamo–LA (expressing VGLUT2) synapses by analyzing the intensity of apposed VGLUT2/PSD95 clusters (Fig. 5*D*) (see Materials and Methods). Strikingly, in PSD95/VGLUT2 appositions, the VGLUT2 levels were significantly lower in *il1rapl1* KO mice (−35% of integrated intensity; Fig. 5D_2, bottom, $p < 0.05$), whereas PSD95 clusters were unaffected (Fig. 5D_2). As these results point to an impact of the mutation at the presynaptic level, we compared paired pulse recordings at thalamo–LA synapses but failed to detect changes in presynaptic release probability (Fig. 5*E*). Thus, our data suggest that Il1rapl1 controls both functional and morphological parameters at thalamo–LA excitatory synapses.

Ubiquitous distribution of *il1rapl1* mRNA in neuronal populations of amygdala

To get some insights on the rationale to *il1rapl1* −/y induced I/E imbalance, we then set out to examine the distribution of *il1rapl1* mRNA in the brain. Previous work raised some evidence for *il1rapl1* expression in olfactory bulb, hippocampus, and cortex (Carrié et al., 1999). However, no robust and detailed demonstration of *il1rapl1* expression pattern has yet been published. We thus performed *in situ* hybridization of *il1rapl1*, together with *vglut1* and *gad67*, to allow for the comparison of its relative expression in inhibitory and excitatory brain regions. Indeed, *vglut1* labels the major glutamatergic population of cells in the cortical forebrain regions (Fig. 6*A*,*C*), whereas *gad67* labels all GABAergic neurons in the brain (Fig. 6*A*,*B*). Slides were first exposed to phosphor imager screen (Fig. 6*A*), and then the cellular resolution was obtained through dipping into photographic emulsion combined with toluidine blue counter staining (see Materials and Methods). *il1rapl1* was probed using 7 oligonucleotides spread over the different exons of the gene. All probes provided the same profile of expression. As expected, probe number 6 (data not shown) and 7 raised within the deleted exon 5 provided no signal when incubated over *il1rapl1* −/*y* slices (Fig. 6*A*). Overall, *il1rapl1* expression was very low compared with that of *vglut1* or *gad67*. Higher expression levels were recurrently seen in olfactory bulbs (data not shown) and in dentate gyrus of the hippocampus (Fig. 6*A*). In the amygdaloid complex, expression spans all excitatory (basolateral amygdala) and inhibitory (intercalated cells and central amygdala) regions homogeneously. Regional observations were confirmed by the investigations on slides at the cellular levels (for better visualization, silver dots were converted to red in Fig. 6*B–D*). Although GABAergic and glutamatergic territories are well delineated in Figure 6*B*, *C*, *il1rapl1* specific pattern appeared homogeneously distributed ruling out the possibility for a selective lack of expression in one or the other subclass of neurons (see quantifications in Fig. 6*B–D*). However, a specific lack of expression in a subclass of interneurons cannot be ruled out.

Cued fear learning is rescued by preconditioning infusion of GABAA-R blockers in the LA of *il1rapl1*-deficient mice

Yet, a scenario emerges in which *il1rapl1* KO mice's impairment in associative learning is the result of exacerbated I/E balance in the LA during CS/US association. *Ex vivo* experiments suggest that this could in turn lead to lower LTP induction in *il1rapl1* KO animals. The next series of experiments aimed at normalizing behavior in KO mice by restoring I/E balance before learning. In this line, previous studies used local or systemic treatment increasing GABAergic transmission to interfere with the acquisition or expression of the conditioned fear response (Sanger and Joly, 1985).

We thus depressed intra-LA GABAA-R-mediated inhibition during the CS/US association (Fig. 7) by infusing the specific antagonist bicuculline into the LA of *il1rapl1*−/*y* and +/*y* littermates before conditioning (Fig. 7). To that end, mice were chronically implanted above the LA (guide cannula positions in Fig. 7*B*), and local infusion of bicuculline was performed bilaterally 30–60 min before the fear conditioning session (see Materials and Methods). Importantly, first attempts using doses previously used in rats (50 ng/200 nl per side) were readily leading to epileptic seizures immediately after infusion (Berlau and McGaugh, 2006). We thus lowered the dose to 20 ng/200 nl and retained only the animals in which the guide cannula tips were immediately above the LA to avoid unspecific effects (Fig. 7*B*). With these safeguards, no obvious seizures were observed during the drug treatment, although we noticed a slight effect of drug treatment on animal locomotor activity (ANOVA, $F_{(1,53)} = 8{,}115$; $p = 0.006$) (Fig. 7*C*). However, there was no difference in general locomotion between WT and KO-treated animals (SNK *post hoc*, $p = 0.706$), thus allowing comparing the behavioral consequences of the treatment in both genotypes. We then compared the freezing levels obtained during and 24 h after the fear conditioning session and compared with nonimplanted mice (Fig. 7*D*,*E*). Although we present the whole acquisition curve, bicuculline treatment did not reach significance until the fifth CS presentation, and comparisons between groups were done at this time point. Two-way ANOVA revealed an interaction effect between genotype and treatment (ANOVA, $F_{(1,57)} = 5{,}043$; $p = 0.029$). In control animals, as shown before, the fear response exhibited by KO mice at the fifth CS/US presentation during the conditioning session was lower than their WT littermates (SNK *post hoc*, $p = 0.011$) (Figs. 1*A*, 7*D*). Strikingly, in bicuculline-treated animals, freezing levels at the fifth CS/US presentation were found indistinguishable between genotypes (SNK *post hoc*, $p = 0.399$), and a significant effect of the treatment was found in KO (SNK *post hoc*, $p = 0.002$) but not WT animals (SNK *post hoc*, $p = 0.850$). When looking at freezing levels during recall, we noticed a significant interaction between genotype and drug treatment (ANOVA, $F_{(1,57)} = 4{,}820$; $p = 0.032$), leading to a normalization of the freezing deficit (control, SNK *post hoc*, $p = 0.008$; treated, SNK *post hoc*, $p = 0.479$; Fig. 7*E*). Normalization of acquisition only became significant at the fifth CS presentation, probably because of incomplete blockade of inhibitory system or a lack of excitation by incoming inputs at initial CS/US associations. However, together, these observations convincingly show a normalization of cued fear acquisition and recall after *in vivo* pharmacological manipulations of the LA ionotropic GABAergic system at the time of CS/US association.

Accordingly, bicuculline treatment in conditioned *il1rapl1* −/*y* mice also restored thalamo–LA LTP occlusion (*il1rapl1*−/*y*: LTP_{naive}, 161 ± 18%, $LTP_{5CS/US+bicu}$, 88 ± 8%, $p < 0.05$; Fig. 7*F*). These results indicate that restoring I/E balance before learning may suffice to allow LTP induction *in vivo* in *il1rapl1* KO animals. We thus propose the existence of a causal link between the deficit in associative learning, the failure of LTP induction, and I/E imbalance within the lateral amygdala.

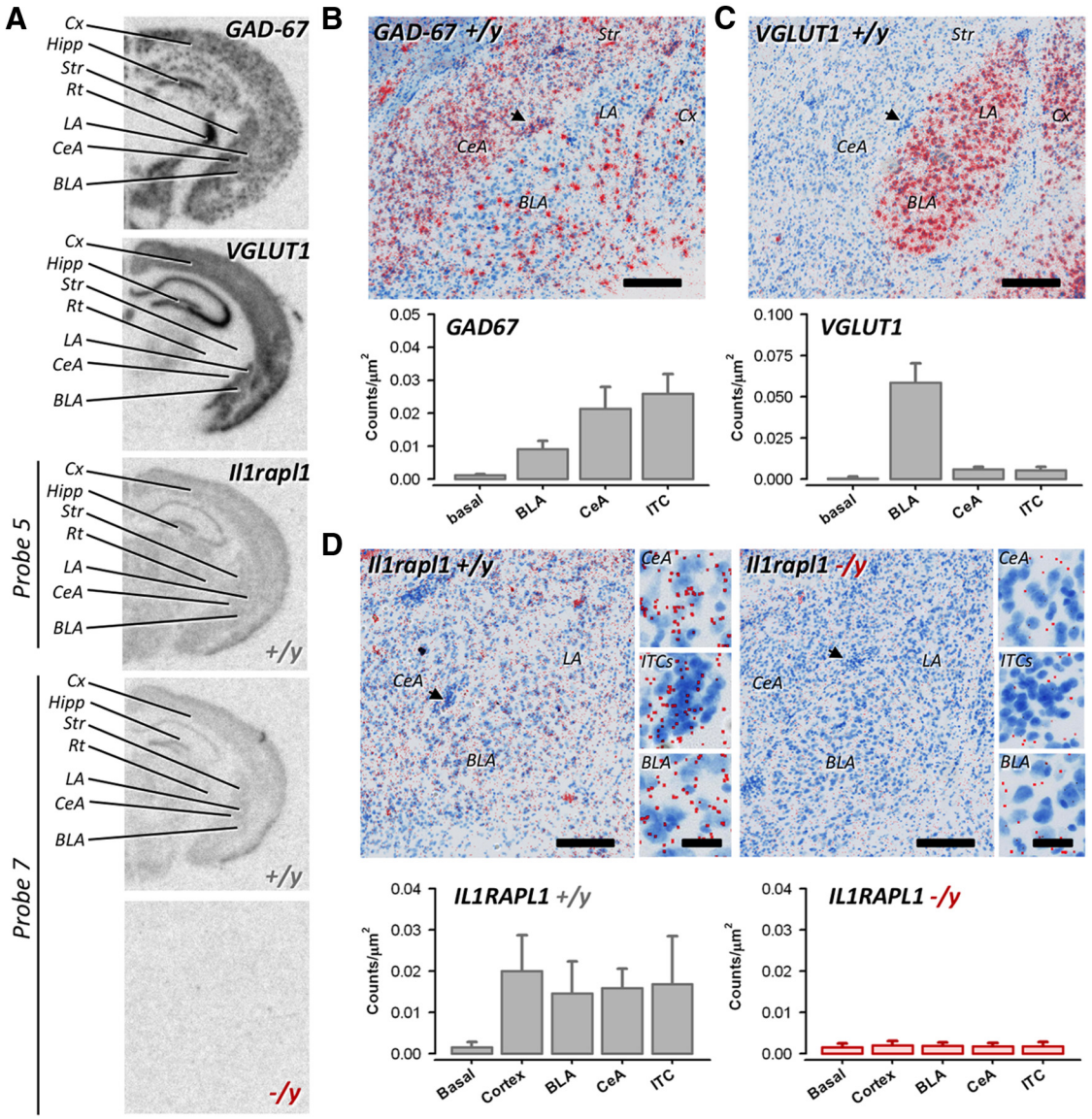

Figure 6. Ubiquitous distribution of *il1rapl1* mRNA in amygdala neurons. ***A***, Regional distribution of *gad67*, *vglut1*, and *il1rapl1*. *il1rapl1* was probed with 7 oligonucleotides; here probe 5 and 7 are shown. Probe 7 is specific of the exon 5, deleted in the knockout model. There is absence of signal when probe 7 is incubated on −/*y* slices. ***B–D***, Emulsion dipping of slices from ***A***. Silver dots were systematically masked and converted to red for display purpose. ***B***, Cellular distribution of *gad67* mRNA in the amygdala. There is dense labeling in the central nucleus, whereas sparse interneurons are depicted in the basolateral divisions. ***C***, Cellular distribution of *vglut1* mRNA in the amygdala. There is dense labeling of neurons in the basolateral division, whereas the central nucleus is devoid of labeling. ***D***, Cellular distribution of *il1rapl1* mRNA in the amygdala. Lower expression levels are detected compared with *gad67* and *vglut1*, but −/y slices display much lower background signals (right panels). *il1rapl1* expression covers all divisions of amygdala. Arrows point to ITCs. Scale bars: 250 μm; insets, 30 μm. Cx, Cortex; hipp, hippocampus; Str, striatum; Rt, reticular nucleus of the thalamus; LA, lateral amygdala; CeA, central amygdala; BLA, basolateral amygdala; ITC, intercalated cells.

Direct optical activation of LA cells during acquisition of associative cued fear normalizes fear learning in *il1rapl1*-deficient mice

During associative fear learning, US is thought to act as a detonator inducing depolarization and firing of LA principal cells, instructing plasticity at synapses conveying the CS onto the same cells (Rosenkranz and Grace, 2002; Maren, 2005). This phenomenon was spectacularly demonstrated recently by Johansen et al. (2010): by pairing auditory CS with optical activation of LA principal cells, they showed that direct activation of LA principal cells was sufficient to drive cued associative fear conditioning. We implemented a similar strategy to bypass an eventual fading of the US "detonation" in *il1rapl1*-deficient mice (Fig. 8). To this aim, LA cells were transfected with AAV2/9.CAG.ChR2-Venus.W.SV40-p1468 (U-Penn vector core) introduced through chronically implanted cannula, which also permitted the delivery of timely controlled light pulses within the LA via an optical fiber (see Materials and Methods) (Fig. 8*B–G*).

First, to control for the efficacy of the opsin strategy, we tested the light activation of LA principal neurons *in vitro* (Fig. 8*A*). In all transfected neurons, we observed that continuous 1 s, 460 nm light-applications were leading to continuous AP discharge (Fig. 8*A*). We also tested the capability of transfected neurons to respond to repeated short (2 ms long) flashes of 460 nm light, a condition previously used *in vivo* in the amygdala (Johansen et al., 2010). By varying flash frequencies, we observed that most ChR2-expressing neurons were able to strictly follow flashes up to 20 Hz before exhibiting discharge failures (Fig. 8*A*). Thus, 20 Hz trains were retained for *in vivo* experiments.

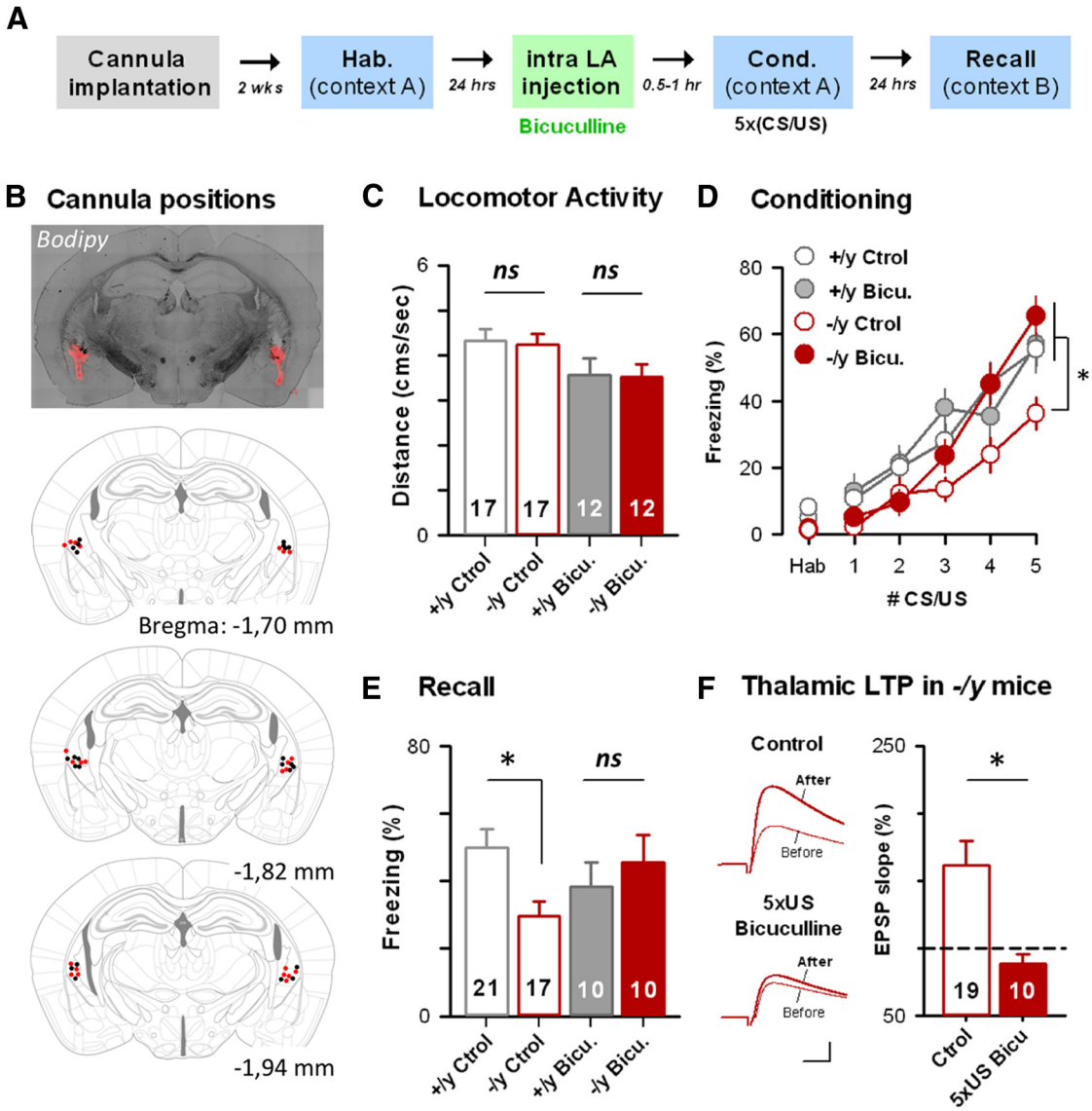

Figure 7. Cued fear learning deficit is restored by preconditioning infusion of the GABAA-R blocker bicuculline in the lateral amygdala. ***A***, Experimental paradigm. ***B***, Mice were bilaterally implanted above the LA to allow drug application in awake animals just before the fear conditioning. Top, Bodipy (500 nl each side) diffusion allowing assessment of drug diffusion in the amygdala region. Bottom, Cannula positions for all +/*y* (black dots) and −/*y* (red dots) animals considered for statistics. ***C***, Locomotor activity in control and bicuculline-injected animals was measured by tracking of animal movement before the acquisition phase (2 first minutes in Context A). ***D***, ***E***, Freezing levels exhibited by bicuculline injected *il1rapl1* +/*y* and −/*y* animals were measured during conditioning (***D***) and recall (***E***) and compared with nontreated, control KO, and WT mice. *ns*, Not significant. *$p < 0.05$. Number of animals is indicated. ***F***, Fear learning induced complete thalamo–LA LTP occlusion in bicuculline-treated *il1rapl1*−/*y* mice. Left, Typical EPSPs recorded before and after pairing in naive and conditioned control (Ctrl) and bicuculline-treated (5 × US bicu) KO mice. Calibration: 4 mV, 5 ms. Right, Mean LTP in *il1rapl1*−/*y* naive (Ctrl) and conditioned (5 × US Bicu) bicuculline-treated adult mice. Number of recorded cells is indicated.

Then, a first cohort of 7 ChR2-transduced mice of each genotype was exposed to an associative fear learning (CS/US) + light delivery procedure (Fig. 8*B–D*). During conditioning sessions, light applications (unilateral, 460 nm, 2 ms flashes at 20 Hz during 30 s, 6–8 mW output light power) were repeatedly applied together with CS^+/US presentations (Fig. 8*B*, *C*). Importantly, our *in vivo* light stimulations were proven to be efficient in activating LA neurons as the expression of the activity-reporter C-fos was specifically increased at the illuminated side (data not shown). We then score the freezing levels exhibited by WT and KO mice during CS^+ presentations within the conditioning phase (Fig. 8*C*). Strikingly, both KO and WT cohorts then exhibited very similar freezing levels, comparable with the one observed in WT animals submitted to CS/US pairings (Fig. 1). Interestingly, at the recall test, WT and KO mice did exhibit a high level of freezing reaction at the CS^+ presentation (WT light, 44 ± 13%; KO light, 54 ± 11%), indicating that the improvement of fear memory was maintained (Fig. 8*D*). However, KO mice also displayed a high degree of generalization (KO light CS^-, 55 ± 11%), suggesting that CS/US/Light protocol might have abnormally activated the amygdala, leading to a CS^-/US association. Importantly, we controlled that the light-application effect was depending on the presence of the US (Fig. 8*E–G*). Indeed, it has been previously shown that repeated Light/CS presentation could lead to the generation of an associative conditioned response to the CS (Johansen et al., 2010). Thus, in another implanted cohort of 8 +/*y* and 8 −/*y* animals, we could show that the application of 5 CS^+/Light was not able to induce robust conditioned fear response (Fig. 8*E–G*).

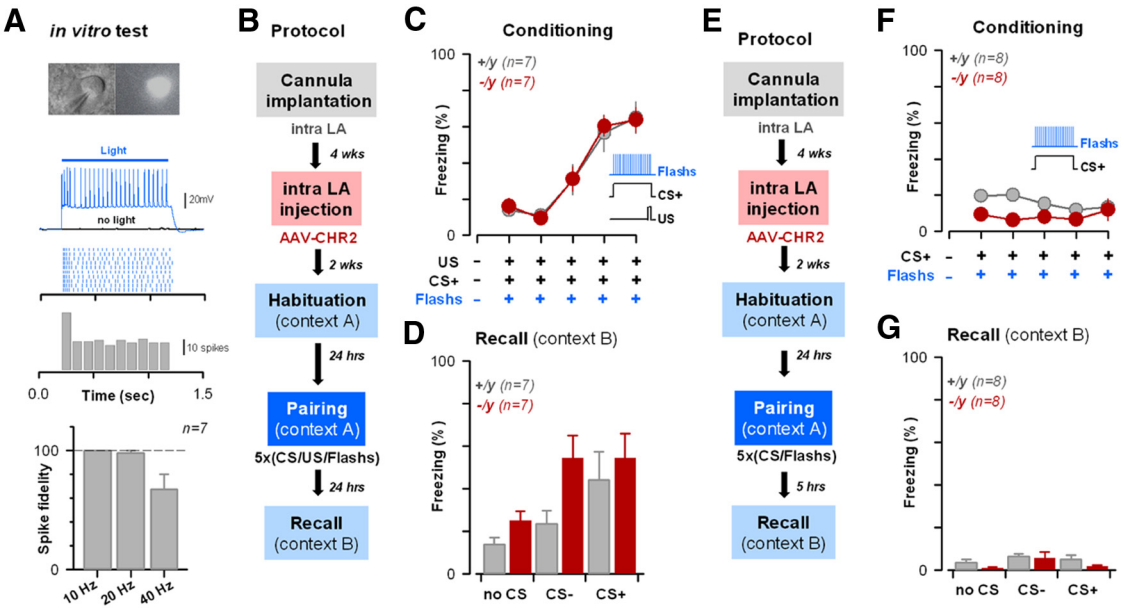

Figure 8. Direct optical activation of LA cells induces comparable associative cued fear learning in normal and *il1rapl1*-deficient mice. ***A***, Light activation of LA neuronal cells using opsin-based strategy. Top, Light flashes (1-s-long, 460 nm) induced continuous spiking discharge in AAV-ChR2-transfected LA cells. Bottom, Short flashes (5 ms) were applied at different frequencies, and discharge fidelity was measured. No failure in LA principal cell spiking was observed up to 20 Hz. ***B***, Experimental paradigm used for opsin-based conditioning protocol. It includes chronic cannula implantation, LA infection with AAV-ChR2 constructs, and 460 nm blue light/CS/US paired applications (see Materials and Methods). ***C***, ***D***, Freezing levels observed during the conditioning (***C***) and the recall (***D***) sessions in CS/US/light conditioned WT and KO mice. ***E–G***, Same presentation as in ***B–D***, but for CS/light pairings.

Collectively, pharmacological (Fig. 7) and opsin-based strategies (Fig. 8) led us to conclude that, once bypassing the requirement of postsynaptic depolarization in LA principal cells, *il1rapl1*-deficient and their WT littermates exhibited comparable amygdala-related learning capabilities. LA-targeted *in vivo* strategies correcting or bypassing the I/E imbalance at the time of CS/US associations seem successful in normalizing cued fear learning in *il1rapl1* mutant mice, pointing to the crucial role of this structure in generating the observed deficit.

Discussion

Using a combined approach at behavioral, cellular, and synaptic levels, we provide a thorough characterization of the consequences of *il1rapl1* deletion on cued fear related amygdala neuronal networks. Several lines of evidence indicate that the mutation impacts specifically excitatory synapses onto glutamatergic cells, leaving connections to GABAergic cells intact. The working model, strengthened here by *in vivo* approaches, proposes that local I/E imbalances in amygdala neuronal circuits led to deficits in the acquisition of cued fear memory by lowering LA PN activation, thereby decreasing associative LTP induction. Thus, discrete behavioral deficits may arise from the heterogeneous vulnerability of excitatory synapses to ID gene deficiency.

I/E imbalance and behavioral consequences after *il1rapl1* deletion

We propose here that *il1rapl1* deficiency leads to an I/E imbalance in the LA, perturbing cued fear memory formation, but not cued fear memory expression. Indeed, LA-dedicated experiments aiming at depressing or bypassing the LA-GABAergic system immediately before the CS/US association (i.e., at the exact timing of associative synaptic plasticity induction) were efficiently normalizing for the cued fear deficit during the recall tests (Figs. 7 and 8), long after that correcting treatments were passed. This indicates that, once properly acquired, cued fear memory expression is not impaired in *il1rapl1*-deficient mice. Thus, we propose that, after *il1rapl1* mutation, I/E imbalance in LA impairs cued fear memory formation by preventing associative LTP gating at major excitatory entries conveying CS and US modalities (Ehrlich et al., 2009). In addition, our data suggest that LA I/E balance may not be of crucial importance in the reactivation of LA neurons participating to the cued fear memory trace stored in the LA (Han et al., 2009). In this line, former *in vivo* observations pointed to a depression of the amygdala GABAergic system after cued fear conditioning (Chhatwal et al., 2005). However, because some modalities of the conditioned fear (i.e., $CS^+/CS-$ discrimination during recall; Fig. 8) and the kinetic of freezing behavior during acquisition (Fig. 7) are not entirely corrected by our *in vivo* treatments, we cannot exclude that additional mechanisms upstream or downstream to LA integration contribute to the observed cued fear learning phenotype.

The possible impairment of LTP induction in *il1rapl1* KO mice is reminiscent of previous observations made on hippocampal memory formation in a Down syndrome mouse model (Kleschevnikov et al., 2004) and more generally in line with an increasing number of reports linking ID/ASD mutations with discrete I/E imbalance in specific networks (Chao et al., 2010; Baroncelli et al., 2011; Pizzarelli and Cherubini, 2011; Yizhar et al., 2011). For Il1rapl1-dependent mechanisms, our view is that associative memory formation may be mainly impaired in the brain areas in which (1) the presence of Il1rapl1 in association with specific molecular partners is crucial for the maintenance/consolidation/function of excitatory synapses onto principal cells (see below), and (2) in which induction of associative LTP is strongly depending on feedforward inhibition and more globally on local I/E balance.

I/E imbalance is induced by the heterogeneous synaptic vulnerability to *il1rapl1* removal

Interestingly, our results pointed the differential vulnerability of excitatory synapses to *il1rapl1* mutation, especially regarding the identity (e.g., GABAergic or glutamatergic) of the postsynaptic cell (Figs. 3 and 4). Our efforts to better characterize the expression pattern of *il1rapl1* led to the identification of a specific but ubiquitous expression of weak levels of the mRNA in most likely all neuron types of the basolateral amygdala complex (Fig. 6). Thereby, the simplistic explanation of *il1rapl1* −/*y* phenotype through the differential expression in interneuron and principal cells is ruled out. Interestingly, Il1rapl1 protein recently emerged through the efforts of several groups as a new trans-synaptic adhesion and signaling molecule entering an heterophilic interaction with presynaptic PTP-∂ (Valnegri et al., 2011; Yoshida et al., 2011). This interaction promotes the aggregation of presynaptic (bassoon and VGLUT1) and postsynaptic (PSD95 and Shank2) proteins at excitatory, but not at inhibitory, contacts in dissociated neuron cultures and in cortical slices (Valnegri et al., 2011; Yoshida et al., 2011). In addition, a recent study proposed that the modulation of RhoA/ROCK signaling by the IL1RAPL1 TIR domain, through an interaction with Mcf2l (Hayashi et al., 2013), mediates both IL1RAPL1-mediated spinogenesis and control of AMPAR trafficking (Hayashi et al., 2013), possibly linking functional and morphological phenotypes. In the amygdala, feedforward inhibition is elicited through the activation of AMPAR- and NMDAR-containing postsynapses on low-spiny GABAergic interneurons (Szinyei et al., 2000, 2003; Spampanato et al., 2011). Taking this into account, one can imagine that *il1rapl1* mutation does not affect interneurons the same way it does principal cells. In this line, recent work strikingly brought evidence for a mirror role of the postsynaptic protein Erbin only at excitatory synapse formed with GABAergic neurons (Tao et al., 2013). Further work will be necessary to understand whether there is a causal relationship between the absence of dendritic spine and the absence of functional consequence of *il1rapl1* mutation. Indeed, one may anticipate that the impact of many ID gene mutations may not be ubiquitous at central synapses and that similar functional I/E imbalance generated by this heterogeneity may also be found in other ID models.

Recently, the emergence of several families of trans-synaptic adhesion molecules important for synapse specification raised a lot of interest by pointing to an unexpected possible wealth of heterogeneity in synaptic functions and plasticity (McMahon and Díaz, 2011; Siddiqui and Craig, 2011). Beyond the diversity in genes, many splice variants were also shown to occur at these loci (Missler and Südhof, 1998a). Additionally, secreted binding partners (e.g., neurexophilins) exist that can alter trans-synaptic adhesions (Missler and Südhof, 1998b). More striking is the activity-dependent regulation of neurexin1 binding through alternative splicing (Iijima et al., 2011). Thus, the synaptic code determining the balance of expression of this mixture of molecules at a given synapse is of key importance to understand how complex brain circuits are wired. Clearly, our work points to the functional heterogeneity of excitatory synaptic inputs involved in the fulfillment of complex behavioral functions. Although *il1rapl1* mRNA seems to be expressed at all cell types of amygdala, additional experiments will be required to understand the molecular rational behind the differential vulnerability of excitatory synapses to *il1rapl1* deletion.

We further show that deletion of *il1rapl1* results in fading of excitatory transmission and morphological impairments at thalamo–LA Vglut2-PSD95 (Fig. 5). Indeed, medial geniculate medial part and postintralaminar thalamic nuclei that project to LA both express robust levels of *vglut2* mRNA (Fremeau et al., 2001). Although we bring here convincing *in situ* hybridization of *il1rapl1* mRNA, the lack of comprehensive morphological description of the Il1rapl1 and PTP-∂ distributions hampers our ability to fully overview the system we dissected. Nevertheless, our data suggest that either the functional Il1rapl1/PTP-∂ complex is formed mainly at thalamo–LA synapses, or that it is formed at all excitatory synapses but is only critical at the thalamo–LA connection. In the latter scenario, functional redundancy may blur the phenotype of the deletion at most other synapses. Alternatively, we cannot rule out that our observations result from Il1rapl1-induced extrasynaptic alterations that in turn unravel existing presynaptic heterogeneity to neuromodulation. Indeed, Chu et al. (2012) recently illustrated the target-specific suppression of GABAergic transmission by dopamine.

Interestingly, we did not observe a loss of dendritic spines in LA pyramidal neurons from *il1rapl1* −/y animals (Fig. 5*A*), somehow contrasting with the I/O curves showing a functional disappearance of these long range connections (Fig. 3). Further, we also observed very little effects of the mutation on miniature EPSCs recorded in LA principal cells (Fig. 5). This paradox opens the interesting possibility that the mutation introduces a switch from long range to local synaptic connectivity, a model also proposed for neurodevelopmental disorders (Geschwind and Levitt, 2007). The neurodevelopmental disorder theory states that neurons are hyperconnected at the local network level, but in contrast, show decreased long-range connectivity between cortical brain circuits. For example, prominent hyperconnectivity was recently shown in local medial prefrontal cortical networks of a genetic mouse model for intellectual disability and autism (Testa-Silva et al., 2012). Addressing this question would require assessment of LA-LA principal cell connectivity in *il1rapl1* KO mice. Hyperconnectivity observations would then redefine *il1rapl1* mutations as causing a neurodevelopmental disorder syndrome.

In conclusion, our work unravels heterogeneity in synaptic dependency to Il1rapl1 function and its role in the fine-tuning of I/E balance in discrete circuits of the brain. We suggest that constitutive absence of Il1rapl1 disrupts this balance, possibly explaining the deficit in LTP induction *in vivo* and the behavioral deficits observed in KO mice. Beyond providing a first mechanistic explanation to I/E imbalance, a phenotype frequently associated with cognitive disorders, our results force one to not only examine the impact of a particular ID mutation onto a single synaptic type but rather to consider all physiological determinants driving a functional neuronal circuit. Conversely, the use of ID/ASD models may also allow identifying new sources of behaviorally relevant synaptic heterogeneity.

References

Baroncelli L, Braschi C, Spolidoro M, Begenisic T, Maffei L, Sale A (2011) Brain plasticity and disease: a matter of unhibition. Neural Plast 2011: 1–11. CrossRef Medline

Berlau DJ, McGaugh JL (2006) Enhancement of extinction memory consolidation: the role of the noradrenergic and GABAergic systems within the basolateral amygdala. Neurobiol Learn Mem 86:123–132. CrossRef Medline

Bissière S, Humeau Y, Lüthi A (2003) Dopamine gates LTP induction in lateral amygdala by suppressing feedforward inhibition. Nat Neurosci 6:587–592. CrossRef Medline

Bliss TV, Lomo T (1973) Long-lasting potentiation of synaptic transmission in the dentate area of the anaesthetized rabbit following stimulation of the perforant path. J Physiol 232:331–356. Medline

Carrié A, Jun L, Bienvenu T, Vinet MC, McDonell N, Couvert P, Zemni R, Cardona A, Van Buggenhout G, Frints S, Hamel B, Moraine C, Ropers

HH, Strom T, Howell GR, Whittaker A, Ross MT, Kahn A, Fryns JP, Beldjord C, et al. (1999) A new member of the IL-1 receptor family highly expressed in hippocampus and involved in X-linked mental retardation. Nat Genet 23:25–31. CrossRef Medline

Chao HT, Chen H, Samaco RC, Xue M, Chahrour M, Yoo J, Neul JL, Gong S, Lu HC, Heintz N, Ekker M, Rubenstein JL, Noebels JL, Rosenmund C, Zoghbi HY (2010) Dysfunction in GABA signalling mediates autism-like stereotypies and Rett syndrome phenotypes. Nature 468: 263–269. CrossRef Medline

Chhatwal JP, Myers KM, Ressler KJ, Davis M (2005) Regulation of gephyrin and GABAA receptor binding within the amygdala after fear acquisition and extinction. J Neurosci 25:502–506. CrossRef Medline

Chu HY, Ito W, Li J, Morozov A (2012) Target-specific suppression of GABA release from parvalbumin interneurons in the basolateral amygdala by dopamine. J Neurosci 32:14815–14820. CrossRef Medline

Dani VS, Chang Q, Maffei A, Turrigiano GG, Jaenisch R, Nelson SB (2005) Reduced cortical activity due to a shift in the balance between excitation and inhibition in a mouse model of Rett syndrome. Proc Natl Acad Sci U S A 102:12560–12565. CrossRef Medline

Ehrlich I, Humeau Y, Grenier F, Ciocchi S, Herry C, Lüthi A (2009) Amygdala inhibitory circuits and the control of fear memory. Neuron 62:757–771. CrossRef Medline

Fremeau RT Jr, Troyer MD, Pahner I, Nygaard GO, Tran CH, Reimer RJ, Bellocchio EE, Fortin D, Storm-Mathisen J, Edwards RH (2001) The expression of vesicular glutamate transporters defines two classes of excitatory synapse. Neuron 31:247–260. CrossRef Medline

Gabernet L, Jadhav SP, Feldman DE, Carandini M, Scanziani M (2005) Somatosensory integration controlled by dynamic thalamocortical feed-forward inhibition. Neuron 48:315–327. CrossRef Medline

Gambino F, Pavlowsky A, Béglé A, Dupont JL, Bahi N, Courjaret R, Gardette R, Hadjkacem H, Skala H, Poulain B, Chelly J, Vitale N, Humeau Y (2007) IL1-receptor accessory protein-like 1 (IL1RAPL1), a protein involved in cognitive functions, regulates N-type Ca^{2+}-channel and neurite elongation. Proc Natl Acad Sci U S A 104:9063–9068. CrossRef Medline

Gambino F, Kneib M, Pavlowsky A, Skala H, Heitz S, Vitale N, Poulain B, Khelfaoui M, Chelly J, Billuart P, Humeau Y (2009) IL1RAPL1 controls inhibitory networks during cerebellar development in mice. Eur J Neurosci 30:1476–1486. CrossRef Medline

Gambino F, Khelfaoui M, Poulain B, Bienvenu T, Chelly J, Humeau Y (2010) Synaptic maturation at cortical projections to the lateral amygdala in a mouse model of Rett syndrome. PLoS One 5:e11399. CrossRef Medline

Geschwind DH, Levitt P (2007) Autism spectrum disorders: developmental disconnection syndromes. Curr Opin Neurobiol 17:103–111. CrossRef Medline

Han JH, Kushner SA, Yiu AP, Hsiang HL, Buch T, Waisman A, Bontempi B, Neve RL, Frankland PW, Josselyn SA (2009) Selective erasure of a fear memory. Science 323:1492–1496. CrossRef Medline

Hayashi T, Yoshida T, Ra M, Taguchi R, Mishina M (2013) IL1RAPL1 associated with mental retardation and autism regulates the formation and stabilization of glutamatergic synapses of cortical neurons through RhoA signaling pathway. PLoS One 8:e66254. CrossRef Medline

Herry C, Ciocchi S, Senn V, Demmou L, Müller C, Lüthi A (2008) Switching on and off fear by distinct neuronal circuits. Nature 454:600–606. CrossRef Medline

Hong I, Kim J, Lee J, Park S, Song B, Kim J, An B, Park K, Lee HW, Lee S, Kim H, Park SH, Eom KD, Lee S, Choi S (2011) Reversible plasticity of fear memory-encoding amygdala synaptic circuits even after fear memory consolidation. PLoS One 6:e24260. CrossRef Medline

Humeau Y, Herry C, Kemp N, Shaban H, Fourcaudot E, Bissière S, Lüthi A (2005) Dendritic spine heterogeneity determines afferent-specific hebbian plasticity in the amygdala. Neuron 45:119–131. CrossRef Medline

Humeau Y, Reisel D, Johnson AW, Borchardt T, Jensen V, Gebhardt C, Bosch V, Gass P, Bannerman DM, Good MA, Hvalby Ø, Sprengel R, Lüthi A (2007) A pathway-specific function for different AMPA receptor subunits in amygdala long-term potentiation and fear cconditioning. J Neurosci 27:10947–10956. CrossRef Medline

Humeau Y, Gambino F, Chelly J, Vitale N (2009) X-linked mental retardation: focus on synaptic function and plasticity. J Neurochem 109: 1–14. CrossRef Medline

Iijima T, Wu K, Witte H, Hanno-Iijima Y, Glatter T, Richard S, Scheiffele P (2011) SAM68 regulates neuronal activity-dependent alternative splicing of neurexin-1. Cell 147:1601–1614. CrossRef Medline

Johansen JP, Hamanaka H, Monfils MH, Behnia R, Deisseroth K, Blair HT, LeDoux JE (2010) Optical activation of lateral amygdala pyramidal cells instructs associative fear learning. Proc Natl Acad Sci U S A 107:12692–12697. CrossRef Medline

Kleschevnikov AM, Belichenko PV, Villar AJ, Epstein CJ, Malenka RC, Mobley WC (2004) Hippocampal long-term potentiation suppressed by increased inhibition in the Ts65Dn mouse, a genetic model of Down syndrome. J Neurosci 24:8153–8160. CrossRef Medline

LeDoux JE (2000) Emotion circuits in the brain. Annu Rev Neurosci 23: 155–184. CrossRef Medline

Maren S (2005) Synaptic mechanisms of associative memory in the amygdala. Neuron 47:783–786. CrossRef Medline

McDonald AJ (1982) Neurons of the lateral and basolateral amygdaloid nuclei: a Golgi study in the rat. J Comp Neurol 212:293–312. CrossRef Medline

McMahon SA, Díaz E (2011) Mechanisms of excitatory synapse maturation by trans-synaptic organizing complexes. Curr Opin Neurobiol 21:221–227. CrossRef Medline

Missler M, Südhof TC (1998a) Neurexins: three genes and 1001 products. Trends Genet 14:20–26. CrossRef Medline

Missler M, Südhof TC (1998b) Neurexophilins form a conserved family of neuropeptide-like glycoproteins. J Neurosci 18:3630–3638. Medline

Moutsimilli L, Farley S, Dumas S, El Mestikawy El S, Giros B, Tzavara ET (2005) Selective cortical VGLUT1 increase as a marker for antidepressant activity. Neuropharmacology 49:890–900. CrossRef Medline

Pavlowsky A, Gianfelice A, Pallotto M, Zanchi A, Vara H, Khelfaoui M, Valnegri P, Rezai X, Bassani S, Brambilla D, Kumpost J, Blahos J, Roux MJ, Humeau Y, Chelly J, Passafaro M, Giustetto M, Billuart P, Sala C (2010) A postsynaptic signaling pathway that may account for the cognitive defect due to IL1RAPL1 mutation. Curr Biol 20:103–115. CrossRef Medline

Pavlowsky A, Chelly J, Billuart P (2011) Emerging major synaptic signaling pathways involved in intellectual disability. Mol Psychiatry 17: 682–693. CrossRef Medline

Piton A, Michaud JL, Peng H, Aradhya S, Gauthier J, Mottron L, Champagne N, Lafrenière RG, Hamdan FF, Hamdan FF, Joober R, Fombonne E, Marineau C, Cossette P, Dubé MP, Haghighi P, Drapeau P, Barker PA, Carbonetto S, Rouleau GA (2008) Mutations in the calcium-related gene IL1RAPL1 are associated with autism. Hum Mol Genet 17:3965–3974. CrossRef Medline

Pizzarelli R, Cherubini E (2011) Alterations of GABAergic signaling in autism spectrum disorders. Neural Plast 2011:1–12. CrossRef Medline

Pouille F, Scanziani M (2001) Enforcement of temporal fidelity in pyramidal cells by somatic feed-forward inhibition. Science 293:1159–1163. CrossRef Medline

Purpura DP (1974) Dendritic spine "dysgenesis" and mental retardation. Science 186:1126–1128. CrossRef Medline

Rodriguez A, Ehlenberger DB, Dickstein DL, Hof PR, Wearne SL (2008) Automated three-dimensional detection and shape classification of dendritic spines from fluorescence microscopy images. PLoS One 3:e1997. CrossRef Medline

Rosenkranz JA, Grace AA (2002) Dopamine-mediated modulation of odour-evoked amygdala potentials during Pavlovian conditioning. Nature 417:282–287. CrossRef Medline

Rumpel S, LeDoux J, Zador A, Malinow R (2005) Postsynaptic receptor trafficking underlying a form of associative learning. Science 308:83–88. CrossRef Medline

Sanger DJ, Joly D (1985) Anxiolytic drugs and the acquisition of conditioned fear in mice. Psychopharmacology (Berl) 85:284–288. CrossRef Medline

Siddiqui TJ, Craig AM (2011) Synaptic organizing complexes. Curr Opin Neurobiol 21:132–143. CrossRef Medline

Sosulina L, Meis S, Seifert G, Steinhäuser C, Pape HC (2006) Classification of projection neurons and interneurons in the rat lateral amygdala based upon cluster analysis. Mol Cell Neurosci 33:57–67. CrossRef Medline

Sosulina L, Graebenitz S, Pape HC (2010) GABAergic interneurons in the mouse lateral amygdala: a classification study. J Neurophysiol 104:617–626. CrossRef Medline

Spampanato J, Polepalli J, Sah P (2011) Interneurons in the basolateral amygdala. Neuropharmacology 60:765–773. CrossRef Medline

Szinyei C, Heinbockel T, Montagne J, Pape HC (2000) Putative cortical and

thalamic inputs elicit convergent excitation in a population of GABAergic interneurons of the lateral amygdala. J Neurosci 20:8909–8915. Medline

Szinyei C, Stork O, Pape HC (2003) Contribution of NR2B subunits to synaptic transmission in amygdaloid interneurons. J Neurosci 23:2549–2556. Medline

Tamamaki N, Yanagawa Y, Tomioka R, Miyazaki J, Obata K, Kaneko T (2003) Green fluorescent protein expression and colocalization with calretinin, parvalbumin, and somatostatin in the GAD67-GFP knock-in mouse. J Comp Neurol 467:60–79. CrossRef Medline

Tao Y, Chen YJ, Shen C, Luo Z, Bates CR, Lee D, Marchetto S, Gao TM, Borg JP, Xiong WC, Mei L (2013) Erbin interacts with TARP γ-2 for surface expression of AMPA receptors in cortical interneurons. Nat Neurosci 16:290–299. CrossRef Medline

Testa-Silva G, Loebel A, Giugliano M, de Kock CP, Mansvelder HD, Meredith RM (2012) Hyperconnectivity and slow synapses during early development of medial prefrontal cortex in a mouse model for mental retardation and autism. Cereb Cortex 22:1333–1342. CrossRef Medline

Vaillend C, Poirier R, Laroche S (2008) Genes, plasticity and mental retardation. Behav Brain Res 192:88–105. CrossRef Medline

Valnegri P, Montrasio C, Brambilla D, Ko J, Passafaro M, Sala C (2011) The X-linked intellectual disability protein IL1RAPL1 regulates excitatory synapse formation by binding PTP and RhoGAP2. Hum Mol Genet 20:4797–4809. CrossRef Medline

van Bokhoven H (2011) Genetic and epigenetic networks in intellectual disabilities. Annu Rev Genet 45:81–104. CrossRef Medline

Yizhar O, Fenno LE, Prigge M, Schneider F, Davidson TJ, O'Shea DJ, Sohal VS, Goshen I, Finkelstein J, Paz JT, Stehfest K, Fudim R, Ramakrishnan C, Huguenard JR, Hegemann P, Deisseroth K (2011) Neocortical excitation/inhibition balance in information processing and social dysfunction. Nature 477:171–178. CrossRef Medline

Yoshida T, Yasumura M, Uemura T, Lee SJ, Ra M, Taguchi R, Iwakura Y, Mishina M (2011) IL-1 receptor accessory protein-like 1 associated with mental retardation and autism mediates synapse formation by trans-synaptic interaction with protein tyrosine phosphatase. J Neurosci 31:13485–13499. CrossRef Medline

2 Publication 2: "The hippocampo-amygdala control of contextual fear expression is affected in a model of intellectual disability

2.1 Results summary

The starting point of this second paper was the initial finding that *Il1rapl1* KO mice also presented a deficit of fear when re-exposed to the conditioning context. Indeed, in the initial "screening" experience we found a deficit in freezing levels during renewal of fear in *Il1rapl1* KO animals (see page 77), suggesting some dysfunctions in the neural circuits underlying formation and/or expression of contextual fear memory. Contextual fear can be defined as a conditioned fear response that is elicited in a given context in which the animal had a previous noxious experience. We decided to further explore this behavioral deficit because all treatments that were efficiently correcting for cued fear learning in *Il1rapl1* KO mice were unable to correct for the deficit in contextual fear in the same animals (Figure 27), pointing that it must originate in a different mechanism. Indeed, all treatments correcting for cued fear were performed just before the learning phase (and not the testing phase), thus acting specifically on the formation of fear memory. Taken together, these results suggested that the underlying cause of the contextual fear deficit could originate in the expression of the fear memory instead than the initial formation of the fear memory. Because renewal of fear combines cued and contextual aspects of fear memory, I then developed a pure contextual fear learning task where the animal associates the context only with the occurrence of foot shocks. Interestingly, when re-exposed to the conditioning context *Il1rapl1* KO mice showed lower fear levels than their WT littermates (publ. Figure 1).

In order to identify what brain region(s) could be responsible to the lack of freezing response upon fearful context re-exposure, we then measured neuronal activation on both basolateral amygdala (BLA) and hippocampal regions. Coherent with the lack of freezing behavior, *Il1rapl1* KO mice presented a strong reduction in the activation of BLA but surprisingly only a mild reduction in the caudal region of hippocampus known to project to the BLA, and even an over-activation of the dorsal dentate gyrus region of the hippocampus (publ. Figure 2).

Treatment	Cued fear learning	Contextual fear
Pre-training bicuculline	Corrected	Not corrected
Pre-training α5IA (IP)	Corrected	Not corrected
Opsin-based conditioning	Corrected	Not corrected
Reinforced conditioning	Corrected	Not corrected

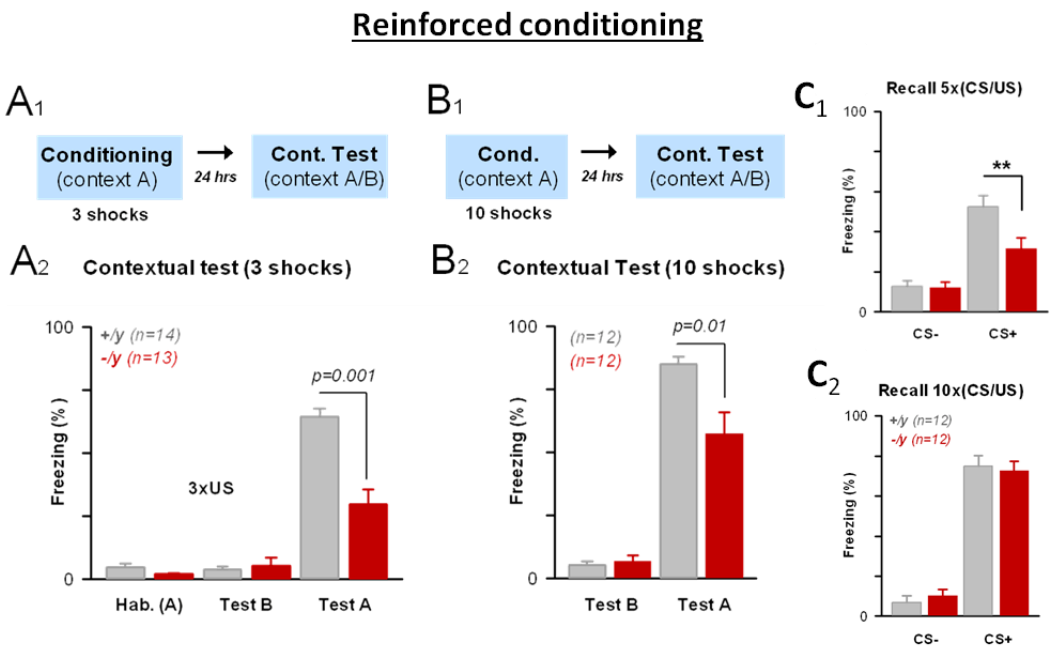

Figure 27: Pre-training treatments aiming at correcting cued fear learning were not efficient in correcting contextual fear. Indeed, pre-training bicuculline, pre-training α5IA, opsin-based conditioning and reinforced conditioning didn't rescue contextual renewal of fear. Reinforced conditioning consists of increasing the number of CS/US presentations (for cued fear) or the number of shock applications (for contextual fear) to test if the deficit originates in an inability to form the memory. A_1: Classical pure contextual fear protocol using three shocks; 24hrs later animals are resubmitted to the fearful context. A_2: *Il1rapl1* KO animals have a strong deficit when re-exposed to the fearful context specifically. B1: Same protocol as in A1 except we increased the number of shocks. B2: Increasing the number of shocks didn't rescue the deficit in *Il1rapl1* KO mice. C1: Recall of cued fear after using 5 CS/US pairings during conditioning was impaired in *Il1rapl1* KO mice. C2: Recall of cued fear after increasing CS/US pairings was rescued in *Il1rapl1* KO mice.

Projections from caudal hippocampus to BLA (hippocampo-BLA) are thought to be important for contextual fear memory expression (Maren et al., 2013). However, relatively little is known

about their synaptic properties and biological function *in vivo*. Because of the strong impairment in BLA neuronal activation, I hypothesized that hippocampo-BLA projections could be dysfunctional in *Il1rapl1*-deficient mice, possibly leading to lower BLA principal cell activation. With the aim of characterizing hippocampo-BLA projections and their possible dysfunction in *Il1rapl1*-deficient mice, I used an opsin-based strategy to isolate functionally the fibers from the hippocampus reaching the BLA *in vitro*. Indeed, even if positioned at the right place (medially to the CeA), electrical stimulations wouldn't differentiate between hippocampal projections to BLA from unrelated ones (for example, from prefrontal cortex). In contrast, localized injections of opsins allow stimulation of their axonal projections in brain regions of interest (Figure 28).

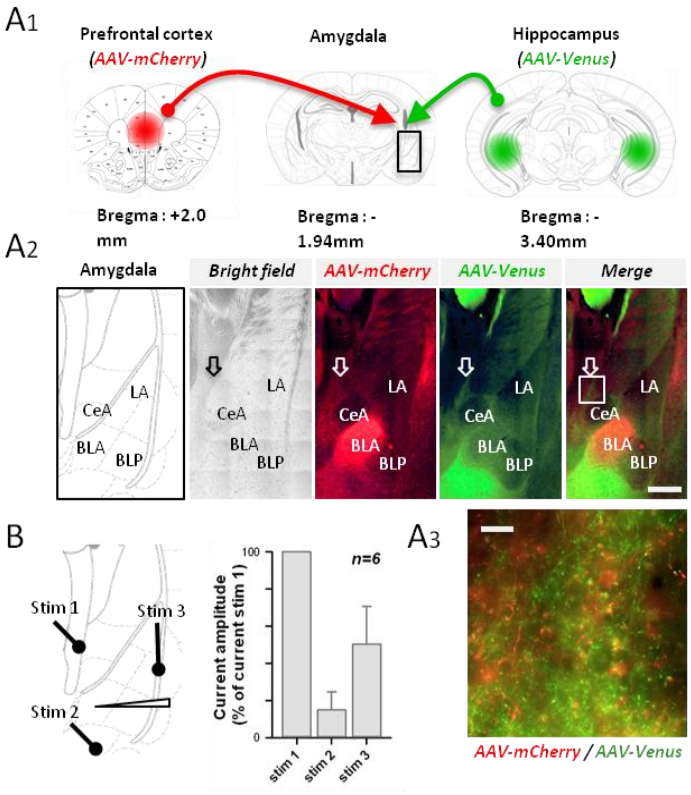

Figure 28: Optogenetic isolation of hippocampo-and prefrontal projections to amygdala. A_1: AAV-mCherry and AAV-Venus were injected in prefrontal cortex and ventral hippocampus respectively. A_2: Amygdala brain slice and corresponding images of prefrontal (red) and hippocampal (green) projections impinging onto BLA. Projections bordered the CE laterally and reached the BLA through a dense fiber bundle. A_3: Merged zoomed picture of prefrontal and hippocampal projections taken in the square box (fiber bundle). B: Electrical stimulations confirmed that placing an electrode in the fiber bundle (Stim1) led to the highest current amplitudes on BLA principal cells.

Thus, infection of ventral hippocampus with channelrhodopsin (ChR2) allowed me to stimulate hippocampal projections in BLA and measure evoked responses of BLA principal cells. First, using acute brain slices, I recorded for excitatory and inhibitory transmission on BLA principal cells following light stimulation of hippocampal afferents. Similarly as in lateral amygdala, BLA principal cells from *Il1rapl1* KO mice received less excitation whereas measured inhibition was kept unaltered, leading to a local I/E imbalance in BLA (publ. Figure 3). This finding raised the question whether this local I/E imbalance in BLA may actually contribute to the contextual fear memory expression deficit of *Il1rapl1*-deficient mice. To test for a possible involvement of hippocampo-BLA projections in contextual fear expression, we designed an experiment allowing me to potentiate these projections using *in vivo* light stimulation, based on the demonstration that in slices, bursting light stimulations were efficient in boosting synaptic transmission at hippocampo-BLA synapses (publ. Figure 4).

At that time, our *in vivo* "rescue" protocol was pretty original because we aimed at potentiating a given synaptic population (hippocampo-BLA synapses) in order to observe the consequences of this synaptic intervention at behavioral levels. Interestingly, using the advantages of local injections of channelrhodopsin we were able to test for the functional importance of both of pre- and/or postsynaptic compartments (that is vHPC and BLA) in the mediation of the contextual fear response. Indeed, by injecting ChR2 in vHPC only, we could separate the specific contribution of hippocampo-BLA projections (presynaptic only; Figure 29). Hippocampo-BLA projections were potentiated outside the testing context (more precisely in mice homecage) in order to avoid possible confusion that could have occurred if this had been realized in the "fearful" context. Using this strategy we reinforced all hippocampal projections reaching BLA before the animal was re-exposed to the "fearful" context. When animals are resubmitted to the "fearful" context, memory is recalled and potentiated hippocampal projections become activated again, leading to the normalization of the fear response in *Il1rapl1* KO animals (publ. Figure 4; Figure 29). In contrast, restricting the potentiation to the postsynaptic compartment alone (that is achieved by infecting BLA with ChR2) wasn't sufficient to restore contextual fear expression in *Il1rapl1* KO mice (publ. Figure 4; postsynaptic only Figure 29). This experiment

provided strong evidence that the specific potentiation of hippocampo-BLA projections was sufficient to restore contextual fear in KO animals.

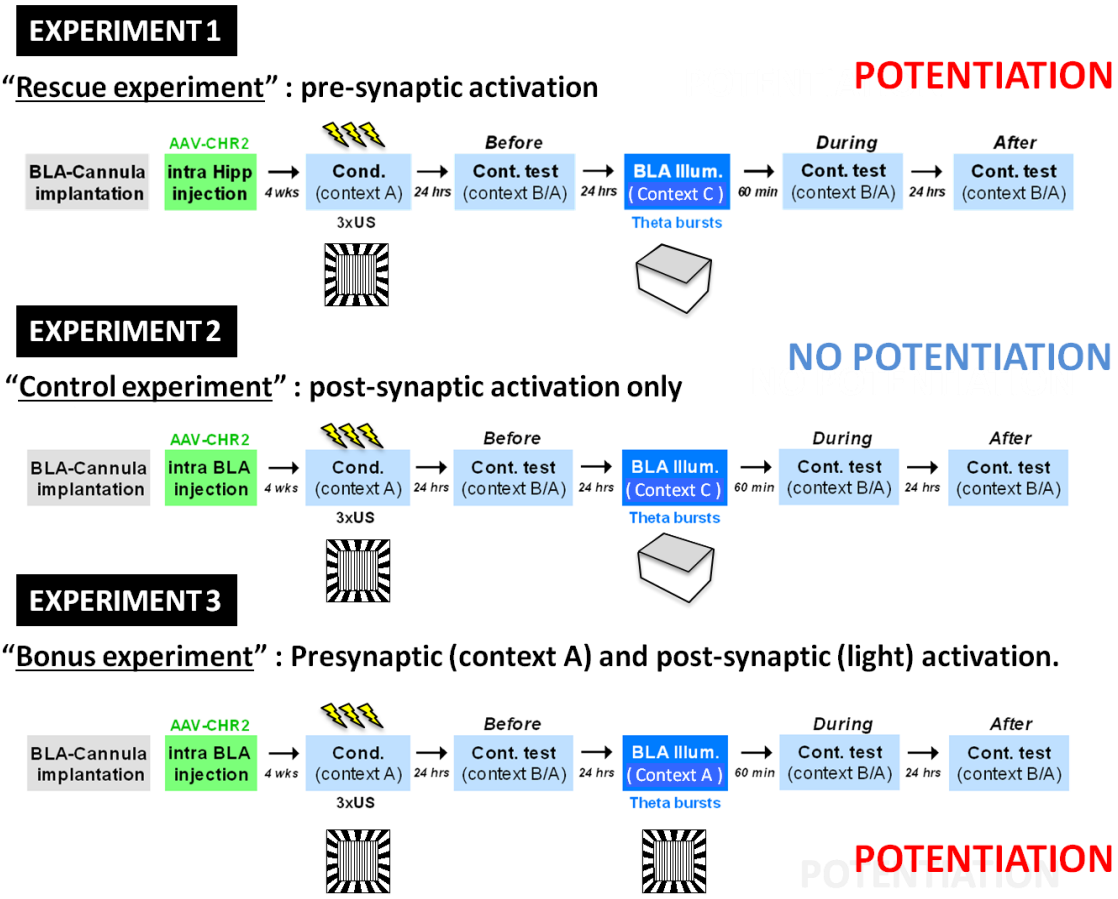

Figure 29: Three different experiments to test for the contribution of pre and/or postsynaptic compartments (vHPC and BLA) in the mediation of contextual fear memory expression. In experiment 1 we tested contextual fear before and after *in vivo* illumination of hippocampo-BLA projections, thus restricting the potentiation to the presynaptic compartment. In experiment 2 the protocol is the same except BLA was injected with Chr2, thus restricting the potentiation to the postsynaptic compartment only. Finally, in experiment 3 both pre-and postsynaptic compartment's involvement was assessed. Indeed, presynaptic activation was achieved by performing the potentiation in the "fearful" context while postsynaptic activation was again achieved by illuminating BLA.

Moreover, we realized a last experiment where the postsynaptic compartment (BLA) was potentiated but during the re-exposure of animals to the "fearful" context contrasting with the previous two experiments were this occurred in the homecage (bonus experiment; Figure 29). Thus, this experiment combines both pre-and postsynaptic compartments because re-exposing animals to the "fearful" context activates hippocampo-BLA projections and postsynaptic

activation is achieved by BLA illuminations. In this case, we were able to restore contextual fear expression in *Il1rapl1* KO mice (data not shown), but we didn't include these data in the manuscript as the normalization of behavior was more likely to result from unspecific effects of BLA illumination on fear expression. Taken together these three experiments show that we were able to specifically isolate the functional importance of hippocampal projections to BLA in the mediation of contextual fear memory expression. We conclude that the behavioral impairment of *Il1rapl1* KO animals results from a lack of BLA principal cells activation following local I/E imbalance and incoming hippocampal input during re-exposure to "fearful" contexts.

2.2 Discussion

In this work we show that removal of the *Il1rapl1* gene led to deficits in expression of previously formed contextual fear memory. In line with my previous observations, we propose that local I/E imbalances in BLA participate in the contextual fear memory expression deficit in *Il1rapl1* KO animals. Indeed we obtained evidence that I/E balance in BLA controls fear memory expression because injecting a $GABA_A$ agonist in BLA before re-exposure to the "fearful" context decreased freezing levels in WT animals (data not shown). However, these pharmacological interventions are quite invasive possibly leading to unspecific effects. In the future, efforts should be made in providing stronger links with our *in vivo* priming experiment and I/E imbalance in BLA. Importantly, this paper suggests that I/E imbalance following *Il1rapl1* removal can impact memory at multiple levels.

The local I/E imbalance in BLA is very similar to what I observed on LA principal cells following stimulation of thalamic afferents. Following stimulation of hippocampal projections, BLA principal cells received less excitation and inhibition seemed preserved (publ. Figure 3). However, in this work, we didn't study whether excitatory drive on BLA inhibitory neurons was affected. Thus, we cannot exclude that *Il1rapl1* mutation impacts a subclass of BLA interneurons that would be contributing to the feed-forward inhibition at these particular long-range afferents. To my knowledge, the role of BLA interneurons in contextual fear memory expression has not yet been addressed. Interestingly, a recent anatomical report found that projections from ventral hippocampus also make strong connections with BLA interneurons (Muller et al.,

2012). Similarly to what has been recently published, demonstrating a different role of interneuron subtypes in cued fear learning (Wolff et al., 2014), *in vivo* recordings and manipulation of specific interneurons during contextual fear expression could help in resolving this issue. However, taken together with my previous report we can expect excitation on interneurons to be preserved. Thus, it is likely that the BLA also shows target-specific effects that are limited to excitatory synapses made on BLA principal cells (see general discussion).

The functional relevance as to recruit FFI circuits in BLA by hippocampal projections remains unclear and made even more complex by the high heterogeneity of BLA interneurons (Capogna, 2014). A particularly interesting matter would be to know if FFI is induced in the BLA *in vivo* during expression of fear and if this is mediated by vHPC projections. Recently, a team has used *ex vivo* recordings of previously conditioned animals to study the role of mPFC-BLA pathway during extinction and they were able to show that mPFC-BLA FFI-circuits were not affected by fear extinction (Cho et al., 2013). Thus, it would be interesting to use a similar strategy to further characterize the role of hippocampo-BLA FFI circuits in the regulation of fear behavior. Another possibility would be to manipulate the activity of different interneuron populations by optogenetics during behavior.

Also, although we have potentiated hippocampal projections in BLA by optogenetic priming, the synaptic mechanisms underlying this remain poorly characterized. Although I observed a potentiation of hippocampo-BLA synapses onto BLA principal cells after optogenetic bursting, the synaptic mechanisms underlying them remain unstudied. In this line, it would be interesting to know whether our stimulation protocol involves pre-and/or postsynaptic mechanisms. Chr2 was expressed only in hippocampal projections, suggesting that our priming protocol leads to an increase of neurotransmitter release at hippocampal axonal terminals, in line with previous results showing that light stimulation of axons leads to a high probability of release (Zhang and Oertner, 2007). To test for this, I have recorded PPR values just before and just after induction of optogenetic LTP and I observed a reduction in PPR after LTP induction (data not shown), suggesting that our priming protocol leads to an increase of neurotransmitter release. A recent report showed that it is possible to activate or inactivate cued fear memory by potentiating or depressing auditory inputs to the LA with optogenetics (Nabavi et al., 2014). Interestingly, their

LTP stimulation protocol led to higher AMPA/NMDA ratio on LA principal cells, suggesting that new AMPA receptors were inserted in the postsynaptic membrane. Whether our stimulation protocol led to similar postsynaptic changes is unknown. Recently, it was shown that coupling Chr2-induced postsynaptic depolarization with glutamate uncaging was able to potentiate synaptic transmission and to recruit CAMKII to the observed spine, thus suggesting that optogenetic stimulation does recruit similar signaling cascades than physiological-induced LTP (Zhang et al., 2008). Recently, I have started using optogenetics and calcium-imaging in acute brain slices to study how BLA principal cells integrate synaptic information from vHPC. This could be an interesting technical approach to compare synaptic integration in BLA between genotypes following stimulation of hippocampal projections.

In contrast to the pathophysiological mechanisms leading to cued fear learning deficits in the same mice, this paper supports that contextual memory formation is unaffected in *Il1rapl1* mutant mice. Nevertheless, our data suggest the possible existence of intra-hippocampal deficits in absence of IL1RAPL1. Indeed, we did observe a significant over-activation of the dentate gyrus formation in the dorsal hippocampus following fearful context re-exposure in *Il1rapl1*-deficient mice (publ. Figure 2), suggesting that the contextual memory engram may not be properly established and/or retrieved. This however do not seems to significantly perturb the discriminative capacity of the animals. Some future dedicated experiments with closely similar contexts may evidence some contextual encoding deficits in *Il1rapl1*-deficient mice. Nevertheless, after optogenetic priming of hippocampal projections to BLA, mice were still capable of discriminating between the fearful and the not conditioned context, as the normalization of freezing levels in *Il1rapl1* KO mice was specific to the fearful context. It suggests that hippocampal contextual processing is roughly preserved and that the synaptic mechanisms leading to the formation of contextual fear memory are unaffected or resistant to the pathologic consequences of *Il1rapl1* deficiency.

2.3 Conclusion

The main message of this study is that *Il1rapl1* KO mice have deficits in the expression of contextual fear memory and that this is consecutive to a local I/E imbalance in the BLA. Thus,

local I/E imbalances following *Il1rapl1* mutation not only impact the formation of memories (see publication 1), but also the expression of previously formed memories.

Importantly, we unraveled the functional importance of caudal hippocampal projections to BLA in the regulation of contextual fear memory expression. Before this report, no studies had addressed the biological significance of these projections *in vivo*. Taking advantage of the lower BLA activation in *Il1rapl1* KO mice, we tested whether potentiating hippocampal projections to BLA could improve expression of contextual fear memory in *Il1rapl1* KO animals. *In vivo* optogenetic priming of hippocampo-BLA fibers presumably restores/bypass local I/E imbalance in BLA, leading to increased fear levels during expression of fear memories.

We have performed some additional experiments to test for the functional contribution of vHPC in contextual fear expression. To achieve this, we inhibited vHPC using optogenetics before re-exposure to the "fearful" context in WT animals (Figure 30). By plotting the freezing levels across time we observed a marked deficit in freezing levels during the first 90 seconds of contextual re-exposure before returning to baseline levels (Figure 30). This opens the intriguing possibility that vHPC could be involved in the establishment of the contextual fear response.

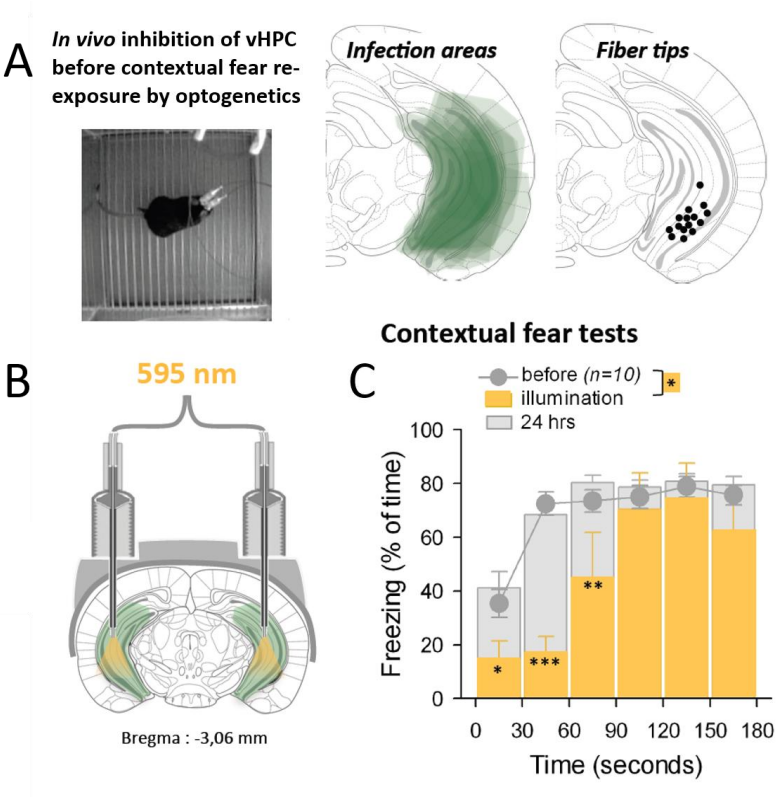

Figure 30: ***In vivo*** **optogenetic inhibition of vHPC before re-exposure to the "fearful" context. A: Mice were infected with Arch in vHPC (see infection areas) and optogenetic inhibition was achieved by inserting a fiber through implanted cannulas. B: Bilateral yellow light was applied just before contextual re-exposure. C: Illumination decreased freezing levels during the initial 90 seconds of fear onset.**

Brain Struct Funct
DOI 10.1007/s00429-014-0882-x

ORIGINAL ARTICLE

The hippocampo-amygdala control of contextual fear expression is affected in a model of intellectual disability

Chun-Lei Zhang · Xander Houbaert · Marilyn Lepleux · Melissa Deshors · Elisabeth Normand · Frédéric Gambino · Etienne Herzog · Yann Humeau

Received: 11 June 2014 / Accepted: 20 August 2014

Abstract The process of learning mainly depends on the ability to store new information, while the ability to retrieve this information and express appropriate behaviors are also crucial for the adaptation of individuals to environmental cues. Thereby, all three components contribute to the cognitive fitness of an individual. While a lack of behavioral adaptation is a recurrent trait of intellectually disabled patients, discriminating between memory formation, memory retrieval or behavioral expression deficits is not easy to establish. Here, we report some deficits in contextual fear behavior in knockout mice for the intellectual disability gene *Il1rapl1*. Functional in vivo experiments revealed that the lack of conditioned response resulted from a local inhibitory to excitatory (I/E) imbalance in basolateral amygdala (BLA) consecutive to a loss of excitatory drive onto BLA principal cells by caudal hippocampus axonal projections. A normalization of the fear behavior was obtained in adult mutant mice following opsin-based in vivo synaptic priming of hippocampo-BLA synapses in adult *il1rapl1* knockout mice, indicating that synaptic efficacy at hippocampo-BLA projections is crucial for contextual fear memory expression. Importantly, because this restoration was obtained after the learning phase, our results suggest that some of the genetically encoded cognitive deficits in humans may originate from a lack of restitution of genuinely formed memories rather than an exclusive inability to store new memories.

Keywords Contextual fear expression · Hippocampal projections · Optogenetic · Intellectual disability

C.-L. Zhang and X. Houbaert contributed equally to the work.

Electronic supplementary material The online version of this article (doi:10.1007/s00429-014-0882-x) contains supplementary material, which is available to authorized users.

C.-L. Zhang · X. Houbaert · M. Lepleux · M. Deshors · E. Normand · F. Gambino · E. Herzog · Y. Humeau
Team Synapse in Cognition, Institut Interdisciplinaire de NeuroScience, Centre National de la Recherche Scientifique CNRS UMR5297, Université de Bordeaux, Bordeaux, France

M. Deshors · E. Normand
Pole In Vivo, Institut Interdisciplinaire de NeuroScience, Centre National de la Recherche Scientifique CNRS UMR5297, Université de Bordeaux, Bordeaux, France

Y. Humeau (✉)
UMR5297 Institut Interdisciplinaire de NeuroScience, Centre de Génomique Fonctionnelle, 146 rue Léo Saignat, 33077 Bordeaux Cedex, France
e-mail: yann.humeau@u-bordeaux.fr

Introduction

Learning and memory processes are crucial to adapt our behaviors to environmental cues and highly depend on the ability of discrete neuronal circuits to integrate sensory information to elicit correct behavioral responses. Genetically encoded intellectual disability (ID) mostly results from mutations in genes functioning in neuronal and synaptic signaling cascades (Pavlowsky et al. 2011). Among these, *IL1RAPL1* is a member of a novel family of IL1/Toll receptors thought to be expressed at excitatory synapses (Pavlowsky et al. 2010) and mutations in *IL1RAPL1* gene have been shown to induce autism and ID in humans (Carrié et al. 1999; Piton et al. 2008). At the cellular level, IL1RAPL1 is thought to be a trans-synaptic adhesion protein promoting pre- and post-synaptic effectors important for the formation, maintenance and function of excitatory synapses (Gambino et al. 2007; Yoshida et al. 2011; Valnegri et al. 2011; Hayashi et al. 2013). At the

Published online: 27 August 2014

physiological level, we have recently shown that *Il1rapl1*-mutant mice have a deficit in cued fear memory formation due to a lack of synaptic plasticity induction at long-range projections to the lateral amygdala (LA) (Houbaert et al. 2013). We established that the impact of IL1RAPL1 removal is focused at excitatory synapses formed on LA principal neurons, while those contacting interneurons remain unaffected. As a result, the local I/E balance is disrupted and prevents the adequate induction of long-term potentiation and associated memory formation (Ledoux 2000; Rumpel et al. 2005). Indeed, an increasing variety of neuronal processes depend on local inhibition (Kullmann et al. 2012) and, remarkably, I/E imbalances are now frequently reported in the etiology of brain disorders such as schizophrenia (Lisman et al. 2008) or ID (Gatto and Broadie 2010; Baroncelli et al. 2011). Thus, more functional circuits and related cognitive processes may suffer from local I/E imbalances in *Il1rapl1*-deficient mice.

Re-exposure to the context in which an aversive stimulus was previously delivered induces fear behavior in mice that can be quantified by the level of freezing (16). While the dorsal hippocampus (dHPC) is thought to associate and store together the different olfactory, auditory, tactile, and visual elements of the context in which fear conditioning occurs (Rudy et al. 2004; Goosens 2011; Liu et al. 2012), activation of the caudal hippocampus (cHPC) and basolateral amygdala (BLA) appears to be necessary for contextual fear expression (Muller et al. 1997; Anagnostaras et al. 2001; Pentkowski et al. 2006). Interestingly, evidence for direct connections between cHPC and BLA have been obtained both morphologically (Pitkänen et al. 2000) and functionally (Bienvenu et al. 2012; Hübner et al. 2014). We here performed an integrated dissection of contextual fear deficits in *il1rapl1*-/y mice. We unravel a dysregulation of hippocampo-BLA projections with consequences on contextual memory expression in mice that had previously experienced and learned from the fearful context.

Results

Contextual fear deficit in il1rapl1-deficient mice

In the course of *Il1rapl1*-/y characterization, we recurrently observed a lack of contextual fear reaction (Maren et al. 2013). To better characterize this deficit, a cohort of *Il1rapl1+/y* and *-/y* mice was submitted to a discriminative contextual fear conditioning, receiving electric shocks in context A, and being re-exposed to the same context (Test A) or to an unrelated one (Test B) 24 h later (Fig. 1a; see "Materials and methods"). The conditioned fear response was strongly impaired in *Il1rapl1-/y* mice (Fig. 1a), although context discrimination (Tests B in Fig. 1a), pain perception and locomotor activity (Houbaert et al. 2013) were not affected in these mice. To evaluate the onset of the contextual fear deficit, conditioned mice of both genotypes were re-exposed to the fearful context at different time points (Fig. 1b). The deficit in *Il1rapl1* KO mice was detected as early as 12 h after the shock applications (Fig. 1b). Finally, the difference was still observed when using a strong conditioning procedure (10 shocks, instead of 3; Fig. 1c), suggesting that the deficit was independent of the intensity of sensory processing.

Neuronal activation during contextual fear is affected by Il1rapl1 null mutation

Next, to detect neuronal activation in brain regions important for contextual fear (Rudy et al. 2004; Goosens 2011; Liu et al. 2012; Maren et al. 2013), we analyzed the expression of *c-Fos* early gene in *Il1rapl1 +/y* and *-/y* mice (Herry and Mons 2004) after contextual fear conditioning and aversive context re-exposure (Fig. 2a; see "Materials and methods"). Interestingly, in dHPC, dentate gyrus activation was high in both tested (Test A, re-exposure) and non-tested groups (no re-exposure, Fig. 2c–e). In contrast, we observed that in both mouse genotypes, re-exposure to the fearful context was driving significant dorsal CA1, caudal CA1 and BLA activations (Fig. 2d, e). However, some differences exist between genotypes: in *Il1rapl1 -/y* mice, BLA activation was markedly reduced, cHPC activation was mildly reduced and dHPC activation (DG) was increased compared to *+/y* littermates (Fig. 2c–e). Thus, *Il1rapl1* KO mice most likely exhibit a reduction in the activation of neuronal circuits thought to be responsible for contextual fear expression.

A potential contribution of the lack of cHPC and BLA activation onto fear expression at the testing time was first assessed by in vivo pharmacological experiments: acute and local application of the $GABA_AR$ agonist muscimol before contextual re-exposure confirmed that the activation of both structures is essential for the conditioned fear response to express (supplementary Fig. 1). Then, reciprocal pharmacological experiments forcing the activation of BLA at the testing time—but not before learning (data not shown)—was able to restore normal conditioned fear response in the KO mice (supplementary Fig. 2).

Constitutive *Il1rapl1* mutation leads to I/E imbalance at hippocampo-BLA synapses

Next, we tested the possibility that BLA activation deficit in -/y mice was caused by alterations of hippocampo-BLA projections which were recently shown to contribute to contextual aversive memory expression (Orsini et al. 2011;

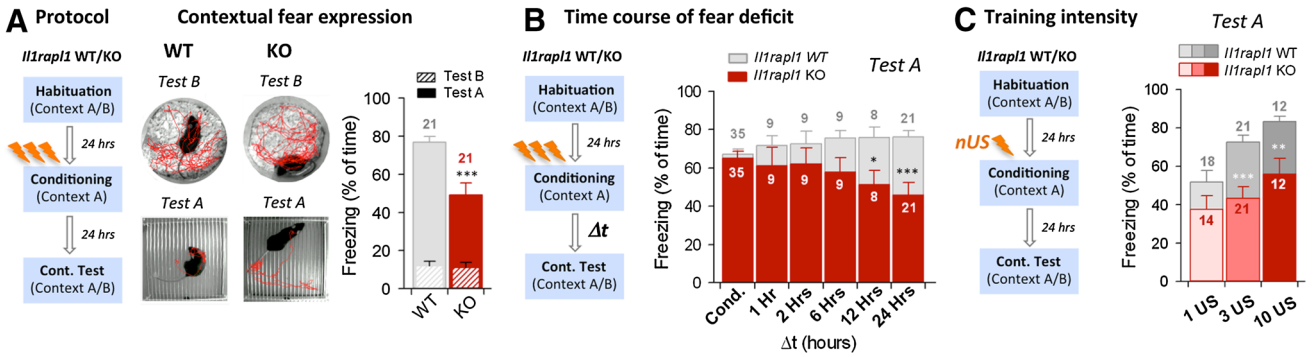

Fig. 1 Deletion of the ID gene *Il1rapl1* is associated with a lack of contextual fear. **a** Experimental protocol generating discriminative contextual fear. Conditioned WT mice exhibit typical freezing response solely in context A ($p < 0.001$, Student's t test), and discriminative contextual fear is impaired in *Il1rapl1* KO mice ($p < 0.001$, Student's t test). **b** A group of 56 WT and 56 KO animals were similarly conditioned using three shock applications in context A, and then tested once for contextual fear response at different timings after the shock application. The numbers of animals are indicated. The "Cond" condition corresponds to the freezing behavior observed for 2 min after the last shock delivery. **c** The deficit in conditioned response was independent of the strength of the conditioning. Cohorts of WT and KO animals were conditioned using 1, 3 or 10 US (shocks) applications, and the conditioned response was tested 24 h later. Overtraining did not restore the conditioned response in overtrained *Il1rapL1* KO mice (Student's t test, 3US WT vs. KO $p < 0.001$; 10 US WT vs. KO, $p < 0.01$)

Knapska et al. 2012; Maren et al. 2013). To functionally isolate hippocampo-BLA synapses, we used an opsin-based strategy using in vivo stereotaxic injections of AAV-ChR2 viral constructs in the cHPC (Hübner et al. 2014; Morozov et al. 2011) (Fig. 3a) (see "Materials and methods" and supplementary Fig. 3). We then recorded BLA principal neurons in coronal acute slices while stimulating hippocampal axons using 1 ms-long flashes of 460 nm light (Fig. 3b). When BLA principal cells were recorded at −70 mV, we successfully isolated light-evoked inward currents sensitive to the AMPA receptor blocker CNQX (Fig. 3b) and the voltage-gated sodium channel blocker tetrodotoxin (TTX, Fig. 3b), indicating that they were evoked by physiological action potentials. Interestingly, in the presence of TTX, light-evoked EPSCs were completely restored—albeit slightly more slowly—by incubating TTX-treated slices with 100 µM of the potassium channel blocker 4AP (Fig. 3b) demonstrating that hippocampal projections to BLA neurons were monosynaptic (Petreanu et al. 2007; Felix-Ortiz et al. 2013).

Then, we tested the efficacy of hippocampal synapses to recruit local interneurons (feedforward inhibition circuit) (FFI; Fig. 3c) (Hübner et al. 2014). To achieve these measurements in single cells, AMPAR- and $GABA_A$R-mediated currents were separated based on their reversal potentials (Fig. 3c) (Houbaert et al. 2013). Strikingly, the I/E balance recorded in *Il1rapl1 -/y* BLA neurons is significantly shifted toward inhibition due to a decrease of the AMPAR component (Fig. 3d). This is in accordance with our previous findings at cortical and subcortical projections to the LA of *Il1rapl1 -/y* mice (Houbaert et al. 2013), suggesting that I/E imbalance may be a general synaptic deficit associated with this ID mutation. To test if this could lead to a lack of BLA activation upon hippocampal activation, we light stimulated AAV-ChR2-infected cHPC from anesthetized GAD-67-eGFP *Il1rapl1* WT and KO animals before performing BLA *c-fos* detection (supplementary Fig. 4) (see "Materials and methods"). Interestingly, in *Il1rapl1* KO mice, the proportion of GFP-expressing *c-fos* positive cells was increased, suggesting a lack of BLA PNs activation by incoming hippocampal inputs in the absence of *Il1rapl1*.

Post-training hippocampo-BLA functional stimulation restores a normal fear expression in *Il1rapl1*-deficient mice

To establish a causal link between the lack of efficacy at hippocampus–BLA synapses and the decrease in contextual fear response, we designed an in vivo "priming" experiment. Indeed, in vitro opsin experiments show that application of high-frequency bursts of 460 nm light potentiate hippocampo-BLA connections over minutes to hours (Fig. 4a; see "Materials and methods"). We therefore tested the efficacy of similar bursting illuminations in vivo in restoring normal freezing levels in conditioned *Il1rapl1-/y* mice (Fig. 4b–d). Importantly, as others (Felix-Ortiz et al. 2013), we chose to separate the locus of AAV-ChR2 infection (cHPC, Fig. 4b) from the locus of illumination (BLA, Fig. 4b). We thereby restricted the presence of light-sensitive compartments to efferent axonal projections from hippocampal neurons contacting the amygdala (hippocampo-BLA synapses). *Il1rapl1 +/y* and *-/y* animals were infected within the cHPC with the AAV-ChR2

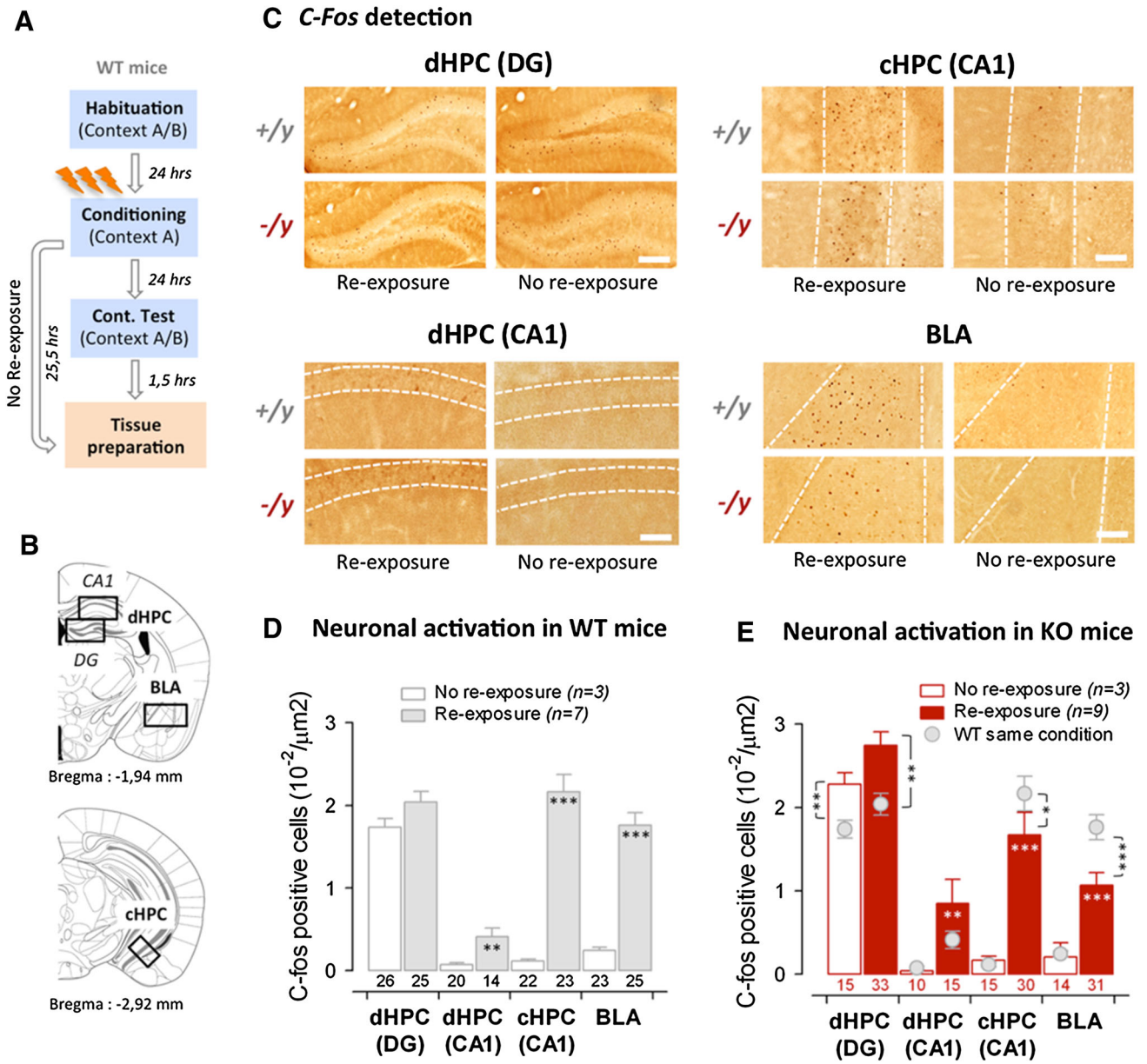

Fig. 2 Neuronal activation during contextual fear is affected by *Il1rapl1* null mutation. **a** Experimental protocol. 10 WT and 12 KO mice were conditioned, and tissue prepared for C-Fos immunodetection 25.5 h later. A sub-group of mice (re-exposure, $n = 7$ WT and 9 KO) was submitted to the fearful context A 1.5 h before killing. Another group of mice ($n = 3$ WT and 3 KO) was not re-exposed to the fearful context (no re-exposure). **b** Scheme of the analyzed regions. The following were included in the analysis: dorsal hippocampus (dHPC, dentate gyrus and CA1 regions), the basolateral amygdala (BLA) and the caudal hippocampus (CA1 region). See "Materials and methods" for more details. **c** Typical pictures of *C-Fos* immune-reactive neurons in indicated areas and conditions. Fearful context re-exposure leads to activation of both the BLA and cHPC. *Scale bars* dHPC DG, 200 µm; dHPC CA1, 100 µm; BLA, 180 µm, cHPC CA1, 100 µm. **d** *C-Fos* levels show specific dHPC-CA1, cHPC-CA1 and BLA activation upon fearful context re-exposure in WT mice (Student's *t* test, $p < 0.01$). The number of analyzed brain slices is indicated. **e** Early gene c-Fos activation during context A re-exposure shows a strong reduction of BLA activation (Mann–Whitney, $p < 0.001$) and a mild reduction in cHPC (Mann–Whitney, $p < 0.05$) in KO mice. The number of analyzed slices is indicated

viruses and chronically implanted above the BLA to allow optical fiber insertion (Fig. 4b). After being submitted to contextual fear conditioning and a first test A/B (before in Fig. 4b, c), optic fibers were inserted in both groups. Bursts of 460 nm light were delivered to their home cage, 1 h before conducting another test A/B sequence ("1 h after" in Fig. 4b, c). Strikingly, the amount of freezing exhibited by "primed" *-/y* mice increased dramatically, and became undistinguishable from that of similarly treated *+/y* mice, on which the "priming" effect was negligible (Fig. 4c).

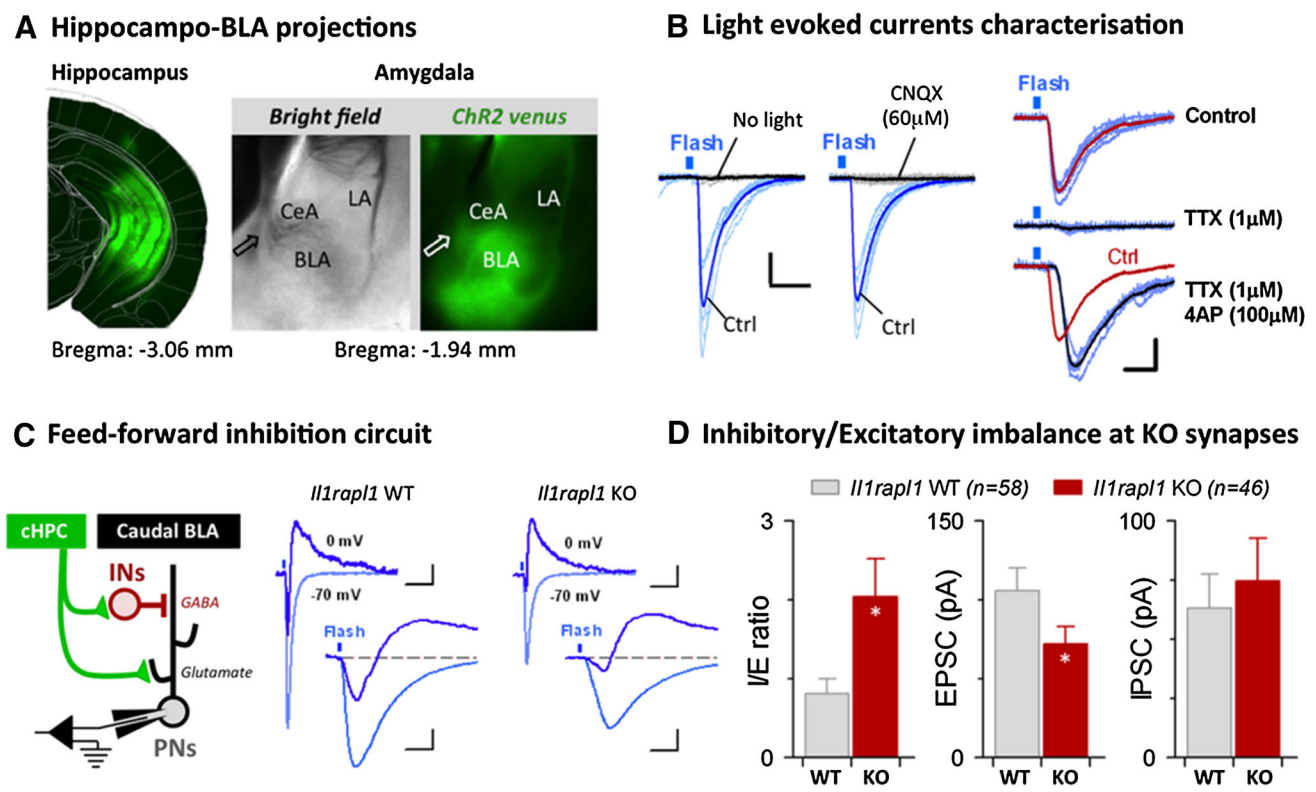

Fig. 3 Impaired I/E balance at hippocampo-BLA synapses in *Il1rapl1* KO mice. **a** AAV-ChR2-venus infection areas targeting caudal hippocampus in WT and KO animals always included the CA1 regions, and occasionally dentate gyrus and subiculum regions. **b** *Left* light-evoked excitatory currents were abolished by both AMPAR-blocker CNQX and voltage-gated sodium channel blocker tetrodotoxin (TTX), indicating that excitatory synapses are light stimulated in a physiological manner. *Scale bars: left*, 20 pA and 20 ms. In TTX-treated slices, light-evoked EPSCs could be completely restored by adding 4AP to the perfusion medium, suggesting monosynaptic inputs to BLA neurons. *Scale bars* 20 pA and 10 ms. **c**, **d** Optogenetic functional isolation of hippocampo-BLA fibers unveils I/E imbalance in *Il1rapl1* KO mice. Note that excitatory currents are decreased in *Il1rapl1* KO mice (paired *t* test, $p = 0.044$). *Scale bars*: *top*, 10 pA and 50 ms; *bottom*, 15 pA and 10 ms

Importantly, no effect was observed in both genotypes during context B re-exposure (Fig. 4c and data not shown, $p > 0.05$). Conclusively, the phenotypic rescue was absent when mice of both genotypes were infected and implanted within the BLA (Fig. 4d), allowing the sole activation of BLA neurons but not the potentiation of hippocampo-BLA synapses (data not shown). However, after illumination of BLA neurons, we observed an increase of freezing levels in context B potentially resulting from activation of anxiety-related brain structures by BLA projections (Felix-Ortiz et al. 2013; Felix-Ortiz and Tye 2014). We conclude that the restoration of contextual fear expression in *il1rapl1-/y* mice only occurs through the potentiation of hippocampo-BLA synapses at the testing time and specifically in the conditioning context.

Discussion

Learning, together with the retrieval and behavioral expression of previously encoded memories, contributes jointly to the cognitive fitness of individuals. In the present work we show that the intellectual disability gene *Il1rapl1* is necessary for the relevant expression of previously formed contextual fear memory.

While we recently revealed that *Il1rapl1*-deficient mice exhibit I/E imbalance at thalamic projections to the LA with consequences on cued fear learning (Houbaert et al. 2013), we observe here a very similar cellular phenotype at functionally isolated hippocampo-BLA projections with consequences on contextual fear memory expression but not learning per se (see below). In *Il1rapl1 -/y*, thalamo-LA excitatory synapses impinging onto principal cells are deficient, but synapses of the same projection contacting interneurons seem unaltered (Houbaert et al. 2013). Although we did not specifically re-address whether the excitatory drive onto local BLA interneurons was preserved, we may nevertheless propose that a lack of excitation at long-range projections causing a local I/E imbalance is a functional signature of *Il1rapl1* mutation in the mouse brain. This is further supported by the ubiquitous

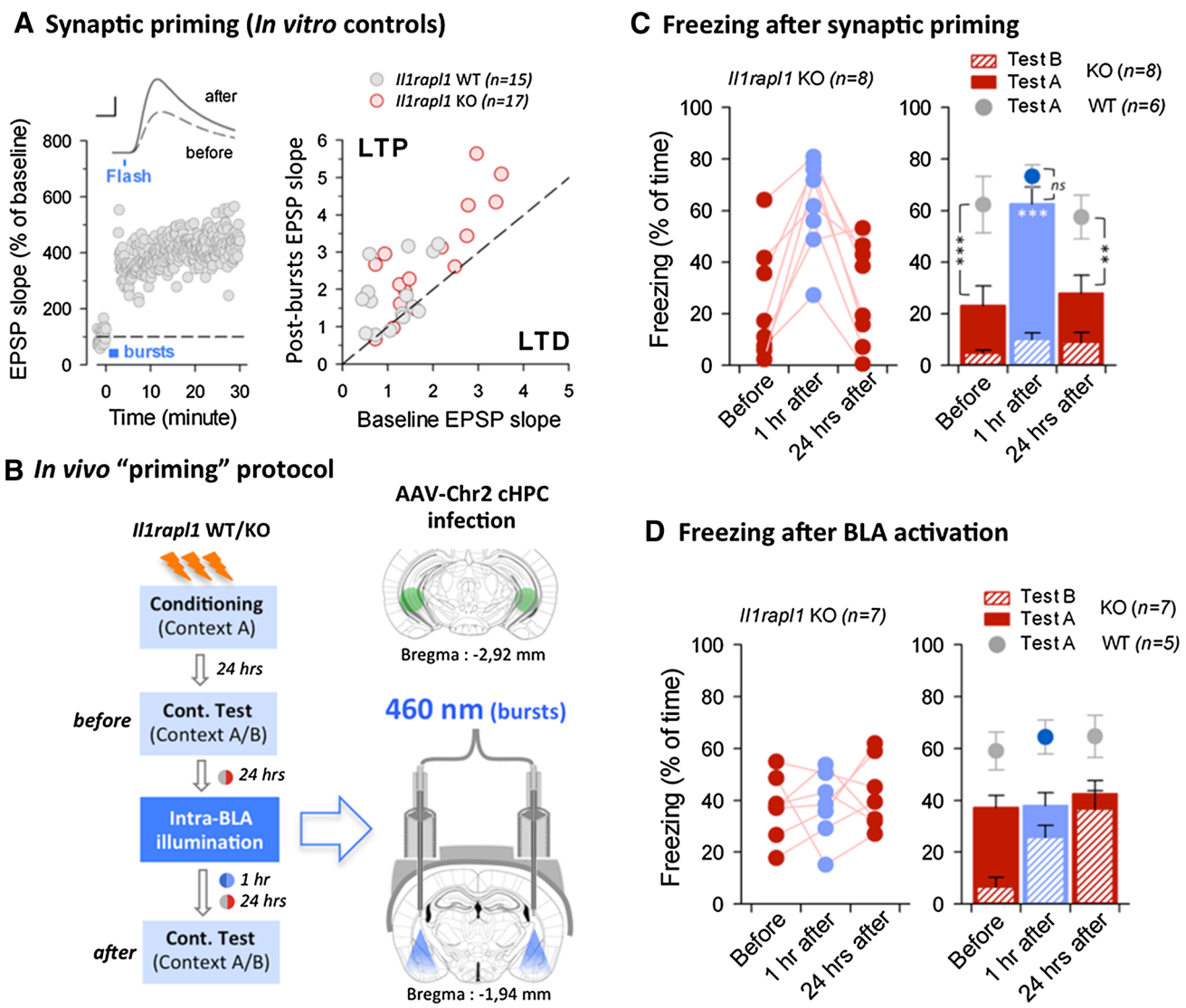

Fig. 4 Hippocampo-BLA synaptic priming restores fear expression in Il1rapl1 mutant mice. **a** Light-bursting stimulation of hippocampo-BLA terminals leads to stable potentiation of synaptic efficacy onto BLA pyramidal neurons. *Scale bars:* 3 mV and 5 ms. **b** Experimental design of the in vivo "priming" experiment. **c** Burst illumination of hippocampo-BLA terminals normalizes contextual fear in *Il1rapl1* KO mice. Two-way ANOVA revealed a significant effect of genotype (ANOVA $F_{(1,36)} = 17{,}641$; $p < 0.001$) and of illumination (ANOVA $F_{(2,45)} = 7{,}113$; $p = 0.007$), but no interaction between genotype and illumination (ANOVA $F_{(2,45)} = 1{,}781$; $p = 0.183$) as the illumination did not have an significant effect on WT freezing levels. SNK post hoc multiple comparisons were used to test for differences between groups. They showed a strong effect of illumination on KO freezing levels (SNK before vs. 1 h after; $p = 0.001$). The difference observed between WT and KO animals before illumination (SNK before WT vs. KO; $p = 0.001$) disappeared after illumination, with KO animals reaching similar levels to WT animals (SNK 1 h after WT vs. KO; $p > 0.05$). 24 h after treatment, a difference between WT and KO animals was observed again (SNK 24 h later WT vs. KO $p < 0.05$), showing that activation of hippocampo-BLA fibers transiently rescues KO phenotype. **d** Illumination of BLA neurons did not normalize contextual fear to context A in *Il1rapl1* KO mice. Two-way ANOVA revealed a significant effect of genotype (ANOVA $F_{(1,30)} = 22{,}868$; $p < 0.001$) and no significant effect of illumination (ANOVA $F_{(2,30)} = 0{,}407$; $p = 0.669$). SNK post hoc multiple comparisons were used to test for differences between groups. Indeed, the initial contextual fear deficit of *Il1rapl1* KO mice before light (SNK before WT vs. KO; $p = 0.016$) was not rescued by light stimulation of BLA (SNK 1 h after WT vs. KO; $p = 0.004$) and remained 24 h after light stimulation (SNK 24 h after WT vs. KO; $p = 0.014$). Illumination of BLA neurons increased freezing levels in KO animals to unspecific context B (one-way repeated measures ANOVA; $F_{(2,12)} = 8{,}025$; $p < 0.01$; SNK post hoc: before vs. 1 h after $p < 0.05$; before vs. 24 h after $p < 0.01$). The same treatment had no effect on WT freezing levels in context B (one-way repeated measures ANOVA; $F_{(2,8)} = 2{,}135$; $p > 0.05$)

and homogeneous expression of *Il1rapl1* mRNA throughout the brain (Houbaert et al. 2013).

Yet, in contrast to the pathophysiological mechanisms leading to cued fear learning deficits in the same mice, our current dataset supports that contextual memory formation—and the synaptic contacts accounting for—are either unaffected or resistant to the pathologic consequences of *Il1rapl1* deficiency. Indeed, we observed that upon contextual fear reactivation, dHPC activation was high in *Il1rapl1* -/y mice, suggesting that the contextual fear engram is properly established (Goshen et al. 2011) (Fig. 2). Accordingly, *Il1rapl1*-deficient mice are capable of exhibiting normal discriminative fear behavior after optogenetic priming stimulations (Fig. 4). Furthermore, in our previous report focusing on LA, treatments aiming at correcting or bypassing the LA I/E imbalance were efficient only if applied immediately before the CS/US association, that is at the exact timing of associative synaptic plasticity induction and memory formation (Houbaert et al. 2013). In the present work, none of the pre-training treatments, such as overtraining in the conditioning context (Fig. 1) or BLA bicuculline infusion (data not shown), was efficient in correcting the lack of contextual fear reaction during the tests (Houbaert et al. 2013). In contrast, it was sufficient to improve the neurotransmission efficacy at hippocampo-BLA connections during the contextual tests to normalize the freezing behavior of *Il1rapl1* mutant mice. Interestingly, restoration of conditioned response in *Il1rapl1*-deficient mice was only temporary as freezing levels returned to their initial values 24 h after the "priming" experiment (Fig. 4c). This may indicate that stabilization of LTP is not completed using rather artificial light-induced stimulation protocols that possibly exclude endogenous neuromodulations. Furthermore, contextual discrimination was preserved in these "phenotypic restoration" experiments, and behavioral restoration was not obtained through the sole induction of firing at targeted BLA neurons (Fig. 4). We thereby exclude that behavioral improvement results from general changes in activity levels and/or general anxiety induced by alterations of the BLA to vHPC projections (Felix-Ortiz et al. 2013; Felix-Ortiz and Tye 2014).

Altogether, our approach enabled fine characterization of pathologically relevant phenotypes of the *Il1rapl1* ID mouse model. We could show that altered I/E balance at the hippocampo-BLA projections leads to a deficit in contextual memory expression rather than memory formation. Thereby, our data suggest that cognitive disability in humans may result from the deficiency of synapses involved at different steps of the cognitive process, including memory restitution and behavioral expression.

Materials and methods

Animals

All experiments were performed using male *Il1rapl1* -/y (*Il1rapl1* KO) and their control +/y (*Il1rapl1* WT) littermates (C57BL/6 J background, 2–4 months old), housed in 12/12 LD with ad libitum feeding. Every effort was made to minimize the number of animals used and their suffering. The experimental design and all procedures were in accordance with the European guide for the care and use of laboratory animals and the animal care guidelines issued by the animal experimental committee of Bordeaux Universities (CE50) (A5012009).

Fear conditioning

Mice were housed individually in a ventilated area before the start of behavioral training. To avoid excessive stress during the experiments, animals were handled every day before the start of the experiment during a week. On day 1, animals were transferred to the conditioning context (context A) for habituation. On day 2, we proceeded with the conditioning phase. The protocol typically consisted of 3× foot shock of 0.6 mA for 2 s with 60 s time interval between shocks. Discriminative contextual fear memory was tested 24 h after conditioning by analyzing the freezing levels in context B vs. context A (Tests B/A). Freezing behavior was quantified automatically in each behavioral session using a CCD camera connected to automatic freezing detection software (Ugo Basile, Italy). To test for animal exploration and activity, the animal displacement in the context was traced and analyzed with software programmed and provided by Dr. Jiyun Peng (Fudan University, Shanghai, China). In Fig. 1b, different groups of conditioned mice were submitted to single contextual test A only once at 1, 2, 6, 12 or 24 h after the shock applications. In the under/overtraining experiments (Fig. 1c) the protocol was modified to either 1 or 10× foot shock of 0.6 mA for 1 s with 30–75 s interval between shocks.

Stereotaxic viral infections and cannula implantations

AAV injections

Adeno-associated viruses [AAV2/9.CAG.ChR2-Venus.W.SV40-p1468, ref Addgene-20071, $5.82E^{12}$ vector genomes (vg)/ml] (Figs. 3, 4) were packaged at the University of Pennsylvania Vector Core. Around 2 months old mice (over 20 g) were prepared for the stereotaxic injection. Beforehand, mice were treated with buprenorphine (0.1 mg/kg, i.p) and positioned in a stereotaxic apparatus (David Kopf Instruments, Tujunga, CA) under continuous

anesthesia with isoflurane. During the surgery, the mice were warmed on a 33–35 °C heating pad. The virus was bilaterally pressure injected through glass pipettes (Hirschmann Laborgerate, ringcaps, tips pulled O.D 30–50 µm) using a Picosprizer (Parker Co). The positions of bregma and lambda points were defined and adjusted to the same horizontal level. Coordinates for the BLA are: (AP) −1.5–1.7 mm, (ML) ±3.2–3.4 mm, (DV) −4.8 mm; or caudal HPC: (AP) −3.1–3.3 mm, (ML) ±3.2–3.4 mm, (DV) −4.0 mm.

Cannula implantation

Stainless steel guide cannula (26 or 24 gauge; Plastics-One, Roanoke, VA, USA) were bilaterally implanted above the BLA: (AP) −1.5–1.7 mm, (ML) ±3.2–3.4 mm, (DV) −3.4–3.5 mm; or caudal HPC: (AP) −3.1–3.3 mm, (ML) ±3.2–3.4 mm, (DV) −3.0–3.1 mm. The cannula was secured to the skull using dental cement (Super-Bond, Sun Medical Co. Ltd, Moriyama, Shiga, Japan). Finally, a dummy cannula was inserted into the guide cannula to reduce the risk of infection. During the proceeding 2 weeks of cannula surgery recovery, or 4–6 weeks of virus transfection, body weight and symptoms of sickness were monitored carefully.

Optical stimulation and behavioral testing

To be tightly fixed to the guide cannula pedestal, an optical polymer fiber (200 or 250 µm of diameter, Prizmatix Ltd, Israel) was glued through an infusion cannula housing holder and assembled with a locking cap collar (Plastics-One, US). The projection distance out of the guide cannula tip (1–1.5 mm) was set to allow positioning of the fiber above the BLA (Fig. 4).

After being submitted to a classical habituation/conditioning/test sequence, cHPC-(priming) and BLA- (control, data not shown) infected mice were bilaterally illuminated through BLA cannula in their home cages 1 h before being re-exposed to the fearful context. Bursting light stimulations were similar to the one used in vitro (see below). Note that both in vivo and in vitro, 20 Hz, instead of 100 Hz trains, gave similar results (data not shown).

Electrophysiology

Acute slices preparations

We prepared coronal BLA- or cHPC-containing acute slices from mice infected with the AAV-Chr2 constructs in the cHPC. Due to animal age (3–4 months old), we used the "protective recovery method" described in http://www.brainslicemethods.com. Briefly, mice were anesthetized with a mixture of ketamine/xylazine (100 and 10 mg/kg, respectively) and cardiac-perfused with ice-cold, oxygenated (95 % O_2, 5 % CO_2) NMDG-based cutting solution containing (in mM): 93 NMDG, 93 HCl, 2.5 KCl, 1.2 NaH_2PO_4, 30 $NaHCO_3$, 25 Glucose, 10 $MgSO_4$, 0.5 $CaCl_2$, 5 sodium ascorbate, 3 sodium pyruvate, 2 thiourea and 12 mM *N*-acetyl-L-cystéïne (pH 7.3–7.4, with osmolarity of 300–310 mOsm). The brains were rapidly removed and placed in the ice-cold and oxygenated NMDG cutting solution described above. Coronal slices (300 µm) were prepared using a Vibratome (VT1200S, Leica Microsystems, USA) and transferred to an incubation chamber held at 32 °C and containing the same NMDG cutting solution. After this incubation the slices were maintained at room temperature in oxygenated modified ACSF containing (mM): 92 NaCl, 2.5 KCl, 1.2 NaH_2PO_4, 30 $NaHCO_3$, 20 HEPES, 25 glucose, 2 $MgSO_4$, 2 $CaCl_2$, 5 sodium ascorbate, 3 sodium pyruvate, 2 thiourea and 12 mM *N*-acetyl-L-cystéïne (pH 7.3–7.4, with osmolarity of 300–310 mOsm) until recording.

Recordings

Whole-cell recordings from BLA principal neurons were performed at 30–32 °C in a superfusing chamber as previously described (Houbaert et al. 2013). Neurons were visually identified with infrared videomicroscopy using an upright microscope equipped with a 60× objective. Patch electrodes (3–5 MΩ) were pulled from borosilicate glass tubing and filled with a low-chloride solution containing (in mM): 140 Cs-methylsulfonate, 5 QX314-Cl, 10 HEPES, 10 phosphocreatine, 4 Mg-ATP and 0.3 Na-GTP (pH adjusted to 7.25 with CsOH, 295 mOsm).

Feedforward inhibition

BLA principal neurons were recorded in voltage clamp mode at −70 mV (to record AMPAR-mediated EPSCs) or 0 mV (to record GABAAR-mediated IPSCs) as previously described (Houbaert et al. 2013). Hippocampo-BLA monosynaptic EPSCs and di-synaptic IPSCs were elicited by 1 ms light stimulations delivered by an ultrahigh power 460 nm LED (Prizmatix Ltd, Israel) at maximal intensity.

LTP experiments

In these dedicated current-clamp experiments, Cs-methylsulfonate was replaced with equimolar K-gluconate. All experiments were performed in the absence of picrotoxin. Hippocampo-BLA monosynaptic EPSPs were elicited by 1 ms light stimulations delivered by an ultrahigh power 460 nm LED (Prizmatix Ltd, Israel). Light intensity was adjusted to obtain baseline EPSP amplitudes of ∼5 mV.

The induction "bursting" protocols are composed of five burst episodes separated by 30 s. Each burst is composed of 20 trains (applied at 5 Hz) of four light flashes (intra-train frequency: 100 Hz). Baseline transmission is obtained at 0.2 Hz.

Data acquisition and analysis

Data were recorded with a Multiclamp700B (Molecular Devices, USA), filtered at 2 kHz and digitized at 10 kHz. Data were acquired and analyzed with pClamp10.2 (Molecular Devices). In all LTP experiments, series resistance was monitored throughout the experiment, and if it changed by more than 15 %, the data were not included in the analysis. Changes were quantified by normalizing and averaging EPSC amplitude or EPSP slope during the last 5 min of the experiments relative to the 5 min of baseline prior to LTP induction.

c-Fos detection

90 min after the contextual test, mice were deeply anesthetized with pentobarbital and fixed by intracardiac perfusion with 4 % paraformaldehyde in PBS. Brains were removed, post-fixed overnight and preserved in PBS. Coronal slices, 50-µm thick, were obtained using a vibratome (Leica 1,200 s). For *c-Fos* immunostaining, brain sections were maintained in a blocking buffer (PBS solution containing 0.3 % Triton X-100 and 2 % gelatin) for 1 h at room temperature. Thereafter, sections were incubated at 4 °C overnight with polyclonal antibody against *c-Fos* (1:20,000; Merck-Millipore, PC38) diluted in the blocking buffer. Slices were rinsed three times in PBS and incubated for 1 h 30 min at room temperature with goat anti-rabbit, biotinylated secondary antibody. After being rinsed in PBS, we incubated them with avidin–biotin complex (Vector Laboratories); slices were rinsed in PBS and c-Fos was detected using the DAB substrate kit for peroxidase (Vector Laboratories).

All slice images were taken by a Nanozoomer 2.0 HT (Hamamatsu Photonics, Massy, France) using objective UPS APO 20× NA 0.75 combined with an additional lens 1.75×, leading to a final magnification of 35×. Virtual slides were acquired with a TDI-3CCD camera. Regions of interest for the c-Fos counting were identified with reference to the Paxinos and Watson brain atlas. Regions of interest included: the cellular layer of the dentate gyrus (bregma: −1.34 to −1.94 mm) and CA1 (bregma: dHPC: −1.34 to −1.94 mm; cHPC: −2.92 to −3.52 mm) regions of the hippocampus, and the BLA (bregma: −1.34 to −1.94 mm). To automatize the analysis, a homemade macro was written using NIH's ImageJ. A combination of a threshold and a size selection with the Analyze Particles plugin performed on each region of interest allowed us to count the number of positive cells. We also controlled that *Il1rapl1* deletion did not affect cell density in selected regions of interest. To this aim, 3 *Il1rapl1* WT and 3 KO mice were deeply anesthetized with pentobarbital and fixed with 4 % paraformaldehyde/PBS using intra-cardiac perfusion. Brains were removed, post-fixed overnight and preserved in PBS. Coronal slices, 60-µm-thick, were obtained using a vibratome (Leica 1,200 s). dHPC/BLA sections (bregma: −1.34 to −1.94 mm) and cHPC (bregma: −2.92 to −3.52 mm) were mounted in hard-set vectashield containing DAPI before being imaged using an upright epifluorescence microscope, Nikon Eclipse Ni-U (Nikon France S.A) using 40× objective CFI Plan Fluor NA 0.75. Regions of interest for the c-Fos counting were identified with reference to the Paxinos and Watson brain atlas as for c-Fos counting. Automatized image processing was made possible using a homemade ImageJ (NIH, USA) macro based on the automatic nuclei counter plugin. No difference in cellular density was observed in any of the analyzed areas between *Il1rapl1* WT and KO animals.

Statistical analysis

Detailed statistics are described in each figure legend. Briefly, when comparing the effect of one factor in a group, Student's *t* test was used. However, when data were not following a normal distribution, we applied the Mann–Whitney rank-based statistical test. When studying the impact of two factors (genotype and treatment) in optogenetic experiments, we used two-way ANOVA followed by Student–Newman–Keuls (SNK) post hoc analysis to test for differences between groups of interest. For all tests, statistical difference was concluded when $p < 0.05$.

Reagents

Tetrodotoxin was purchased from Latoxan and stock solution prepared in acetate buffer at pH 4.5. Bicuculline and muscimol were purchased from Ascent Scientific (Cambridge, UK) and 4-AP from Sigma Aldrich (Saint Louis, USA).

Acknowledgments We thank Drs. Cyril Herry, Andréas Luthi and Andrew Penn for fruitful discussions and corrections of the manuscript. We are grateful to Dr. P. Billuart and J. Chelly for their help and for providing us with *Il1rapl1* mutant mice, and Dr. Jiyun Peng for helping in the tracking of mouse activities. We acknowledge Ed Boyden, Ph.D., and the Massachusetts Institute of Technology for kindly providing AAV-ArchT constructs to the research community and Dr. C. Herry for providing us with AAV viruses. We also thank the Pole in vivo and animal facilities of the Bordeaux University for the animal care. The microscopy was done in the Bordeaux Imaging Centre of the University of Bordeaux, with the help of Sébastien Marais. This study was supported by grants from the Agence

Nationale pour la Recherche (ANR-10-BLAN-1434, ANR-12-JSV4-0005-01, ANR-12-SAMA-001-03 and ANR-10-LABX-43 BRAIN to E.H. and Y.H.), the European Neuroscience Institutes Network (Y.H.), the Gencodys FP7 program (Y.H.).

References

Anagnostaras SG, Gale GD, Fanselow MS (2001) Hippocampus and contextual fear conditioning: recent controversies and advances. Hippocampus 11:8–17 doi:10.1002/1098-1063(2001) 11:1<8:AID-HIPO1015>3.0.CO;2-7

Baroncelli L, Braschi C, Spolidoro M et al (2011) Brain plasticity and disease: a matter of inhibition. Neural Plast 2011:1–11. doi:10.1155/2011/286073

Bienvenu TCM, Busti D, Magill PJ et al (2012) Cell-type-specific recruitment of amygdala interneurons to hippocampal theta rhythm and noxious stimuli in vivo. Neuron 74:1059–1074. doi:10.1016/j.neuron.2012.04.022

Carrié A, Jun L, Bienvenu T et al (1999) A new member of the IL-1 receptor family highly expressed in hippocampus and involved in X-linked mental retardation. Nat Genet 23:25–31. doi:10.1038/12623

Felix-Ortiz AC, Tye KM (2014) Amygdala inputs to the ventral hippocampus bidirectionally modulate social behavior. J Neurosci 34:586–595. doi:10.1523/JNEUROSCI.4257-13.2014

Felix-Ortiz AC, Beyeler A, Seo C et al (2013) BLA to vHPC inputs modulate anxiety-related behaviors. Neuron 79:658–664. doi:10.1016/j.neuron.2013.06.016

Gambino F, Pavlowsky A, Begle A et al (2007) IL1-receptor accessory protein-like 1 (IL1RAPL1), a protein involved in cognitive functions, regulates N-type Ca^{2+}-channel and neurite elongation. Proc Natl Acad Sci 104:9063–9068. doi:10.1073/pnas.0701133104

Gatto CL, Broadie K (2010) Genetic controls balancing excitatory and inhibitory synaptogenesis in neurodevelopmental disorder models. Front Synaptic Neurosci 2:4. doi:10.3389/fnsyn.2010.00004

Goosens KA (2011) Hippocampal regulation of aversive memories. Curr Opin Neurobiol 21:460–466. doi:10.1016/j.conb.2011.04.003

Goshen I, Brodsky M, Prakash R et al (2011) Dynamics of retrieval strategies for remote memories. Cell 147:678–689. doi:10.1016/j.cell.2011.09.033

Hayashi T, Yoshida T, Ra M et al (2013) IL1RAPL1 associated with mental retardation and autism regulates the formation and stabilization of glutamatergic synapses of cortical neurons through RhoA signaling pathway. PLoS One 8:e66254. doi:10.1371/journal.pone.0066254.s002

Herry C, Mons N (2004) Resistance to extinction is associated with impaired immediate early gene induction in medial prefrontal cortex and amygdala. Eur J Neurosci 20:781–790. doi:10.1111/j.1460-9568.2004.03542.x

Houbaert X, Zhang CL, Gambino F et al (2013) Target-specific vulnerability of excitatory synapses leads to deficits in associative memory in a model of intellectual disorder. J Neurosci 33:13805–13819. doi:10.1523/JNEUROSCI.1457-13.2013

Hübner C, Bosch D, Gall A et al (2014) Ex vivo dissection of optogenetically activated mPFC and hippocampal inputs to neurons in the basolateral amygdala: implications for fear and emotional memory. Front Behav Neurosci 8:64. doi:10.3389/fnbeh.2014.00064

Knapska E, Macias M, Mikosz M et al (2012) Functional anatomy of neural circuits regulating fear and extinction. Proc Natl Acad Sci 109:17093–17098. doi:10.1073/pnas.1202087109

Kullmann DM, Moreau AW, Bakiri Y, Nicholson E (2012) Plasticity of inhibition. Neuron 75:951–962. doi:10.1016/j.neuron.2012.07.030

Ledoux JE (2000) Emotion circuits in the brain. Annu Rev Neurosci 23:155–184. doi:10.1146/annurev.neuro.23.1.155

Lisman JE, Coyle JT, Green RW et al (2008) Circuit-based framework for understanding neurotransmitter and risk gene interactions in schizophrenia. Trends Neurosci 31:234–242. doi:10.1016/j.tins.2008.02.005

Liu X, Ramirez S, Pang PT et al (2012) Optogenetic stimulation of a hippocampal engram activates fear memory recall. Nature 484:381–385. doi:10.1038/nature11028

Maren S, Phan KL, Liberzon I (2013) The contextual brain: implications for fear conditioning, extinction and psychopathology. Nat Rev Neurosci. doi:10.1038/nrn3492

Morozov A, Sukato D, Ito W (2011) Selective suppression of plasticity in amygdala inputs from temporal association cortex by the external capsule. J Neurosci 31:339–345

Muller J, Corodimas KP, Fridel Z, Ledoux JE (1997) Functional inactivation of the lateral and basal nuclei of the amygdala by muscimol infusion prevents fear conditioning to an explicit conditioned stimulus and to contextual stimuli. Behav Neurosci 111:683–691

Orsini CA, Kim JH, Knapska E, Maren S (2011) Hippocampal and prefrontal projections to the basal amygdala mediate contextual regulation of fear after extinction. J Neurosci 31:17269–17277. doi:10.1523/JNEUROSCI.4095-11.2011

Pavlowsky A, Gianfelice A, Pallotto M et al (2010) A postsynaptic signaling pathway that may account for the cognitive defect due to IL1RAPL1 mutation. Curr Biol 20:103–115. doi:10.1016/j.cub.2009.12.030

Pavlowsky A, Chelly J, Billuart P (2011) Emerging major synaptic signaling pathways involved in intellectual disability. Mol Psychiatry. doi:10.1038/mp.2011.139

Pentkowski NS, Blanchard DC, Lever C et al (2006) Effects of lesions to the dorsal and ventral hippocampus on defensive behaviors in rats. Eur J Neurosci 23:2185–2196. doi:10.1111/j.1460-9568.2006.04754.x

Petreanu L, Huber D, Sobczyk A, Svoboda K (2007) Channelrhodopsin-2-assisted circuit mapping of long-range callosal projections. Nat Neurosci 10:663–668. doi:10.1038/nn1891

Pitkänen A, Pikkarainen M, Nurminen N, Ylinen A (2000) Reciprocal connections between the amygdala and the hippocampal formation, perirhinal cortex, and postrhinal cortex in rat. A review. Ann N Y Acad Sci 911:369–391

Piton A, Michaud JL, Peng H et al (2008) Mutations in the calcium-related gene IL1RAPL1 are associated with autism. Hum Mol Genet 17:3965–3974. doi:10.1093/hmg/ddn300

Rudy JW, Huff NC, Matus-Amat P (2004) Understanding contextual fear conditioning: insights from a two-process model. Neurosci Biobehav Rev 28:675–685. doi:10.1016/j.neubiorev.2004.09.004

Rumpel S, LeDoux J, Zador A, Malinow R (2005) Postsynaptic receptor trafficking underlying a form of associative learning. Science 308:83–88. doi:10.1126/science.1103944

Valnegri P, Montrasio C, Brambilla D et al (2011) The X-linked intellectual disability protein IL1RAPL1 regulates excitatory synapse formation by binding PTP and RhoGAP2. Hum Mol Genet 20:4797–4809. doi:10.1093/hmg/ddr418

Yoshida T, Yasumura M, Uemura T et al (2011) IL-1 receptor accessory protein-like 1 associated with mental retardation and autism mediates synapse formation by trans-synaptic interaction with protein tyrosine phosphatase. J Neurosci 31:13485–13499. doi:10.1523/JNEUROSCI.2136-11.2011

IX) General discussion

Identification of neuronal dysfunctions associated with intellectual disability represents an important challenge in modern neuroscience. Using a mouse model mutated for the *Il1rapl1* gene, my findings shed some light on the consequences of the removal of this ID gene at the behavioral and synaptic level, providing a strong link between synaptic abnormalities and learning/memory impairments (Figure 31). The mutation of *Il1rapl1* led to local inhibitory/excitatory imbalances in amygdala by the target-specific disruption of excitatory synapses of principal cells. This resulted in behavioral deficits in both the ability to form new memories and express previously formed memories (Figure 31). Most importantly, *in vivo* interventions aiming at restoring I/E imbalance in *Il1rapl1* KO mice were effective in normalizing behavior, suggesting that some corrections must be effective in adult individuals. Also, my work highlights the importance of studying all components of a particular neural circuit to understand the functional consequences of a given mutation as it may act at discrete cellular and/or synaptic levels.

A major consequence of my work was to define *Il1rapl1* deficiency as a cause of I/E imbalances in neuronal circuits. I believe that this is an important step in our understanding of *Il1rapl1*-associated cognitive deficiencies. Indeed, I/E imbalances potentially interfere with information processing at multiple levels affecting numerous and various functional aspects of neuronal function. It is strongly believed that the synchronization between synaptic excitation and inhibition is of key importance for the triggering of neuronal activity, the duration and time course of spike discharge, and eventually its synchronization at the millisecond scale (Isaacson and Scanziani, 2011). Noteworthy, too low or too high inhibition leads to brain dysfunction and neuropsychological diseases (Baroncelli et al., 2011; Gatto and Broadie, 2010).

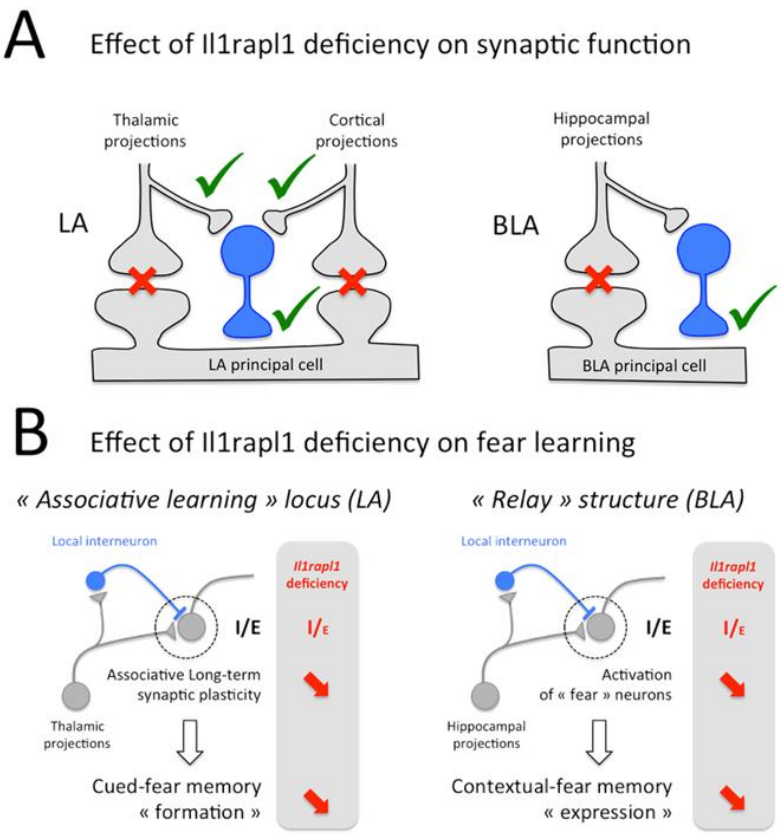

Figure 31: Scheme representing the effects of Il1rapl1 deficiency on synaptic function and fear learning. A. In LA (left), *Il1rapl1* deficiency leads to the target-specific disruption of excitatory synapse on principal cells. Excitatory synapses on interneurons and FFI are preserved. In BLA (right), excitatory synapses on principal cells were disrupted and FFI preserved. B. Target-specificity led to a local I/E imbalance in both LA and BLA. In LA, I/E imbalance led to a deficit in associative synaptic plasticity underlying the formation of the cued fear memory. In BLA, local I/E imbalance led to a lower activation of BLA principal cells following incoming information from ventral hippocampus and the consequent deficit in contextual fear memory expression.

However, many questions still remain unanswered at the end of my PhD work. For example, one could wonder whether I/E imbalances are generalized throughout the brain or if they are discrete, affecting some brain areas and leaving others untouched. Understanding I/E imbalances following IL1RAPL1 deficiency requires answering the general question of how, where and when I/E imbalances are generated in the brain upon IL1RAPL1 deficiency. Undoubtedly, understanding how IL1RAPL1 deficiency affects I/E imbalance will require continuous efforts and the use of various cellular molecular, functional and genetic approaches to further unravel how synaptic heterogeneity in the brain is causing the I/E imbalance. A crucial step will be to define the onset and the time-course of I/E imbalances throughout animal's life,

as it may drive the development of targeted therapeutic interventions that would aim to intervene at periods when IL1RAPL1 is functionally more important. In the following paragraphs I'll try to consider these points by opening some perspectives and proposing some experimental strategies combining behavioral, cellular, synaptic and molecular strategies.

1 How and where does IL1RAPL1 absence impact the synapse?

My work mostly concentrated on the *in vivo* consequences of IL1RAPL1 absence at both synaptic and behavioral levels. However, I didn't further study the molecular mechanisms underlying IL1RAPL1 function in the brain. Indeed most experimental data on IL1RAPL1 function at the synapse have been obtained on *in vitro* neuronal cultures. The identities of the cellular and/or molecular mechanisms underlying IL1RAPL1 function at the synapse are still not completely understood, especially when taking into account the large synaptic heterogeneity in the brain. The next chapter aims at discussing how and where IL1RAPL1 absence leads to I/E imbalances in the brain.

1.1 IL1RAPL1, a synaptogenic protein

Understanding the precise role of a synaptic protein requires a fine understanding of the exact localization of the protein at the synapse. Thus, it is somehow surprising that no clear-cut consensus emerged yet about the cellular localization of IL1RAPL1. As stated in the introduction, IL1RAPL1 is expressed in several brain regions throughout the brain in both excitatory and inhibitory cells. Remarkably, it is still not clear if the protein product is present at both pre-and postsynaptic compartments. In neuronal cultures, over-expressed tagged IL1RAPL1 is highly enriched in postsynaptic compartments, particularly in dendritic spines (Pavlowsky et al., 2010b; Valnegri et al., 2011; Yoshida et al., 2011). One of these studies however does report a weak signal for IL1RAPL1 protein in axons but without further exploring this finding (Yoshida et al., 2011). We have tried localizing endogenous IL1RAPL1 protein in brain slices but none of the currently available antibodies were capable of localizing it (data not shown). Further efforts were made by our collaborators in the Cochin institute (P. Billuart, M. Ramos) in order to

generate more specific IL1RAPL1 antibodies, using different epitopes. These attempts remained unsuccessful. Given the rather "artificial conditions" that were used in previous studies (over-expression in cultured neurons) to determine the localization of IL1RAPL1, I would not yet consider IL1RAPL1 solely as a postsynaptic protein.

1.1.1 Postsynaptic IL1RAPL1 mediates synapse formation/maintenance

Recently a model has emerged where postsynaptic IL1RAPL1 is believed to mediate excitatory synapse formation by trans-synaptic interactions with presynaptic protein PTPδ. Indeed, interaction of presynaptic PTPδ with postsynaptic IL1RAPL1 in cultured cells leads to recruitment of pre- and postsynaptic partners (Valnegri et al., 2011; Yoshida et al., 2011) mediating synapse differentiation and formation. However, the exact molecular partners and signaling pathways that mediate postsynaptic spine formation are not clearly established. Following formation of the PTPδ/IL1RAPL1 complex, RhoGAP2 is recruited to the postsynaptic site and binds to IL1RAPL1 (Valnegri et al., 2011). Interestingly, a lot of ID-gene mutations are found in proteins of the family of small GTP-ases (Ba et al., 2013). RhoGAP2 inhibits Rac1 activity, a protein involved in neuronal development and spine morphogenesis through effects on the actin cytoskeleton (Etienne-Manneville and Hall, 2002). However, this report didn't address whether IL1RAPL1/RhoGAP2 interaction really leads to the inhibition of Rac1 pathway and how this could impact cytoskeletal organization. Interestingly, interaction of IL1RAPL1 with the newly characterized partner Mcf2l activates downstream RhoA/ROCK signaling cascade which has been shown to be important in cytoskeleton dynamics (Hayashi et al., 2013). Together, these results suggest that IL1RAPL1/PTPδ interaction recruits postsynaptic effectors that mediate cytoskeleton organization, a crucial step in the formation and morphology of dendritic spines (Govek et al., 2005). However, it is quite surprising that *in vivo*, in a more constraint environment, the density and morphology of dendritic spines was found to be roughly normal (but see mild effects found in (Pavlowsky et al., 2010b), suggesting strong functional redundancies. Interestingly, because of the aspiny or low-spiny nature of interneurons, one can imagine that the vulnerability of excitatory synapses onto these cells to IL1RAPL1 deficiency may be less important, thereby generating I/E imbalance.

The presynaptic compartment is also strongly enriched in actin cytoskeleton and undergoes strong remodeling during synaptic formation and elimination. Thus, if IL1RAPL1 localizes presynaptically it could potentially impact actin cytoskeleton organization at the presynaptic compartment. However, because of the presynaptic localization of PTPδ, this is unlikely to occur through formation of a transsynaptic IL1RAPL1/PTPδ complex. The increasing evidence of IL1RAPL1/PTPδ in synapse formation urges researchers to develop tools that would allow imaging this complex at more integrated levels to confirm *in vitro* findings (but see (Yoshida et al., 2011)). Indeed, the precise cellular and synaptic distribution of PTPδ and IL1RAPL1 protein *in vivo* is still lacking, which makes it difficult to know how and where PTPδ/IL1RAPL1 complex could be formed. This could potentially be achieved by creating transgenic mouse lines where both PTPδ and IL1RAPL1 would be fused to fluorophores. However, creating double transgenic mouse lines is energy consuming and not easy to achieve. Recently, a technique was developed that allows mapping synaptic connectivity in the brain called GRASP (GFP reconstitution across synaptic partners). This technique is based on the functional complementation between a pre- and postsynaptic partner, each of them being fused with a solely non-functional GFP fragment. Upon close apposition, fluorescence is recovered and synaptic connectivity can be imaged. Expression of the pre-and postsynaptic fragments is achieved by genetic interventions combining in utero electroporation and Cre-Lox technology (Kim et al., 2012). However, because this technique uses over-expression manipulations, using proteins with possible synaptogenenic properties (as PTPδ and IL1RAPL1) could lead to artifacts that don't reflect the endogenous role of the transsynaptic complex *in vivo*.

At the postsynaptic site, IL1RAPL1 interacts with PSD-95 whose recruitment to the PSD is regulated by JNK activity (Pavlowsky et al., 2010b). PSD-95 interacts with a lot of postsynaptic scaffold proteins and loss of interaction with IL1RAPL1 could potentially disrupt general organization of the PSD by altering the distribution and function of others scaffold proteins of the PSD, leading to deficits in general function/anatomy of the postsynaptic site. Interestingly, PSD-95 interacts with NR-2 subunit of NMDA receptors thereby controlling its dynamics (Kornau et al., 1995), suggesting that *Il1rapl1* deletion could disrupt excitatory transmission. In addition, interaction of IL1RAPL1 with MCF2L seems to promote AMPA receptor dynamics at the

postsynaptic site, leading to the insertion of GluA2/A3 subunit-containing AMPA receptors at the synapse. This insertion was shown to depend on Mcf2l/RhoA/ROCK pathway (Yoshida et al., 2011). Taken together, these results suggest that *Il1rapl1* mutation could lead to deficits in basal excitatory synaptic transmission by impacting glutamate receptor dynamics. This is an important issue as I observed that AMPAR-mediated excitatory transmission was affected at some long-range projections in *Il1rapl1*-deficient mice (Pavlowsky et al., 2010b).

In conclusion, IL1RAPL1 interacts with post-and transsynaptic effectors to mediate spine formation and/or maintenance possibly through actions on the actin cytoskeleton or general organization of the PSD. The absence of IL1RAPL1 would then disturb these processes leading to morphological abnormalities in dendritic spines. An important question is to understand if the heterogeneity in the impact of *Il1rapl1* deficiency onto spine morphology is resulting from IL1RAPL1 itself (various expression levels of IL1RAPL1 or of some important partners) or from heterogeneous expression of redundancy mechanisms. This would be not so surprising when considering the large number of protein/protein interactions contributing to synaptogenesis.

1.1.2 Heterogeneity defines vulnerability to IL1RAPL1 absence

What are the mechanisms governing the specific vulnerability of excitatory synapses of *Il1rapl1* mutation? We excluded that this could result from a differential expression of *Il1rapl1* between principal cells (affected synapses) and interneurons (unaffected synapses) using in situ hybridization. As mentioned above, a more likely possibility resides in the fact that excitatory synapses on principal cells and interneurons differ in their anatomical properties, the molecular mechanisms leading to synapse formation, and their molecular equipment once formed. While the molecular partners leading to excitatory synapse formation on glutamatergic cells are starting to be well documented, little is known about mechanisms of excitatory synapse formation in interneurons. Recently however, it was shown that the postsynaptic protein Erbin interacts with a specific isoform of a TARP protein controlling AMPA receptor trafficking and insertion in cortical interneurons (Tao et al., 2013). This led to the formation of excitatory synapses with recruitment of AMPA receptors and this effect was only observed on interneurons and not principal cells. Thus, the specific expression of particular subtypes of

AMPAR scaffolds in interneurons and not principal cells could lead to synaptic specificity. Another report highlights the role of NRG-1 (neuregulin), a neurotrophic factor, in binding ErbB4 receptor to mediate synaptogenesis on interneurons specifically, possibly through stabilization of PSD-95 (Ting et al., 2011). Both these reports show that excitatory synapse development on interneurons depends on specific interactions that are not present on glutamatergic cells, proving the diversity in mechanisms leading to synapse formation. Beyond the diversity in genes mediating synaptic formation, many splice variants were shown to occur in genes involved in synaptogenesis (Craig and Kang, 2007), providing an additional level of complexity in synaptic formation and specificity. Interestingly, interaction of presynaptic PTPδ with postsynaptic Slitrk3 protein is important in mediating inhibitory synapse development (Takahashi et al., 2012). An interesting question would be to know of PTPδ/IL1RAPL1 and PTPδ/Slitrk3 interactions compete to generate correct excitatory/inhibitory synapse development. Interestingly, PTPδ contains three spliced exons in the extracellular Ig-like domains and splicing of these exons in the meA and meB positions regulate interaction with IL1RAPL1 (Yoshida et al., 2011). Thus, it is possible that differential splicing of presynaptic PTPδ in GABA-ergic versus glutamatergic axons contributes to selectivity in partner binding and function, similar to what is observed in neurexins (Aoto et al., 2013).

Whether IL1RAPL1 could be involved in excitatory synapse formation of interneurons remains unstudied, but it seems that consequences of *Il1rapl*1 removal are specific to excitatory synapses of spiny glutamatergic cells. An intriguing question would be whether *Il1rapl1* mutation would also impact excitatory synapses on spiny interneurons, as some interneurons do possess those specialized structures, for example the medium spiny neurons (MSNs) of striatum. This issue could be resolved by looking at electrophysiological and morphological characteristics of these neurons using a similar strategy as the one used in the publication 1, namely by using GAD67-eGFP reporter line to record from interneurons.

In conclusion, these results suggest the mechanisms regulating synaptogenesis are highly heterogeneous and that some synapse specificities exist between principal excitatory and local inhibitory interneurons. Taken together, the examples discussed above suggest that heterogeneity can have both pre-and postsynaptic origins. However, most currently available

experimental evidence suggests that synaptic heterogeneity is mostly expressed at the postsynaptic level. Because of this strong postsynaptic heterogeneity, synaptogenic proteins like IL1RAPL1 could possibly act specifically at certain synaptic types. Consecutively, during early synaptogenesis, the synaptic contact with the axon would not be correctly made, leading to irreversible deficits in long-range wiring and loss of afferents on certain brain regions. Thus, the use of tools that allow characterizing full-brain connectivity in ID mouse models can be essential. Recently, a technology called CLARITY has been developed that allows looking at global brain connectivity in mouse brains (Chung and Deisseroth, 2013). In theory, comparing *Il1rapl1* KO brains with WT brains could reveal some deficits in connectivity between brain regions, an information that could then be used to target the next region of the brain that one can explore at functional as well as behavioral levels.

Crucial information is missing in our current knowledge of the impact of Ilrapl1 deficiency at synaptic level: the intimate morphology of the synaptic compartments. Electron microscopy (EM) has proven to be effective in finding morphological and functional differences between different synapses. Indeed, electron microscopy allows visualizing small structures like the PSD, the active zone and small organelles with very high resolution. Also, it differentiates between symmetrical and asymmetrical synapses allowing distinguishing excitatory and inhibitory synapses. To me, it seems essential to use this technique to study the consequences of IL1RAPL1 removal on synaptic function and morphology at different synaptic levels. Most importantly, EM could potentially provide some information on the exact synaptic localization of IL1RAPL1 and provide the first evidence for a potential heterogeneous distribution of IL1RAPL1 depending on the synapse type studied. To me, EM studies would then be coupled to immune-localization (with gold particles) of particular IL1RAPL1 partners or important synaptic proteins, and/or cellular determination of the pre/postsynaptic compartments by the use of fixable EM labeling. In this line, it is encouraging that the deficit in excitatory synapses in hippocampus following IL1RAPL1 removal was also found in EM sections of KO mice (Pavlowsky et al., 2010b).

1.1.3 Does IL1RAPL1 have a presynaptic function?

While a lot of data point for a role of IL1RAPL1 in synapse formation mainly through trans-and postsynaptic effectors, few data currently exists for a presynaptic role of IL1RAPL1. The currently available data suggest that IL1RAPL1 could be involved in both the building up (Yoshida and Mishina, 2008) of the presynapse and in the regulation of synaptic transmission (Gambino et al., 2007). However, strong evidence for this is still lacking mainly because of the lack of studies in which sole presynaptic *Il1rapl1* expression was manipulated. *In vitro* electrophysiology allows assessing some presynaptic properties. For example, paired pulse ratio (PPR) is a parameter that is calculated by making a ratio between the amplitudes of two postsynaptic responses induced by two closely (50ms) separated presynaptic stimulations and informs on the release properties of presynaptic terminals. PPR can be facilitating, meaning the amplitude of the second response is bigger than the first one or depressing when the amplitude of the second response is smaller. For example, thalamo-LA and cortico-LA afferents have different presynaptic properties illustrated by different PPR values (Humeau et al., 2005). The mechanisms underlying release probability are thought to be essentially presynaptic and are mediated by concentration of calcium ions in the presynaptic terminal. The residual calcium hypothesis states that during the second stimulation, vesicle-mediated neurotransmitter release is increased leading to facilitation (Zucker and Regehr, 2002). Interestingly, we detected strong alteration of the PPR at Cortico-LA synapses of *Il1rapl1*-deficient mice (manuscript in preparation), suggesting that some presynaptic properties may be affected. In this line, presynaptic, PKA dependent Cortico-LA LTP was also abolished (manuscript in preparation), whereas the control of spontaneous fusion events remained unaffected. Thus, direct or indirect consequences of IL1RAPL1 deficiency may exist at the presynaptic level.

Further characterization of the possible role of IL1RAPL1 in presynaptic function would require the use of experimental approaches that allow removing the protein in the presynaptic compartment only. In cultured neurons, this can be achieved by recording pairs of cells with WT or KO genotypes using fluorescent reporter lines: for example, by using crossings of *Il1rapl1* KO mice with X-GFP mice, WT cells can be identified by GFP expression. Then, the recording all four combinations of KO and WT cells as pre-synapse or post-synapse allow understanding in which

synaptic compartment a given protein plays a functional role. However, cultured cells do not reproduce the complexity of neural circuitry in the brain and it is possible that this strategy would not unveil the entire repertoire played by the protein *in vivo*. Alternatively, the use of Cre-lox technology allows the suppression of the protein in brain regions of interest resulting in the absence of the protein in the soma but also in axonal terminals. Then, by looking at a particular projection in the brain, one can easily study the presynaptic role of the protein. However, this requires the creation of a transgenic mouse line where the *Il1rapl1* gene mutation would be flanked by loxP sites, a mouse model that was not available during my PhD. Recently, in a collaborative study, I used this approach to study the consequences of the absence of ID-related protein ATP6AP2 at both pre-and postsynaptic compartments. There, we used hippocampo-BLA projections as a synaptic model (data not shown). To achieve this, ATP6AP2 was removed pre (in vHPC) or postsynaptically (in BLA) by Cre-dependent viruses and hippocampo-BLA currents were evoked by optogenetics as previously described. Thus, this strategy allowed me to specifically record for the consequences of pre-or postsynaptic absence of this ID-related protein in a preserved adult neuronal circuit. The same strategy could be soon be reproduced using floxed-*Il1rapl1* mice that will be shortly available in the lab, and would finally demonstrate if IL1RAPL1 exerts a role at some presynapses.

1.1.4 A proteomic approach to study the consequence of IL1RAPL1 absence at the synapse

The absence of I1rapl1 in the brain and more particularly at the synapse could potentially perturb several interactions with identified or yet to be discovered protein partners. As a consequence, the quantity of certain proteins could change in *Il1rapl1*-deficient mice, participating to the pathophysiology of this ID gene. Alternatively, the absence of IL1RAPL1 could also lead to the activation of compensatory mechanisms that counterbalance IL1RAPL1 deficiency by regulating the levels of redundant proteins. In order to identify possible consequences of IL1RAPL1 absence on synaptic protein levels we used a proteomic approach to test for protein levels between *Il1rapl1* KO and WT animals. To isolate synaptic compartments, we prepared synaptosomes of *Il1rapl1* KO and WT mice brain homogenates. Synaptosomes are functional synaptic particles consisting of a resealed presynaptic compartment and part of the

postsynaptic element that can be obtained following fractionation of mouse brain tissue. They have allowed unraveling a number of mechanisms regulating synaptic function and stability, mainly through the identification of proteins through proteomic determination. However, a major problem resides in the fractionation methods that often lead to a contamination of the neuronal fraction with glial and non-neuronal particles. Recently however, an amelioration of the purity of the synaptosomal fraction was obtained by sorting GFP-expressing synaptic particles. This technique, called FASS (Fluorescence Activated Synaptosome Sorting), is based on the sorting of Venus-positive synaptosomes that have been obtained from a VGLUT1-Venus mouse using FACS technology (Biesemann et al., 2014). Thus, this technique allows the isolation of the main glutamatergic (VGLUT1-positive) synapses in the mouse brain.

Synaptosomal preparations were submitted to different treatments in order to isolate synaptic proteins. Then, proteins of both KO and WT samples were submitted to mass spectrometer chromatography in order to identify proteins that could be up or down-regulated following removal of IL1RAPL1. Using this technique, we have identified about 113 candidates that were significantly up or down regulated in *Il1rapl1* KO mice (Figure 32). I regrouped these proteins in categories reflecting their biological function at the synapse. These categories include: cytoskeletal organization, cell adhesion, transmembrane transporter activity, signaling, vesicle mediated transport, protein binding, neurotransmitter secretion and metabolic processes (Figure 32).

Several findings emerged from this: we observed an up-and down-regulation of several proteins involved in cytoskeletal organization, a down-regulation of several proteins involved in neurotransmitter release as well as in protein regulating endocytosis and finally a down regulation of few proteins involved in organization of the PSD. Taken together, these first results confirmed previous reports, including ours, showing a role of IL1RAPL1 in the organization/morphology of the pre-and postsynaptic compartment and in synaptic function in general, and suggest that the chronic absence of IL1RAPL1 could potentially interfere with all these biological processes. Each particular case cannot be discussed here. I choose to discuss a few examples that make sense regarding previous reports about *Il1rapl1* deficiency phenotypes.

Surprisingly we observed a strong upregulation (more than tenfold) of GluR3 subunit of AMPA receptors. Interestingly, *GluR3* is located on the X chromosome and mutations have been found in patients with ID (Wu et al., 2007). However, the precise role of this subunit in AMPAR function remains unclear and electrophysiological recordings in CA1 region of hippocampus (Meng et al., 2003) or in LA (Humeau et al., 2007) did not reveal strong abnormalities in *GluR3* KO mice. Moreover, *GluR3* KO mice did not show behavioral abnormalities to both cued and contextual fear (Humeau et al., 2007) with only a delay in the appearance of the freezing response during the acquisition session, thereby mimicking the *Il1rapl1* phenotype. Interestingly, a deficit in LTP at Cortico-LA synapses is also seen in *GluR3* KO mice, as in *GluR1* KO mice and *Il1rapl1* KO mice (Humeau et al., 2007) (data not shown). Recently, the IL1RAPL1/MCF2L complex has been shown to be important for the insertion of GluR2/R3-containing AMPA receptors (Hayashi et al., 2013). Unfortunately, we couldn't identify RhoGAP2 or MCF2L in our synaptosomal sorting, possibly because of technical limitations in retrieving soluble proteins in purified synaptosomes. Taken together, our results suggest a functional link between IL1RAPL1 and GluR3. However, results at different analytical levels are quite divergent, with up and down-regulation of IL1RAPL1 and GluR3 leading to similar consequences. Our current explanation is the fact that not all measurements examine the same cellular or subcellular compartments. For example, our proteomic approach purifies synaptic particles, thus the increase in GluR3 levels must be consecutive to an increase of GluR3 to the synaptic compartment. It has to be noted that all other subunits of AMPAR subunits were not up or down-regulated in *Il1rapl1* KO preparations. Interestingly, AMPA and NMDA receptors have been shown to move from extrasynaptic sites to synaptic sites, a highly dynamic and regulated process (Groc and Choquet, 2006). Thus, the increase of GluR3 in synaptosomes could reflect an increase of GluR3 subunit from extrasynaptic sites to the PSD. Interestingly, whereas PSD95 remained unchanged, two proteins of the PSD were shown to be strongly down-regulated in *Il1rapl1* KO preparations. For example, we found a down-regulation of SAP-97, a scaffold protein that is important for dynamics of AMPA glutamate receptors (Howard et al., 2010) and has been shown to interact with IL1RAPL1 (Pavlowsky et al., 2010b). Interestingly, we also observed a strong down-regulation of the olfactomedin-1 protein which has been shown to

interact with AMPARs subunits, amongst which GluR2. Although the mechanisms by which olfactomedin-1 regulates AMPARs function and/or dynamics remain unknown, it would sure deserve to be looked into. Surrounding teams in the institute have developed tools to track the dynamics of the different subunits of AMPA receptors (Groc and Choquet, 2006), and will soon be used to resolve AMPARs dynamics in absence of IL1RAPL1. It will be of particular interest to analyze the AMPAR dynamic in both principal cells and interneurons, as a differential change in the dynamic of AMPAR in both cell types could potentially lead to the I/E imbalance in *Il1rapl1* KO mice.

Regarding the proteins involved in cytoskeletal organization, about half of them were up-regulated and the other half down-regulated, yet not allowing to let emerge any conclusion. However, in line with reported effects of *Il1rapl1* deficiency onto dendritic spine density and morphology it suggests that modifications in molecular cascades controlling synaptic morphology occurs in *Il1rapl1* KO mice. Interestingly, we observed a down regulation in a lot of proteins involved in endocytosis, amongst which we identified amphyphysin and endophilin A1. Endocytosis plays a crucial role in both the recycling of vesicles at the presynaptic terminal but also in the dynamics of AMPA and NMDA receptors at the postsynaptic compartment. Thus, deregulation of endocytosis in *Il1rapl1* KO mice could potentially disturb these processes and impact neurotransmitter release.

Interestingly, two well-known presynaptic proteins, synapsin 1 and 2 were shown to be down-regulated in *Il1rapl1* KO synaptosomes. Synapsins are thought to be important actors in the regulation of synaptic vesicle pools at the presynaptic terminal by tethering them to the actin cytoskeleton (Cesca et al., 2010). Mutations in synapsins cause hyper-excitability of networks and lead to epilepsy and more recently a mutation in *Syn1* was shown to be associated with ASD (Fassio et al., 2011). Recent work realized in our lab for a collaborative study has started addressing the synaptic consequences of *Syn1* absence in LA. Using *Syn1*/GAD67eGFP mice, E. Lugara, a master student from F. Benfenati lab (IIT, Italy) analyzed evoked excitation of LA principal and interneurons following stimulation of both thalamic and cortical projections. Although preliminary, an I/E imbalance seems to be present at these long range projections, a phenotype that resemble the one observed in *Il1rapl1* KO mice.

Although very preliminary, our proteomic data combined with the available functional data of IL1RAPL1 points to an important role of IL1RAPL1 in both pre- and postsynaptic compartment at both morphological and functional levels. More interesting are the potential roles of IL1RAPL1 in the control of dendritic spine dynamic/morphology (actin cytoskeleton), presynaptic vesicular dynamic (endocytosis, reserve pool), and AMPAR trafficking (PSD, GluRs subunits). The impact onto these key synaptic phenomena will have to be addressed in a cell specific manner, as IL1RAPL1 must act differentially in principal cells and interneurons. In the near future we are planning on realizing western blots on purified synaptosomes to confirm the findings we obtained by proteomics (Figure 32).

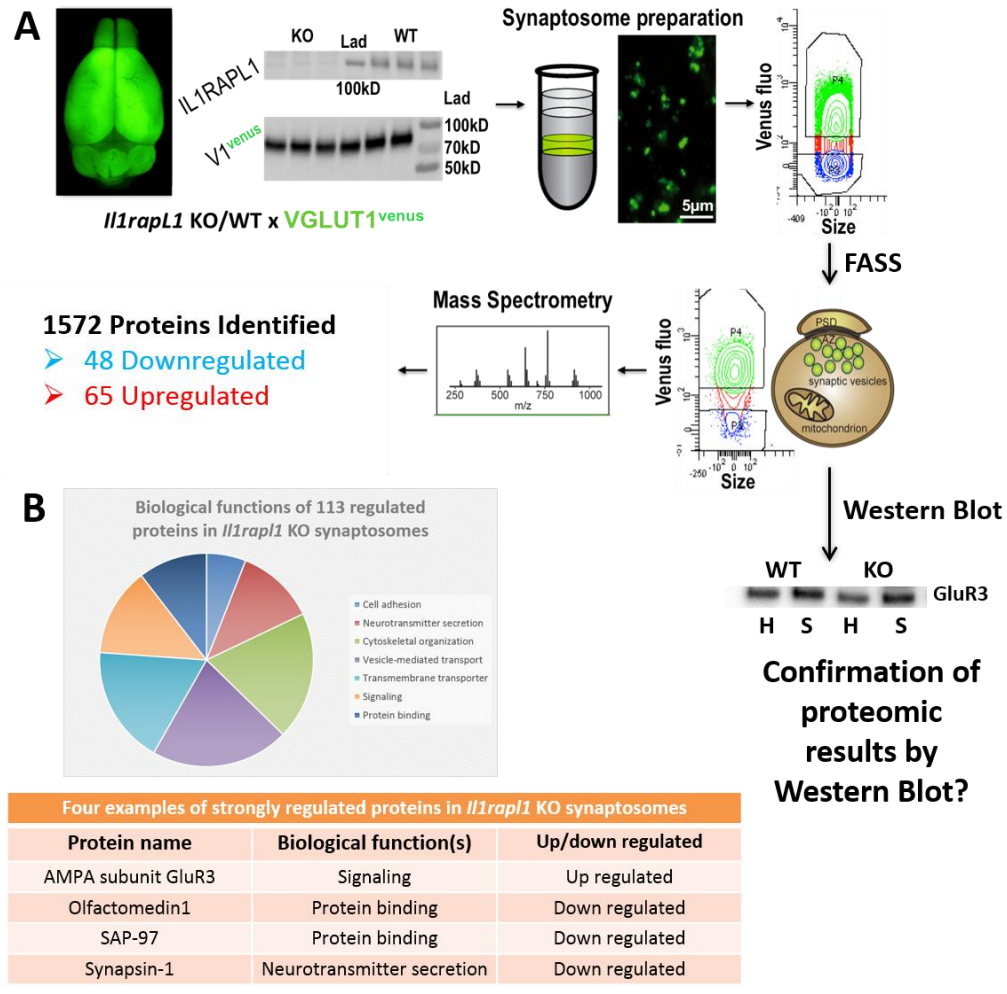

Four examples of strongly regulated proteins in *Il1rapl1* KO synaptosomes		
Protein name	**Biological function(s)**	**Up/down regulated**
AMPA subunit GluR3	Signaling	Up regulated
Olfactomedin1	Protein binding	Down regulated
SAP-97	Protein binding	Down regulated
Synapsin-1	Neurotransmitter secretion	Down regulated

Figure 32: A. Scheme representing the strategy to purify synaptosomes from Il1rapl1 KO/WT x vGlut1-Venus mice. On top left is represented the brain of a vGlut1-Venus mice. The Western Blot confirms the absence of IL1RAPL1 protein in Il1rapl1 KO/vGlut1-venus mice. Synaptosomes were prepared from fractionation of brain homogenates. FACS analysis of the synaptosomal preparation revealed two clear populations of particles (Venus+ in green and Venus- in blue). FASS sorting led to a very pure preparation as seen by the sorting profile. FASS-sorted Venus+ samples were submitted to mass spectrometry to test for protein levels in *Il1rapl1* KO animals. We identified 1572 protein, 48 were down regulated and 65 up regulated in *Il1rapl1*-deficient preparations.

2 When is IL1RAPL1 important at the synapse?

During development, neural circuits are established with extensive remodeling of synapses. Most *in vitro* evidence for IL1RAPL1 in synaptic formation was realized on neuronal cultures taken and prepared from young mice. In contrast, most of my results were realized on adult mice, a period where brain development is complete. However, morphological remodeling of synapses and synaptic turnover also occur at later stages throughout life. Indeed, synapses have been shown to appear and disappear following learning and memory processes and experience-dependent synaptic plasticity (Holtmaat et al., 2008). Thus, knowing whether IL1RAPL1 could alter spine dynamics *in vivo* during adult life is an essential question we would like to answer in the future.

Therapeutic interventions have more chances of success if they correct the deficits at temporally relevant times. The finding that we could rescue contextual fear memory expression in *Il1rapl1*-deficient animals is particularly fascinating because it supposes that some cognitive deficits in ID could be corrected after the initial formation of memories, more specifically during their retrieval and behavioral expression. Although I was able to rescue behavioral deficits in *Il1rapl1* KO mice, possibly by restoring I/E imbalance, the most convincing way of proving the causal role of a protein in behavioral deficits is to reintroduce it *in vivo* and test if behavior can be normalized. In the near future, we'll plan to reintroduce protein constructs of functional IL1RAPL1 by stereotaxy in different brain regions of interest. By reintroducing IL1RAPL1 *in vivo*, we could potentially make more causal links with the absence of the protein in particular brain regions and the observed behavioral deficits. For example, we could test whether injecting IL1RAPL1 in BLA is sufficient to restore contextual fear memory expression. Similarly, reintroducing IL1RAPL1 in different regions of hippocampus could potentially unveil some upstream dysfunctions in hippocampal function during contextual fear expression. In parallel we will inject different mutant versions of IL1RAPL1 lacking some functional important domains to further explore and dissect how IL1RAPL1 structure relates to its synaptic function.

2.1 Consequences of IL1RAPL1's absence on information processing and behavior?

It remains to be studied whether other forms of learning or memory are impaired in *Il1rapl1*-deficient mice and if this can be linked with local I/E imbalances. ID and ASD patients often show impairments in social interactions (Baroncelli et al., 2011; Gatto and Broadie, 2010) and recently a report has shown that strong optogenetic excitation of mPFC neurons leads to deficits in social interactions. Thus, I/E imbalance in mPFC is crucial for appropriate social behavior (Yizhar et al., 2011). Interestingly, excessive excitation is a common feature in a lot of ASD models and explains certain cognitive deficits. *Il1rapl1* mutation in humans can lead to ASD (Piton et al., 2008) but until now nobody has addressed whether *Il1rapl1* KO mice also present some forms of social interaction deficits. A more thorough behavioral screening of *Il1rapl1* KO mice seems necessary. It would be interesting to record for I/E balance in mPFC possibly linking it with social behavior. However, the report of Yizhar et al. supports that excessive excitation underlies social interactions when we report a loss of excitatory transmission at long-range projections. It remains to be studied if decrease in excitation can lead to social interaction deficits.

Working memory is another important aspect of cognitive abilities. It is defined by the capacity of the brain to store information for short period of time. Short term spatial working memory is highly dependent on mPFC and synchronized activity between mPFC and hippocampus (O'Neill et al., 2013). Keeping in mind that *Il1rapl1* KO mice present a small reduction in spine density in hippocampus and in cortical structures, deficits in spatial working memory are likely to emerge in this mouse model. Thus, it would be interesting to submit *Il1rapl1* KO mice to spatial working memory tasks and try to record for I/E balance in relevant brain structures, eventually making links with synaptic- and cognitive dysfunctions.

2.1.1 *In vivo* imaging as a tool to study synapse dynamics

The development of two-photon laser-scanning microscopy in the living brain (Grienberger and Konnerth, 2012) has allowed unprecedented high-resolution imaging of the structural dynamics of synapses. Indeed, it allowed the chronic monitoring of the same portion of dendrite in the

living animal over periods of weeks to months without the need for repeated invasive surgery. We have recently implemented this technique in the laboratory which would allow us to study spine dynamics over long periods of time and at different developmental stages throughout the life of *Il1rapl1*-deficient mice. *In vivo* imaging becomes really fascinating when coupled to behavior. Indeed, a recent study has shown that pyramidal neurons of layer V in the FrA region of the prefrontal cortex showed spine dynamics following learning and extinction of fear conditioning in mice(Lai et al., 2012). Thus, we have the ambition to study the impact of fear conditioning on spine dynamics in cortical structures of *Il1rapl1*-deficient mice. However, these techniques possess the main disadvantage of being limited in depth. As a consequence, only superficial layers 2/3 (L2/3) of cortical structures are usually imaged *in vivo*. Nonetheless, L2/3 synapses are thought to be critical for learning new skills (Huber et al., 2012; Komiyama et al., 2010). In addition, because of the ubiquitous expression of *Il1rapl1* in the cortex and the high order cognitive deficits in ID patients, pathological consequences of IL1RAPL1 absence are likely to emerge in these structures too.

Recently, a report has benefited from the recent development of genetically-encoded calcium indicators to look at neuronal ensemble activity in the somatosensory cortex of *Fmr1* KO mice by combining *in vivo* two photon calcium imaging and electrophysiology (Gonçalves et al., 2013). They showed that cortical networks are hyper-excitable in a brain-state dependent manner during a critical period of experience-dependent synaptic plasticity, possibly explaining some behavioral deficits. Surely, the comprehension of ID would benefit from the implementation of these techniques in mouse models. In this line, neighboring mPFC neurons of *Fmr1* KO mice were hyper-connected during a critical period in early development of mPFC (Testa-Silva et al., 2012). Thus, *in vivo* imaging can be used to image synapse dynamics during behavior but also to study global connectivity in brain regions of interest.

2.1.2 Catching behaviorally relevant cells

When trying to establish a link between synaptic and neuronal function and learning and memory events, an important source of cellular heterogeneity in the neuronal populations is their actual contribution – or not - to this information coding. Episodic and contextual memories

can be retrieved months and years after they have been formed. During retrieval of memory, it is believed that there is a reactivation of neurons that were activated during memory formation (Tayler et al., 2013). Indeed, during learning a subset of neurons store the memory trace (also called the memory engram) and reactivation of these cells is necessary for expression of behavior (Reijmers et al., 2007). When animals are re-exposed to a fearful context, BLA neuronal ensembles that were activated during learning are recruited during re-exposure (Nonaka et al., 2014). Similarly, in the dorsal dentate gyrus of hippocampus, optogenetic activation of cells that were previously recruited in the memory trace was sufficient to induce fear expression (Liu et al., 2012). Knowing where, how and when memory traces are stored and recalled is an essential question in neuroscience and particularly in the context of ID. Indeed, this approach could allow us to restrict our observations and manipulations to physiologically relevant cells and refine our knowledge about the ID-genes in learning and memory.

Recently, it was also shown that BLA neurons show output specificity to the mPFC and that this defined their behavioral role (Senn et al., 2014). Indeed, BLA cells projecting to PL were shown to be preferentially active during high fear while BLA cells projecting to IL are recruited during extinction. An intriguing question would be to know whether BLA-projecting cells to PL are also preferentially recruited by vHPC during high states of fear. This could potentially be answered by combining retrobeads injections in mPFC (IL and PL) and some optogenetic stimulation of hippocampal projections in BLA. Injected retrobeads are taken up by the axonal terminals and travel back to the soma, allowing patching selectively BLA-projecting cells to mPFC.

I successfully used this strategy to answer a specific question: because *Il1rapl1* KO animals presented deficits in contextual fear memory expression I tested whether BLA principal cells that received hippocampal inputs were also preferentially connected to PL. To achieve this, retrobeads were injected in both PL and IL part of mPFC to assess whether BLA-projecting cells could be differentially connected to vHPC and if they showed different characteristics in *Il1rapl1* KO and WT animals. No difference was detected between the two BLA cell populations (projecting to IL VS PL), in both genotypes. However, this strategy was validated in the lab and will be used in the future to improve the postsynaptic specification *in vivo*. In line with this, comparing retrobeads-positive and retrobeads-negative cells in BLA by stimulating hippocampal

projections didn't reveal a difference between the two populations (Hübner et al., 2014). Thus, it doesn't seem that BLA projecting cells to PL and IL are differentially connected by vHPC.

Several strategies allow the labeling of activated cells during certain phases of behavior. Most of them are based on the fact that learning and memory induce expression of immediate early genes (IEG) like c-Fos, Arc… Recently, a technique was developed that allows identifying physiologically relevant neurons several days or weeks after their stimulus dependent activation (during memory formation, retrieval…). This technique is based on the use of a newly developed mouse line where the tetracycline transactivator (tTA) protein is under control of the immediate early gene c-Fos promoter. During neuronal activation (c-Fos activation), tTA is produced and will specifically bind on TetO sequences on the genome, allowing expression of a downstream functional protein – opsin - or fluorescent reporter (Liu et al., 2012; Tayler et al., 2013). TetO constructs can be delivered in specific brain areas through localized injections (Liu et al., 2012) or by crossing mice with TetO transgenic animals (Tayler et al., 2013). To restrict tTa production to physiologically relevant time-windows, animals are submitted to a special food diet. When doxycycline is added to the food, there is inhibition of tTA binding to TetO sequences and removing doxycycline treatment opens a time window allowing the tagging of activated neurons during a particular moment of learning. Putting the animals back on doxycycline closes the window, avoiding any unspecific labeling.

This particular model could be very useful to label cells that were specifically activated during contextual re-exposure in *Il1rapl1* KO mice. Indeed, although we proved the efficacy of hippocampo-BLA fibers in regulating contextual fear expression intensity, our optogenetic stimulation protocol stimulated all Chr2-expressing fibers. However, *in vivo*, only a small proportion of caudal CA1 cells is reactivated during contextual re-exposure (Tayler et al., 2013). It would be particularly interesting to know if the manipulation of projections originating from the activated cells only is sufficient for restoring contextual fear memory. This would require breeding *Il1rapl1* KO mice with cFos-tTA mice and to infect caudal hippocampus with a TetO-Chr2 construct. Then, by relieving doxycycline treatment during contextual fear memory expression, cFos would be limited to the cells that are reactivated during the test leading to Chr2 expression in specific cellular types. cFos-tTA mice could also be particularly useful to

perform *ex vivo* recordings of cells involved in a particular behavioral phase (fluorescent labeling). Indeed, behaviorally activated cells often show different molecular and electrophysiological properties compared to non-activated cells (Zhou et al., 2009). Thus, recordings from behaviorally relevant cells will be a necessary step to understand how ID gene mutations impact integrative neuronal properties.

X) Conclusion

During my PhD thesis I have shown that absence of the synaptic protein IL1RAPL1 leads to target-specific disruption of excitatory synapses on principal cells leading to local I/E imbalances in amygdala. Interestingly I/E imbalances in LA and BLA impacted both memory formation and expression of previously formed memories, providing strong links with synaptic function and cognition. Most importantly, my work highlights the heterogeneous vulnerability of synapses induced by the absence of IL1RAPL1 depending on the identity of the postsynaptic cell (principal vs. interneuron). Indeed, synaptic heterogeneity contributes to cognitive fitness of individuals and many behavioral features of ID are likely to result from specific alterations in neural circuits. Both pre-and postsynaptic compartments are highly heterogeneous in their molecular composition suggesting that the absence of many other synaptic proteins could affect brain function differentially depending on the studied synaptic structure. In the future, efforts should be made in the study of all cellular and/or synaptic types at integrated levels in ID animal models, as this is probably the best strategy to link cognitive abnormalities with synaptic dysfunctions. This will require the development of tools that allow discriminating between synaptic types. Continuous efforts will also have to be made in the identification of interacting partners of IL1RAPL1 and the signaling pathways mediated by these interactions. Signaling pathways are still the main target for therapeutic interventions and their comprehension is crucial for the understanding of disease. IL1RAPL1 is believed to be important for synaptogenesis during development of the brain but whether this also holds for synaptic remodeling in adult life remains unknown. Altogether, my work opened some intriguing questions that will have to be answered in the future for a more comprehensive understanding of IL1RAPL1 at the synapse.

XI) Bibliography

Acuna, C., Guo, Q., Burré, J., Sharma, M., Sun, J., and Südhof, T.C. (2014). Microsecond Dissection of Neurotransmitter Release: SNARE-Complex Assembly Dictates Speed and Ca(2+) Sensitivity. Neuron *82*, 1088–1100.

Alabi, A.A., and Tsien, R.W. (2013). Perspectives on kiss-and-run: role in exocytosis, endocytosis, and neurotransmission. Annu. Rev. Physiol. *75*, 393–422.

Aligianis, I.A., Johnson, C.A., Gissen, P., Chen, D., Hampshire, D., Hoffmann, K., Maina, E.N., Morgan, N. V, Tee, L., Morton, J., et al. (2005). Mutations of the catalytic subunit of RAB3GAP cause Warburg Micro syndrome. Nat. Genet. *37*, 221–223.

Ammar, M.-R., Humeau, Y., Hanauer, A., Nieswandt, B., Bader, M.-F., and Vitale, N. (2013). The Coffin-Lowry syndrome-associated protein RSK2 regulates neurite outgrowth through phosphorylation of phospholipase D1 (PLD1) and synthesis of phosphatidic acid. J. Neurosci. *33*, 19470–19479.

Anggono, V., and Huganir, R.L. (2012). Regulation of AMPA receptor trafficking and synaptic plasticity. Curr. Opin. Neurobiol. *22*, 461–469.

Aoto, J., Martinelli, D.C., Malenka, R.C., Tabuchi, K., and Südhof, T.C. (2013). Presynaptic neurexin-3 alternative splicing trans-synaptically controls postsynaptic AMPA receptor trafficking. Cell *154*, 75–88.

Atasoy, D., Schoch, S., Ho, A., Nadasy, K.A., Liu, X., Zhang, W., Mukherjee, K., Nosyreva, E.D., Fernandez-Chacon, R., Missler, M., et al. (2007). Deletion of CASK in mice is lethal and impairs synaptic function. Proc. Natl. Acad. Sci. U. S. A. *104*, 2525–2530.

Ba, W., van der Raadt, J., and Nadif Kasri, N. (2013). Rho GTPase signaling at the synapse: implications for intellectual disability. Exp Cell Res *319*, 2368–2374.

Bahi, N. (2003). IL1 receptor accessory protein like, a protein involved in X-linked mental retardation, interacts with Neuronal Calcium Sensor-1 and regulates exocytosis. Hum Mol Genet *12*, 1415–1425.

Banerjee, S., Riordan, M., and Bhat, M.A. (2014). Genetic aspects of autism spectrum disorders: insights from animal models. Front Cell Neurosci *8*, 58.

Baroncelli, L., Braschi, C., Spolidoro, M., Begenisic, T., Maffei, L., and Sale, A. (2011). Brain plasticity and disease: a matter of inhibition. Neural Plast *2011*, 286073.

Barot, S.K., Chung, A., Kim, J.J., and Bernstein, I.L. (2009). Functional imaging of stimulus convergence in amygdalar neurons during Pavlovian fear conditioning. PLoS One *4*, e6156.

Bauer, E.P., and LeDoux, J.E. (2004). Heterosynaptic long-term potentiation of inhibitory interneurons in the lateral amygdala. J Neurosci *24*, 9507–9512.

Behnecke, A., Hinderhofer, K., Bartsch, O., Nümann, A., Ipach, M.-L., Damatova, N., Haaf, T., Dufke, A., Riess, O., and Moog, U. (2011). Intragenic deletions of IL1RAPL1: Report of two cases and review of the literature. Am. J. Med. Genet. A *155A*, 372–379.

Berkel, S., Tang, W., Treviño, M., Vogt, M., Obenhaus, H.A., Gass, P., Scherer, S.W., Sprengel, R., Schratt, G., and Rappold, G.A. (2012). Inherited and de novo SHANK2 variants associated with autism spectrum disorder impair neuronal morphogenesis and physiology. Hum. Mol. Genet. *21*, 344–357.

Berlau, D.J., and McGaugh, J.L. (2006). Enhancement of extinction memory consolidation: the role of the noradrenergic and GABAergic systems within the basolateral amygdala. Neurobiol Learn Mem *86*, 123–132.

Bianchi, V., Farisello, P., Baldelli, P., Meskenaite, V., Milanese, M., Vecellio, M., Mühlemann, S., Lipp, H.P., Bonanno, G., Benfenati, F., et al. (2009). Cognitive impairment in Gdi1-deficient mice is associated with altered synaptic vesicle pools and short-term synaptic plasticity, and can be corrected by appropriate learning training. Hum. Mol. Genet. *18*, 105–117.

Bienvenu, T.C., Busti, D., Magill, P.J., Ferraguti, F., and Capogna, M. (2012). Cell-type-specific recruitment of amygdala interneurons to hippocampal theta rhythm and noxious stimuli in vivo. Neuron *74*, 1059–1074.

Biesemann, C., Gronborg, M., Luquet, E., Wichert, S.P., Bernard, V., Bungers, S.R., Cooper, B., Varoqueaux, F., Li, L., Byrne, J.A., et al. (2014). Proteomic screening of glutamatergic mouse brain synaptosomes isolated by fluorescence activated sorting. EMBO J *33*, 157–170.

Bissière, S., Humeau, Y., and Lüthi, A. (2003). Dopamine gates LTP induction in lateral amygdala by suppressing feedforward inhibition. Nat. Neurosci. *6*, 587–592.

Van Bokhoven, H. (2011). Genetic and epigenetic networks in intellectual disabilities. Annu Rev Genet *45*, 81–104.

Born, T.L., Smith, D.E., Garka, K.E., Renshaw, B.R., Bertles, J.S., and Sims, J.E. (2000). Identification and characterization of two members of a novel class of the interleukin-1 receptor (IL-1R) family. Delineation of a new class of IL-1R-related proteins based on signaling. J Biol Chem *275*, 29946–29954.

Bosch, M., and Hayashi, Y. (2012). Structural plasticity of dendritic spines. Curr Opin Neurobiol *22*, 383–388.

Bosch, M., Castro, J., Saneyoshi, T., Matsuno, H., Sur, M., and Hayashi, Y. (2014). Structural and molecular remodeling of dendritic spine substructures during long-term potentiation. Neuron *82*, 444–459.

Boyden, E.S., Zhang, F., Bamberg, E., Nagel, G., and Deisseroth, K. (2005). Millisecond-timescale, genetically targeted optical control of neural activity. Nat Neurosci *8*, 1263–1268.

Branco, T., and Häusser, M. (2010). The single dendritic branch as a fundamental functional unit in the nervous system. Curr. Opin. Neurobiol. *20*, 494–502.

Braudeau, J., Delatour, B., Duchon, A., Pereira, P.L., Dauphinot, L., de Chaumont, F., Olivo-Marin, J.-C., Dodd, R.H., Hérault, Y., and Potier, M.-C. (2011). Specific targeting of the GABA-A receptor α5 subtype by a selective inverse agonist restores cognitive deficits in Down syndrome mice. J. Psychopharmacol. *25*, 1030–1042.

Burgoyne, R.D. (2007). Neuronal calcium sensor proteins: generating diversity in neuronal Ca2+ signalling. Nat. Rev. Neurosci. *8*, 182–193.

Capogna, M. (2014). GABAergic cell type diversity in the basolateral amygdala. Curr. Opin. Neurobiol. *26*, 110–116.

Caporale, N., and Dan, Y. (2008). Spike timing-dependent plasticity: a Hebbian learning rule. Annu Rev Neurosci *31*, 25–46.

Carper, R. (2002). Cerebral Lobes in Autism: Early Hyperplasia and Abnormal Age Effects. Neuroimage *16*, 1038–1051.

Carrié, A., Jun, L., Bienvenu, T., Vinet, M.C., McDonell, N., Couvert, P., Zemni, R., Cardona, A., Van Buggenhout, G., Frints, S., et al. (1999). A new member of the IL-1 receptor family highly expressed in hippocampus and involved in X-linked mental retardation. Nat. Genet. *23*, 25–31.

Cesca, F., Baldelli, P., Valtorta, F., and Benfenati, F. (2010). The synapsins: key actors of synapse function and plasticity. Prog Neurobiol *91*, 313–348.

Chelly, J., Khelfaoui, M., Francis, F., Cherif, B., and Bienvenu, T. (2006). Genetics and pathophysiology of mental retardation. Eur J Hum Genet *14*, 701–713.

Cho, J.H., Deisseroth, K., and Bolshakov, V.Y. (2013). Synaptic encoding of fear extinction in mPFC-amygdala circuits. Neuron *80*, 1491–1507.

Choquet, D., and Triller, A. (2013). The dynamic synapse. Neuron *80*, 691–703.

Chow, B.Y., Han, X., Dobry, A.S., Qian, X., Chuong, A.S., Li, M., Henninger, M.A., Belfort, G.M., Lin, Y., Monahan, P.E., et al. (2010). High-performance genetically targetable optical neural silencing by light-driven proton pumps. Nature *463*, 98–102.

Chung, K., and Deisseroth, K. (2013). CLARITY for mapping the nervous system. Nat. Methods *10*, 508–513.

Citri, A., and Malenka, R.C. (2008). Synaptic plasticity: multiple forms, functions, and mechanisms. Neuropsychopharmacology *33*, 18–41.

Courtin, J., Bienvenu, T.C.M., Einarsson, E.Ö., and Herry, C. (2013). Medial prefrontal cortex neuronal circuits in fear behavior. Neuroscience *240*, 219–242.

Courtin, J., Chaudun, F., Rozeske, R.R., Karalis, N., Gonzalez-Campo, C., Wurtz, H., Abdi, A., Baufreton, J., Bienvenu, T.C., and Herry, C. (2014). Prefrontal parvalbumin interneurons shape neuronal activity to drive fear expression. Nature *505*, 92–96.

Craig, A.M., and Kang, Y. (2007). Neurexin-neuroligin signaling in synapse development. Curr Opin Neurobiol *17*, 43–52.

D'Adamo, P., Masetti, M., Bianchi, V., More, L., Mignogna, M.L., Giannandrea, M., and Gatti, S. (2014). RAB GTPases and RAB-interacting proteins and their role in the control of cognitive functions. Neurosci Biobehav Rev.

Dalva, M.B., McClelland, A.C., and Kayser, M.S. (2007). Cell adhesion molecules: signalling functions at the synapse. Nat Rev Neurosci *8*, 206–220.

Dani, V.S., Chang, Q., Maffei, A., Turrigiano, G.G., Jaenisch, R., and Nelson, S.B. (2005). Reduced cortical activity due to a shift in the balance between excitation and inhibition in a mouse model of Rett syndrome. Proc. Natl. Acad. Sci. U. S. A. *102*, 12560–12565.

Darnell, J.C., and Klann, E. (2013). The translation of translational control by FMRP: therapeutic targets for FXS. Nat. Neurosci. *16*, 1530–1536.

DeFelipe, J., Lopez-Cruz, P.L., Benavides-Piccione, R., Bielza, C., Larranaga, P., Anderson, S., Burkhalter, A., Cauli, B., Fairen, A., Feldmeyer, D., et al. (2013). New insights into the classification and nomenclature of cortical GABAergic interneurons. Nat Rev Neurosci *14*, 202–216.

Deidda, G., Bozarth, I.F., and Cancedda, L. (2014). Modulation of GABAergic transmission in development and neurodevelopmental disorders: investigating physiology and pathology to gain therapeutic perspectives. Front Cell Neurosci *8*, 119.

Delorme, R., Ey, E., Toro, R., Leboyer, M., Gillberg, C., and Bourgeron, T. (2013). Progress toward treatments for synaptic defects in autism. Nat Med *19*, 685–694.

Dong, H., O'Brien, R.J., Fung, E.T., Lanahan, A.A., Worley, P.F., and Huganir, R.L. (1997). GRIP: a synaptic PDZ domain-containing protein that interacts with AMPA receptors. Nature *386*, 279–284.

Durand, C.M., Perroy, J., Loll, F., Perrais, D., Fagni, L., Bourgeron, T., Montcouquiol, M., and Sans, N. (2012). SHANK3 mutations identified in autism lead to modification of dendritic spine morphology via an actin-dependent mechanism. Mol Psychiatry *17*, 71–84.

Ehrlich, I., Humeau, Y., Grenier, F., Ciocchi, S., Herry, C., and Luthi, A. (2009). Amygdala inhibitory circuits and the control of fear memory. Neuron *62*, 757–771.

Endele, S., Rosenberger, G., Geider, K., Popp, B., Tamer, C., Stefanova, I., Milh, M., Kortüm, F., Fritsch, A., Pientka, F.K., et al. (2010). Mutations in GRIN2A and GRIN2B encoding regulatory subunits of NMDA receptors cause variable neurodevelopmental phenotypes. Nat. Genet. *42*, 1021–1026.

Esteban, J.A., Shi, S.-H., Wilson, C., Nuriya, M., Huganir, R.L., and Malinow, R. (2003). PKA phosphorylation of AMPA receptor subunits controls synaptic trafficking underlying plasticity. Nat. Neurosci. *6*, 136–143.

Etienne-Manneville, S., and Hall, A. (2002). Rho GTPases in cell biology. Nature *420*, 629–635.

Fanselow, M.S., and Dong, H.W. (2010). Are the dorsal and ventral hippocampus functionally distinct structures? Neuron *65*, 7–19.

Fanselow, M.S., and Poulos, A.M. (2005). The neuroscience of mammalian associative learning. Annu Rev Psychol *56*, 207–234.

Fassio, A., Patry, L., Congia, S., Onofri, F., Piton, A., Gauthier, J., Pozzi, D., Messa, M., Defranchi, E., Fadda, M., et al. (2011). SYN1 loss-of-function mutations in autism and partial epilepsy cause impaired synaptic function. Hum. Mol. Genet. *20*, 2297–2307.

Fernandez, F., and Garner, C.C. (2007). Over-inhibition: a model for developmental intellectual disability. Trends Neurosci *30*, 497–503.

Fernandez, F., Morishita, W., Zuniga, E., Nguyen, J., Blank, M., Malenka, R.C., and Garner, C.C. (2007). Pharmacotherapy for cognitive impairment in a mouse model of Down syndrome. Nat Neurosci *10*, 411–413.

Fourcaudot, E., Gambino, F., Humeau, Y., Casassus, G., Shaban, H., Poulain, B., and Luthi, A. (2008). cAMP/PKA signaling and RIM1alpha mediate presynaptic LTP in the lateral amygdala. Proc Natl Acad Sci U S A *105*, 15130–15135.

Fremeau, R.T., Kam, K., Qureshi, T., Johnson, J., Copenhagen, D.R., Storm-Mathisen, J., Chaudhry, F.A., Nicoll, R.A., and Edwards, R.H. (2004). Vesicular glutamate transporters 1 and 2 target to functionally distinct synaptic release sites. Science *304*, 1815–1819.

Frints, S., Froyen, G., Marynen, P., and Fryns, J.-P. (2002). X-linked mental retardation: vanishing boundaries between non-specific (MRX) and syndromic (MRXS) forms. Clin. Genet. *62*, 423–432.

Fyffe, S.L., Neul, J.L., Samaco, R.C., Chao, H.T., Ben-Shachar, S., Moretti, P., McGill, B.E., Goulding, E.H., Sullivan, E., Tecott, L.H., et al. (2008). Deletion of Mecp2 in Sim1-expressing neurons reveals a critical role for MeCP2 in feeding behavior, aggression, and the response to stress. Neuron *59*, 947–958.

Gambino, F., and Holtmaat, A. (2012). Synapses let loose for a change: inhibitory synapse pruning throughout experience-dependent cortical plasticity. Neuron *74*, 214–217.

Gambino, F., Pavlowsky, A., Begle, A., Dupont, J.L., Bahi, N., Courjaret, R., Gardette, R., Hadjkacem, H., Skala, H., Poulain, B., et al. (2007). IL1-receptor accessory protein-like 1 (IL1RAPL1), a protein involved in cognitive functions, regulates N-type Ca2+-channel and neurite elongation. Proc Natl Acad Sci U S A *104*, 9063–9068.

Gambino, F., Kneib, M., Pavlowsky, A., Skala, H., Heitz, S., Vitale, N., Poulain, B., Khelfaoui, M., Chelly, J., Billuart, P., et al. (2009). IL1RAPL1 controls inhibitory networks during cerebellar development in mice. Eur. J. Neurosci. *30*, 1476–1486.

Gatto, C.L., and Broadie, K. (2010). Genetic controls balancing excitatory and inhibitory synaptogenesis in neurodevelopmental disorder models. Front Synaptic Neurosci *2*, 4.

Gecz, J., Gedeon, A.K., Sutherland, G.R., and Mulley, J.C. (1996). Identification of the gene FMR2, associated with FRAXE mental retardation. Nat. Genet. *13*, 105–108.

Giannandrea, M., Bianchi, V., Mignogna, M.L., Sirri, A., Carrabino, S., D'Elia, E., Vecellio, M., Russo, S., Cogliati, F., Larizza, L., et al. (2010). Mutations in the small GTPase gene RAB39B are responsible for X-linked mental retardation associated with autism, epilepsy, and macrocephaly. Am. J. Hum. Genet. *86*, 185–195.

Gilissen, C., Hehir-Kwa, J.Y., Thung, D.T., van de Vorst, M., van Bon, B.W., Willemsen, M.H., Kwint, M., Janssen, I.M., Hoischen, A., Schenck, A., et al. (2014). Genome sequencing identifies major causes of severe intellectual disability. Nature *511*, 344–347.

Godlee, C., and Kaksonen, M. (2013). Review series: From uncertain beginnings: initiation mechanisms of clathrin-mediated endocytosis. J. Cell Biol. *203*, 717–725.

Gonçalves, J.T., Anstey, J.E., Golshani, P., and Portera-Cailliau, C. (2013). Circuit level defects in the developing neocortex of Fragile X mice. Nat. Neurosci. *16*, 903–909.

Gordon, S.L., and Cousin, M.A. (2013). X-linked intellectual disability-associated mutations in synaptophysin disrupt synaptobrevin II retrieval. J Neurosci *33*, 13695–13700.

Govek, E.E., Newey, S.E., and Van Aelst, L. (2005). The role of the Rho GTPases in neuronal development. Genes Dev *19*, 1–49.

Gradinaru, V., Zhang, F., Ramakrishnan, C., Mattis, J., Prakash, R., Diester, I., Goshen, I., Thompson, K.R., and Deisseroth, K. (2010). Molecular and cellular approaches for diversifying and extending optogenetics. Cell *141*, 154–165.

Graf, E.R., Zhang, X., Jin, S.X., Linhoff, M.W., and Craig, A.M. (2004). Neurexins induce differentiation of GABA and glutamate postsynaptic specializations via neuroligins. Cell *119*, 1013–1026.

Grienberger, C., and Konnerth, A. (2012). Imaging calcium in neurons. Neuron *73*, 862–885.

Groc, L., and Choquet, D. (2006). AMPA and NMDA glutamate receptor trafficking: multiple roads for reaching and leaving the synapse. Cell Tissue Res. *326*, 423–438.

Guy, J., Gan, J., Selfridge, J., Cobb, S., and Bird, A. (2007). Reversal of neurological defects in a mouse model of Rett syndrome. Science (80-.). *315*, 1143–1147.

Hamdan, F.F., Gauthier, J., Dobrzeniecka, S., Lortie, A., Mottron, L., Vanasse, M., D'Anjou, G., Lacaille, J.C., Rouleau, G.A., and Michaud, J.L. (2011). Intellectual disability without epilepsy associated with STXBP1 disruption. Eur J Hum Genet *19*, 607–609.

Han, J.H., Kushner, S.A., Yiu, A.P., Cole, C.J., Matynia, A., Brown, R.A., Neve, R.L., Guzowski, J.F., Silva, A.J., and Josselyn, S.A. (2007). Neuronal competition and selection during memory formation. Science (80-.). *316*, 457–460.

Han, Y., Kaeser, P.S., Südhof, T.C., and Schneggenburger, R. (2011). RIM determines Ca^2+ channel density and vesicle docking at the presynaptic active zone. Neuron *69*, 304–316.

Hayashi, T., Yoshida, T., Ra, M., Taguchi, R., and Mishina, M. (2013). IL1RAPL1 associated with mental retardation and autism regulates the formation and stabilization of glutamatergic synapses of cortical neurons through RhoA signaling pathway. PLoS One *8*, e66254.

Herry, C., Ciocchi, S., Senn, V., Demmou, L., Muller, C., and Luthi, A. (2008). Switching on and off fear by distinct neuronal circuits. Nature *454*, 600–606.

Herry, C., Ferraguti, F., Singewald, N., Letzkus, J.J., Ehrlich, I., and Luthi, A. (2010). Neuronal circuits of fear extinction. Eur J Neurosci *31*, 599–612.

Herzog, É. (2004). Comprendre les neurones glutamatergiques chez les mammifères: un ménage à trois. M/S Médecine Sci.

Holtmaat, A., and Svoboda, K. (2009). Experience-dependent structural synaptic plasticity in the mammalian brain. Nat Rev Neurosci *10*, 647–658.

Holtmaat, A., De Paola, V., Wilbrecht, L., and Knott, G.W. (2008). Imaging of experience-dependent structural plasticity in the mouse neocortex in vivo. Behav Brain Res *192*, 20–25.

Hong, I., Kim, J., Song, B., Park, K., Shin, K., Eom, K.D., Han, P.L., Lee, S., and Choi, S. (2012). Fear conditioning occludes late-phase long-term potentiation at thalamic input synapses onto the lateral amygdala in rat brain slices. Neurosci Lett *506*, 121–125.

Howard, M.A., Elias, G.M., Elias, L.A.B., Swat, W., and Nicoll, R.A. (2010). The role of SAP97 in synaptic glutamate receptor dynamics. Proc. Natl. Acad. Sci. U. S. A. *107*, 3805–3810.

Huber, D., Gutnisky, D.A., Peron, S., O'Connor, D.H., Wiegert, J.S., Tian, L., Oertner, T.G., Looger, L.L., and Svoboda, K. (2012). Multiple dynamic representations in the motor cortex during sensorimotor learning. Nature *484*, 473–478.

Hübner, C., Bosch, D., Gall, A., Lüthi, A., and Ehrlich, I. (2014). Ex vivo dissection of optogenetically activated mPFC and hippocampal inputs to neurons in the basolateral amygdala: implications for fear and emotional memory. Front. Behav. Neurosci. *8*, 64.

Humeau, Y., Shaban, H., Bissière, S., and Lüthi, A. (2003). Presynaptic induction of heterosynaptic associative plasticity in the mammalian brain. Nature *426*, 841–845.

Humeau, Y., Herry, C., Kemp, N., Shaban, H., Fourcaudot, E., Bissiere, S., and Luthi, A. (2005). Dendritic spine heterogeneity determines afferent-specific Hebbian plasticity in the amygdala. Neuron *45*, 119–131.

Humeau, Y., Reisel, D., Johnson, A.W., Borchardt, T., Jensen, V., Gebhardt, C., Bosch, V., Gass, P., Bannerman, D.M., Good, M.A., et al. (2007). A pathway-specific function for different AMPA receptor subunits in amygdala long-term potentiation and fear conditioning. J. Neurosci. *27*, 10947–10956.

Humeau, Y., Gambino, F., Chelly, J., and Vitale, N. (2009). X-linked mental retardation: focus on synaptic function and plasticity. J Neurochem *109*, 1–14.

Isaacson, J.S., and Scanziani, M. (2011). How inhibition shapes cortical activity. Neuron *72*, 231–243.

Isshiki, M., Tanaka, S., Kuriu, T., Tabuchi, K., Takumi, T., and Okabe, S. (2014). Enhanced synapse remodelling as a common phenotype in mouse models of autism. Nat Commun *5*, 4742.

Jamain, S., Quach, H., Betancur, C., Rastam, M., Colineaux, C., Gillberg, I.C., Soderstrom, H., Giros, B., Leboyer, M., Gillberg, C., et al. (2003). Mutations of the X-linked genes encoding neuroligins NLGN3 and NLGN4 are associated with autism. Nat Genet *34*, 27–29.

Johansen, J.P., Hamanaka, H., Monfils, M.H., Behnia, R., Deisseroth, K., Blair, H.T., and LeDoux, J.E. (2010). Optical activation of lateral amygdala pyramidal cells instructs associative fear learning. Proc. Natl. Acad. Sci. U. S. A. *107*, 12692–12697.

Kaeser, P.S., Deng, L., Wang, Y., Dulubova, I., Liu, X., Rizo, J., and Sudhof, T.C. (2011). RIM proteins tether Ca2+ channels to presynaptic active zones via a direct PDZ-domain interaction. Cell *144*, 282–295.

Kamp, M.A., Hänggi, D., Steiger, H.-J., and Schneider, T. (2012). Diversity of presynaptic calcium channels displaying different synaptic properties. Rev. Neurosci. *23*, 179–190.

Kaufmann, W.E. (2000). Dendritic Anomalies in Disorders Associated with Mental Retardation. Cereb. Cortex *10*, 981–991.

Kelemen, E., and Fenton, A.A. (2010). Dynamic grouping of hippocampal neural activity during cognitive control of two spatial frames. PLoS Biol *8*, e1000403.

Khelfaoui, M., Denis, C., van Galen, E., de Bock, F., Schmitt, A., Houbron, C., Morice, E., Giros, B., Ramakers, G., Fagni, L., et al. (2007). Loss of X-linked mental retardation gene oligophrenin1 in mice impairs spatial memory and leads to ventricular enlargement and dendritic spine immaturity. J Neurosci *27*, 9439–9450.

Kim, J., Zhao, T., Petralia, R.S., Yu, Y., Peng, H., Myers, E., and Magee, J.C. (2012). mGRASP enables mapping mammalian synaptic connectivity with light microscopy. Nat. Methods *9*, 96–102.

Kim, J., Kwon, J.T., Kim, H.S., Josselyn, S.A., and Han, J.H. (2014). Memory recall and modifications by activating neurons with elevated CREB. Nat Neurosci *17*, 65–72.

Kleschevnikov, A.M., Belichenko, P. V, Villar, A.J., Epstein, C.J., Malenka, R.C., and Mobley, W.C. (2004). Hippocampal long-term potentiation suppressed by increased inhibition in the Ts65Dn mouse, a genetic model of Down syndrome. J Neurosci *24*, 8153–8160.

Komiyama, T., Sato, T.R., O'Connor, D.H., Zhang, Y.-X., Huber, D., Hooks, B.M., Gabitto, M., and Svoboda, K. (2010). Learning-related fine-scale specificity imaged in motor cortex circuits of behaving mice. Nature *464*, 1182–1186.

Kornau, H.C., Schenker, L.T., Kennedy, M.B., and Seeburg, P.H. (1995). Domain interaction between NMDA receptor subunits and the postsynaptic density protein PSD-95. Science *269*, 1737–1740.

Kroon, T., Sierksma, M.C., and Meredith, R.M. (2013). Investigating mechanisms underlying neurodevelopmental phenotypes of autistic and intellectual disability disorders: a perspective. Front Syst Neurosci *7*, 75.

Kwon, S.-K., Woo, J., Kim, S.-Y., Kim, H., and Kim, E. (2010). Trans-synaptic adhesions between netrin-G ligand-3 (NGL-3) and receptor tyrosine phosphatases LAR, protein-tyrosine phosphatase delta (PTPdelta), and PTPsigma via specific domains regulate excitatory synapse formation. J. Biol. Chem. *285*, 13966–13978.

Lai, C.S., Franke, T.F., and Gan, W.B. (2012). Opposite effects of fear conditioning and extinction on dendritic spine remodelling. Nature *483*, 87–91.

Li, D., Herault, K., Silm, K., Evrard, A., Wojcik, S., Oheim, M., Herzog, E., and Ropert, N. (2013). Lack of evidence for vesicular glutamate transporter expression in mouse astrocytes. J Neurosci *33*, 4434–4455.

Lin, J.Y. (2011). A user's guide to channelrhodopsin variants: features, limitations and future developments. Exp Physiol *96*, 19–25.

Liu, X., Ramirez, S., Pang, P.T., Puryear, C.B., Govindarajan, A., Deisseroth, K., and Tonegawa, S. (2012). Optogenetic stimulation of a hippocampal engram activates fear memory recall. Nature *484*, 381–385.

Maren, S., and Quirk, G.J. (2004). Neuronal signalling of fear memory. Nat Rev Neurosci *5*, 844–852.

Maren, S., Fanselow, M.S., and Angeles, L. (1995). Synaptic Plasticity in the Basolateral Hippocampal Formation Stimulation Amygdala in viva Induced by. *15*.

Maren, S., Phan, K.L., and Liberzon, I. (2013). The contextual brain: implications for fear conditioning, extinction and psychopathology. Nat Rev Neurosci *14*, 417–428.

Markram, H., Toledo-Rodriguez, M., Wang, Y., Gupta, A., Silberberg, G., and Wu, C. (2004). Interneurons of the neocortical inhibitory system. Nat Rev Neurosci *5*, 793–807.

Matsuzaki, M., Honkura, N., Ellis-Davies, G.C.R., and Kasai, H. (2004). Structural basis of long-term potentiation in single dendritic spines. Nature *429*, 761–766.

Maurin, T., Zongaro, S., and Bardoni, B. (2014). Fragile X Syndrome: From molecular pathology to therapy. Neurosci Biobehav Rev.

McGaugh, J.L. (2004). The amygdala modulates the consolidation of memories of emotionally arousing experiences. Annu. Rev. Neurosci. *27*, 1–28.

Meng, Y., Zhang, Y., and Jia, Z. (2003). Synaptic Transmission and Plasticity in the Absence of AMPA Glutamate Receptor GluR2 and GluR3. Neuron *39*, 163–176.

Michalon, A., Sidorov, M., Ballard, T.M., Ozmen, L., Spooren, W., Wettstein, J.G., Jaeschke, G., Bear, M.F., and Lindemann, L. (2012). Chronic pharmacological mGlu5 inhibition corrects fragile X in adult mice. Neuron *74*, 49–56.

Moretti, P., Levenson, J.M., Battaglia, F., Atkinson, R., Teague, R., Antalffy, B., Armstrong, D., Arancio, O., Sweatt, J.D., and Zoghbi, H.Y. (2006). Learning and memory and synaptic plasticity are impaired in a mouse model of Rett syndrome. J Neurosci *26*, 319–327.

Muller, J.F., Mascagni, F., and McDonald, A.J. (2007). Serotonin-immunoreactive axon terminals innervate pyramidal cells and interneurons in the rat basolateral amygdala. J. Comp. Neurol. *505*, 314–335.

Muller, M., Faber-Zuschratter, H., Yanagawa, Y., Stork, O., Schwegler, H., and Linke, R. (2012). Synaptology of ventral CA1 and subiculum projections to the basomedial nucleus of the amygdala in the mouse: relation to GABAergic interneurons. Brain Struct Funct *217*, 5–17.

Murphy, J.A., Stein, I.S., Lau, C.G., Peixoto, R.T., Aman, T.K., Kaneko, N., Aromolaran, K., Saulnier, J.L., Popescu, G.K., Sabatini, B.L., et al. (2014). Phosphorylation of Ser1166 on GluN2B by PKA is critical to synaptic NMDA receptor function and Ca2+ signaling in spines. J. Neurosci. *34*, 869–879.

Nabavi, S., Fox, R., Proulx, C.D., Lin, J.Y., Tsien, R.Y., and Malinow, R. (2014). Engineering a memory with LTD and LTP. Nature *511*, 348–352.

Nadif Kasri, N., Nakano-Kobayashi, A., Malinow, R., Li, B., and Van Aelst, L. (2009). The Rho-linked mental retardation protein oligophrenin-1 controls synapse maturation and plasticity by stabilizing AMPA receptors. Genes Dev *23*, 1289–1302.

Nadif Kasri, N., Nakano-Kobayashi, A., and Van Aelst, L. (2011). Rapid synthesis of the X-linked mental retardation protein OPHN1 mediates mGluR-dependent LTD through interaction with the endocytic machinery. Neuron *72*, 300–315.

Nair, D., Hosy, E., Petersen, J.D., Constals, A., Giannone, G., Choquet, D., and Sibarita, J.-B. (2013). Super-resolution imaging reveals that AMPA receptors inside synapses are dynamically organized in nanodomains regulated by PSD95. J. Neurosci. *33*, 13204–13224.

Nakano-Kobayashi, A., Kasri, N.N., Newey, S.E., and Van Aelst, L. (2009). The Rho-linked mental retardation protein OPHN1 controls synaptic vesicle endocytosis via endophilin A1. Curr. Biol. *19*, 1133–1139.

Nakano-Kobayashi, A., Tai, Y., Nadif Kasri, N., and Van Aelst, L. (2014). The X-linked mental retardation protein OPHN1 interacts with Homer1b/c to control spine endocytic zone positioning and expression of synaptic potentiation. J Neurosci *34*, 8665–8671.

Nonaka, A., Toyoda, T., Miura, Y., Hitora-Imamura, N., Naka, M., Eguchi, M., Yamaguchi, S., Ikegaya, Y., Matsuki, N., and Nomura, H. (2014). Synaptic Plasticity Associated with a Memory Engram in the Basolateral Amygdala. J. Neurosci. *34*, 9305–9309.

O'Neill, P.K., Gordon, J.A., and Sigurdsson, T. (2013). Theta oscillations in the medial prefrontal cortex are modulated by spatial working memory and synchronize with the hippocampus through its ventral subregion. J Neurosci *33*, 14211–14224.

Opazo, P., and Choquet, D. (2011). A three-step model for the synaptic recruitment of AMPA receptors. Mol. Cell. Neurosci. *46*, 1–8.

Opazo, P., Labrecque, S., Tigaret, C.M., Frouin, A., Wiseman, P.W., De Koninck, P., and Choquet, D. (2010). CaMKII triggers the diffusional trapping of surface AMPARs through phosphorylation of stargazin. Neuron *67*, 239–252.

Orsini, C.A., Kim, J.H., Knapska, E., and Maren, S. (2011). Hippocampal and prefrontal projections to the basal amygdala mediate contextual regulation of fear after extinction. J Neurosci *31*, 17269–17277.

Orsini, C.A., Yan, C., and Maren, S. (2013). Ensemble coding of context-dependent fear memory in the amygdala. Front Behav Neurosci *7*, 199.

Papagiakoumou, E. (2013). Optical developments for optogenetics. Biol Cell *105*, 443–464.

Pape, H.-C., and Pare, D. (2010). Plastic synaptic networks of the amygdala for the acquisition, expression, and extinction of conditioned fear. Physiol. Rev. *90*, 419–463.

Pavlowsky, A., Zanchi, A., Pallotto, M., Giustetto, M., Chelly, J., Sala, C., and Billuart, P. (2010a). Neuronal JNK pathway activation by IL-1 is mediated through IL1RAPL1, a protein required for development of cognitive functions. Commun. Integr. Biol. *3*, 245–247.

Pavlowsky, A., Gianfelice, A., Pallotto, M., Zanchi, A., Vara, H., Khelfaoui, M., Valnegri, P., Rezai, X., Bassani, S., Brambilla, D., et al. (2010b). A postsynaptic signaling pathway that may account for the cognitive defect due to IL1RAPL1 mutation. Curr Biol *20*, 103–115.

Pavlowsky, A., Chelly, J., and Billuart, P. (2012). Emerging major synaptic signaling pathways involved in intellectual disability. Mol Psychiatry *17*, 682–693.

Paylor, R., Yuva-Paylor, L.A., Nelson, D.L., and Spencer, C.M. (2008). Reversal of sensorimotor gating abnormalities in Fmr1 knockout mice carrying a human Fmr1 transgene. Behav Neurosci *122*, 1371–1377.

Peca, J., Feliciano, C., Ting, J.T., Wang, W., Wells, M.F., Venkatraman, T.N., Lascola, C.D., Fu, Z., and Feng, G. (2011). Shank3 mutant mice display autistic-like behaviours and striatal dysfunction. Nature *472*, 437–442.

Pinard, A., Seddik, R., and Bettler, B. (2010). GABAB receptors: physiological functions and mechanisms of diversity. Adv. Pharmacol. *58*, 231–255.

Pinard, C.R., Muller, J.F., Mascagni, F., and McDonald, A.J. (2008). Dopaminergic innervation of interneurons in the rat basolateral amygdala. Neuroscience *157*, 850–863.

PITKÄNEN, A., PIKKARAINEN, M., NURMINEN, N., and YLINEN, A. (2006). Reciprocal Connections between the Amygdala and the Hippocampal Formation, Perirhinal Cortex, and Postrhinal Cortex in Rat: A Review. Ann. N. Y. Acad. Sci. *911*, 369–391.

Piton, A., Michaud, J.L., Peng, H., Aradhya, S., Gauthier, J., Mottron, L., Champagne, N., Lafreniere, R.G., Hamdan, F.F., team, S.D., et al. (2008). Mutations in the calcium-related gene IL1RAPL1 are associated with autism. Hum Mol Genet *17*, 3965–3974.

Pouille, F., and Scanziani, M. (2004). Routing of spike series by dynamic circuits in the hippocampus. Nature *429*, 717–723.

Purpura, D.P. (1974). Dendritic spine “dysgenesis” and mental retardation. Science *186*, 1126–1128.

Quirk, G.J., Armony, J.L., and LeDoux, J.E. (1997). Fear Conditioning Enhances Different Temporal Components of Tone-Evoked Spike Trains in Auditory Cortex and Lateral Amygdala. Neuron *19*, 613–624.

Reijmers, L.G., Perkins, B.L., Matsuo, N., and Mayford, M. (2007). Localization of a stable neural correlate of associative memory. Science (80-.). *317*, 1230–1233.

Rizzoli, S.O. (2014). Synaptic vesicle recycling: steps and principles. EMBO J *33*, 788–822.

Ronesi, J.A., Collins, K.A., Hays, S.A., Tsai, N.-P.P., Guo, W., Birnbaum, S.G., Hu, J.-H.H., Worley, P.F., Gibson, J.R., and Huber, K.M. (2012). Disrupted Homer scaffolds mediate abnormal mGluR5 function in a mouse model of fragile X syndrome. Nat Neurosci *15*, 431–40, S1.

De Roo, M., Klauser, P., and Muller, D. (2008). LTP promotes a selective long-term stabilization and clustering of dendritic spines. PLoS Biol. *6*, e219.

Rumpel, S., LeDoux, J., Zador, A., and Malinow, R. (2005). Postsynaptic receptor trafficking underlying a form of associative learning. Science (80-.). *308*, 83–88.

Rzhetsky, A., Bagley, S.C., Wang, K., Lyttle, C.S., Cook Jr., E.H., Altman, R.B., and Gibbons, R.D. (2014). Environmental and state-level regulatory factors affect the incidence of autism and intellectual disability. PLoS Comput Biol *10*, e1003518.

Sah, P., Westbrook, R.F., and Luthi, A. (2008). Fear conditioning and long-term potentiation in the amygdala: what really is the connection? Ann N Y Acad Sci *1129*, 88–95.

Sakisaka, T., and Takai, Y. (2005). Cell adhesion molecules in the CNS. J Cell Sci *118*, 5407–5410.

Sala, C., and Segal, M. (2014). Dendritic spines: the locus of structural and functional plasticity. Physiol. Rev. *94*, 141–188.

Sanders, M.J., Wiltgen, B.J., and Fanselow, M.S. (2003). The place of the hippocampus in fear conditioning. Eur. J. Pharmacol. *463*, 217–223.

Senn, V., Wolff, S.B.E., Herry, C., Grenier, F., Ehrlich, I., Gründemann, J., Fadok, J.P., Müller, C., Letzkus, J.J., and Lüthi, A. (2014). Long-range connectivity defines behavioral specificity of amygdala neurons. Neuron *81*, 428–437.

Shaban, H., Humeau, Y., Herry, C., Cassasus, G., Shigemoto, R., Ciocchi, S., Barbieri, S., van der Putten, H., Kaupmann, K., Bettler, B., et al. (2006). Generalization of amygdala LTP and conditioned fear in the absence of presynaptic inhibition. Nat Neurosci *9*, 1028–1035.

Shen, J., Tareste, D.C., Paumet, F., Rothman, J.E., and Melia, T.J. (2007). Selective activation of cognate SNAREpins by Sec1/Munc18 proteins. Cell *128*, 183–195.

Sheng, M., and Kim, E. (2011). The postsynaptic organization of synapses. Cold Spring Harb Perspect Biol *3*.

Shin, R.M., Tully, K., Li, Y., Cho, J.H., Higuchi, M., Suhara, T., and Bolshakov, V.Y. (2010). Hierarchical order of coexisting pre- and postsynaptic forms of long-term potentiation at synapses in amygdala. Proc Natl Acad Sci U S A *107*, 19073–19078.

Shin, S.M., Zhang, N., Hansen, J., Gerges, N.Z., Pak, D.T.S., Sheng, M., and Lee, S.H. (2012). GKAP orchestrates activity-dependent postsynaptic protein remodeling and homeostatic scaling. Nat. Neurosci. *15*, 1655–1666.

Smith, D.M., and Bulkin, D.A. (2014). The form and function of hippocampal context representations. Neurosci Biobehav Rev *40*, 52–61.

Sosulina, L., Graebenitz, S., and Pape, H.C. (2010). GABAergic interneurons in the mouse lateral amygdala: a classification study. J Neurophysiol *104*, 617–626.

Sotres-Bayon, F., Sierra-Mercado, D., Pardilla-Delgado, E., and Quirk, G.J. (2012). Gating of fear in prelimbic cortex by hippocampal and amygdala inputs. Neuron *76*, 804–812.

Spampanato, J., Polepalli, J., and Sah, P. (2011). Interneurons in the basolateral amygdala. Neuropharmacology *60*, 765–773.

Spencer, C.M., Graham, D.F., Yuva-Paylor, L.A., Nelson, D.L., and Paylor, R. (2008). Social behavior in Fmr1 knockout mice carrying a human FMR1 transgene. Behav Neurosci *122*, 710–715.

Spruston, N. (2008). Pyramidal neurons: dendritic structure and synaptic integration. Nat Rev Neurosci *9*, 206–221.

Sudhof, T.C. (2004). The synaptic vesicle cycle. Annu Rev Neurosci *27*, 509–547.

Sudhof, T.C. (2008). Neuroligins and neurexins link synaptic function to cognitive disease. Nature *455*, 903–911.

Sudhof, T.C. (2013). Neurotransmitter release: the last millisecond in the life of a synaptic vesicle. Neuron *80*, 675–690.

Südhof, T.C. (2013). A molecular machine for neurotransmitter release: synaptotagmin and beyond. Nat. Med. *19*, 1227–1231.

Szinyei, C., Narayanan, R.T., and Pape, H.C. (2007). Plasticity of inhibitory synaptic network interactions in the lateral amygdala upon fear conditioning in mice. Eur J Neurosci *25*, 1205–1211.

Tabolacci, E., Pomponi, M.G., Pietrobono, R., Terracciano, A., Chiurazzi, P., and Neri, G. (2006). A truncating mutation in the IL1RAPL1 gene is responsible for X-linked mental retardation in the MRX21 family. Am. J. Med. Genet. A *140*, 482–487.

Takahashi, H., Katayama, K., Sohya, K., Miyamoto, H., Prasad, T., Matsumoto, Y., Ota, M., Yasuda, H., Tsumoto, T., Aruga, J., et al. (2012). Selective control of inhibitory synapse development by Slitrk3-PTPdelta trans-synaptic interaction. Nat Neurosci *15*, 389–98, S1–2.

Tamamaki, N., Yanagawa, Y., Tomioka, R., Miyazaki, J., Obata, K., and Kaneko, T. (2003). Green fluorescent protein expression and colocalization with calretinin, parvalbumin, and somatostatin in the GAD67-GFP knock-in mouse. J Comp Neurol *467*, 60–79.

Taniguchi, H. (2014). Genetic dissection of GABAergic neural circuits in mouse neocortex. Front Cell Neurosci *8*, 8.

Tao, Y., Chen, Y.J., Shen, C., Luo, Z., Bates, C.R., Lee, D., Marchetto, S., Gao, T.M., Borg, J.P., Xiong, W.C., et al. (2013). Erbin interacts with TARP gamma-2 for surface expression of AMPA receptors in cortical interneurons. Nat Neurosci *16*, 290–299.

Tarpey, P., Parnau, J., Blow, M., Woffendin, H., Bignell, G., Cox, C., Cox, J., Davies, H., Edkins, S., Holden, S., et al. (2004). Mutations in the DLG3 gene cause nonsyndromic X-linked mental retardation. Am J Hum Genet *75*, 318–324.

Tarpey, P.S., Smith, R., Pleasance, E., Whibley, A., Edkins, S., Hardy, C., O'Meara, S., Latimer, C., Dicks, E., Menzies, A., et al. (2009). A systematic, large-scale resequencing screen of X-chromosome coding exons in mental retardation. Nat Genet *41*, 535–543.

Tayler, K.K., Tanaka, K.Z., Reijmers, L.G., and Wiltgen, B.J. (2013). Reactivation of neural ensembles during the retrieval of recent and remote memory. Curr Biol *23*, 99–106.

Testa-Silva, G., Loebel, A., Giugliano, M., de Kock, C.P., Mansvelder, H.D., and Meredith, R.M. (2012). Hyperconnectivity and slow synapses during early development of medial prefrontal cortex in a mouse model for mental retardation and autism. Cereb Cortex *22*, 1333–1342.

Thalhammer, A., and Cingolani, L.A. (2014). Cell adhesion and homeostatic synaptic plasticity. Neuropharmacology *78*, 23–30.

Ting, A.K., Chen, Y., Wen, L., Yin, D.M., Shen, C., Tao, Y., Liu, X., Xiong, W.C., and Mei, L. (2011). Neuregulin 1 promotes excitatory synapse development and function in GABAergic interneurons. J Neurosci *31*, 15–25.

Tritsch, D., Chesnoy-Marchais, D., and Feltz, A. (1998). Physiologie du neurone.

Tropea, D., Giacometti, E., Wilson, N.R., Beard, C., McCurry, C., Fu, D.D., Flannery, R., Jaenisch, R., and Sur, M. (2009). Partial reversal of Rett Syndrome-like symptoms in MeCP2 mutant mice. Proc Natl Acad Sci U S A *106*, 2029–2034.

Tsvetkov, E., Carlezon, W.A., Benes, F.M., Kandel, E.R., and Bolshakov, V.Y. (2002). Fear Conditioning Occludes LTP-Induced Presynaptic Enhancement of Synaptic Transmission in the Cortical Pathway to the Lateral Amygdala. Neuron *34*, 289–300.

Tyagarajan, S.K., and Fritschy, J.M. (2014). Gephyrin: a master regulator of neuronal function? Nat Rev Neurosci *15*, 141–156.

Tye, K.M., and Deisseroth, K. (2012). Optogenetic investigation of neural circuits underlying brain disease in animal models. Nat Rev Neurosci *13*, 251–266.

Vaillend, C., Poirier, R., and Laroche, S. (2008). Genes, plasticity and mental retardation. Behav Brain Res *192*, 88–105.

Valnegri, P., Montrasio, C., Brambilla, D., Ko, J., Passafaro, M., and Sala, C. (2011). The X-linked intellectual disability protein IL1RAPL1 regulates excitatory synapse formation by binding PTPdelta and RhoGAP2. Hum Mol Genet *20*, 4797–4809.

Waites, C.L., Craig, A.M., and Garner, C.C. (2005). Mechanisms of vertebrate synaptogenesis. Annu. Rev. Neurosci. *28*, 251–274.

Waites, C.L., Specht, C.G., Härtel, K., Leal-Ortiz, S., Genoux, D., Li, D., Drisdel, R.C., Jeyifous, O., Cheyne, J.E., Green, W.N., et al. (2009). Synaptic SAP97 isoforms regulate AMPA receptor dynamics and access to presynaptic glutamate. J. Neurosci. *29*, 4332–4345.

Whibley, A.C., Plagnol, V., Tarpey, P.S., Abidi, F., Fullston, T., Choma, M.K., Boucher, C.A., Shepherd, L., Willatt, L., Parkin, G., et al. (2010). Fine-scale survey of X chromosome copy number variants and indels underlying intellectual disability. Am J Hum Genet *87*, 173–188.

Williams, S.R., and Atkinson, S.E. (2008). Dendritic synaptic integration in central neurons. Curr Biol *18*, R1045–7.

Wolff, S.B., Grundemann, J., Tovote, P., Krabbe, S., Jacobson, G.A., Muller, C., Herry, C., Ehrlich, I., Friedrich, R.W., Letzkus, J.J., et al. (2014). Amygdala interneuron subtypes control fear learning through disinhibition. Nature *509*, 453–458.

Won, H., Lee, H.R., Gee, H.Y., Mah, W., Kim, J.I., Lee, J., Ha, S., Chung, C., Jung, E.S., Cho, Y.S., et al. (2012). Autistic-like social behaviour in Shank2-mutant mice improved by restoring NMDA receptor function. Nature *486*, 261–265.

Won, H., Mah, W., and Kim, E. (2013). Autism spectrum disorder causes, mechanisms, and treatments: focus on neuronal synapses. Front Mol Neurosci *6*, 19.

Woo, J., Kwon, S.-K., Choi, S., Kim, S., Lee, J.-R., Dunah, A.W., Sheng, M., and Kim, E. (2009). Trans-synaptic adhesion between NGL-3 and LAR regulates the formation of excitatory synapses. Nat. Neurosci. *12*, 428–437.

Woodruff, A.R., and Sah, P. (2007). Inhibition and synchronization of basal amygdala principal neuron spiking by parvalbumin-positive interneurons. J Neurophysiol *98*, 2956–2961.

Wragg, R.T., Snead, D., Dong, Y., Ramlall, T.F., Menon, I., Bai, J., Eliezer, D., and Dittman, J.S. (2013). Synaptic vesicles position complexin to block spontaneous fusion. Neuron *77*, 323–334.

Wu, Y., Arai, A.C., Rumbaugh, G., Srivastava, A.K., Turner, G., Hayashi, T., Suzuki, E., Jiang, Y., Zhang, L., Rodriguez, J., et al. (2007). Mutations in ionotropic AMPA receptor 3 alter channel properties and are associated with moderate cognitive impairment in humans. Proc. Natl. Acad. Sci. U. S. A. *104*, 18163–18168.

Xue, M., Atallah, B. V, and Scanziani, M. (2014). Equalizing excitation-inhibition ratios across visual cortical neurons. Nature *511*, 596–600.

Yan, Q.J., Rammal, M., Tranfaglia, M., and Bauchwitz, R.P. (2005). Suppression of two major Fragile X Syndrome mouse model phenotypes by the mGluR5 antagonist MPEP. Neuropharmacology *49*, 1053–1066.

Yizhar, O., Fenno, L.E., Prigge, M., Schneider, F., Davidson, T.J., O'Shea, D.J., Sohal, V.S., Goshen, I., Finkelstein, J., Paz, J.T., et al. (2011). Neocortical excitation/inhibition balance in information processing and social dysfunction. Nature *477*, 171–178.

Yoshida, T., and Mishina, M. (2008). Zebrafish orthologue of mental retardation protein IL1RAPL1 regulates presynaptic differentiation. Mol Cell Neurosci *39*, 218–228.

Yoshida, T., Yasumura, M., Uemura, T., Lee, S.J., Ra, M., Taguchi, R., Iwakura, Y., and Mishina, M. (2011). IL-1 receptor accessory protein-like 1 associated with mental retardation and autism mediates synapse formation by trans-synaptic interaction with protein tyrosine phosphatase delta. J Neurosci *31*, 13485–13499.

Youngs, E.L., Henkhaus, R., Hellings, J.A., and Butler, M.G. (2012). IL1RAPL1 gene deletion as a cause of X-linked intellectual disability and dysmorphic features. Eur J Med Genet *55*, 32–36.

Zhang, Y.P., and Oertner, T.G. (2007). Optical induction of synaptic plasticity using a light-sensitive channel. Nat Methods *4*, 139–141.

Zhang, J., Muller, J.F., and McDonald, A.J. (2013). Noradrenergic innervation of pyramidal cells in the rat basolateral amygdala. Neuroscience *228*, 395–408.

Zhang, Y.P., Holbro, N., and Oertner, T.G. (2008). Optical induction of plasticity at single synapses reveals input-specific accumulation of alphaCaMKII. Proc Natl Acad Sci U S A *105*, 12039–12044.

Zhou, Q., Homma, K.J., and Poo, M. (2004). Shrinkage of dendritic spines associated with long-term depression of hippocampal synapses. Neuron *44*, 749–757.

Zhou, Y., Won, J., Karlsson, M.G., Zhou, M., Rogerson, T., Balaji, J., Neve, R., Poirazi, P., and Silva, A.J. (2009). CREB regulates excitability and the allocation of memory to subsets of neurons in the amygdala. Nat Neurosci *12*, 1438–1443.

Zucker, R.S., and Regehr, W.G. (2002). Short-term synaptic plasticity. Annu Rev Physiol *64*, 355–405.